JOHN VAN GEEST
CANCER RESEARCH CENTRE
Nottingham Trent University

Assessment of a novel mutated Prostatic Acid Phosphatase-derived vaccine for the treatment of Prostate Cancer

Pauline Le Vu

A thesis submitted in partial fulfilment of the requirements of Nottingham Trent University for the degree of Doctor of Philosophy

Supervisors: Dr. Stephanie E.B McArdle
Prof. Alan G. Pockley

September 2019

DECLARATION OF OWNERSHIP

This submission is the result of my work. All help and advice, other than that received from tutors, has been acknowledged and primary and secondary sources of information have been properly attributed. Should this statement prove to be untrue, I recognise the right and duty of the Board of Examiners to recommend what action should be taken in line with the University's regulations on assessment contained in the Handbook.

Copyright Statement

Acknowledgments

Table of Contents

Abbreviations

AA	Amino acids
ACT	Adoptive cell transfer
ADCC	Antibody-dependent cell mediated cytotoxicity
ADT	Androgen deprivation therapy
APC	Antigen-presenting cells
AR	Androgen receptor
beta2m	Beta2 microglobulin
CAF	Cancer associated fibroblast
CAF	Cationic adjuvant formulation
CAR	Chimeric antigen receptor
cDNA	Complementary deoxyribonucleic acid
CDRs	Complementarity determining regions
CIML	Cytokine-induced memory-like
CMV	Cytomegalovirus
CR	Complete response
CRPC	Castrate resistant prostate cancer
CTL	Cytotoxic T lymphocytes
CTLA-4	Cytotoxic T-lymphocyte–associated antigen 4
CTRL	Control
DC	Dendritic cells
DNA	Deoxyribonucleic acid
DRE	Digital rectal examination
EBV	Epstein-Barr virus
ELISA	Enzyme-linked immunosorbent assay
ER	Endoplasmic reticulum
FACS	Fluorescent assay cell sorting
FADD	Fas-associated death domain
FCS	Fetal calf serum
FDA	Food and Drug Administration
FITC	Fluorescein isothiocyanate
FLUa	Influenza A
GAPDH	Glyceraldehyde-3-phosphate dehydrogenase
GM-CSF	Granulocyte macrophage-colony stimulating factor
HLA	Human Leucocyte Antigen
ICS	Intracellular cytokine staining
IDO	Indoleamine 2,3-dioxygenase
IFN	Interferon
Ig	Immunoglobulin
IL	Interleukin
ILT-2	Human inhibitory receptors Ig-Like Transcript 2
LAG3	Lymphocyte-activation gene 3
LPS	Lipopolysaccharide
mAbs	Monoclonal antibodies
MDSC	Myeloid derived suppressor cells
MHC	Major histocompatibility complex
mRNA	Messenger ribonucleic acid

NK	Natural killer cells
NKG2D	NK cell activating receptor
OS	Overall survival
PAMPs	Pathogen-associated molecular patterns
PAP	Prostatic acid phosphatase
PAP42mer	Prostatic acid phosphatase 42 amino acid sequence
PBMC	Peripheral blood mononuclear cells
PCa	Prostate cancer
PD-1	Programmed death 1
PD-L1	Programmed death ligand 1
Poly I:C	Polyinosinicpolycytidylic acid
PSA	Prostate-specific antigen
RNA	Ribonucleic acid
ROS	Reactive oxygen species
RNS	Reactive nitrogen species
RT	Room temperature
RT-PCR	Reverse transcriptase-polymerase chain reaction
SDS-PAGE	Sodium dodecyl sulphate-polyacrylamide gel electrophoresis
Treg	Regulatory T-cells
TAA	Tumour-associated antigens
TAM	Tumour associated macrophages
TAP	Transporter associated with antigen processing (TAP)
TCM	Central memory T-cell
TCR	T cell receptor
TEM	Effector memory T cells
TGFβ	Transforming growth factor b
Th	T helper lymphocytes
TIL	Tumour infiltrating lymphocytes
TLR	Toll-like receptor
TME	Tumour micro-environment
TNF	Tumour necrosis factor
TNM	Tumour-Node-Metastasis
TPTPB	Transperineal template prostate biopsy
TRAIL	TNF-related apoptosis-inducing ligand
TRM	Tissue resident memory T-cell
TRUS	Transrectal ultrasonography
TSCM	Stem central memory T-cell
VEGF	Vascular endothelial growth factor
WT	Wild type

List of figures

List of tables

Abstract

Prostate cancer is the second most frequent cancer in men. Patients with a localized disease are treated with local therapies such as prostatectomy or radiation therapy whereas patients with a metastatic disease are treated with androgen deprivation therapies (ADT). However, patients ultimately develop resistance to ADT, thereby leading to a castrate resistant prostate cancer (CRPC). The treatment options for such disease are limited and not curative, with a median survival from diagnosis of 14 months. Among these treatments, the Sipuleucel-T based vaccine, FDA approved in 2010, has been shown to prolong the overall survival by 4 months. However, while this approach demonstrated the efficacy of targeting the Prostatic Acid Phosphatase (PAP) antigen, overexpressed in prostate cancer, to stimulate the patient's immune system to treat CRPC, it remains extremely expensive and limited in its efficacy.

The aim of the study was to develop a new, less expensive and more effective PAP-based vaccine for the treatment of advanced prostate cancer. A 15mer PAP-derived vaccine, when injected as a DNA vaccine, was previously shown to induce PAP-specific T-cell responses and to reduce tumour growth in a syngeneic heterotopic murine prostate cancer model. A new form of the vaccine was subsequently developed by elongating (to 42mer) and introducing a single mutation to the PAP-derived peptide.

Two pre-clinical murine models (C57Bl/6 mice and HHDII/DR1 transgenic) were used to assess the efficacy of the vaccine. The mutated PAP42mer sequence was the most immunogenic sequence in both models when administered as a peptide-based vaccine, as demonstrated by the higher number of IFNγ-releasing splenocytes following *in vitro* stimulation with PAP-derived class-I and class-II epitopes and by the higher functional avidity obtained. The vaccine immunogenicty was further enhanced by using stronger adjuvants and delivery systems. CAF09 adjuvant and ImmunoBody® DNA vaccine were superior to CpG adjuvant in inducing PAP-specific immune responses. This was demonstrated by the expression of activation and inhibitory markers, by the induction of a memory response and by the functional phenotype (cytokines release, proliferation, and degranulation) of CD8$^+$ T cells following *in vitro* stimulation with shorter-vaccine-derived peptides. Splenocytes from vaccinated mice were capable of lysing target cells in a PAP-dependant manner *in vitro*. Vaccination slowed down the growth of human-PAP$^+$ expressing tumours implanted in the HHDII/DR1 model but no anti-tumour effect was observed against TRAMP-C1 tumours in the C57Bl/6 model. Finally, circulating PAP42mer derived-specific CD8$^+$ T cells were detected in the blood of patients with prostate cancer.

In summary, this study demonstrated that a unique vaccine strategy could induce a robust anti-PAP immunity but with little effect on the growth of implanted PAP-expressing cancer cell-derived tumours *in vivo*. The presence of PAP-specific CD8$^+$ T cells in the periphery of patients with advanced prostate cancer suggests that these patients could benefit from this new approach.

Chapter 1: Introduction

1.1. Prostate cancer

1.1.1. Epidemiology and risk factors

Prostate cancer (PCa) is the second most frequent cancer in men worldwide and the fifth cause of death due to cancer in men (Ferlay, et al. 2015). Worldwide, deaths due to PCa represents 6.6% of total deaths from cancer in male. In the UK, deaths from PCa represent 7% of deaths from all cancers in male (Cancer research UK website: https://www.cancerresearchuk.org/health-professional/cancer-statistics/statistics-by-cancer-type/prostate-cancer#heading-One).

Over the last decade, PCa age-standardised mortality rates decreased by 12%. PCa mortality rates are expected to decrease by 16% by 2035.

The survival rate is estimated at 84% in the UK (Cancer research UK website: https://www.cancerresearchuk.org/health-professional/cancer-statistics/statistics-by-cancer-type/prostate-cancer#heading-One). Following diagnosis, the 1-year survival rate is estimated at 96.6%, the 5 years survival rate at 86.6% and the 10 years survival rate at 77.6%. The age range at which the survival rate is the highest is between 60 to 69 years old with 94% and drops to 66% for 80-99 years old. In the last 40 years, there has been an improvement of the overall survival (OS) rate from 25 to 84%. The survival rate depends on the stage of the disease at diagnosis, going from 100% for stage I to 30% for stage IV. In Europe, the mean age-standardised 5-year survival rate is at 83.4%. It is the highest between 55-64 years of age and the lowest from 85 years of age (De Angelis, et al. 2014). In African Americans, the 5-year survival is nearly 100% for early diagnosis (localised disease) but drops to 32.6% for late diagnosis (distant metastases) (Taitt 2018).

In 2012, almost 70% of all prostate cancers were diagnosed in developed regions. Indeed, the incidence rate is the highest in Australia/New Zealand, followed by Northern America, Western Europe, Northern Europe, the Caribbean, Southern Africa, Southern America and then Asia where the incidence rate is relatively low. The variation for prostate cancer incidence worldwide is partially due to more frequent diagnosis using Prostate Specific Antigen (PSA) testing in developed regions, with 23-42% of new PCa cases in Europe and the United States which could be due to over diagnosis (Quinn and Babb 2002). There is less variation in mortality rates than in incidence rates, with a higher number of deaths due to PCa in less developed regions. The mortality rate is high in populations of African descent, intermediate in the Americas and Oceania and low in Asia (Ferlay, et al. 2015). According to Taitt it seems clear that men of African descent outside the African continent are at higher risk of developing PCa, although it is less evident for Black men living in Africa, suggesting that environmental factors could be implicated (Taitt 2018). The same was observed for Asian men. The access to diagnostic, health-care services and recommendations for PCa testing are factors than vary depending on countries, which increases the fluctuations in

incidence and mortality rates worldwide. Overall, the incidence and mortality rates are decreasing in developed regions but incidence seem to be increasing worldwide.

The difference in incidence rate across racial and ethnic groups is also due to genetic factors. Multiple PCa genetic risk loci identified in a genome-wide association study in men of European and Asian descent allowed to identify variants that are more common in men of African than European descent (Haiman, et al. 2011).

Hassanipour-Azgomi *et al*. conducted a study assessing the incidence and mortality of PCa and their relationship with the Human Development Index (life expectancy at birth, mean years of schooling and income level per person of the population) worldwide (Hassanipour-Azgomi, et al. 2018). They concluded that there was a positive correlation between the Standardized Incidence Rate of PCa and the Human Development Index and a negative correlation between the standardized mortality rate and the Human Development Index. Despite the high incidence rate, the mortality rate is decreasing for PCa patients with increasing levels of Human Development Index, due to the improvement of diagnosis and efficacy of treatment.

Family history of PCa has been shown to impact the risk of PCa. There is a two to three-fold increased risk of PCa for men whose brother or father have had PCa and a nine fold increase in the case of both having had PCa (Hemminki and Czene 2002). Another study associated the risk of dying from PCa with family history of PCa. In that case, the risk of death from PCa is two times higher for a man whose brother or father died of PCa (Brandt, et al. 2012). More than 105 prostate cancer risk loci explain about one-third of the heritability (Hoffmann, et al. 2015). However, the majority of identified germline risk loci are not strongly associated with lethal or nonlethal prostate cancer (Shui, et al. 2014), suggesting that inherited factors may be involved early in prostate carcinogenesis (Pernar, et al. 2018).

PCa incidence is highly related to age with the highest incidence rates occurring in older men, with a peak in the 75-79 age group (Cancer research UK website: https://www.cancerresearchuk.org/health-professional/cancer-statistics/statistics-by-cancer-type/prostate-cancer#heading-One). The implementation of PSA screening in the U.S. led to a shift in the average age at PCa diagnosis, which is now 66 years of age (Howlader, et al. 2016). By the age of 79, the probability to develop PCa is 1 in 14 for men worldwide, 1 in 47 for men in low to middle sociodemographic index countries and 1 in 6 for men in high sociodemographic index countries (Fitzmaurice, et al. 2017). Although PCa occurs mainly in older men, 10% of men diagnosed with PCa in the U.S. in 2012 were 55 years old or less. This early onset PCa may have distinct etiology and clinical phenotype (Salinas, et al. 2014).

Pernar *et al.* have summarized in a comprehensive review the risk factors for advanced and fatal PCa specifically (Pernar, et al. 2018).

- ➤ Obesity, weight gain and waist circumference. Obesity was shown to be associated with a higher risk of PCa recurrence and mortality. Weight gain was also linked to higher risk of recurrence after a prostatectomy. Waist circumference was suggested to be positively associated with the risk of advanced PCa.
- ➤ Taller height probably increases the risk of PCa, in particular the risk advanced PCa.
- ➤ Smoking was positively associated with increased risk of death from PCa and of advanced PCa.
- ➤ Calcium and dairy products have both been positively associated with PCa and in some studies with advanced or lethal PCa.

On the contrary, some factors have been identified as protective against PCa.

- ➤ Fish consumption has been linked with decreased PCa mortality and recurrence.
- ➤ Coffee intake has shown no association with PCa but some studies showed an inverse association with risk of advanced PCa.
- ➤ Lycopene and tomatoes. Lycopene is a strong anti-oxidant and is present in tomatoes. Higher consumption of tomato-based products and higher concentrations of lycopene in the serum/plasma were linked to a lower risk of PCa and possibly a lower risk of PCa progression.
- ➤ Cholesterol and statins. Cholesterol was shown to increase the risk of PCa. Inversely, the use of statins was negatively associated with lethal PCa. Moreover, the use of statins during Androgen Deprivation Therapy (ADT) showed a slower progression of the disease (Van Rompay, et al. 2019)
- ➤ Physical activity was linked to a lower risk of developing advanced and aggressive PCa. For men diagnosed with PCa, physical activity was shown to improve the survival and to decrease the progression of the disease.

1.1.2.Pathophysiology

The prostate is an exocrine gland composed of three zones: peripheral (70% of total volume), central (25%) and transition (5%) zones. The majority of PCa cases develop from the peripheral zone (75%), 20% develop from the transitional zone, while 5% arise from the central zone (McNeal 1988). Most PCa cases are adenocarcinomas as they are derived from the prostate epithelium (Nelson, et al. 2003). Although the exact aetiology of prostate cancer is unknown, literature supports the hypothesis that both genetic and environmental factors are responsible (Kolonel, et al. 2004). Human studies indicate that inflammation might have a role in the development of PCa (De Marzo,

et al. 2007), and in particular in the progression from localized to metastatic disease (Ammirante, et al. 2010; Luo, et al. 2007).

Several molecular mechanisms, involved in infection or inflammation, lead to a proliferative inflammatory atrophy, then leading to prostatic intraepithelial neoplasia, to localised PCa, to metastatic PCa and finally to Androgen-independent PCa (Nelson, et al. 2003).

PCa is usually a slow developing cancer, offering a large therapeutic window. The 5-year survival rate for patients diagnosed with a localized or regional disease is nearly 100%, however, it decreases to 28% for patients with a metastatic disease at diagnosis (Siegel, et al. 2015).

1.1.3.Screening and diagnostic

Early stages PCa are usually asymptomatic, while locally advanced and metastatic PCa are symptomatic. Specific tests are therefore needed for diagnosis, as early diseases are potentially curable.

Prostate cancer is usually diagnosed by a PSA blood test and a digital rectal exam (DRE), followed by a transrectal ultrasonography (TRUS). More than 60% of PCas are diagnosed in asymptomatic patients with normal DRE and elevated PSA (Descotes 2019).

Since the 1990s, PSA testing has become the most common screening tool used to diagnose PCa (Borley and Feneley 2009). PSA is a serine protease that was first purified in 1979 (Wang, et al. 1979). It is produced by the prostatic epithelium and the periurethral glands. Its expression is prostate-specific but not cancer specific as it is present in normal prostate tissue. As a result, its expression increases with age, concurrently with the volume of the prostate. The introduction of PSA screening is responsible for the increased incidence of PCa due to over diagnosis (Telesca, et al. 2008).

PSA has a low sensitivity, with 15% of men who have a PSA value between 0 and 4 ng/ml, having PCa and 15% of those are high Gleason score (Thompson, et al. 2004; Lucia, et al. 2008).

Although PSA testing reduced the mortality due to PCa (Shroder, et al. 2014), the resulting over diagnosis leads to unnecessary biopsies (Loeb, et al. 2014).

The use of PSA screening led to diagnosis at an earlier stage of the disease because of the lead time (time from screen detection to clinical diagnosis) of PCa, estimated from 3 to 10 years (Etzioni, et al. 2008).

Due to the controversial PSA threshold to recommend a biopsy, new PSA-derived methods have been developed (Descotes., 2019): 1) implementation of age-adjusted PSA thresholds, 2) calculation of the ratio free-PSA to total-PSA, 3) calculation of the PSA density (total-PSA divided by the total prostate volume) and 4) the PSA velocity/PSA doubling time, which considers the increase of total-PSA over time.

Along with the PSA test, the DRE is one of the primary tests for the diagnosis of PCa. This test allows to detect non-PSA secreting tumours (Borley and Feneley 2009). However, it fails to detect many cancers and detects them at more advanced stages, in comparison to the PSA test (Smith and Catalona 1995). The European randomized study of screening for prostate cancer (ERSPC), Rotterdam, reported that the positive predictive value of an abnormal DRE, alongside an elevated PSA value, for detecting the presence of PCa was 48.6% in the first round of screening, decreasing to 29.9% and 21.2% in the second and third rounds, respectively (Gosselaar, et al. 2008). Nonetheless, there was a significant increase of risk of PCa with a Gleason score superior than 7 in men with a suspicious DRE in each screening rounds.

Once there is suspicion of PCa, a TRUS-guided biopsy is performed. TRUS procures imaging of the prostate and seminal vesicles.

This technique was demonstrated to be superior to digitally directed biopsies (Hodge, et al. 1989). However, TRUS-guided biopsies give 15 to 46% of false negatives and under-grade the Gleason score up to 38% in comparison to the result at radical prostatectomy (Kvale, et al. 2009). TRUS biopsy can lead to error such as sampling errors, missing a high-grade cancer or over diagnosing a low-grade cancer (Descotes, et al. 2019). To avoid these mistakes, improved TRUS biopsy techniques have been developed using Magnetic Resonance Imaging (MRI) in order to localise PCa within the prostate gland more accurately. Moreover, transperineal template prostate biopsy (TPTPB) was shown to increase the PCa detection rate in comparison to TRUS biopsies in biopsy naive patients with PSA <20ng/mL (Nafie, et al. 2014).

1.1.4. Classification of prostate cancer: grades and stages

The Gleason score, described by Gleason and Mellinger in 1974, is the most commonly used grading system (Gleason and Mellinger 1974). It is based on the histology of carcinoma cells in Haematoxylin and eosin stained sections conferring a score from 1 to 5 (least to most aggressive). Two grades are assigned for each patient, the first one describing the largest tumour area and the second one describing the second largest tumour area. Both grades are added up to obtain a histologic score ranging from 2 to 10 (Figure 1.1) (Humphrey 2004).
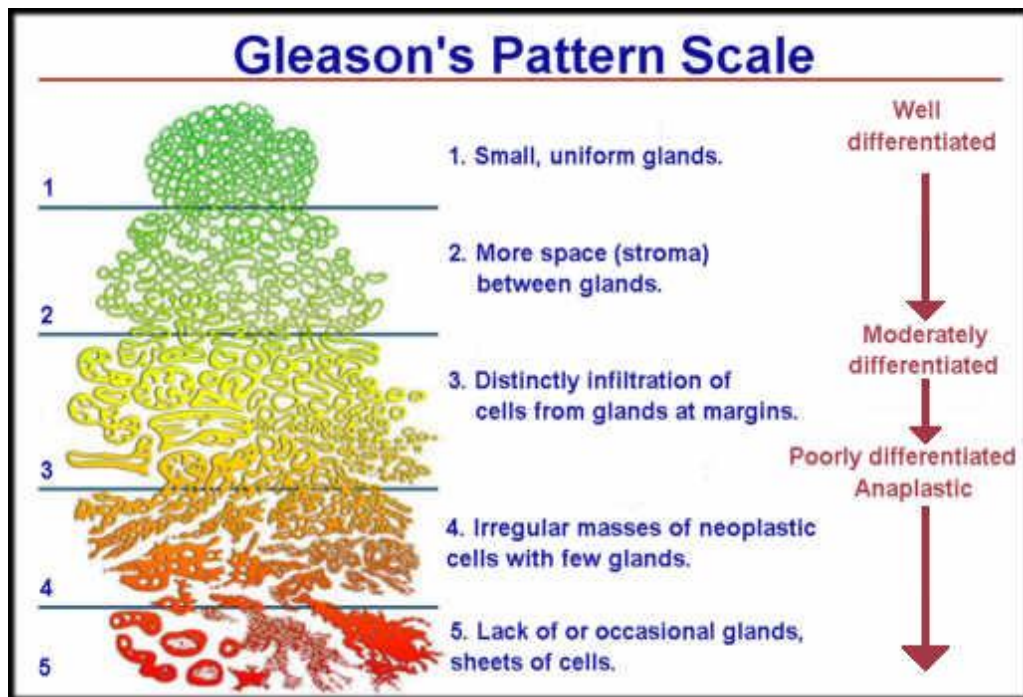
Figure 1.1: Gleason's pattern scale (adapted from Humphrey 2004) (Reprinted by permission from [Springer Nature Customer Service Centre GmbH]: [Springer Nature] [MODERN PATHOLOGY] [GLEASON GRADING AND PROGNOSTIC FACTORS IN CARCINOMA OF THE PROSTATE, HUMPHREY), [COPYRIGHT] (2004))

The Gleason grading system evolved following two meetings organised by the international Society of Urologic Pathology in 2005 and 2014, resulting into a new Grade Group system which was adopted by the 2016 World Health Organization classification of tumours of the prostate (Chen and Zhou 2016).

According to the new Grade Group system, Gleason Scores range from 6-10. A score of 6 describes a cancer that will progress slowly, while a score of 7 suggests an intermediate risk for aggressive cancer. However, a score of 7 can be divided into two grade groups: a 3+4 suggests a better prognostic than a 4+3. A score ≥ 8 suggests a high risk for aggressive cancer that will metastasize rapidly.

The Gleason grade is related to clinical end points such as the clinical stage, the PSA value, the progression to metastatic disease, the response to different therapies and the survival (Humphrey 2004).

The Tumour-Node-Metastasis (TNM) system is used to determine the pathological stage of the disease. The American Joint Committee on Cancer published in 2017 the eighth edition Cancer staging manual (Buyyounouski, et al. 2017). Staging of PCa is necessary to categorise the severity of the disease, estimate the prognosis and recommend treatment. The vast majority of prostate cancer, approximately 95%, are clinically localized to the prostate without definite evidence of metastasis. The T category, referring to the size and extent of the primary tumour, is based on physical examination, imaging, endoscopy, biopsy and biochemical tests. The N category, indicating

if the tumour has spread to the lymph nodes, is evaluated via clinical examination and imaging. Finally, the M category, indicative of the extent of the metastases, is based on physical examination, imaging, skeletal studies and biochemical tests (Sobin and Witterkind 2002).

The D'amico classification, introduced in 1999, divides patients with localized disease into three categories: low, intermediate or high risk (D'amico, et al. 1999). It combines the PSA value, the Gleason score, and the TNM stage (table 1.1: Risk stratification for clinically localized cancer).

Table 1.1: Risk stratification for clinically localized cancer (adapted from https://www.cancernetwork.com/cancer-management/prostate-cancer/page/0/1)

	PSA value (ng/mL)		Highest biopsy Gleason score		Clinical stage
Low risk	<10	and	≤6	and	T1c or T2a
Intermediate risk	≥10 but <20	or	7	or	T2b
High risk	≥20	or	≥8	or	T2c/T3

1.1.5. Current treatments

Treatments options for PCa patients depend on the stage of the disease.

The treatments available for patients diagnosed with localised disease include active surveillance, external beam radiotherapy and radical prostatectomy (surgery). Active surveillance, which consists in monitoring the evolution of the disease using PSA testing, DRE and a confirmatory biopsy, is recommended for low risk patients (Gleason 6, grade I), to provide better quality of life (Witherspoon, et al. 2019). The possibility of managing some intermediate risk patients (Gleason 7 (3+4), grade II) through active surveillance is considered but controversial (Loeb, et al. 2019).

According to a 2010 study by Schymura *et al.*, 39.7% of patients with localized PCa undergo radical prostatectomy, 31.4% receive radiation therapy, 10.3% receive hormone therapy and 18.6% are managed with active surveillance (Schymura, et al. 2010). The two major side effects following radiotherapy and prostatectomy are urinary incontinence and erectile dysfunction (Potosky, et al. 2004). Ultimately, one third of these patients develop recurrence or metastasis and require Androgen Deprivation Therapy (ADT) (McNeel, et al. 2016). ADT is obtained by surgical castration or chemical castration in order to suppress androgen production (Velcheti, et al. 2008). However, ADT has a limited period of efficacy as patients eventually become resistant and develop Castrate Resistant prostate cancer (CRPC) which requires secondary hormonal interventions, chemotherapy or other treatments (De Maeseneer, et al. 2015).

Mechanisms of hormone resistance are classified into three categories: DNA-based alterations in the androgen receptor (AR) gene, AR-growth factors cross-talk and activation of alternative pathways of survival and proliferation (Velcheti, et al. 2008).

A recent study characterised the involvement of IL-23-secreting Myeloid-Derived Suppressor Cells (MDSCs) in the development of CRPC, thereby establishing a role of immunosuppression in the pathophysiology of CRPC (Calcinotto, et al. 2018).

Treatments for mCRPC include androgen signalling inhibitors (Enzalutamide and Abiraterone), chemotherapy (Carbazitaxel and Docetaxel), the radiopharmaceutical agent radium-223 and Sipuleucel-T vaccine (Figure 1.2) (Kirby, et al. 2011).
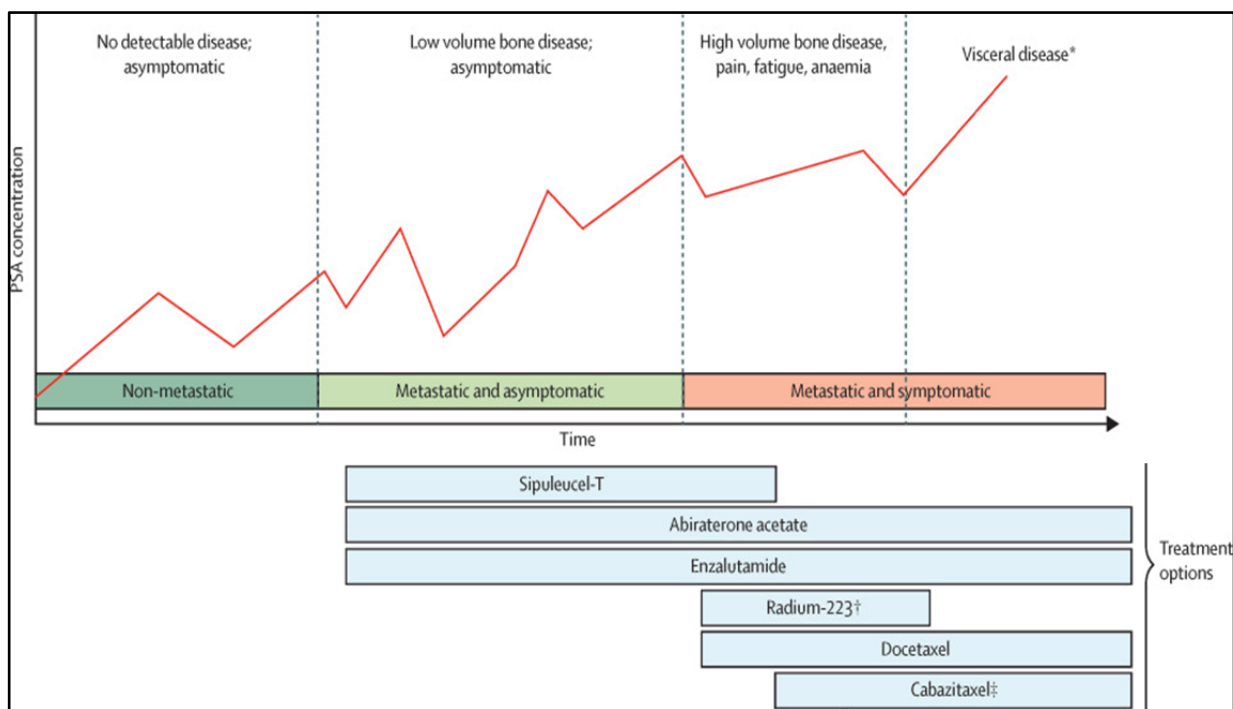
Figure 1.2: Typical progression of metastatic castration-resistant prostate cancer (Reprinted from The Lancet Oncology, Volume 16, Issue 6, Lorente, et al., Sequencing of agents in castration-resistant prostate cancer, pages e279-e292, Copyright (2015), with permission from Elsevier.)

The survival benefit of Docetaxel was confirmed in two 2004 trials: the TAX-327 and the SWOG-99-16, which reported an improved median OS of 2.9 months and 1.9 months respectively (Berthold, et al. 2008; Petrylak, et al. 2004). Docetaxel in combination with prednisone was established as the standard of care. Prednisone is a corticosteroid providing both palliative benefits and anti-tumour responses in PCa (Teply, et al. 2016).

Carbazitaxel, another chemotherapy, was approved in 2010 for post-docetaxel patients. The TROPIC trial showed an improved median OS of 2.4 months (Bahl, et al. 2013).

Enzalutamide and abiraterone acetate are used in chemotherapy-naive and docetaxel-treated mCRPC patients (Lorente, et al. 2015). Enzalutamide, FDA-approved in 2012, is a second-generation androgen that blocks the AR at three levels: 1) binding to androgens to inhibit their binding to ARs, 2) inhibition of nuclear translocation of ARs and 3) inhibition of binding of ARs to chromosomal DNA (Saad 2013). It showed an improved median OS of 4.8 months over placebo in the phase 3 AFFIRM trial (Scher, et al. 2012). Abiraterone acetate, approved in 2011, suppresses the synthesis of

androgen through inhibition of the cytochrome p450 17A1 (Richards, et al. 2012). An improved median OS of 4.6 months was observed in the COU-AA-301 trial between abiraterone acetate and prednisone or prednisone alone (Fizazi, et al. 2012).

The radiopharmaceutical agent radium-223 is recommended for CRPC patients with bone metastasis but no visceral metastasis (Lorente, et al. 2015). It emits high energy α-particles to break double-strand DNA in increased bone turn-over areas. The ALSYMPCA trial reported an improved median OS of 5.1 months (Parker, et al. 2013).

Sipuleucel-T therapeutic vaccine, approved in 2010, is recommended in early stage CRPC. It is based on the *in vitro* stimulation of patient's Peripheral Blood Mononuclear Cells (PBMCs) with a fusion protein composed of Prostatic Acid Phosphatase (PAP) and Granulocyte/Monocyte Colony Stimulating Factor (GM-CSF), followed by the re-infusion of these cells into the patients. Its efficacy was demonstrated in the phase 3 IMPACT trial which reported an improved median OS of 4.1 months (Kantoff, et al. 2010). However, although patients had a Gleason score ≤7, the vaccine had no effect on the time to disease progression.

Overall, between 10% and 20% of prostate cancer patients progress to CRPC within 5 years following diagnosis, a state for which the treatments options are limited and not curative, with a median survival from diagnosis of 14 months (Kirby, et al. 2011). Indeed, patients ultimately developed resistance to AR-targeted therapies and to taxane-based chemotherapy (Galletti, et al. 2017).
New therapies are therefore needed for the treatment of mCRPC patients.
As demonstrated with Sipuleucel-T vaccine, immunotherapies are promising for the treatment of PCa. There is currently an abundance of ongoing clinical trials assessing immunotherapies for the treatment of PCa, as stand-alone, in combination with other immunotherapies or in combination with conventional therapies (McNeel, et al. 2016).

1.2. The immune system
Understanding of the immune system and its cellular components is necessary to comprehend the principle of cancer immunotherapy.

1.2.1. Overview of the immune system
The immune system is divided in two responses: the innate and the adaptive response (Parkin and Cohen 2001).

The innate response is the first line of defence against pathogens and foreign molecules, it is rapidly put into place and not antigen-specific. The cells providing this first line of defence are granulocytes (neutrophils, eosinophils and basophils), monocytes, macrophages, natural killer (NK) cells, NKT cells and γδ T-cells.

NK cells are lymphocytes capable of recognizing and lyse abnormal cells such as virus-infected cells or tumour cells via three mechanisms (Abel, et al. 2018). The first one involves the binding of their own immunoglobulin receptor (FcR) to antibodies on the surface of target cells, called Antibody-Dependant Cellular Cytotoxicity (ADCC) (Wang, et al. 2015). The other mechanism depends on the recognition of MHC class-I molecule on the surface of target cells (Abel, et al. 2018). The absence of MHC class-I molecules on target cells leads to the secretion of perforins which creates pores in the membrane of the target cells, through which granzymes are injected to induce the apoptosis of the cell. The third one relies on the expression of ligands for death receptor: Fas-L and Tumour Necrosis Factor (TNF)-Related Apoptosis Inducing Ligand (TRAIL), inducing the apoptosis of the target cell.

The adaptive response is much more complex, slower to develop and is antigen-specific (Chaplin 2010). T and B lymphocytes recognise antigens via their T-Cell Receptor (TCR) and B-Cell Receptor, respectively. T and B cells derive from progenitor cells in the bone marrow. While B-cells remain in the bone marrow until becoming mature, T-cells migrate to the thymus as thymocytes.

1.2.2.T-cells development

TCRs are the product of a process of random rearrangement and splicing of multiple DNA segments coding for the areas of the receptor responsible for the antigen binding, which happens before exposure to the antigen (Kumar, et al. 2018). This process leads to a naive repertoire of over 10^8 TCRs (Arstila, et al. 1999). The TCR molecule is a heterodimer composed either of an α and a β chain, each containing a constant and a variable domain or composed of γ and δ chains (~5% of T-cells) (Koch and Radtke 2011). The TCR forms a complex with the CD3 molecule and binds to 8 to 10mer peptides which are derived from previously broken-down proteins by intracellular processing. Following TCR rearrangement, thymocytes migrate to the thymus for maturation and selection processes (Koch and Radtke 2011). Positive selection consists of selection of TCRs recognizing self-MHC molecule with peptide with sufficient affinity. However, TCRs that bind too strongly to self-MHC molecule with peptide will undergo apoptosis (negative selection). At that stage, T-cells express both CD4 and CD8 co-receptors and will lose one of them before exiting the thymus and circulating in the periphery.

Naive T-cells enter lymph nodes to encounter Antigen Presenting Cells (APCs) which will present antigens at the surface of Major Histocompatibility Complex (MHC) class-I and class-II molecules (Gaudino and Kumar 2019). Different cell types can hold the function of APCs. Dendritic cells (DCs) are "professional" APCs and are essential for activating naive T-cells, but macrophages and B-cells can also present antigens at their surface.

1.2.3.MHC and antigen presentation

There are two types of MHC molecules: class-I and class-II, each composed of 2 chains and four domains (Figure 1.3) (Janeway, et al. 2001). MHC class-I molecules are expressed by almost all nucleated cells of an organism and present at their surface endogenous antigens (normal, viral or tumour proteins) to CD8$^+$ T-cells. They are composed of 3 α domains and one β2-microglobulin domain.

MHC class-II molecules are only expressed by APCs and present at their surface exogenous antigens, taken up by endocytosis, to CD4$^+$ T-cells. There are composed of 2 α domains and 2 β domains.
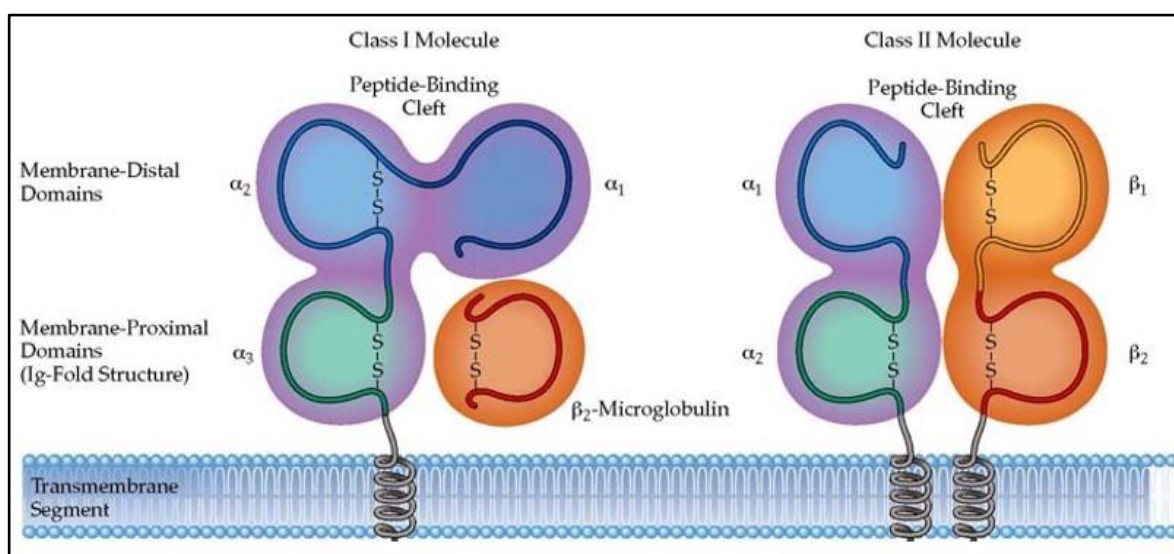
Figure 1.3 Structure of MHC class-I and MHC class-II molecules (adapted from https://www.onlinebiologynotes.com/major-histocompatibility-complex-mhc-structure-types-and-functions/)

In both cases, the antigen processing differs (Blum, et al. 2013).

Briefly, the pathway of endogenous antigen begins with self- (mutated, overexpressed or misfolded in the case of a tumour cell) or viral proteins produced and released into the cytoplasm where they are digested by the proteasome (a group of enzymes specialised in digesting ubiquitinated proteins). The peptides produced are then chaperoned to the endoplasmic reticulum where they enter with the help of the Transporter associated with Antigen Processing (TAP) systems. Peptide/MHC complexes then detach from the TAP transporter to be delivered to the cell surface in order to be available for CD8 TCR recognition.

In the case of exogenous antigens, protein antigens enter the cell by endocytosis and are digested into peptides fragments in acidic endosomes. Acidic endosomes then fuse with MHC class-II molecules containing endosomes which will bind to the antigen peptide. Finally, the complex migrates to the cell surface for CD4 TCR recognition.

1.2.4.T-cell priming and activation

T-cells are primed by APCs in secondary lymphoid organs such as lymph nodes or spleens. The activation of T-cells is based on three signals (Condotta and Richer 2017). The first signal is initiated by the binding of the appropriate peptide-MHC complex to the TCR of the T-cell. This binding induces the phosphorylation of the CD3 complex and the transmission of signals through downstream pathways (Huse 2009). The second signal depends on the binding of ligands such as CD80 (B7-1) and CD86 (B7-2), expressed on the surface of DCs, to the activating co-receptor CD28 (Chen, et al. 2013). DCs express high levels of CD80 and CD86, rendering them highly capable of activating naive T-cells (Lim, et al. 2012). The third signal rely upon the secretion of cytokines by DCs to guide the T-cell response (De Jong, et al. 2005). These 3 signals lead to the division and clonal expansion of the primed T-cell. Effector cells then migrate to the disease site through the attraction of organ-specific adhesion molecules (Sallusto, et al. 1999), where they can recognise target cells. A portion of these effector cells will become memory cells, characterised by a long lifespan and a fast reaction upon subsequent exposure to their antigen (Omilusik and Goldrath 2017).

Since the discovery of the CD28 to CD80/CD86 interaction, many other co-receptors/ligands were discovered (Figure 1.4) (Chen, et al. 2013). Depending on their impact on T-cells, they are divided into co-stimulatory and co-inhibitory receptors. The first one leading to immunity and the second to tolerance by inducing T-cell anergy or exhaustion of the T-cell.
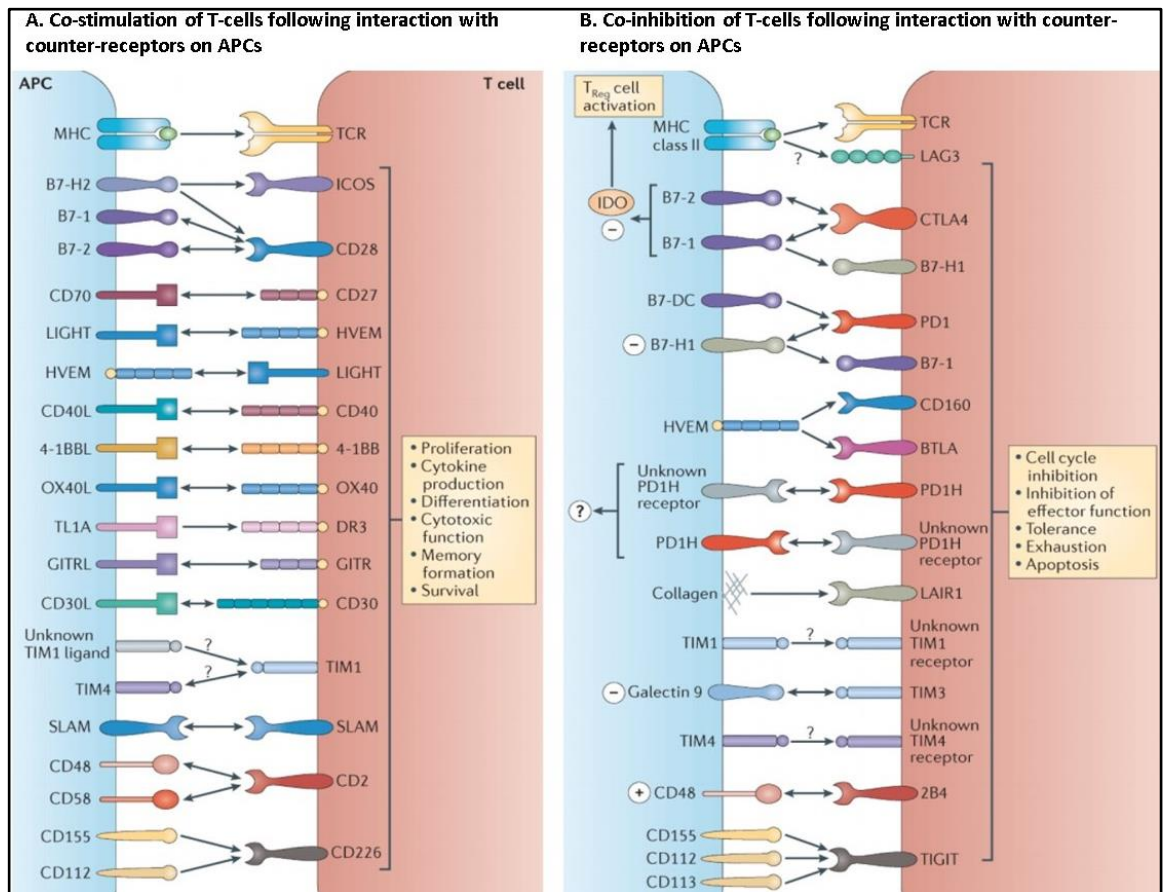
Figure 1.4: Co-signalling interactions in T cells (Reprinted by permission from [Springer Nature Customer Service Centre GmbH]: [Springer Nature] [NATURE REVIEWS IMMUNOLOGY] [MOLECULAR MECHANISMS OF T CELL CO-STIMULATION AND CO-INHIBITION, CHEN AND FLIES), [COPYRIGHT] (2013))

1.2.5. Role of CD4^{+} and CD8^{+} T-cells

As mentioned earlier, T-cells are divided into CD4^{+}, helper, and CD8^{+}, cytotoxic, T-cells, each exhibiting distinctive roles.

1.2.5.1. CD4^{+} T-cells

CD4^{+} T-cells are involved in infectious diseases, autoimmune diseases, asthma, allergic responses and tumour immunity. They are defined by their role of helping other immune cells such as B cells, CD8^{+} T-cells or macrophages. They are highly plastic cells that can differentiate into several subsets. Each subset is defined by the cytokines and transcription factors inducing them and the cytokine pattern they secrete following TCR activation. Caza *et al.* describes 8 subsets: Th1, Th2, Th9, Th17, Th22, Th25, follicular T-cells and regulatory T- cells (Tregs) (Caza, et al. 2015). Among other roles, Th1 cells have a role in the clearance of tumours cells. On the other hand, Tregs have an inhibitory role on other T-cells, such as cytotoxic CD8^{+} T-cells.

1.2.5.2. CD8^{+} T-cells

CD8^{+} T-cells are characterised by their direct cytotoxicity against cells presenting their specific antigen onto MHC class-I molecules. They induce cytotoxicity by two mechanisms (Martinez-Lostao,

et al. 2015). One is through perforation of the target cell membrane with perforin and injection of cytotoxic granzyme molecules into its cytoplasm leading to apoptosis. The other mechanism induces apoptosis via the expression of death ligands: FAS-ligand and TRAIL. The expression of FAS-L and TRAIL at the surface of CD8$^+$ T-cells leads to their binding to FAS and TRAIL receptors on the surface of the target cell. Both mechanisms involve caspases to induce apoptosis. CD8$^+$ T-cells are classified into different subsets according to their capacity to proliferate and their differentiation state (Golubovskaya, et al. 2017). Subsequent to priming by DCs, naive T-cells become T stem cell memory cells, then T central memory cells, T effector memory cells and finally, T effector cells. The loss of the memory function is inversely proportional to the gain of effector function. Effector CD8$^+$ T-cell, also called Cytotoxic T Lymphocyte (CTL), are characterised by the expression of IFN-γ, TNF-α, perforin and granzyme (Zhang, et al. 2011).

1.3. Cancer immunology

The concept of using the immune system of a patient against their own tumour is recent as it relied on the acceptance by the scientific community that the immune system is able to distinguish transformed from normal cells and to eradicate tumours. The concept of immunosurveillance evolved slowly since the beginning of the past century. Indeed, Paul Ehrlich formulated the hypothesis that the immune system could prevent transformed cells from developing into tumors more than a century ago (Ehrlich 1909). The hypothesis of immunological surveillance was proposed by Burnet (Burnet 1970) on the basis of previous theories formulated both by Burnet and Thomas from the year 1957. Over the years, several arguable experiments contradicted this hypothesis leading to its dismissal. Stutman demonstrated that athymic nude mice, lacking T-cells, developed as many spontaneous or methylcholantrene-induced tumors than control mice, suggesting no active role of thymus-dependent immunity against tumour growth (Stuman 1974).

The regained interest for the immunological surveillance hypothesis followed findings demonstrating the implication of both IFNγ and perforin molecules and of lymphocytes in controlling tumour growth (Street, et al. 2001; Russel and Ley 2002).

These findings led to the concept of immune-editing.

1.3.1. Concept of cancer immuno-editing

In 2002, Dunn described the concept of immuno-editing (Dunn, et al. 2002). This concept is based on three consecutive processes: elimination, equilibrium and escape.

The elimination process incorporates the concept of immunological surveillance. Briefly, the tumour causes an inflammation leading to the recruitment firstly of innate immune cells such as NK, NKT, γδ T-cells, macrophages and DCs. NK, NKT and γδ T-cells secrete IFNγ and induce apoptosis in tumour cells. DCs ingest tumours debris and migrate to the lymph nodes to present tumour

antigens to CD4^{+} and CD8^{+} specific T-cells which then migrate to the tumour site where CD8^{+} T-cells can lyse tumour cells in an antigen-specific manner.

The equilibrium process relies on the hypothesis that non-immunogenic tumour cells have been selected during the elimination process, rendering them "invisible" to the immune system. This process can last for years as it relies on the balance between the capacity of immune cells to kill tumours cells and the capacity of tumours cells to resist to the immune system's cytotoxic mechanisms.

Finally, the escape process consists in the uncontrollable proliferation of resistant tumour cells variants leading to tumour growth and development of metastasis.

This concept holds the idea that the immune system has two contradictory roles in cancer: it destroys tumour cells, but by doing so, it selects for immune-resistant tumour cells.

1.3.2. Immune tolerance and cancer

Immune tolerance aims at avoiding auto-immunity and is classified into two categories: central and peripheral tolerance. Central tolerance consists in the destruction of self-reactive T-cells during the negative selection in the thymus (Kyewski, et al. 2006). Self-reactive cells that escaped the central tolerance process are eliminated in the periphery by peripheral tolerance, which is regulated via two different types of mechanisms (Nurieva, et al. 2013). The first mechanism is intrinsic to the T-cell: induction of anergy and apoptosis. The second mechanism is controlled by immunosuppressive immune cells such as Tregs and tolerogenic DCs.

Both categories of tolerance have different implications in cancer. Central tolerance renders the detection of Tumour Associated Antigen (TAA) difficult as most T-cell clones carrying TCRs specific for a TAA would have been depleted. Therapies such as vaccination aim at stimulating TAA-specific T-cell clones that might have escaped central tolerance. On the other hand, peripheral tolerance mechanisms are regulated by molecules and cells at the tumour site that therapies aim to neutralize with treatments such as Immune Checkpoint Blockade (ICB). These mechanisms will be described in details in the next section.

1.3.3. Tumour microenvironment

Several factors influence the induction of immunity or tolerance in a tumour: tumour genetics/epigenetics, host genetics, the microbiome and the tumour microenvironment (TME).

The gut microbiome affects oncogenesis (Yoshimoto, et al. 2013) (Dapito, et al. 2012), tumor progression, as well as the response to anti-cancer therapy (Zitvogel, et al. 2015). For instance, some species of intestinal bacteria were shown to modulates the anticancer immune effects of cyclophosphamide chemotherapy by generating specific T helper 17 cells and memory Th1 immune responses (Viaud, et al. 2013). Moreover, abnormal gut microbiome composition can lead to

resistance to ICB, such as anti PD-1/PD-L1 antibodies, which lead to the possibility of improving ICB efficacy through Fecal microbiota transplantation (Routy, et al. 2018).

As discussed previously, although the immune system develops an anti-tumour immunity, several immuno-suppressive mechanisms are put in place within the micro-environment.

Chen *et al.* describes three types of immune profiles within tumours from patients (Chen, et al. 2017). The first type is called immune-inflamed as it is characterized by the presence of T-cells, myeloid cells and monocytic cells in the tumour parenchyma. The second profile, named immune-excluded, is characterized by the presence of immune cells contained in the stroma, unable to enter the tumour. Finally, the profile characterised by the rarity of T-cells is called immune-desert. This phenotype suggests the absence of tumour-specific T-cells. The last two phenotypes are considered as non-inflamed tumours.

The TME is defined by the type of cytokines and cells (immune and non-immune) present in a tumour. The remaining of this section will focus on describing these elements, to understand the mechanisms put in place to counteract the establishment of an anti-tumour immune response or the efficacy of a pre-existing one.

1.3.3.1. Direct immunosuppressive mechanisms of tumour cells

Tumour cells employ various mechanisms to escape the immune system and induce immune tolerance. To avoid T-cells recognition, antigen presentation is downregulated by antigen loss, downregulation of MHC class-I molecules and of antigen-processing machineries such as TAP molecules (Marincola, et al. 2000). Mutations in death receptor signalling pathways (FAS and TRAIL) (Takahashi, et al. 2006 and Shin, et al. 2001, respectively) and over-expression of anti-apoptotic molecules render tumour cells less sensitive to lymphocytes killing (Hinz, et al. 2000).

Tumour cells induce T-cell anergy by expression of ligands to inhibitory receptors expressed by lymphocytes (Figure 1.5), such as Programmed death ligand 1 (PD-L1) which binds to Programmed death 1 (PD-1) (Dong, et al. 2002; Yamamoto, et al. 2008), galectin-9 which binds to Tim-3 (Zhou, et al. 2018), galectin-1 (Liu, et al. 2005), HLA-G (Agaugue, et al. 2011) or HLA-E (Derré, et al. 2006). Galectin-1 inhibits the activation, the proliferation and the secretion of pro-inflammatory cytokines by T-cells, and induces the apoptosis of activated T-cells (Liu, et al. 2005).

HLA-G induces MDSCs, inhibits T-cells and promotes the pro-tumorigenic Th2 profile (Agauge, et al. 2011). It also inhibits NK cells through the Human inhibitory receptors Ig-Like Transcript 2 (ILT2) receptor (Favier, et al. 2010).

HLA-E is induced by IFNγ and inhibits NK cells and CTL via binding to NKG2A inhibitory receptor (Derré, et al. 2006).

Other mechanisms employed by tumour cells consists in the secretion of immunosuppressive factors that recruit or promote the differentiation and expansion of immunosuppressive cells.

1.3.3.2. Immunosuppressive soluble factors

A number of immunosuppressive chemokines and cytokines are produced by tumour cells within the tumour environment. The mechanism of action of some of the critical ones are described below.

Tumour Growth Factor-β (TGF-β) inhibits T-cell priming and infiltration (Mariathasan, et al. 2018), and suppresses effector cell cytotoxicity by inhibiting the expression of perforin, granzyme A, granzyme B, Fas ligand, and IFNγ (Thomas and Massague 2005).

Vascular Endothelial Growth Factor (VEGF) promotes the angiogenesis. It also inhibits the effector function and the proliferation of T-cells via enhancing the expression of PD-1, CTLA-4, LAG-3 and Tim-3 on T-cells, as well as PD-L1 on DCs (Khan, et al. 2018). It can inhibit DCs maturation and therefore antigen presentation to T-cells (Gabrilovich, et al. 1996).

Interleukin-10 (IL-10) is a cytokine inducing T-cell anergy via CTLA-4 inhibitory receptor (Steinbrink, et al. 2002). It inhibits the cytokine secretion by activated macrophages (Fiorentino, et al. 1991) and inducible Nitric Oxide Synthase (iNOS) production by macrophages (Dokka, et al. 2001).

Indoleamine 2,3-dioxygenase (IDO) production by stromal cells is induced by the secretion of IFNγ by CD8^{+} T-cells in the TME (Labadie, et al. 2019). IDO is also produced by MDSCs. This enzyme catalyses the conversion of tryptophan to kynurenine leading to a depletion in tryptophan (essential amino acid) responsible for inducing cell cycle arrest and anergy in T-cells. Moreover, the accumulation of kynurenine was shown to induce Tregs (Mellor, et al. 2004).

1.3.3.3. Immunosuppressive cells

Tregs are part of the T-cell compartment and are divided into natural Tregs and inducible Tregs (Sakaguchi, et al. 2008). Naive CD4^{+} T-cells can differentiate into inducible Tregs in the presence of TGF-β (Josefowicz, et al. 2012). Tregs not only suppress the functions of T-cells but also of NK cells, NKT cells, macrophages and DCs (Sakaguchi, et al. 2008). Mechanisms to induce immunosuppression include the secretion of immunosuppressive factors such as TGFβ and IL-10, IL-2 deprivation and cell-contact dependant suppression.

MDSCs derive either from monocytes or granulocytes. MDSCs immunosuppressive mechanisms are directed both on the immune system and on other non-immune elements (Ugel, et al. 2015).

MDSCs secrete TGF-β and IL-10 which promotes the formation of Tregs and blocks the activation of NK cells. MDSCs also inhibit T-cell migration to the tumour site and induce T-cells anergy by expressing markers such as PD-L1. They produce Reactive Oxygen Species (ROS) and reactive nitrogen species (RNS) thereby inhibiting the activation and proliferation of T-cells. Finally, they deplete the environment in metabolites essential to lymphocytes survival: L-arginine (due to expression of arginase) and L-tryptophan (due to expression of IDO).

Other mechanisms that promote tumour growth include the induction of angiogenesis and vasculogenesis, the promotion of metastasis and of tumour cells stemness.

Tumour Associated Macrophages (TAMs) are similar to immunosuppressive M2 polarised macrophages and differentiate from circulating monocytes. Once in the tumour they are found in areas of hypoxia and necrosis (Li, et al. 2007). Similarly to MDSCs, TAMs use immunosuppressive mechanisms directly on the immune system as well as induce angiogenesis, vasculogenesis, metastasis and tumour cells stemness (Ugel, et al. 2015). TAMs induce apoptosis in T-cells via the expression of TRAIL-R and of FAS and the secretion of TGF-β. They induce T-cell anergy via expression of PD-L1 and PD-L2, B7-1/2 (binding to CTLA-4) and production of RNS. They promote Tregs via secretion of IL-10 and TGF-β and recruit them to the TME. Finally, they also deplete lymphocytes of essential metabolites.

Cancer-associated Fibroblasts (CAFs) are part of the tumour stroma therefore promoting the proliferation of tumour cells and the creation of a metastatic niche through production of growth factors, chemotactic factors and angiogenesis factors (Li, et al. 2007). Moreover, CAFs recruit monocytes to the tumour site and induce their differentiation into PD-1 expressing TAMs (Gok Yavuz, et al. 2019).

1.3.4. T-cells in cancer

DCs can capture tumour cells debris and cross-present TAAs to T-cells, leading to the expansion of TAA-specific $CD8^+$ and $CD4^+$ T-cells (Nouri-Shirazi, et al. 2000). The presence of $CD8^+$ and $CD4^+$ T-cells in the tumour correlates with a good prognosis (Naito, et al. 1998; Galon, et al. 2006; Meng, et al. 2018).

1.3.4.1. $CD8^+$ T-cells

Activated $CD8^+$ T-cells differentiate into effector cells under cytokines such as IL-2, IL-12, IL-21 and IL-27 (Zhang, et al. 2011). As described section 1.2.5.2, anti-tumour CTL effector functions relies on both the secretion of pro-inflammatory cytokines (IFNγ and TNFα) and on the killing of tumour cells.

1.3.4.1.1. Cytotoxicity

CTLs use diverse mechanisms to lyse target cells (Martinez-Lostao, et al. 2015).

The perforin/Granzyme B pathway was described as the most efficient mechanism to kill tumour cells. Granzyme B enters target cells through perforin pores and induces cell death by different pathways. Firstly, by direct cleavage and activation of pro-apoptotic caspases 3 and 7. Secondly, by cleavage of pro-apoptotic molecule Bid (part of Bcl-2 family) inducing a cascade of event leading to the release of cytochrome C from the mitochondria. This event leads to the formation of the

apoptosome activating the pro-apoptotic caspase 9. The third mechanism involves the release of Bim (part of Bcl-2 family) to activated the mitochondrial pathway.

On the contrary, the effect of granzyme A to induce apoptosis is not as clear. Granzyme A is believed to contribute to the inflammasome leading to the caspase 1-dependant production of IL-1β. Another pathway involves mitochondrial depolarization and the production of ROS leading to DNA damage-driven cell death.

Other Granzymes molecules have been described: C, F, H, K and M. Granzymes K and M were shown to regulate the production of pro-inflammatory cytokines.

The death ligands pathway is characterised by the binding of Fas-L and TRAIL to their respective receptors (Fas and TRAIL-receptor 1 and 2) which promotes receptors oligomerization leading to the recruitment of Fas-associated death domain (FADD) and activation of the caspase 8. Caspase 8 can trigger two different apoptotic pathways: caspase 3 induces direct apoptosis while Bid triggers the mitochondrial pathway.

Apoptosis via this pathway can be inhibited and replaced by necrotic cell death. Moreover, mechanisms blocking the apoptosis can lead to TRAIL-driven proliferation and survival signals.

1.3.4.1.2.Secretion of pro-inflammatory cytokines

IFNγ is secreted by CTLs, CD4^{+} T-cells, NK cells, γδ T-cells and macrophages (Albini, et al. 2018; Xiang, et al. 2018). It promotes anti-tumour M1 rather than pro-tumour M2 macrophages. This cytokine stimulates adaptive immunity (Smyth, et al. 2002) and was shown to mediate anti-metastatic effect through inhibition of angiogenesis (Hayakawa, et al. 2002). IFNγ promotes the motility and cytotoxic functions of CTLs (Bhat, et al. 2017). It also increased the expression of MHC class-I molecules at the surface of tumour cells (Zhou 2009) rendering them more sensitive to CTL killing. IFNγ also induces the expression of the immunoproteasome (Tanaka et Kasahara, 1998), allowing the presentation of different epitopes by MHC-class I molecules at the surface of tumour cells and therefore their recognition by T-cells. Moreover, IFNγ induces the expression of MHC class-II molecules by cancer cells (Steimle, et al. 1994), which can lead to recognition and killing of tumour cells via cytotoxic CD4^{+} T-cells in an MHC-II-CD4 restricted manner (Quezada, et al. 2010) (Xie, et al. 2010).

Howerer, IFNγ also exhibits anti-inflammatory properties such as the induction of PD-L1 expression (Abiko, et al. 2015) and the production of IDO by CD8^{+} T-cells cells and MDSCs (Labadie, et al. 2019).

TNFα is produced by CTLs and macrophages and is identified both as a pro-tumour and an anti-tumour cytokine (Balkwill 2009). It can induce the activation and proliferation of T-cells or the apoptosis of highly activated effector T-cells (Mehta, et al. 2018) and is known to induce apoptosis

or necrosis of tumour cells (Wang, et al. 2008). However, its anti-tumour role is characterised by: 1) promotion of Tregs, regulatory B cells and MDSCs, 2) inhibition of CTL responses, 3) induction of PD-L1 on tumour cells and 4) induction of angiogenesis and metastasis (Bertrand, et al. 2017; Wang, et al. 2008).

IL-2 is mainly produced by antigen-simulated CD4^{+} T cells but is also produced by CD8^{+} T-cells, NK cells and DCs (Jiang, et al. 2016). It has a major role in maintaining Tregs, but also promotes the proliferation of NK cells, CD4^{+} T-cells and CTLs. Moreover, it favours the differentiation of CD8^{+} T-cells into CTLs rather than memory cells (Pipkin, et al. 2010). IL-2 also stimulates the production of IFN-γ, perforin and granzyme as well as promotes the migration of CTL to peripheral tissues (Rollings, et al. 2018). This cytokine has been used as a cancer treatment since it showed cancer regression in a patient, who remained disease free for 29 years, in 1984 (Rosenberg 2014).

1.3.4.1.3. Concept of exhaustion

Antigen persistence and sustained pro-inflammatory milieu induce the expression of co-inhibitory receptors in CTLs. This state called exhaustion is characterised by the loss of effector functions and the incapacity to develop memory cells (Figure 1.5) (Wherry and Kurachi 2015). Exhausted tumour-specific CD8^{+} T-cells have been described by many (Baitsch, et al. 2011).

Exhausted T-cells lose their capacity to proliferate, to secrete pro-inflammatory cytokines (IL-2, IFNγ, and TNFα) and to degranulate (Wherry and Kurachi 2015). Moreover, they lose their memory phenotype characterised by the expression of CD44, CD62L, CD127 or CXCR3. Finally, they co-express several inhibitory co-receptors: CTLA-4, PD-1, LAG-3, Tim-3, TIGIT, 2B4, BTLA or also CD160. It is however important to note that exhausted T-cells are not inactive and maintain some functional capacities.

Although the concept of exhaustion in cancer is mainly attributed to CTLs, CD4^{+} T-cells can also express co-inhibitory receptors and lose their effector functions (Goding, et al. 2013).

The existence of inhibitory receptors is essential as these negative regulatory pathways control auto reactivity and maintain peripheral tolerance (Sharpe, et al. 2007). Their expression appears transiently on effector T-cells following their activation.

Figure 1.5: Progressive development of T-cell exhaustion (Reprinted by permission from [Springer Nature Customer Service Centre GmbH]: [Springer Nature] [NATURE REVIEWS IMMUNOLOGY] [MOLECULAR AND CELLULAR INSIGHTS INTO T CELL EXHAUSTION, WHERRY AND KURACHI], [COPYRIGHT] (2015))

1.3.4.1.4.Memory T-cells

The generation of memory T-cells is crucial in cancer to obtain a long-lasting anti-tumour immune response (Reading, et al. 2018). Differentiation of T-cells into memory T-cells is facilitated by antigen exposure and inflammatory milieu (Shaulo, et al. 2008). Memory T-cells are characterised by a long lifespan and a proliferative potential upon antigen re-challenge.

Three subsets of circulating memory CD8+ T-cells were described: Stem central memory (Tscm), Central memory (Tcm) and effector memory (Tem). Tscm have the capacity to differentiate into Tcm or Tem upon antigen stimulation and display a naive phenotype (Gattinoni, et al. 2011). Tcm can differentiate into Tem upon antigen stimulation and hold a stem-cell like phenotype. Tem are more differentiated and display similar functions to effector T-cells.

Tissue resident memory T-cells (Trm) were described as skin resident T-cells enhancing local immunity against pathogens following an infection (Gebhardt, et al. 2009). They can derive from either Tcm or Tem cells, secrete pro-inflammatory cytokines (IFNγ, IL-2 and TNFα) upon TCR activation, thereby recruiting NK cells and DCs, and produce Granzyme B (Schenkel, et al. 2014).

The incapacity to generate functional tumour-specific memory T-cells can be due to several mechanisms such as the deletion of tumour associated self-antigen, the low avidity of TCR-peptide and MHC interactions, the dysfunction of T-cells (anergy, tolerance, exhaustion) or their incapacity to migrate to the tumour site (Reading, et al. 2018).

1.3.4.1.5. TCR affinity and avidity

The TCR affinity depends on the strength of the interaction between a TCR and an MHC-peptide complex (Figure 1.6) (Stone, et al. 2009). A high TCR affinity was shown to correlate with higher cytotoxicity and IFNγ production (Tian, et al. 2007). The avidity is defined as the strength between multiple TCRs and MHC-peptide complexes (Vigano, et al. 2012). The functional avidity relates to the overall clonal T-cell response towards its antigen. Although it is often the case, the TCR affinity does not always correlate with the TCR avidity. Indeed, external factors such as inhibitory molecules can dampen the T-cell response in spite of a strong TCR/MHC-peptide interaction.

In cancer, high avidity T-cells have been described as highly cytotoxic (Dutoit, et al. 2001; Pudney, et al. 2010). High avidity TCR/MHC-peptide interaction correlates with the expression of PD-1 (Harari, et al. 2007; Simon, et al. 2015). However, supra-optimal TCR stimulation of high avidity T-cells was described to induce exhausted T-cells with impaired cytotoxic functions (Brentville, et al. 2010). Indeed, Janicki *et al*. described high avidity CD8^{+} T-cells differentiating into CTL within the tumour-draining lymph node but losing their effector function once reaching the tumour site (Janicki, et al. 2008).
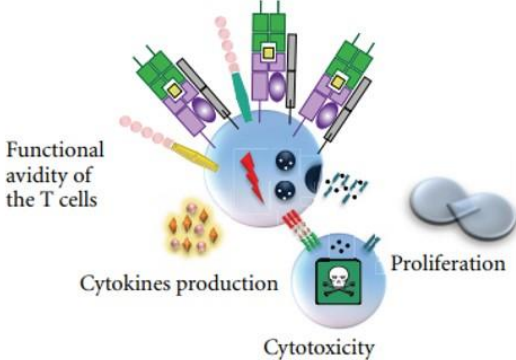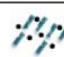
	Schematic representation	Definition	Technique of measurement	Measurement readout
TCR affinity		Strength of the binding between one peptide-MHC (pMHC) molecule and one TCR	Surface plasmon resonance (SPR)	- Direct assessment of ligand binding to surface immobilized receptors - K_D values, on- and off-rates, and $T_{1/2}$ can precisely be determined
TCR avidity		Strength of interaction between multiple TCR and pMHC molecules	Surface staining with fluorescent peptide-MHC multimers	- Fluorescence intensity of surface bound pMHC multimers - Cell surface bound tetramer off-rates
Functional avidity of the T cells	Cytokines production / Cytotoxicity / Proliferation	Antigen sensitivity (activation threshold)	Assessment of T-cell functions in presence of decreasing antigen concentration	Biological read-out: - Cytokines production - Cytotoxic activity (ability to lyse target cells) - Proliferation capacity

Peptide-MHC (pMHC) molecule and TCR   Coreceptor   Granzymes and perforin

Costimulatory/coinhibitory molecules and their ligands   Fas/FasL

Figure 1.6: Schematic representation, definition, technique of measurement and readout of TCR affinity and functional avidity (Reprinted by permission from [CREATIVE COMMONS ATTRIBUTION LICENSE]: [Clinical & Developmental Immunology], [Vigano, et al., FUNCTIONAL AVIDITY: A MEASURE TO PREDICT THE EFFICACY OF EFFECTOR T CELLS?, (2012)])

1.3.4.2.CD4^{+} T-cells

CD4^{+} T-cells have various roles in anti-tumour immunity. Mainly, they provide help to CD8^{+} T-cells during the priming phase in the secondary lymphoid organs, allowing the generation of a strong and lasting CTL response (Borst, et al. 2018).

According to Borst *et al.*, the priming of T-cells occurs in two consecutive distinct steps. During the first step, DCs independently present antigens to CD4^{+} and CD8^{+} T-cells in the lymph node or spleen. During the second step, both activated CD4 and CD8^{+} T-cells interact with the same DC in the same lymph node allowing the delivery of the help signal (Eickhoff, et al. 2015; Hor, et al. 2015). The CD4^{+} T-cell/DC interaction induces the expression of CD40L in the CD4^{+} T-cell, triggering CD40 signalling in the DC, thus increasing its antigen presentation ability by an increased expression of the co-stimulatory ligands CD80/CD86, CD70 and the secretion of type I interferons and of IL-12 and IL-15 interleukines. CD80/CD86 and CD70 interact with CD28 and CD27, respectively, on the surface of CD8^{+} T-cells, promoting their differentiation and survival (Feau, et al. 2012). DC-derived cytokines

promote the differentiation of CD8^{+} T-cell into CTLs. Moreover, CD4^{+} T-cells-derived IL-2 and IL-21 promote the CTL response.

As a result, CD4^{+} T-cell help promotes both the effector and the memory CD8^{+} T-cell responses (Ahrends, et al. 2017).

Help signals promote cytotoxicity mechanisms by inducing the production of IFNγ, TNFα, FAS-L, granzyme A and B (Ahrends, et al. 2017). Moreover, in the absence of help, non-cytotoxic exhausted CTLs expressing high levels of co-inhibitory receptors such as PD-1 and LAG-3 are generated. CD4^{+} T-cells help selectively promotes functional anti-tumour high avidity antigen-specific CD8^{+} T-cells (Zhu, et al. 2015). Helper T-cells are also required for the induction of a memory response (Janssen, et al. 2003) as in their absence, CD8^{+} T-cells die due to apoptosis during the secondary expansion phase (Janssen, et al. 2005).

Other anti-tumour roles of CD4^{+} T-cells include 1) the recruitment of APCs and NK cells, 2) the inhibition of angiogenesis by Th1 cells, 3) the recruitment of eosinophils by Th2 cells and 4) the secretion of IFNγ and granzyme B by cytolytic CD4^{+} T-cells in some cases (Kim, et al. 2014). Indeed, cytotoxic CD4^{+} T-cells-driven anti-tumour immunity relying on the MHC class-II restricted recognition of tumour cells was described (Quezada, et al. 2010).

Moreover, Th1 cells were shown to induce senescence in cancer cells via an IFNγ/TNFα-dependant mechanism (Braumuller, et al. 2013).

1.4. Immunotherapies for PCa

The recognition of the role of the immune system in fighting cancer and the understanding of the mechanisms involved lead to the development over the years of numerous immunotherapies.

Immunotherapies for cancer can be divided into two categories based on their ability to stimulate the immune system against tumour cells: passive or active (Galluzzi, et al. 2014). Passive immunotherapies have a direct anti-cancer effect, such as tumour-targeting antibodies, adoptive transfer of *in vitro* activated immune cells or oncolytic viruses. On the contrary, active immunotherapies aim at stimulating the host immune system, as DC-based immunotherapies, peptide- and DNA-based vaccines, immunostimulatory cytokines, immunomodulatory monoclonal antibodies or immunogenic cell death inducers.

The remainder of this section will focus on the main immunotherapies for PCa that are either currently in use or being assessed in clinical trials.

1.4.1.Immune infiltration in PCa

To understand the rationale for using immunotherapies for the treatment of PCa, it is crucial to comprehend the immune status in prostate tumours. This will also help understanding the difficulty of developing immunotherapies for PCa that could generate a complete response in patients. Tumours can be categorised as "hot", inflamed, or "cold", non-inflamed. Although the development of prostate tumours is believed to be partly driven by inflammation (Sfanos and De Marzo 2012), prostate tumours are described as cold tumours, with a poor immune infiltrate (Vitkin, et al. 2019). One explanation for this is their low mutational burden that renders them less immunogenic due to the lack of tumour-associated antigens (Vitkin, et al. 2019). Other factors are: 1) defects in the DNA damage response, 2) decreased MHC Class I expression, 3) dysfunctional IFN1 signalling and 4) loss of PTEN protein. The latest has been associated with a decrease of IFNγ, granzyme B and of CD8^{+} Tumour Infiltrating Lymphocytes (TILs) (Sharma, et al. 2018). Futhermore, chronic exposure to type I IFNs is associated with therapy resistance and immunosuppression. Indeed, the subset of interferon-stimulated genes activated after prolonged IFN1 exposure causes radiation and chemotherapy resistance (Minn. Et al, 2015) and promotes cancer growth and metastasis (Cheon, 2014). Chronic IFN1 signaling can also diminish the effect of immunotherapies, such as ICBs, CAR T-cell therapies and oncolytic virus therapies (Budhwani, et al. 2018).

The presence of TILs, in particular of CTLs and helper T-cells is associated with a good prognosis (Fridman, et al. 2017). However, the implication of CD8^{+} TILs in PCa is not clear. Some studies have demonstrated that the presence of TILs is associated with a poor prognosis (Ness, et al. 2014; Leclerc, et al. 2016) with one study linking the presence of TILs and macrophages with worse distant metastasis-free survival (Zhao, et al. 2019). Ness *et al.* suggested that TILs in prostate tumours are dysfunctional (Ness, et al. 2014), which is supported by the fact that the expression of IFNγ and granzyme B was decreased in TILs in comparison to those in normal prostate tissue and was accompanied by an increased PD-1 expression (Ebelt, et al. 2008). Furthermore, the expression of PD-1 on TILs and of PD-L1 on tumour cells have been observed in 19% of a 16 CRPC patients' cohort (Massari, et al. 2016) while an increased expression of PD-L1 and PD-L2 on DCs and of PD-1 on T-cells has been observed in the blood of Enzatulamide-resistant PCa patients (Bishop, et al. 2015). The presence of CD8^{+} TILs exhibiting a restricted TCR repertoire was associated with the expression of PD-1 (Sfanos, et al. 2009). The dysfunction of TILs could also be due to the presence of immunosuppressive factors and cells. The presence in high proportions of both CD4^{+} and CD8^{+} Tregs has been reported (Kiniwa, et al. 2007; Kaur, et al. 2018) and associated with worse progression-free survival and OS (Davidsson, et al. 2013; Nardone, et al. 2016). There is also evidence that soluble factors generate immunosuppressive PD-L1/CD209 (DC marker)-expressing monocytes in the tumour, unable to cross-present tumour-antigens to CD8^{+} T cells and suppressing T-cell

proliferation (Spary, et al. 2014). The decreased proportion of DCs correlates with high Gleason score and worse progression free survival (Liu, et al. 2013). The presence of TAMs was observed in PCa; however, they were abundant in early clinical stages and decreased in the presence of lymph-node metastases (Shimura, et al. 2000). A study on a cohort of 234 patients showed that most TAMs had an immunosuppressive phenotype alongside inactive T-cells (Lundholm, et al. 2015). An increase of MDSCs and Tregs was observed in the blood of PCa patients in comparison to healthy donors (Idorn, et al. 2014). The mechanism of T-cell suppression by MDSCs observed relied on the expression of iNOS enzyme. Another study demonstrated the role of MDSCs-derived IL-23 in the development of CRPC by activation of the androgen receptor pathway in tumour cells, promoting their survival and proliferation in an androgen-independent manner (Calcinotto, et al. 2018). A preclinical study determined that the loss of PTEN lead to the expansion of MDSCs in the TME (Garcia, et al. 2014).

On the other hand, the presence of DCs and NK cells was associated with improved distant metastasis-free survival (Zhao, et al. 2019) and the increase of CD8^{+} T-cells was associated with longer progression free survival following radiotherapy (Nardone, et al. 2016). The presence of NK cells in great amount correlated with lower risk of disease progression (Gannon, et al. 2009). The expression of IFNγ on TILs was increased in PCa patients in comparison to benign prostatic hyperplasia cases (Elsässer-Beile, et al. 2000).

Vitkin *et al.* summarized the factors impacting the immune TME in PCa in figure 1.7 (Vitkin, et al. 2019).
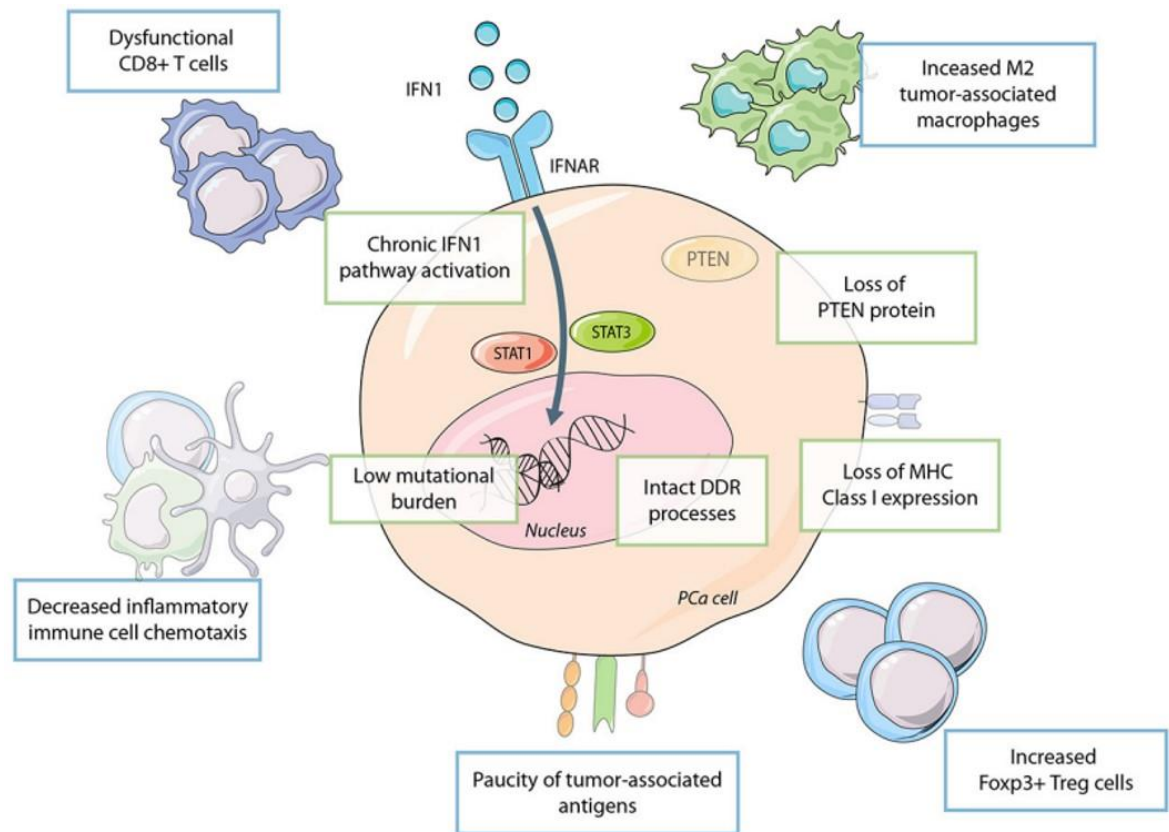
Figure 1.7: Tumour Immune Microenvironnement in PCa (Reprinted by permission from [CREATIVE COMMONS ATTRIBUTION LICENSE]: [FRONTIERS IN IMMUNOLOGY], [Vitkin, et al., THE TUMOR IMMUNE CONTEXTURE OF PROSTATE CANCER, (2019)])

1.4.2. Cancer vaccines

Cancer vaccines can be divided into four categories: tumour cell vaccines, DC-based vaccines, protein- or peptide-based cancer vaccines and genetic vaccines, either DNA, RNA or viral-based (Guo, et al. 2013).

Regardless of the category, every cancer vaccine aims at delivering tumour antigens to DCs and activating DCs in order for them to induce TAA-specific CD4$^+$ and CD8$^+$ T-cell responses.

The choice of the antigen is crucial as the antigen needs to be expressed only (tumour specific antigen) or preferentially (TAA) by cancer cells but not by cells belonging to vital organs in order to avoid any potential side effects. In addition, the antigen needs to be both immunogenic and required by the tumour cells to limit antigen loss due to immuno-editing (Dunn, et al. 2002). The antigen also needs to be expressed by the primary tumour and the metastasis.

The delivery vehicle or the adjuvant to combine with the antigen enhances its immunogenicity.

They can be divided into six categories: cytokines/endogenous immunomodulators such as GM-CSF, microbes and microbial derivatives such as CpG or poly I:C, mineral salts, oil emulsions, particulates and viral vectors such as adenovirus, vaccinia or fowl pox (Melero, et al. 2014).

To date, Sipuleucel-T is the only FDA-approved therapeutic cancer vaccine. Despite many attempts, the development of therapeutic cancer vaccine for all types of cancer has not been so successful, many vaccines failed in phase 3 clinical trial because of inexistent or disappointing clinical efficacy. It becomes clear that therapeutic cancer vaccines as a monotherapy cannot overcome the immunosuppressive TME and the mechanisms of tolerance that T-cells have to face. Therefore, a number of ongoing clinical trials are assessing the effect of multiple therapies together.

Moreover, cancer vaccines are more likely to have a greater benefit for patient with less advanced-stage cancers (Melero, et al. 2014).

1.4.2.1.Sipuleucel-T

Sipuleucel-T was briefly described section 1.1.5.

Its processing is described in figure 1.8. Briefly, isolated PBMCs from patient's blood were stimulated for 36-44 hours with a fusion protein composed of GM-CSF and PAP antigen. GM-CSF is a cytokine that promotes the differentiation and activation of DCs (Steinman, et al. 1991). It was shown to enhance T-cell cross-priming (Zhan, et al. 2011). The cells reinfused back into the patient are believed to induce $CD4^+$ and $CD8^+$ T-cell responses.

The Immunotherapy for Prostate Adenocarcinoma Treatment (IMPACT) trial confirmed the improved survival effect of Sipuleucel-T (Kantoff, et al. 2010). 521 mCRPC patients were enrolled, with 2/3 receiving Sipuleucel-T and 1/3 placebo, and received 3 infusions every two weeks. The improved OS was of 4.1 months, with one patient who had a partial remission. PSA decline of ≥50% was only observed in 2.6% of patients. Antibodies against the fusion protein were detected in 66.2% of patients (2.9% for placebo group) while antibodies against PAP were detected in 28.5% of patients (1.4% in the placebo group). *In vitro* stimulation with the fusion protein induced T-cell proliferation in 73% of Sipuleucel-T treated patients (against 12.1% in the placebo group) while 27.3% of patients exhibited T-cell proliferation in response to PAP stimulation (against 8% in the placebo group). Interestingly, the increase of antibodies targeting PAP or the fusion protein correlated with an improved OS while the T-cell proliferation observed did not.

The majority of patients received docetaxel chemotherapy following either Sipuleucel-T treatment or placebo.

Despite the improved OS in patients with asymptomatic or minimally symptomatic mCRPC, no progression free survival improvement was observed.
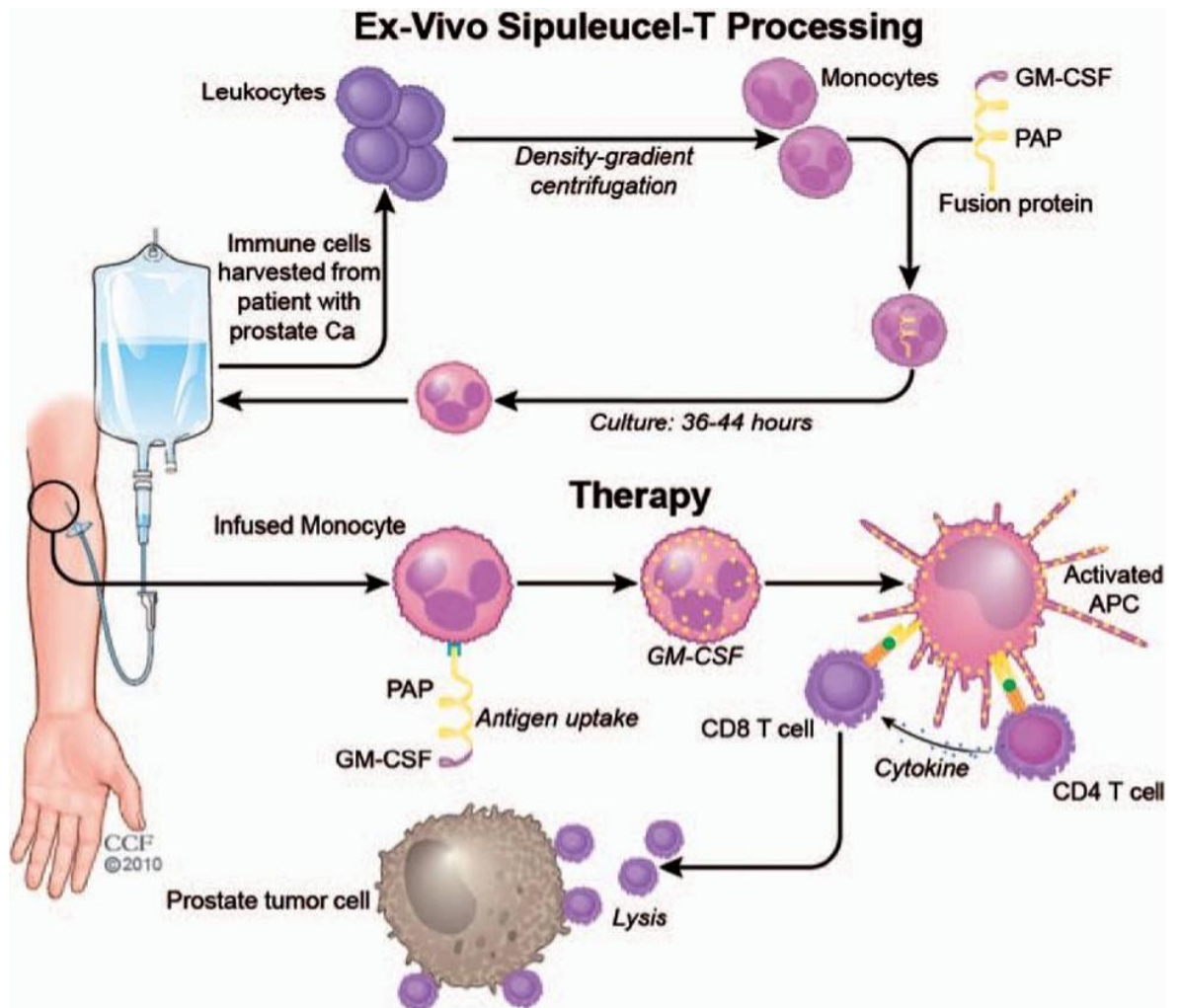
Figure 1:8: Processing of Sipuleucel-T (Reprinted by permission from [SAGE PUBLICATIONS], gratis reuse for doctoral dissertations: [THERAPEUTIC ADVANCES IN MEDICAL ONCOLOGY], [GARCIA, SIPULEUCEL-T IN PATIENTS WITH METASTATIC CASTRATION-RESISTANT PROSTATE CANCER: AN INSIGHT FOR ONCOLOGISTS, (2011)])

Since its FDA-approval, Sipuleucel-T has been studied further to understand its mechanism of action, and has been assessed in combination with diverse (immuno)therapies.

Analysis and comparison of the IMPACT trial with two previous phase III clinical trials (D9901/D9902A) confirmed the in vitro expansion and activation of APCs, characterised by the increased expression of CD54, and suggests the establishment of both cellular and humoral immune responses, all of these parameters correlating with improved OS (Sheikh, et al. 2013). Antonarakis et al. demonstrated the lytic phenotype of circulating PAP-specific CD8^{+} T-cells in Sipuleucel-T treated patients, determined by CD107a degranulation marker expression (Antonarakis, et al. 2018). Moreover, the expression of both IFNγ and granzyme B in PAP-specific T-cells was observed (Wargowski, et al. 2018).

When Sipuleucel-T was administered prior to prostatectomy, it was shown to induce the recruitment of T-cells to the TME (Fong, et al. 2014). The majority of these T-cells expressed PD-1, proliferated, and secreted IFNγ following stimulation with the PAP protein.

Interestingly, the presence of antibodies against other antigens was observed following Sipuleucel-T treatment, in particular against PSA, suggesting antigen spread, and correlated with improved OS (GuhaThakurta, et al. 2015). The transient increase of eosinophils was found to correlate as well with increased OS (McNeel, et al. 2014). As expected, the IMPACT trial showed that a low PSA baseline correlated strongly with improved OS, suggesting that patients with less advanced disease benefit more from the vaccine (Schellhammer, et al. 2013).

The combination of Sipuleucel-T with other currently used treatments for mCRPC, such as Enzatulamide and Abiraterone Acetate, was well tolerated and did not alter the immunological effects observed when Sipuleucel-T was administered alone (Quinn, et al. 2014; Small, et al. 2015). Sipuleucel-T followed by ADT induced stronger anti-tumour responses than ADT followed by Sipuleucel-T in non-metastatic patients with recurrent disease (Antonarakis, et al. 2017).

Although Sipuleucel-T demonstrated clinical benefit for mCRPC patients by improving the OS, there is still no cure for advanced PCa and new therapies are needed. The next section describes some of the vaccines in development for PCa.

1.4.2.2. Vaccines in phase III clinical trials

Considering the great number of PCa therapeutic vaccines under investigation, this section will focus on vaccines that have reach phase III clinical stage or phase II trials that target PAP protein (Table 1.2).

PROSTVAC (also named PSA-TRICOM) is a poxviral-based vaccine that encodes for PSA, its target antigen, and three costimulatory molecules: B7.1 (CD80), ICAM-1 (CD54) and LFA-3 (CD58). To avoid the development of neutralising antibodies against viral proteins which would alter the immune response, a heterologous prime-boost strategy is used. The vaccinia virus rV-PSA is used for priming while the fowlpox virus rF-PSA is used for boosting (6 boosters). The phase II trial showed an improved OS of 8.5 months and a death rate reduction of 44% (Kantoff, et al. 2010), however the results from the PROSPECT phase III trial (NCT01322490) of PROSTVAC in combination with GM-CSF did not reveal any improvement on the OS, leading to its early discontinuation (Gulley, et al. 2015). Nonetheless PROSTVAC was shown to increase the number of PSA-specific T-cells as well as inducing antigen spreading (Gulley, et al. 2014). It is now being assessed in combination with

Enzatulamide (NCT01867333), docetaxel (NCT02649855) and immune checkpoint inhibitors anti-CTLA-4 (NCT02506114) and anti-PD-1 (NCT02933255).

GVAX-PCa is a whole tumour cell vaccine composed of LNCaP and PC3 PCa cell lines, transduced to secrete GM-CSF. These two cell lines are derived from lymph node and bone metastases respectively. LNCap expresses PCa associated antigens such as PSA, PAP or Prostate-Specific Membrane Antigen (PSMA) (Simons and Sacks 2006).

Despite two phase II trials demonstrating decreased blood PSA and development of anti-vaccine antibodies, both phase III trials, VITAL-1 and VITAL-2, assessing the effect of GVAX-PCa on OS were terminated early (Sonpavde, et al. 2010). VITAL-1, evaluating GVAX-PCa *versus* docetaxel + prednisone in asymptomatic chemo-naïve mCRPC patients, was terminated due to the low probably of leading to an improved OS, its endpoint. VITAL-2, evaluating GVAX-PCa + docetaxel *versus* docetaxel + prednisone in symptomatic chemo-naïve mCRPC patients, was terminated due to the toxicity of GVAC-PCa leading to an increased number of deaths.

DCVAC/PCa autologous vaccine consists of *in vitro* activated DCs pulsed with killed LNCaP cells. The single-arm phase I/II trial revealed an OS of 19 months, while predicted median OS was of 11.8 or 13 months (Halabi and MSKCC monograms respectively) (Podrazil, et al. 2015). Circulating PSA-specific T-cells were detected alongside a reduction of Tregs. The VIABLE phase III trial is ongoing (NCT02111577) and results are expected by June 2020.

Another therapeutic vaccine worth mentioning, although it did not reach phase III clinical trial, is a DNA vaccine encoding the whole PAP protein: pTVG-HP. Its evaluation in a phase I/IIa trial demonstrated its capacity to induce PAP-specific T-cell responses, characterised by IFNγ secretion and proliferation in response to PAP stimulation, and to increase the PSA doubling time (McNeel, et al. 2009). Moreover, the immune response observed was amplified by booster immunisations (Becker, et al. 2010). Adaptation of the immunisation schedule based on real-time immune monitoring did not increase the frequency of patients developing PAP-specific T-cell responses (McNeel, et al. 2014). However, the study revealed the presence of effector and effector memory Th1 PAP-specific T-cell responses. A phase II trial is currently ongoing (NCT01341652) to test the effect of pTVG-HP, with GM-CSF *versus* GM-CSF alone, on metastasis free-survival and is expected to be completed by April 2020.

A pilot study assessed the effect of vaccinating with Sipuleucel-T (as per usual regimen: 3 times with 2 weeks intervals) and boosting with pTVG-HP (4 times with two weeks intervals + 2 immunisations with 3 months intervals), *versus* no boosting (Wargowski, et al. 2018). The aim was to determine whether additional immunisation with the pTVG-HP vaccine could prolong or increase the PAP-

specific immune response. However, there was no increased immune response or effect on OS or PSA doubling time. Subsequent studies will assess this combination using pTVG-HP first and boosting with Sipuleucel-T as this strategy is believed to elicit stronger Th1 cellular immunity rather than Th2 immunity.

Therapeutic cancer vaccines are an attractive therapy for cancer patients as, unlike other therapies, they are well tolerated and side effects are usually minimal. However, vaccines were shown to have more clinical benefit in patients with low tumour burden and less aggressive disease. Indeed, efficacy is dampened by the immunosuppressive microenvironment. Therefore, other therapies capable of counteracting the immunosuppression are required, as stand-alone or in combination with PCa vaccines.

Table 1:2: Completed or ongoing phase II and III clinical trials assessing therapeutic vaccines for the treatment of PCa

Vaccine	Antigen	Mechanism of action	Phase	Patients	Outcome	Trial Identifier	Reference
PROSTVAC (PSA-TRICOM)	PSA	Poxviral-based vector encoding PSA + co-stimulatory molecules (CD80, CD54 and CD58)	II	mCRPC (n=125)	8.5 months OS improvement	NCT00078585	Kantoff, et al. 2010 J Clin Oncol
			PROSPECT III	mCRPC (n=1200)	No OS improvement	NCT01322490	Gulley, et al. 2015
GVAX-PCa	PSA, PAP, PSMA	GM-CSF secreting LNCaP and PC3 cell lines	VITAL-1 III	Asymptomatic chemo-naïve mCRPC (n=626)	No OS improvement	NCT00089856	Sonpavde, et al. 2010
			VITAL-2 III	Symptomatic chemo-naïve mCRPC (n=408)	Toxicity	NCT00133224	
DCVAC/PCa	PSA, PAP, PSMA	*In vitro* activated DCs pulsed with killed LNCaP cells	I/II	Progressive mCRPC (n=25)	6-7.2 months OS improvement	Eudra CT 2009-017295-24	Podrazil, et al. 2015
			Viable III	mCRPC (n=1170)	Ongoing	NCT02111577	
pTVG-HP	PAP	DNA vaccine	I/IIa	Non metastatic castrate sensitive PCa (n=22)	PAP-specific T-cell responses		McNeel, et al. 2009
			II	Non-metastatic Prostate Cancer (n=99)	Ongoing	NCT01341652	

1.4.3. Immune checkpoint blockade

ICB have demonstrated their efficacy in a number of cancers since the FDA-approval of Ipilimumab (anti CTLA-4) for the treatment of melanoma in 2011. Subsequently, antibodies targeting PD-1, PD-L1, PD-L2, LAG-3, TIM-3 or VISTA have gained interest and been evaluated.

The outcome of clinical trials assessing ICB targeting the CTLA-4 or PD-1/PD-L1 axis as stand-alone (Table 1.3) and in combination with vaccines (Table 1.4) in PCa are summarised below.

Ipilimumab was tested in mCRPC in two phase III clinical trials: one before (Beer, et al. 2017) and one after chemotherapy treatment (Kwon, et al. 2014). In the first trial performed, patients received Ipilimumab after Docetaxel chemotherapy. Although the primary endpoint of OS was not reached (P=0.53), progression-free survival was increased. Further analyses showed Ipilimumab was more effective and did improve OS in patients with less advanced disease such as no visceral metastases (P = 0.0038). In the second trial, chemotherapy naive patients without visceral metastasis received Ipilimumab and while median progression-free survival was prolonged and PSA decrease was observed, OS was not improved.

Although the clinical efficacy of Ipilimumab in mCRPC was disappointing, studies of tumours pre/post treatment showed an increase of VISTA and PD-L1 molecules on the surface of macrophages, suggesting new possible targets (Gao, et al. 2017).

The first phase I trial assessing the efficacy of Nivolumab (anti PD-1) showed no objective response in mCRPC patients (Topalian, et al. 2012), which can be explained by the known weak PD-L1 expression in human prostate tumours (Martin, et al. 2015). However, a phase II trial assessing Pembrolizumab (anti PD-1) in Enzatulamide-resistant mCRPC patients reported a drop of PSA value in 3 out of 10 patients, with 2 of them achieving a partial response (Graff, et al. 2016), corroborating the fact that PD-L1 expression increases in Enzatulamide resistant tumours (Bishop, et al. 2016). Indeed, further analysis demonstrated that the two responders had a PD-L1 positive biopsy and that one of them presented markers of microsatellite instability. In the phase I KEYNOTE-28 study assessing the effect of Pembrolizumab on advanced PCa patients with at least 1% of tumours expressing PD-L1, 13% of patients had a partial response and 39% had a stable disease (Hansen, et al. 2018). These encouraging results demonstrate the efficacy of anti PD-1 antibodies in selected PCa patients and lead to the phase II KEYNOTE-199 trial. This trial assessed Pembrolizumab in Docetaxel-refractory mCRPC patients and showed antitumor activity and disease control regardless of PD-L1 expression (De Bono, et al. 2018).

Furthermore, the FDA-approval of Pembrolizumab in 2017 for the treatment of mismatch repair-deficient or microsatellite-unstable cancers (Le, et al. 2017) will benefit a proportion of PCa patients (12%) (Pritchard, et al. 2014; Schweizer, et al. 2016). These patients have somatic mutations in

mismatch repair genes leading to microsatellite instability and therefore to hypermutated tumours (Pritchard, et al. 2014), which correlates with response to ICB (anti-CTLA4, anti-PD1, anti-PDL1) in several tumor types.

Several anti PD-L1 antibodies are currently undergoing clinical trials in mCRPC. Although Avelumab (anti PD-L1) did not induce objective responses, 3 out of 18 mCRPC patients had a stable disease for at least 24 months (Fakhrejahani, et al. 2017).

Thereafter, the combination of Ipilimumab and Nivolumab was tested in a phase II trial as it induced a synergistic effect in melanoma. mCRPC patients with ARV7+ tumours (constitutively active androgen-receptor splice variant 7) were selected, expecting these tumours would be enriched in DNA repair mutations and therefore more sensitive to ICB (Boudadi, et al. 2017). Results were encouraging and objectives responses were more common in DNA repair deficient tumours.

Although ICB therapies have not been as successful as hoped in mCRPC patients, there have been some encouraging results which require further investigations and indicate that subsets of patients might respond to ICB. Patients should therefore be selected, by assessing the presence of mutations in mismatch repair genes as well as the expression of PD-L1 in tumours prior to therapy when considering blockade of the PD-1/PD-L1 axis.

Nonetheless, ICB have since been extensively evaluated in combination with other therapies: hormonal therapy, chemotherapy, radiotherapy and therapeutic vaccines. Most of these trials are ongoing and results are not available yet but some are already completed.

A phase I trial assessing the combination of Sipuleucel-T and low dose Ipilimumab was well tolerated and demonstrated an increase of PAP-specific Immunoglobulins in comparison to what is usually observed with Sipuleucel-T treatment alone (Scholz, et al. 2017). Median survival for the 9 patients reached 4 years and although 3 patients died, the 6 remaining had a median PSA value of 5.5, with one patient in durable remission (Ku, et al. 2018).

Ipilimumab was also tested in combination with PSA-TRICOM vaccine in mCRPC patients. 58% of chemotherapy-naive patients had PSA declines with 6 of them having a drop of at least 50% (Madan, et al. 2012). This phase I trial reported a median OS of 2.63 years and identified immune cell subsets that correlated with longer OS (Jochems, et al. 2014). The lower proportion of PD-1$^+$/TIM-3$^-$ CD4 effector memory T-cells, higher proportion of PD-1$^-$/TIM-3$^+$ CD8$^+$ T-cells and the higher proportion of CTLA$^-$ Tregs before immunotherapy correlated with longer OS. On the contrary, the increase of Tim-3$^+$ NK cells post-immunotherapy correlated with longer OS.

Finally, the combination of pTVG-HP DNA vaccine with Pembrolizumab is currently ongoing and preliminary results from this phase II trial showed PSA declines, decreased tumour volumes in several patients, including one partial response, and the presence of circulating Th1 PAP-specific T-cells (McNeel, et al. 2017). This trial was based on a previous trial demonstrating anti-tumour responses when Pembrolizumab was given concurrently to the DNA vaccine and not sequentially (McNeel, et al. 2018).

These trials demonstrate the safety and improved efficacy of therapeutic cancer vaccines in combination with ICB therapies, providing hope for the treatment of for mCRPC.

Table 1:3: Completed selected clinical trials assessing ICB therapies targeting the CTLA-4 or PD-1/PD-L1 axis for the treatment of PCa

Target	Antibody	Phase	Patients	Outcome	Trial Identifier	Reference
CTLA-4	Ipilimumab	III	Docetaxel treated mCRPC (n=988)	No improved OS (P=0.53) Increased PFS Improved OS on patients with less advanced disease (P=0.0038)	NCT00861614	Kwon, et al. 2014
		III	Chemotherapy naive mCRPC (n=837)	No improved OS Increased PFS	NCT01057810	Beer, et al. 2017
PD-1	Nivolumab	I	mCRPC (n=17)	No objective response	NCT00730639	Topalian, et al. 2012
	Pembrolizumab	II	Enzatulamide-resistant mCRPC (n=10)	20% of partial response	NCT02312557	Graff, et al. 2016
		KEYNOTE-28 Ib	PD-L1$^+$ tumour mCRPC (n=23)	13% of partial response 39% of stable disease	NCT02054806	Hansen, et al. 2018
		KEYNOTE-199 II	Docetaxel-refractory mCRPC (n=258)	Anti-tumour activity regardless of PD-L1 expression	NCT02787005	De Bono, et al. 2018
PD-L1	Avelumab	I	mCRPC (n=18)	17% of stable disease	NCT01772004	Fakhrejahani, et al. 2017

Table 1:4: Completed or ongoing selected clinical trials assessing therapeutic vaccines in combination with ICB therapies targeting the CTLA-4 or PD-1/PD-L1 axis for the treatment of PCa

Combination	Phase	Patients	Outcome	Trial Identifier	Reference
Sipuleucel-T + Ipilimumab	I	Docetaxel-naive progressive mCRPC (n=9)	Median survival >4 years for 6 of 9 patients 1 durable remission Increased PAP-specific humoral response (*versus* Sipuleucel-T alone)		Ku, et al. 2018
PROSTVAC + Ipilimumab	I	mCRPC (n=24)	Media OS= 2.63 years	NCT00113984	Jochems, et al. 2014
pTVG-HP + Pembrolizumab	I	mCRPC (n=26)	PSA declines Anti-tumour activity		McNeel, et al. 2018
	II	mCRPC (n=66)	Ongoing Anti-tumour activity observed 1 partial response	NCT02499835	McNeel, et al. 2017

1.4.4.Other immunotherapies

1.4.4.1.Oncolytic virotherapy

Oncolytic viruses exercise their efficacy by replicating within tumour cells, inducing their lysis and the release of tumour antigens thereby activating the innate immune system and promoting the priming and expansion of tumour-specific T-cells.

The FDA-approval of Talimogene laherparepvec in 2015 for the treatment of advanced melanoma has confirmed the clinical benefit of these type of therapies (Conry, et al. 2018), which are now being developed for other cancer types.

ProstAtak (aglatimagene besadenovec) is developed by Advantagene and is currently undergoing two clinical trials. This therapy consists of the intratumoral delivery of an inactivated herpetic virus containing the thymidine-kinase gene (adV-tk), followed by treatment with an anti-herpetic drug (Valacyclovir) (Rojas-Martinez, et al. 2013).

An ongoing phase II trial is assessing the effect of ProstAtak as a stand-alone in patients with localised PCa undergoing active surveillance (NCT02768363), results are expected by September 2020.

ProstAtak is also currently being assessed in combination with radiotherapy in a phase III trial for patients with intermediate-high risk localised PCa (NCT01436968). Results are expected by December 2022. This trial is based on synergistic results observed during the phase II trial, demonstrating a reduced recurrence rate (Aguilar, et al. 2006).

1.4.4.2.Anti-tumour antibodies

Anti-tumour antibodies function by targeting tumour antigens that are highly expressed on tumour cells, leading to ADCC. In PCa, two antibodies have reached phase II clinical trial.

J591 monoclonal antibody, targeting PSMA, assessed with low-dose IL-2 did not show encouraging results (Jeske, et al. 2007). However, J591 radiolabelled with lutetium-177, to facilitate the killing of prostate tumour cells, induced PSA decline in 60% of patients, one partial response and stable disease in 67% of patients with measurable disease (Tagawa, et al. 2013).

Another strategy is to conjugate chemotherapeutic drugs to the antibody in order to deliver it directly to tumour cells. PSMA Antibody drug conjugate (ADC) delivers the chemotherapeutic agent MMAE (Monomethyl auristatin E) to PSMA-expressing cells. A phase II trial demonstrated anti-tumour efficacy, PSA declines in 44% of patients, 61% of stable disease and 13% of partial responses (Petrylak, et al. 2015).

1.4.4.3.Adoptive cellular Therapy (CAR T cells)

This therapy consists in genetically engineering a patient's own T-cells before reinfusion. Generation of Chimeric Antigen Receptor (CAR) T-cells, which target antigens via an antibody-derived single chain variable fragment, rendering the T-cell MHC-independent, is the most promising approach. Targeting of CD19 in B-cell lymphomas using this technique was highly successful, with up to 71% of complete remissions and durable responses, leading to the FDA-approval of 2 anti-CD19 CAR T-cell therapies (Comiskey, et al. 2018).

In PCa, one CAR T-cell targeting PSMA is currently undergoing phase I clinical trial for metastatic PCa (NCT01140373) and demonstrated safety with increased levels of cytokines suggesting activation of the engineered T-cells (Slovin, et al. 2013). Another phase I trial, recently initiated, assesses CAR T-cells targeting the prostate stem cell antigen (PSCA) in mCRPC patients (NCT03873805).

1.4.5.Immune effect of conventional therapies

As immunotherapies developed in PCa aim at treating mCRPC, it is necessary to understand that these patients would have previously received conventional therapies that may have affected their immune system. Indeed, hormonal therapy, chemotherapy and radiotherapy have been shown to display immuno-modulatory properties.

Hormonal therapy

ADT demonstrated immuno-modulatory effects such as 1) reversing thymic involution (Sutherland, et al. 2005), 2) promoting the survival and differentiation of thymocytes into mature T lymphocytes (Dulos and Bagchus 2001; Roden, et al. 2004), 3) attenuating tolerance to prostatic antigens (Drake, et al. 2005) and 4) increasing the immune infiltration in prostate tumours (Mercader, et al. 2001). Roden *et al*. demonstrated that androgen ablation could enhance proliferation induced antigen-specific stimulation and prostatic T-cell infiltration, while Drake *et al*. showed that vaccination could be potentiated following androgen ablation.

Consecutive to ADT, human prostate tumours are enriched in both $CD4^+$ and $CD8^+$ T-cells and in APCs (Mercader, et al. 2001). Moreover, the T-cell response observed appeared to be oligo clonal. Gannon *et al.* also observed an increase of T-cells in prostate tumours following ADT treatment, however, the increase of macrophages reported correlated with a higher risk of disease progression (Gannon, et al. 2009).

These findings led to trials assessing the combination of ADT with immunotherapies such as cancer vaccines in order to potentiate their effect.

Primary results from a study suggested that Sipuleucel-T could be more efficacious if given after ADT (Antonarakis, et al. 2013), however, further assessment of this phase II trial showed that

patients benefited better from Sipuleucel-T when it was given prior to ADT, regarding vaccine-specific induced humoral and cellular responses (Antonarakis, et al. 2017). Another study assessing the combination of PROSTVAC vaccine with ADT also suggested the benefit of vaccinating patients prior to ADT, as OS was improved (P=0.045) (Madan, et al. 2008). However, is it important to bear in mind that these studies were performed on small cohorts and therefore, more data is needed to determine whether vaccines are more efficacious when given before or after ADT.

Chemotherapy

A number of chemotherapy drugs have also been described as having immuno-modulatory effects, in particular by inducing immunogenic cell death, a type of cell death showed to stimulate the immune system by promoting the uptake and processing of tumour antigens by DCs and the antigen presentation to T-cells, resulting in an increased proportion of TILs (Wang, et al. 2018). Chemotherapy-induced cytotoxicity was proposed to induce antigen cascade, rendering more TAAs available to the immune system (Madan, et al. 2012). In the context of PCa, Docetaxel chemotherapy was reported to increase the production of pro-inflammatory cytokines (IFNγ and TNFα) by lymphocytes therefore increasing their cytotoxic functions (Grunberg, et al. 1998). These facts lead to numerous combinatorial trials of Docetaxel with immunotherapies.

Radiation therapy

Radiation can render tumour cells more sensitive to lymphocyte killing by upregulating the expression of 1) tumour antigens, 2) costimulatory molecules, such as CD80, 3) Fas molecules and 4) MHC class-I molecules (Hodge, et al. 2012). Radiation was also reported to create a pro-inflammatory microenvironment characterised by the presence of cytokines, chemokines and adhesion molecules enhancing the recruitment of T-cells (Friedman 2002).

As expected, these findings also lead to combinatorial trials assessing the synergistic effect of radiotherapy and immunotherapy (Finkelstein, et al. 2015).

Radium-223 was described as displaying immunomodulatory effects *in vitro* via increasing the expression of MHC class-I on PCa cell lines, thereby rendering them more susceptible to T-cell mediated lysis (Malamas, et al. 2016).

These facts need to be considered when developing new strategies for the treatment of mCRPC. Indeed, although immunotherapy is extremely promising, it can be used not only in combination with other immunotherapies but with standard therapies that are already FDA-approved and have demonstrated immunomodulatory effects resulting in clinical benefit for patients.

1.4.6. PAP as a target

PAP is a 100 kDa glycoprotein composed of two subunits of about 50kDa each, acting as a tyrosine phosphatase (Muniyan, et al. 2013). Two forms have been described: intracellular and secreted in the seminal fluid. This protein is highly expressed in the prostate tissue, however, other tissues such as bladder, kidney, pancreas, cervix, testis, lung and ovary can also express low amounts of PAP at the mRNA level.

PAP was discovered in the 1930s and was used as a diagnostic biomarker until the identification of PSA. Interestingly, its cellular form decreases as PCa progresses while its secretory form increases with disease progression. The cellular form is described as a tumour suppressor, with prostate tissue expressing low level of PAP being at higher risk of carcinogenesis. Indeed, several *in vitro* and *in vivo* studies with PCa cell lines showed that PAP expression inversely correlates with their growth rate and tumorigenicity.

Apart from being involved in fertility, the role of PAP secretory form is less clear.

Unlike PSA, PAP expression is androgen-independent. The decrease of cellular PAP induces a signalling cascade leading to the survival, proliferation and PSA production of PCa cells in an androgen-independent manner, allowing PCa cells to develop a castration-resistant phenotype (Muniyan, et al. 2013).

PAP relatively restricted expression in prostate tissues makes it a good target for the treatment of prostate cancer. Moreover, PAP is expressed in 95% of primary prostate tumours (Graddis, et al. 2011) and 11% of PCa patients have detectable circulating PAP-specific T helper cells (McNeel, et al. 2001). In addition, serum PAP was found to be increased in patients with bone metastases in comparison to those without metastases (Ahmann and Schifman 1987). Sipuleucel-T vaccine has validated the strategy of therapeutic cancer vaccines and of using PAP as a target for the treatment of PCa. Although it demonstrated clinical benefit by improving the OS of patients by 4 months, its limited efficacy illustrates the necessity of developing new therapeutic strategies.

Its limited efficacy is due, in part, to the immunosuppressive environment of the tumour. Indeed, Fong *et al.* demonstrated the expression of PD-1 on the majority of infiltrating T-cells as well as a small proportion of Tregs at the tumour interface in patients treated with Sipuleucel-T (Fong, et al. 2014).

Previous work conducted at the John van Geest Cancer Research Centre demonstrated that vaccination with a 15mer PAP-derived peptide, containing an HLA-A2 class-I restricted epitope within an HLA-DR1 class-II-restricted epitope, could induce PAP-specific T-cell responses. Furthermore, immunisation with this peptide sequence in a DNA vector format, the ImmunoBody®, generated higher avidity T-cell responses and reduced the tumour growth in established heterotopic TRAMP-C1 murine prostate cancer cell-derived tumours (Saif, et al. 2014). This

sequence was then elongated to 42 amino-acids long in order to increase the number of potential epitopes. The goal was to increase the HLA haplotypes that could present epitopes, thereby becoming applicable to a larger population of patients rather than only to HLA-A2$^+$ patients. Longer peptides, rather than single epitopes, have been shown to induce stronger CD8$^+$ T-cell reactivity *in vivo* (Bijker, et al. 2007) and were able to induce a more efficient and robust protective immune response. Moreover, long synthetic peptides were shown to be highly advantageous by allowing the incorporation of multiple epitopes allowing HLA typing-independent vaccine design (Melief 2008).

A change of amino-acid at position 116 was found to increase the immunogenicity of the previously reported 15mer, this was therefore retained in the elongated sequence. The mutated 42mer PAP-derived peptide was shown to induce stronger PAP-specific T-cell responses towards MHC class-I and class-II epitopes than its WT counterpart which can be explained by its ability to improve the predicted MHC binding score to the epitopes assessed.

This project aims to assess the efficacy of several adjuvant/delivery systems in eliciting strong PAP-specific immune responses and the anti-tumour efficacy of the strongest vaccine strategy in tumour bearing animals.

1.5. Aims of the study

To assess the efficacy of the vaccine, two preclinical murine models were used: C57Bl/6 mice and HHDII/DR1 transgenic mice. In both models, the ability of wild type (WT) and mutated 42mer PAP-peptide sequences to induce PAP-specific immune responses was compared using different delivery systems (peptide-based vaccines *versus* DNA vaccine). Following immunisation, *in vitro* experiments were performed on splenocytes to assess the vaccine-induced PAP-specific immune response as well as the capacity of lymphocytes to recognize and lyse PAP-expressing target cells. These results lead to the selection of the most immunogenic vaccine strategy.

The final aim was to assess the anti-tumour efficacy of the selected vaccine strategy in heterotopic tumour models in both prophylactic and therapeutic settings.

In parallel, the presence of circulating PAP-specific CTLs in the blood of PCa patients was measured to assess whether PCa patients have a pre-existing immune response towards PAP antigen, which differs from that of patients with benign disease.

Chapter 2: Materials and methods

2.1 Materials

2.1.1.Cell culture reagents

	PROVIDER
Media	
TexMACS	MACS Miltenyi Biotec
RPMI 1640	SLS (Lonza)
DMEM	SLS (Lonza)
Opti-MEM®	Thermo Fisher Scientific
CTL wash	Immunospot
Culture media supplements	
Fetal calf serum (FCS)	Fisher (GE Healthcare)
Nu-Serum IV culture supplement	Corning
L-Glutamine	SLS (Lonza)
D-glucose	Sigma
5α-dihydrotestosterone solution (DHT)	Sigma
HEPES	SLS (Lonza)
Sodium Pyruvate	SLS (Lonza)
Pen/strep antibiotic solution	SLS (Lonza)
2-mercaptoethanol	Sigma
Other culture reagents	
Benzonase	Merck
Dimethyl sulfoxide (DMSO)	Insight Biotechnology
Dulbecco's phosphate buffered saline (DPBS)	SLS (Lonza)
Lipopolysaccharide (LPS)	Sigma
Phosphate buffer saline (PBS)	BioWhittaker Europe
Trypan Blue solution 0.4%	Sigma
Trypsin/Versene	SLS (Lonza)
EDTA 0.5M	Ambion
Acetic acid	Fisher Scientific
Anhydrous ethanol	Sigma
Antibiotics	
Puromycin	Sigma
Geneticin (G418)	Sigma
Hygromycin	Sigma
Zeocin	Invitrogen
Cytokines and peptides	
Murine interferon γ	PeproTech
Murine Interleukin 2	PeproTech
Recombinant human IL-2	R&D Systems
Recombinant human IL-15	R&D Systems
Peptides	Genscript

2.1.2.Chemical reagents

	PROVIDER
Agar	Bioline
Ammonium Persulphate (APS)	Geneflow
Ampicillin	Sigma
Bovine serum albumin (BSA)	Merck
Bromophenol blue	Arcos Organics

Butane	Fisher Scientific
Calcium chloride (CaCl2)	Sigma
Chromium-51	Biosciences
Dextran sulphate	Sigma
Double distilled water (ddH2O)	Barnstead, Nanopure
Clarity Western ECL Substrate	Bio Rad
Ethanol	Fisher Scientific
Ethyl alcohol absolute	VWR chemicals
Ethylenediaminetetraacetic acid (EDTA)	Sigma
Gold microcarriers (1.0mm)	BioRad
Glycerol	Sigma
Glycine	Sigma
Isopropanol	Sigma
ISOTON sheath fluid	Beckman Coulter
Lipofectamine 3000 Transfection Reagent	Invitrogen
Liquid nitrogen	BOC
Magnesium chloride (MgCl2)	Sigma
Methanol	Fisher Scientific
Paraformaldehyde	Arcos
Phosphate Buffer Saline (PBS)	Bio Whittaker Europe
Phosphate Buffer Saline (PBS) Tablets	Oxoid
Polyvinyl pyrrolidone (PVP)	Sigma
Protein Assay Dye Reagent Concentrate	Bio-Rad
Protease Inhibitor Cocktail	Sigma
Propidium iodide	Sigma
Protogel (30% Acrylamide mix)	Geneflow
Sodium azide (NaN3)	Sigma
Sodium chloride (NaCl)	Calbiochem
Sodium dodecyl sulphate (SDS)	Sigma
Sodium hydroxide (NaOH)	Fisher Scientific
Spermidine	Sigma
Sucrose	Sigma
2-methylbutane (isopentane)	Acro Organics
TEMED	Sigma
Triton-X-100	Sigma
1M Tris-HCl	Invitrogen
Trizma (Tris) base	Sigma
Tryptone	Sigma
Tween-20	Sigma
Xylene	Fisher Scientific
Yeast extract	Sigma

2.1.3.Antibodies and Flow cytometry/Western blotting reagents

	PROVIDER
Flow cytometry antibodies	Biolegend
Dextramers	Immudex
soluble anti-CD28	Biolegend
soluble anti-CD49d	Biolegend
Human FcR Blocking Reagent	Miltenyi Biotec
Murine FcR Blocking Reagent	Biolegend
LIVE/DEAD Fixable Yellow Dead Cell Reagent	Thermo Fisher Scientific
LIVE/DEAD Fixable Violet Dead Cell Reagent	Thermo Fisher Scientific

BrefeldinA	Biolegend/Sigma
Monensin/Golgi stop	Biolegend/Sigma
Rabbit anti-human PAP	Cell Signalling
Mouse anti-human β-actin	Sigma
Anti-Rabbit IgG HRP-linked Ab	Cell Signalling
Anti-Mouse IgG HRP-linked Ab	Cell Signalling
Precision Plus Protein WesternC Standards	Bio Rad
Precision Protein™ StrepTactin-HRP Conjugate	Bio Rad

2.1.4. Reagent kits

	PROVIDER
Dynabeads Untouched mouse CD8+ T cell isolation	Invitrogen
CytoFix/CytoPerm kit	Invitrogen
PerFix-nc Kit	Beckman Coulter
Murine IFN γ cytokine ELISpot kit	Mabtech
DAB Peroxidase (HRP) Substrate Kit (with Nickel), 3,3'-diaminobenzidine	Vector Laboratories
OneComp eBeads Compensation Beads	Thermo Fisher Scientific
Wizard plasmid DNA miniprep	Promega
RNeasy Mini Kit (250)	QIAGEN
QIAGEN QIAfilter Plasmid Midi	QIAGEN
Taq Universal SYBR green supermix	BIO-RAD

2.1.5. Cell lines

	PROVIDER
TRAMP-C1	ATCC/PROVIDED BY Matteo Belone (Milan University)
TRAMP-C2	ATCC
T2	ATCC
R-MAS	Provided by Colin Brooks (University of Newcastle)
LNCaP	ATCC
HEK-293T	ATCC
B16/HHDII,DR1	Provided by Scancell

2.1.6. Plasmids

	PROVIDER
pBUD CE4.1	Addgene
pGL4.2/puro	Addgene
pLKO.1 puro	Addgene
Lentiviral Envelope and Packaging Plasmids	Addgene
Primers for qPCR	Sigma

2.1.7. Enzymes, buffers and gels

	PROVIDER
dNTPs	Promega
Oligo dT	Promega
KpnI	Promega
XhoI	Promega
AMV reverse transcriptase	Promega
T4 DNA ligase	Promega

RNAse inhibitor	Promega

All enzymes were used in combination with the buffers recommended and provided by the manufacturer.

LB AGAR PLATE	FOR 500 ML
NaCl	5 g
Tryptone	5 g
Yeast Extract	2.5 g
Agar	7.5 g
ddH2O	Up to 500 mL
Autoclaved, cooled down to 50°C	
Ampicillin	100 mg
Kanamycin	50mg
Zeocin	40mg
Poured on Petri dishes, left to solidify and stored at 4°C for up to a week.	
LB BROTH	**FOR 500 ML**
NaCl	5 g
Tryptone	5 g
Yeast Extract	2.5 g
Autoclaved, cooled down to 50°C	
Ampicillin	50 mg
Stored at 4°C for up to a week	
TRIS-EDTA (TE) BUFFER	**FOR 500 ML**
1 M Tris pH 8	5 mL
0.5 M EDTA pH 8	1 mL
ddH2O	Up to 500 mL
TRIS-Acetate EDTA (TAE) BUFFER	**FOR 50x**
1 M Tris base	242g
Disodium EDTA	18.61g
Glacial acetic acid	57.1mL
ddH2O	Up to 1L
Dilute to 1x using distilled water before use, store at 4°C	
4X SDS-PAGE LOADING BUFFER	**FOR 10 ML**
1M Tris-HCl pH 6.8	2.4 mL
Sodium dodecyl sulfate (SDS)	0.8 g
Glycerol	4 mL
DTT	0.5 mL
Bromophenol blue	4 mg
ddH2O	3.1 mL
Aliquots were stored at -80°C.	
5% STACKING GEL	**FOR 6 ML**
ddH2O	4.1 mL
30% Acrylamide mix	1.0 mL
1.0 M Tris (pH 6.8)	0.75 Ml
10% SDS	0.06 mL
10% ammonium persulfate	0.06 mL
TEMED	0.006 mL
10% RESOLVING GEL	**FOR 20 ML**
H2O	6.6 mL
30% Acrylamide mix	8.0 mL
1.5 M Tris (pH 8.8)	5.0 mL
10% SDS	0.2 mL
10% ammonium persulfate	0.2 mL

TEMED	0.008 mL
5X SDS RUNNING BUFFER	**FOR 1 L**
Glycine	94 g
Tris base	15.1 g
10% SDS	50 mL
ddH2O	Up to 1 L

5X Running buffer was diluted with ddH$_2$O to 1X working concentration prior use. Running buffer was stored at 4°C.

TRANSFER BUFFER	**FOR 2 L**
Glycine	5.8 g
Tris base	11.6 g
10% SDS	0.75 g
Methanol	400 mL
ddH2O	Up to 2 L

Transfer buffer was stored at 4°C.

10 X TRIS-BUFFERED SALINE (10 X TBS)	**FOR 1 L**
Trizma base	24.2 g
NaCl	80 g
ddH2O	Up to 1 L
TRIS-BUFFERED SALINE WITH TWEEN (TBST)	**FOR 1 L**
10 X TBS	100 mL
ddH2O	900 mL
Laemilli buffer	**Volume**
10% SDS (w/v) (4% final)	4mL
Glycerol (20%)	2mL
1M Tris-HCL (125mM)	1.2mL
10% 2-mercaptoethanol	1mL
Distilled water	0.8mL
Buffers for tissue cultures	

Trypan Blue: White cell counting solution: 0.1% (v/v) solution of Trypan blue in PBS 0.6% (v/v) acetic acid in PBS

Cell sorting media	**Concentrations**
EMEM	-
L-glutamine	1%
EDTA	3 mM
HEPES	25 mM
Benzonase (95%)	3.513888889
Pen/Strep	2%
Complete T cell media	**Concentrations**
RPMI 1640	-
FCS	10%
L-glutamine	1%
Pen-Strep	2%
HEPES	1%
Fungizone	0.005%
2-mercaptoethanol (to be freshly added)	50mM

2.1.8. Laboratory plastics, glassware and sharps

	PROVIDER
Cell culture flasks (T25,T75,T175)	Sarstedt, UK
Conical flasks (50 ml,100 ml)	Pyrex
Cryovials	TPP

Eppendorf tubes (0.5 ml, 1.5 ml, 2 ml)	Sarstedt, UK
ELISpot plates	Millipore
FACS tubes	Tyco healthcare group
Falcon tubes (50 ml, 15 ml)	Sarstedt, UK
Filter tips (0.5-10µl, 2-20µl, 20-200µl, 200-1000µl)	Greiner bio-one/ Sarstedt
Flat-bottom culture dishes (6, 24, 96-well)	Sarstedt, UK
Glass coverslips	SLS
Glass slides	SLS
Micro tips (0.5-10µl, 20-200µl, 200-1000µl)	Sarstedt, UK
Magnetic cell separators Mini MACS	Miltenyi Biotech
Pasteur pipettes	Sarstedt, UK
Petri dishes	Sarstedt, UK
Pipettes (5mL, 10mL, 25mL)	Sarstedt, UK
Nitrocellulose blotting membrane 0.22µm	GILSON scientific
Scalpels	SLS(Swann Morton)
Multichannel pipette	Sartorius
Syringes (10ml,20ml)	Becton Dickenson
Tefzel tubing	BioRad
Universal tubes (20ml)	Greiner
Western blot filter paper	Schleicher-Schuell
0.45 µm syringe filter	Sartorius
0.22 µm syringe filter	Sartorius
40 µm nylon strainer	Greiner
70 µm nylon strainer	Greiner
25mm Gauge needle	BD microlance

2.1.9. Equipments

	PROVIDER
4°C refrigerators	Lec
-20°C freezers	Lec
-80°C freezers	Revco/ Sanyo
96-well plate reader	Tecan
Autoclave	Rodwell
Bacterial cell orbital incubator 37°C	Stuart
Bacterial cell culture plate incubator 37°C	Genlab
Viral cell culture incubator 37°C, 5% CO_2	IncuSafe
Tissue culture incubator 37°C, 5% CO_2	Sanyo, Binder
Centrifuges	Sanyo, Eppendorf
CCD camera - GBOX –western blot/gel imaging system	Syngene
Class II safety cabinets	Walker
NucleoCounter® NC-250™	Chemometec
FACS cell sorter	Beckman Coulter
Flow cytometer (Gallios)	Beckman Coulter
Haemocytometers	SLS
Heat blocks	Lab-Line
Helios Gene gun	BioRad
Light microscope	Nikon/Olympus
Microcentrifuge	MSE
Mo FloTM cell sorter	Beckman Coulter

Nanodrop 8000 Spectrophotometer	Thermo scientific
NanoDrop ND UV-VIS Spectrophotometer version 3.2.1	Thermo scientific
ELISpot plate reader	**Cellular Technology Limited CTL**
pH meters	Metler Toledo
Pipettes and multichannel pipettes	Gilson, Star Labs, Eppendorf
Plate rocker	VWR, Stuart
Mixer/agitator	Intelli-mixer (ELMI)
Microplate gamma scintillation counter	TopCount (Packard)
Sonicator	VWR
Top count scintillation counter	Packard
Transfer tank	Bio Rad
Tubing prep station	BioRad
Ultracentrifuge Optima TLX	Beckman
Ultrapure water dispenser	Barnstead
Vacuum filtration unit	Sarstedt
Vortex	Scientific industries
Water baths	Clifton

2.1.10.Softwares

	PROVIDER
ELISpot CTL software	CTL
GraphPad Prism 7	Graph Pad software
Kaluza 1.3 version	Beckman Coulter

2.2. Methods

2.2.1.Preparation of target cell lines

2.2.1.1.Cell culture

2.2.1.1.1.Human cell lines

LNCaP cells were obtained from the American Type Culture Collection (ATCC). These cells were grown in RPMI supplemented with 10% fetal calf serum (FCS), 1% L-glutamine, 1% HEPES and 0.20% glucose. LNCaP transfected with the HHDII plasmid were grown in 1mg/mL G418 and those transduced with the Lentiviral plasmid were grown in 1μg/mL puromycin.

HEK293t cells were obtained from the ATCC. These cells were grown in Dulbecco's modified Eagle's medium (DMEM) supplemented with 10% FCS and 1% L-glutamine.

T2 cells were obtained from the ATCC. These cells were grown in RPMI, supplemented with 10% FCS and 1% L-glutamine.

2.2.1.1.2.Murine cell lines

B16F10 HHDII cells were a generous gift from Scancell. This cell line was knocked out for the murine MHC class I and II by Sigma using Zinc finger technology and then knocked in for the human DR1 and a chimeric HHDII (HLA-A0201: human β2M, α1 and α2 but murine α3) by Scancell. These cells were grown in RPMI supplemented with 10% FCS, 500µg/ml G418 and 300µg/ml Hygromycin. B16-HHDII transduced cells to express the human PAP gene were grown with 1µg/mL puromycin.

TRAMP C1 and Tramp C2 cells were obtained from the ATCC. These cells were grown in DMEM supplemented with 5% FCS, Insulin from bovine pancreas (10 mg/ml stock), and 5% Nu-Serum IV culture supplement and 3ng/mL 5α-dihydrotestosterone solution (DHT).
TRAMP-C1 cells were also provided by Matteo Bellone (University of Milan), these cells were grown in DMEM with 10% FCS and 1% L-glutamine.
TRAMP cells transduced with the Lentiviral plasmid were grown in 1µg/mL puromycin.

R-MAS were a generous gift from Colin Brooks (University of Newcastle). These cells were grown in RPMI, supplemented with 10% FCS and 1% L-glutamine.

2.2.1.1.3.Thawing, sub culturing and freezing of cell lines

Cryovials of cells were taken from -80° freezers and thawed quickly in cell culture hood. 20mL of room temperature (RT) cell line required media was added to a 50mL Falcon tube, defrosted cells were transferred and pelleted by centrifugation at 350g for 5 minutes. Supernatant was discarded, pellet was resuspended in media and transferred into a T25 or T75 flask depending on the size of the pellet. Cells were incubated at 37°C 5% CO_2.

When 70%-90% confluency was reached, cells were sub cultured.
For suspension cell lines (T2 and R-MAS), cells in culture media were transferred into a 50mL tubes and centrifuged at 350g for 5 minutes.
For adherent cell lines, media was removed, cells were washed with sterile PBS and 1-2mL RT Trypsin/Versene was added onto the cells and incubated at 37°C until cells detached from the surface. 5-10mL of media was added onto the cells to neutralise the trypsin/Versene and the mixture was transferred into a 15 or 50mL Falcon tube and centrifuged at 350g for 5 minutes.
Following centrifugation, supernatant was discarded and pellet was resuspended in fresh media. Cells were either re-seeded or counted for subsequent use.
Cells to be frozen were resuspended in freezing media (90%FCS + 10% DMSO). Usually, 1/3 of a T75 flask was resuspended in 1mL of freezing media, transferred into a cryovial and frozen at -80°C.

2.2.1.1.4.Cell counting

Cell line suspensions obtained as detailed in section 2.2.1.1.3 were counted using a Haemocytometer for sub culturing purposes. Haemocytometer was wiped with ethanol and a coverslip was placed at the centre. 10µL of cell suspensions was added to 90µL of trypan blue to obtain a 1:10 dilution. 10µL of the dilution was then added onto the edge of the coverslip and cells were counted in the 4 corners with 16 squares under the microscope.

The number of cells per mL was calculated according to this formula:

Concentration = (Total number of cells /number of squares counted) x 10 (dilution factor) x 10^4

Cells obtained from animal tissues (spleens or tumours), from human PBMCs and cell lines for further use in assays (ELISpot, flow cytometry-based or cytotoxicity assays) were counted using the NucleoCounter to obtain more accurate cell concentrations and viability percentages.

Cell suspensions were diluted as required to obtain cell concentrations within the range acceptable for the NucleoCounter ($0.5-5x10^6$ cells/mL). 50µL of the diluted suspension were mixed with 2.5µL of Solution 18 and added onto counting slides before insertion into the NucleoCounter for counting. The percentage of viability and cell concentration were obtained from automatic calculations by the software.

2.2.1.2.Preparation of plasmids: cloning, gel electrophoresis, extraction of DNA from gel, plasmid bulk-up, sequencing

2.2.1.2.1.HumanPAP knock in

pLenti-puro plasmid was obtained from SIGMA in bacterial glycerol stock. The glycerol stock was bulked up in 100mL Laurie Broth media with 100µg/mL ampicillin and incubated overnight at 37°C with shaking at 200rpm. The plasmid was isolated using the QIAGEN Plasmid Midi Kit, according to manufacturer's protocol and the concentration was measured on a Nanodrop instrument.

The human PAP gene was cut out of pBud plasmid using KpnI and XhoI restriction enzymes, it was cut inserted into the pLenti-puro plasmid, the plasmid was then bulked up, extracted, run on a gel to confirm the size and sent to sequencing to confirm the sequence and the correct orientation of the insert. Plasmids were stored immediately at -20°C.
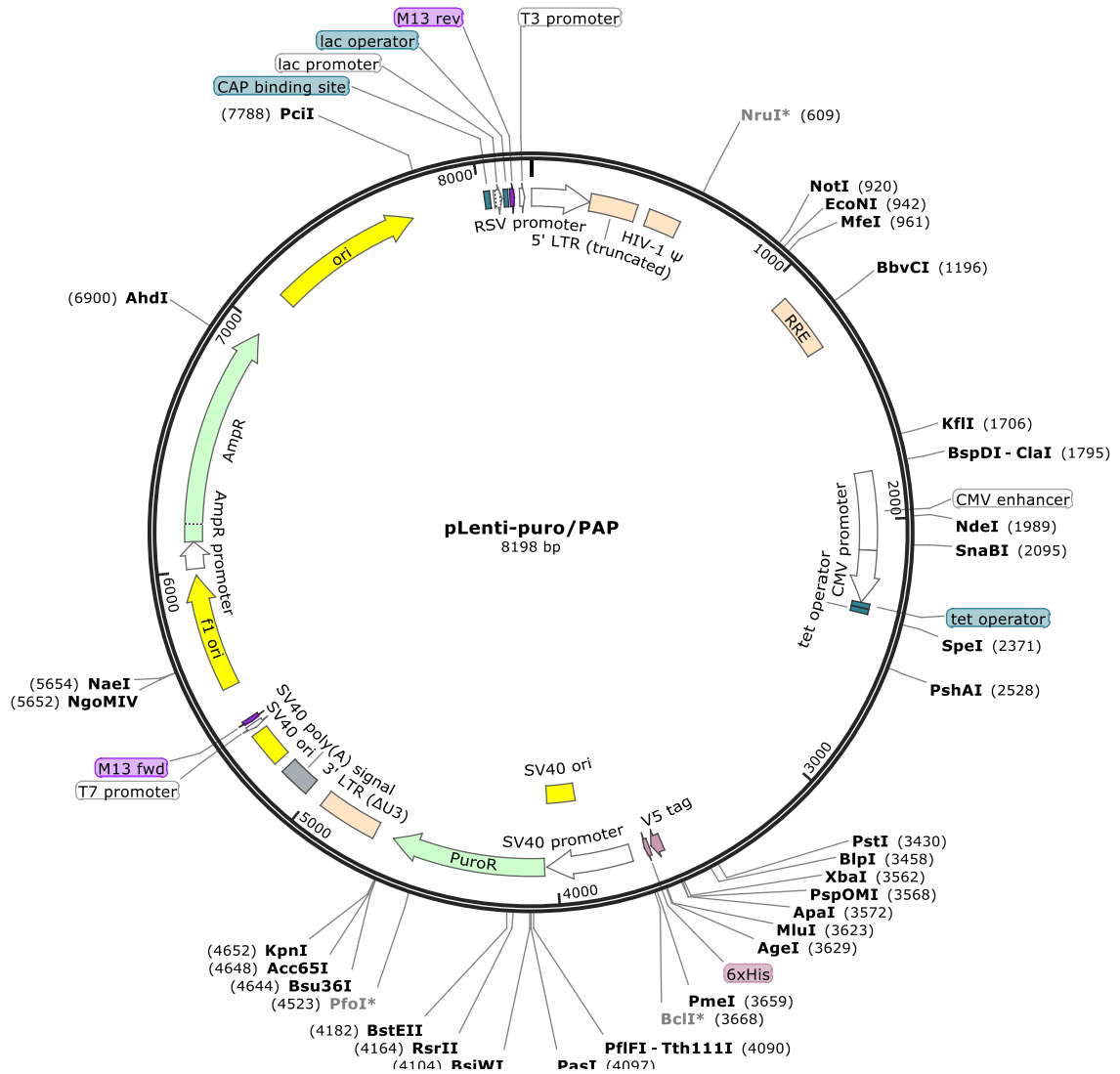
Figure 2.1: pLenti-puro/PAP plasmid map

2.2.1.2.2.MurinePAP and humanPAP knock down

MISSION shRNA plasmids were obtained from SIGMA in Bacterial Glycerol Stock. Two different plasmids were used, one to knock down the human PAP gene and one to knock down the murine PAP gene. The glycerol stock was bulked up in 100mL Laurie Broth media with 100µg/mL ampicillin and incubate overnight at 37°C with shaking at 200rpm. The plasmid was isolated using either the QIAGEN Plasmid Midi Kit or the Wizard® Plus SV Minipreps DNA Purification System, according to manufacturer's protocol and the concentration was measured on a Nanodrop instrument. Plasmids were stored immediately at -20°C.
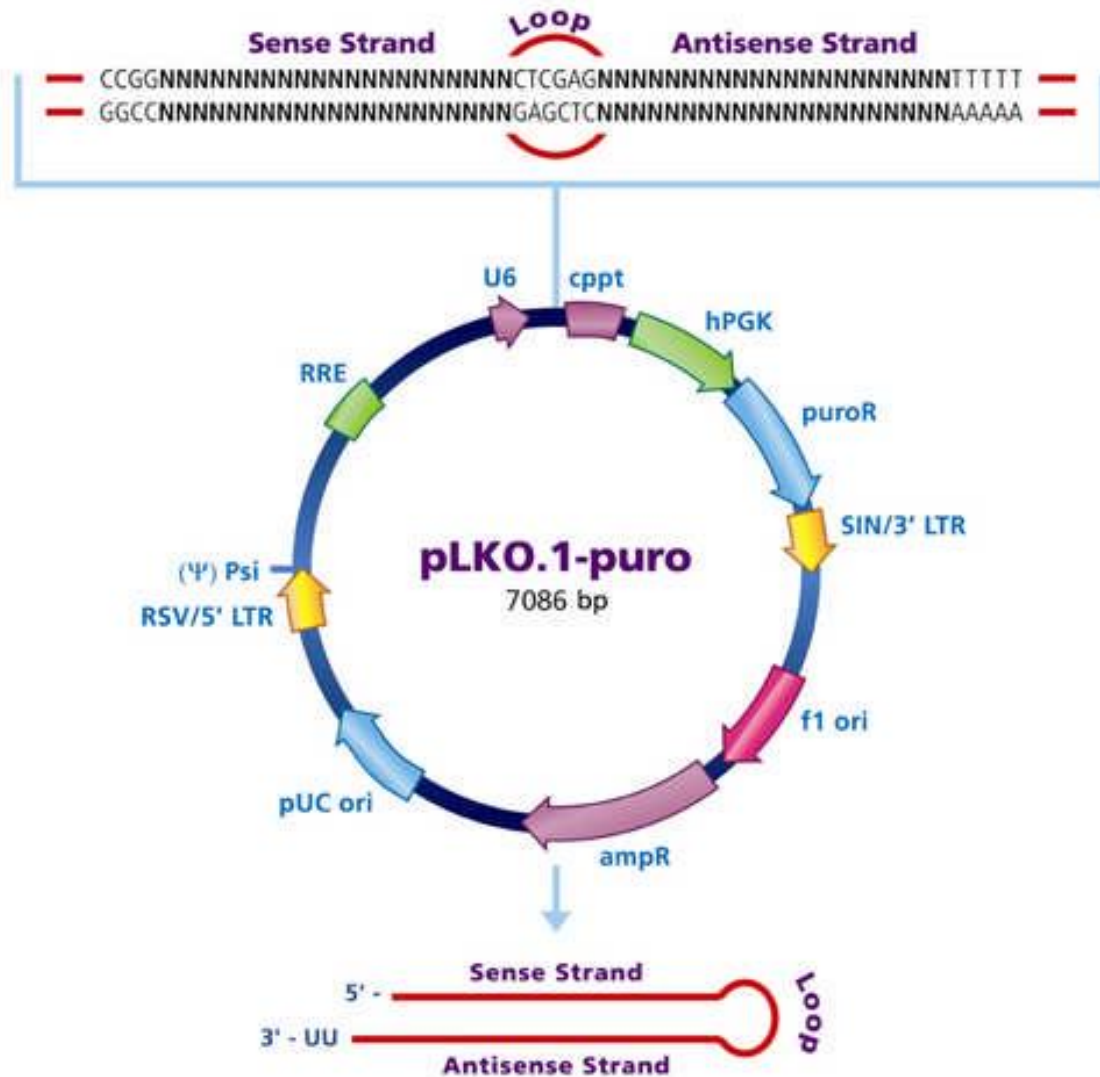
Figure 2.2: pLKO.1-puro plasmid map

2.2.1.3. Lentiviral transduction

2.2.1.3.1. Transfection of packaging cells

HEK293t cells were used as packaging cells to produce viral particles. On day 1, cells were transfected at 50-60% confluency using the lipofectamine 3000 kit by mixing 20μL of Lipofectamine 3000 reagent in 500μL OPTIMEM with 12μL of P3000 reagent in 500μL OPTIMEM and 8μg of plasmid of interest, 6μg of packaging plasmid and 2μg of envelope plasmid. After 30 minutes of incubation at RT, 1mL of the mix was added per T25 flask.

2.2.1.3.2. Virus Collection

Media was changed on day 2, fraction 1 was collected on day 3 and fraction 2 on day 4. Both fractions were filtered through a 450nm filter and immediately frozen at -20°C in cryovials for future use.

2.2.1.3.3.Transduction

Target cells at 70% confluency (LNCaP for the humanPAP knock down; TRAMP-C1 and TRAMP-C2 for the murinePAP knock down) were transduced by adding the virus-containing fractions to the media. The antibiotic for selection of successfully transduced cells, puromycin, was added 24 to 48 hours later at 1μg/mL. The optimal puromycin concentration was previously determined by applying various concentrations and selecting the lowest able to kill 100% of cells within 2 to 4 days.

2.2.1.4.RNA extraction, cDNAs synthesis and RT-PCR

2.2.1.4.1.RNA extraction

Total RNA was extracted from 1-5.10^6 cell pellets (stored at -20°C) using the RNeasy mini extraction kit, according to manufacturer's protocol and the concentration was measured on a Nanodrop instrument. The RNA was stored immediately at -20°C until cDNA synthesis.

2.2.1.4.2.cDNA synthesis

Two μg of RNA in nuclease free water (final volume 9μL) and 1μL of oligo dT were heated at 70°C for 5 minutes. A mix containing 5μL of RT buffer, 1μL of Reverse Transcriptase enzyme, 0.7μL of RNasin, 1μL of dNTP's and 7.3μL of nuclease free water was then added to the reaction and incubated at 40°C for 1 hour. The reaction was heated at 95°C for 5 minutes and frozen immediately at -20°C.

2.2.1.4.3.Real-Time PCR

The RT PCR reaction was performed in a final volume of 13μL by mixing 1μL of cDNA, 6.25μL of Taq Universal SYBR green supermix, 0.5μL of forward and reverse primer (10pM) and 4.75μL of nuclease free water. The relative expression was measured using the 2-^Ct method with one or two housekeeping genes.

Table 2.1: Real-Time PCR conditions

Cycle	Cycle Point
Hold	Hold @ 95°C, 5min 0s
Cycling (35 repeats)	Step 1: Hold @ 95°C, 10s
	Step 2: Hold @ 58°C, 15s
	Step 3: Hold @ 72°C, 20s, acquiring to Cycling A
Melt	Ramp from 58°C to 95°C
	Hold for 90s on the 1st step
	Hold for 5s on next steps,Melt A

Table 2.2: Real-Time PCR primers sequences

Gene	Forward primer	Reverse primer
hHPRT	TGACACTGGCAAAACAATGCA	GGTCCTTTTCACCAGCAAGCT
hPAP	GAGAAGGGGGAGTACTTTG	CTGTTTGTGGTCATACACTC
mHPRT	TGCTCGAGATGTCATGAAGG	TATGTCCCCCGTTGACTGAT
mGAPDH	ACACATTGGGGGTAGGAACA	AACTTTGGCATTGTGGAAGG
mPAP	AAAAGCTGGTCATGTATTCC	GAGGCAGAACTCCATTATA

2.2.1.5.Western Blotting for hPAP

2.2.1.5.1.Sample preparation

PAP protein being secreted, the supernatant of cells in culture was used as a sample instead of cell lysates. B16-HHDII cells were cultured overnight in a confluent T75 flasks with 3mL of media, allowing to just cover the cells to concentrate the protein. 80µL of the supernatant mixed 1:2 with 2X Laemmli buffer was then loaded per well of 1mm, 5-well comb.

2.2.1.5.2.SDS-page and transfer

The gel was run at 100V through the 5% stacking gel and at 130V through the 10% resolving gel for 2 to 3 hours. Proteins were then transferred onto a nitrocellulose membrane for 60 minutes at 100V by wet transfer.

2.2.1.5.3.Immunoprobing

Membranes were stained with Ponceau to ensure the transfer of proteins onto the membrane. The membrane was blocked with 5% skimmed milk powder in TBST for 1hr at RT under constant agitation, washed 5 times for 5 minutes in TBS- 5% tween-20 at RT and then incubated overnight at 4°C with 1:1000 rabbit anti-humanPAP primary antibody in 5% skimmed milk powder in TBS- 5% tween-20. After 5 washes for 5 minutes in TBS- 5% tween-20 at RT, the membrane was incubated with 1:1000 secondary anti-rabbit antibody in 5% skimmed milk powder in TBS- 5% tween-20 for 1hr at RT. After 5 washes for 5 minutes in TBS- 5% tween-20 at RT, the revelation was performed using ECL chemi-luminescence kit.

2.2.1.6.Peptide binding assay for T2 and R-MAS cells

R-MAS or T2 cells were incubated at 26°C overnight to increase the number MHC class-I molecules at the surface of cells. 1 million of cells were incubated for 1 hour (R-MAS cells) or overnight (T2 cells) in 1mL of media containing different concentrations of peptide of interest. Two 9-mer peptides were used: ILL for T2 cells (HLA-A2) and ISI for R-MAS (H2-Db). Six concentrations were tested: 0; 1; 2; 10; 50 and 100µg/mL. Cells were washed in their respective media, counted and 0.5 million were stained with 0.5µL of live dead violet and 1µL of FITC anti- H2-K^b-D^b antibody or 2.5µL of APC anti-HLA-A2 antibody. After washing in PBS and resuspension in Isoton, cells were acquired on a Gallios flow cytometer. Results were analysed on Kaluza software.

2.2.1.7.Interferon γ treatment

Murine cell lines (TRAMP-C1 and TRAMP-C2) at 70% confluency were treated with murine IFNγ respectively. Six concentrations were tested: 0; 0.1; 1; 2; 5 and 10 ng/mL. After 24 hours of

treatment, cells were harvested, counted and 0.5 million were stained with 0.5µL of live dead violet, 1µL of FITC anti- H2-K^b-D^b antibody and 1µL of PE anti-murine PD-L1 antibody. After washing in PBS and resuspension in 300µL Isoton, cells were acquired on a Gallios flow cytometer. Results were analysed on Kaluza software.

2.2.2. Optimisation of the vaccination and assessment of the anti-tumour efficacy of the vaccine

Pre-clinical studies were approved by the Home Office under the Animals (Scientific Procedures) Act under two Project Licences (PPL):

1. 40/3563 valid until the 5th December 2016
2. PB26CF602, granted on the 28th of November 2016 and valid until the 28th of November 2021.

2.2.2.1. Mouse models: HHDII/DR1 and C57Bl/6 mice

Humanized HHDII/DR1 males were bred at Nottingham Trent University animal facility in accordance with the Home Office Codes of Practice for the Housing and Care of Animals. These animals are HLA-A2.1/HLA-DR1- transgenic C57Bl/6 mice. C57Bl/6 mice were purchased from Charles River. Both were used between 7 to 18 weeks old at the start of treatment.

2.2.2.2. Peptides, adjuvants: CpG and CAF09; and ImmunoBody DNA vaccine for Immunisation

2.2.2.2.1. Peptides

Peptides were purchased from GeneScript (USA), resuspended at 10mg/mL in 100% DMSO and stored at -80°C.

Table 2.3: Human and murine PAP42mer peptide sequences

HHDII/DR1 mice Human peptides	Peptide sequences	C57Bl/6 mice Murine peptides
	1 YIRSTDVDRTLMSAMTNLAALFPPEGISIWNPRLLWQPIPVH 42	WT
	1 YIRSTDVDRTLMSLMTNLAALFPPEGISIWNPRLLWQPIPVH 42	1 mutation
WT	1 YIRSTDVDRTLMSAMTNLAALFPPEGVSIWNPILLWQPIPVH 42	2 mutations
1 mutation	1 YIRSTDVDRTLMSLMTNLAALFPPEGVSIWNPILLWQPIPVH 42	3 mutations

2.2.2.2.2. Adjuvants

CpG ODN nucleotide was purchased from Eurofins. CAF09 adjuvant is a liposomal cationic adjuvant developed to generate CD8+ T-cell responses and was a generous gift from Dennis Christensen (Statens Institut, Copenhagen).

2.2.2.2.3. ImmunoBody DNA vaccines

ImmunoBody DNA vaccines were a generous gift from Lindy Durrant (Scancel, Nottingham). The plasmids encoding for the ImmunoBody were bulked up and isolated as described in 2.2.1.2 using law salt Laurie Broth media and 40µg/mL of zeocin antibiotic.

ImmunoBody DNA vaccines were administered to mice using DNA bullets. The preparation consisted in coating expression vectors encoding the IB-PAP42mer onto 1µm gold particles. 200µl of 0.05M spermidine was mixed to 16.6mg of gold microcarriers, then, 36µg of DNA was added to this mixture. Following 5 seconds of sonication, 200µl of CaCl2 (1M) were added dropwise to the mix. For it to precipitate, the mixture was incubated at RT for 10 minutes. The suspension was then washed twice in absolute Ethanol and resuspended in 2ml of PVP solution (0.025mg/ml). After sonication, the solution was loaded into the tubing (Tefzel) and allowed to settle for 10min using a tubing preparation station (Bio-Rad). Following the removal of ethanol using a syringe, the tube was dried using 0.3L/min flowing Nitrogen. Once dried, the tubing was cut using a guillotine. DNA bullets were stored at 4°C until use.

2.2.2.3. Immunisation procedures

For each experiment, mice were immunised 3 times according to the following immunisation schedule.

| Day 1 Prime | Day 14 Boost | Day 28 Boost | Day 35 Splenocytes harvest |
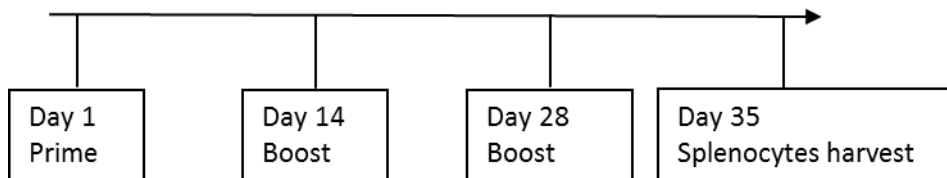
Immunisation using peptide and CpG adjuvant were prepared by mixing 50µg CpG and 30µg of PAP42mer peptide in a final volume of 100µL of PBS. The solution was administered by intramuscular injection at the base of the tail (50µL each side of the base of tail).

Immunisation using peptide and CAF09 adjuvant were prepared by mixing 100µL of CAF09 and 30µg of PAP42mer peptide in a final volume of 200µL of PBS containing 9% sucrose. The solution was administered by intraperitoneal injection.

Immunisation using ImmunoBody DNA vaccines were performed by firing one bullet containing 1µg of DNA using a Helios gene gun (Bio-Rad).

2.2.2.4. Tumour implantation

Cells were harvested as described in section 2.2.1.1.3, counted as described in section 2.2.1.1.4 using the NucleoCounter for accuracy and prepared in either serum free media or in sterile PBS at

the required concentration: 3×10^6 cells/mL for B16-HHDII-PAP cells and 50×10^6 cells/mL for TRAMP-C1 cells. 100µL of the cell suspension was then injected subcutaneously per animal.

2.2.2.5. Processing of tissue samples

2.2.2.5.1. Isolation of splenocytes

Spleens from immunized mice were harvested and placed in a tube containing T-cell media. Each spleen was placed into a sterile petri dish containing 10ml T-cell media and flushed with another 10ml of media using a syringe. The cell suspension was centrifuged at 300g for 10min and re-suspended in 5ml of T-cell media. Cells were then counted using the cell counter NucleoCounter as in 2.2.1.1.4.

2.2.2.5.2. Isolation of tumour cells

Tumours were harvested from animals upon reaching the maximum tumour volume and placed in a tube containing T-cell media. In order to obtain single cell suspensions for flow cytometry assays, tumours were put in a petri dish containing 10mL of T-cell media (50µg/mL of DNase I and 0.1u/mL of collagenase IV) and cut into small pieces using scalpels. The tissue mixture was transferred into a 50mL Falcon tube and setup to gently swirl for 30 minutes (B16 tumours) or 1-2hrs (TRAMP-C1 tumours) at 37°C to help cell dissociation. The mixture was then mashed using the back of a 10mL syringe against a 70µm cell strainer. Another 10mL of T-cell media was used to rinse the cell strainer. The 20mL mixture was then centrifuged at 400g for 5 minutes and resuspended in 2mL (B16 tumours) or 5mL (TRAMP-C1 tumours). 100-200µL of cell suspension was taken into a FACS tube and washed with 2mL of PBS at 400g for 5 minutes before staining with antibodies.

2.2.2.6. IFNg ELISPOT assays

The number of IFNγ releasing PAP-specific T-cells was measured using a murine IFNγ Elispot assay. 96-well filtration plates were activated by adding 50µl/well of 70% Ethanol and washed 5 times with deionised H2O at 200µl/well. Plates were then coated with 50µl of coating antibody (AN18) diluted 1:1000 in sterile PBS and incubated overnight at 4°C. The following day, plates were washed 4 times with sterile PBS and incubated with 100µL/well of T-cell media for 30 minutes at 37°C. After removal of the T-cell media, 0.5×10^6 splenocytes/well were plated in a final volume of 100µL/well. Cells were stimulated with MHC class-I and class-II peptides (see tables 3.2 and 3.3) at 1µg/mL and 10µg/mL respectively in 100µL/well so that the final volume in each well was 200µL/well. Cells with T-cell media alone were used as a negative control. After 48hours of incubation at 37°C, plates were washed 5 times with 200µL/well of PBS+0.05% Tween20. 50µL/well of the biotinylated-detection-antibody (R4-6A2) diluted 1:100 in PBS was added for 2 hours at RT followed by 5 washes again. Then, 50µL/well of streptavidin-AP (AP-conjugate substrate system) diluted 1:100 in PBS was added

for 1hour and 30 minutes at RT. Finally, plates were washed 6 times and the development solution, prepared according to manufacturer's instruction, was added followed by a 10 to 30 minutes incubation in the dark. Once the spots were visible, the reaction was stopped by washing the plates under running tap water. Plates were left to dry overnight. The number of spots were quantified using an Elispot plate reader.

2.2.2.7. Immunophenotyping of splenocytes and TILs

Multi-color flow cytometry was used to assess the expression of activation and exhaustion markers on the surface of T-cells as well as for assessing the presence memory T-cells.

$1x10^6$ of fresh splenocytes were washed in 2mL PBS by centrifugation at 400g for 5 minutes and incubated for 10-15 minutes with 1μL of anti-CD16/CD32 antibody to block their FcR (1μg/tube) for 15 minutes at 4°C. Cells were then incubated with surface antibodies for 30 minutes at 4° in the dark, washed in 2mL PBS by centrifugation at 400g for 5 minutes and resuspended in 300μL isoton. Cells were finally acquired on a Gallios flow cytometer and results were analysed on Kaluza software.

Table 2.4: List of flow cytometry antibodies for exhaustion and memory panel

	Common		Memory panel		Exhaustion panel	
	Antibody	Quantity μg / Volume μl	Antibody	Quantity μg / Volume μl	Antibody	Quantity μg / Volume μl
FITC FL1			CD62L	0.25μg / 0.5μL	GITR (CD357)	1μg / 2μL
PE FL2					OX-40 (CD134)	0.25μg/1.25μL
PE-efluor610 FL3					CTLA-4 (CD152)	0.5μg/2.5μL
PerCp-Cy5.5 FL4					LAG-3 (CD223)	0.5μg/2.5μL
PE-Cy7 FL5					Tim-3 (CD366)	0.5μg/2.5μL
APC FL6			CD44	0.25μg/1.25μL	PD-1	0.5μg / 2.5μL
Alexa-fluor700 FL7	CD4	0.25μg/0.5μL				
APC-Cy7 FL8	CD8	0.5μg/2.5μL				
BV421 FL9	CD45	0.2μg/1μL				
FL10	Live dead	0.5μL				

Intracellular flow cytometry was used to assess the peptide-specific cytokine release, proliferation and degranulation of T-cells by performing Intracellular Cytokine staining (ICS). 1x10^6 fresh splenocytes/well were seeded in 100μl in a 96-wel plate. Three wells/mice were prepared, one containing 100μl of media (negative control), one containing 100μl of class-I peptide (1μg/ml final concentration) in T-cell media and one containing 100μL of class-I peptide (1μg/ml) and class-I peptide (10μg/ml) in T-cell media. Cells were incubated with anti-CD28 and anti-CD49d antibodies (1μg/mL) for co-stimulation, for 1 hour at 37°C. Brefeldin A (5μg/ml) and monensin (2μM) were added to stop the Golgi transport and cells were left at 37°C for a further 5 hours. The plate was then kept at 4°C overnight until staining the following day. Splenocytes were transferred into FACS tubes, washed with 3mL of PBS and resuspended in 50μL FCS. The Fc Receptor was further blocked

using 1μL of anti-CD16/CD32 antibody (1μg/tube) for 15 minutes at 4°C. Surface antibodies were added and incubated for 15 to 30 minutes at 4°C in the dark.

The PerFix-nc Kit (no centrifuge assay kit) was used to fix and permeabilize cells. Cells were fixed with 25μL of fixative agent R1 for 15minutes at 4°C in the dark and permeabilized with 300μl of permeabilizing reagent R2. Intracellular antibodies were added and incubated for 15 to 30 minutes at 4°C in the dark.

Cells were washed with 3mL of 1X R3, re-suspend in 250-300μl of 1X R3 and acquired on a Gallios flow cytometer. Results were analysed on Kaluza software.

The protocol was provided by our collaborator Dennis Christensen (Statens Institut, Copenhagen) who had showed that overnight incubation of splenocytes did not affect the cytokine expression.

Table 2.5: List of flow cytometry antibodies for ICS staining

	Antibody	Fluorochrome/FL	Quantity μg / Volume μl
Surface Abs	CD107a	FITC FL1	1.5μg / 3μl
	CD4	Alexa-fluor700 FL7	0.25μg / 0.5μl
	CD8	APC-Cy7 FL8	0.5μg / 2.5μl
	CD45	BV421 FL9	0.2μg / 1μl
	Live dead	FL10	0.5μl
Intra-cellular Abs	TNF-a	PE FL2	0.25μg / 1.25μL
	Ki67	PE-efluor610 FL3	0.125μg / 0.3μl
	IL-2	PerCp-Cy5.5 FL4	0.6μg / 3μl
	IFNg	PE-Cy7 FL5	0.6μg / 3μl
	Granzyme B	APC FL6	0.5μg / 2.5μl

2.2.2.8. *In vitro* stimulation and killing assays

2.2.2.8.1. Generation of LPs-blast

Splenocytes were stimulated *in vitro* for 6 days to then assess their capacity to kill relevant target cells. LPS-blast were generated to be used as APCs to re-stimulate vaccine-specific T-cells *in vitro*. Spleens from naive mice were treated with LPS (25μg/mL) and Dextran sulphate (7μg/mL) for 48 hours at 37°C. Splenocytes were then washed, treated with mitomycin C (1μg/1x10^6 splenocytes) for 20 minutes at 37°C, washed in T-cell media 4 times and then incubated for 1hr 15 minutes at 37°C with a cocktail of class I peptides at 1 μg/ml (ILL for HHDII/DR1 mice experiments and ISI and SIW for C57Bl/6 mice experiments). Cells were washed, counted and diluted in T-cell media for future use.

2.2.2.8.2. *In vitro* stimulation of splenocytes

30x10^6 splenocytes from each immunised mouse was seeded in T-cell media into 24 well plates at a concentration of 5x10^6/2mL (6 wells/mice). Cells were grown 6 days at 37°C in media containing 50U/mL of mIL-2, 2mM of β-mercaptoethanol and LPS-blasts at a 1:10 ratio (1 LPS-blast for 10 splenocytes from immunised mice).

2.2.2.8.3.51Cr killing assays

Stimulated splenocytes were harvested, counted and seeded in 100µL in 96-well plate (round-bottom) according to the effector:target ratio. Four different effector:target ratios were used: 100:1 (500,000:5,000), 50:1 (250,000:5,000), 25:1 (125,000:5,000), 12.5:1 (62,500:5,000). Target cells were harvested, counted and $2x10^6$ cells were labelled with 1.85 MBq of ^{51}Cr. Cells were incubated for 1hr at 37°C in a water bath followed by 4 washes with specific-cell lines media. For R-MAS and T2 cells, cells were incubated for 1hr at 37°C with class I peptides at 1 µg/ml (ILL for HHDII/DR1 mice experiments and ISI or SIW for C57Bl/6 mice experiments). Cells were then washed 1 more time, counted, diluted in specific-cell lines media and seeded at $5x10^3$ cells/well in 100µL into the 96-well plates containing effector cells. Following 4 hours of incubation at 37°C, 50µL of the supernatant of each well was transferred to Luma plates. Plates were left to dry overnight and were read on the Top Count machine. Target cells alone with media were used as negative control (spontaneous release) and target cells with media and 10µL of 10% SDS were used as positive control (maximum release). Cytotoxicity was calculated according to the following formula:

$$\frac{\text{(Experimental release – spontaneous release)}}{\text{(Maximum release – spontaneous release)}} \times 100 = \textbf{\% of Cytotoxicity}$$

2.2.2.8.4.Negative selection of CD8+ T-cells

CD8+ T-cells were isolated from total splenocytes following 6 days of *in vitro* stimulation with class-I epitopes using the Dynabeads Untouched mouse CD8+ T cell isolation. Manufacturer's protocol was followed.

2.2.2.8.5.Flow-cytometry-based cytotoxicity assay

Target cells (LNCaP cell line) were harvested as described in 2.2.1.1.3 and $1x10^6$ cells was labelled with PK26 fluorescent dye. Manufacturer's protocol was followed. Briefly, cells were washed in serum-free media at 350g for 5 minutes and supernatant was discarded in order to leave no more than 25µL of residual media on the pellet. Cells were resuspended gently with the diluent C provided, by pipetting several times to ensure single cell suspension. A 2X working solution of PKH26 dye (4µM) in diluent C was prepared by mixing 0.8µL of the 1mM stock solution of PK26 dye with 200µL of diluent C. The 200µL cell solution was then added rapidly to the 2X working dye solution to obtain a 2µM final concentration and mixed by pipetting several times. Cells were incubated with the dye for 2-5 minutes and the reaction was stopped by adding an equal volume (400µL) of FCS. Cells were centrifuged at 350g for 5 minutes and then washed three times with complete media. Cell were then counted using the NucleoCounter as in 2.2.1.1.4.

Labelled-target cells and splenocytes were seeded in FACS tubes according to the effector:target ratio and co-incubated for 3 hours. Three different effector:target ratios were used: 20:1 (400,000:20,000), 10:1 (200,000:20,000), 5:1 (10,000:20,000).

At the end of the incubation, cells were washed in PBS and stained with 1μL per tube of LIVE/DEAD Fixable Yellow Dead Cell Reagent (in 100μLof PBS) for 20-30 minutes in the dark. Cells were then topped up with 300μL of Isoton and acquired on a Gallios flow cytometer. Results were analysed on Kaluza software.

Target cells alone were used to determine the spontaneous percentage of dead target cells.

Cytotoxicity was calculated according to the following formula:

$$\frac{(\% \text{ dead target cells} - \% \text{ spontaneous dead target cells})}{(100 - \% \text{ spontaneous dead target cells})} \times 100 = \textbf{\% of Cytotoxicity}$$

2.2.3.PBMC work

Ethical approval for using Human clinical material:

1. Ethical approval for the collection of peripheral blood and the analysis of peripheral blood mononuclear cells (PBMCs) from prostate cancer patients was provided under EoSRES ref no: 14/ES/1014

Whole blood sample from patients with prostate cancer were taken and provided by Dr Masood Khan (Leicester Hospital).

2. Ethical approval for the collection of peripheral blood and the analysis of peripheral blood mononuclear cells (PBMCs) from healthy donors has been provided under application number 435

2.2.3.1.Isolation of PBMCs

PBMCs were isolated from whole blood using Leucosep tubes. Firstly, 15mL of Lymphocyte Separation Medium (LSM) was added per leucosep tube and a quick centrifugation was performed to pass the LSM through the membrane. 30mL of blood diluted in PBS at a 1:1 ratio was then added to the leucosep tubes and centrifuged at 800g for 20 minutes at RT with brakes off. The layer of PBMCs was then collected by pouring the cell suspension into a Falcon tube. The tube was topped up with PBS up to 50mL and centrifuged at RT at 800g for 10 minutes. This washing step was repeated one more time, the pellet was resuspended in 2mL of FCS and cells were counted with the NucleoCounter as described in 2.2.1.1.4.

PBMCs were tested for HLA-A2 expression using an APC-conjugated antibody.

2.2.3.2.Freezing of PBMCs

PBMCs were frozen as described in 2.2.1.1.3 at 10×10^6 cells/mL. Cells were firstly frozen at -80°C for at least 24hrs and then transferred to a liquid nitrogen tank for long-term preservation.

2.2.3.3.Expansion protocol

Cryopreserved PBMCs were thawed out in a prewarmed CTL thaw solution (RPMI with 10% CTL thaw solution and 0.02% benzonase) and then centrifuged at 400g for 10 minutes. The PBMCs were resuspended in 10mL TexMACS media and incubated 37°C, 5% CO_2 for 2hrs. The cells were then centrifuged at 300g for 10 minutes and counted using the NucleoCounter as described in 2.2.1.1.4. PBMCs were prepared at 2×10^6 cells/ml in TexMACS media and 2×10^6 cells were seeded per well in a 24-well plate (number of wells per patient depended on the number of PBMCs recovered).

PBMCs of each patient were stimulated with 3 different conditions: 1) hPAP42mer mutated peptide, 2) ILL 9mer peptide and 3) a mix of EBV, CMV and FLuA class-I peptides. The peptides mixes were prepared in TexMACS media: ILL peptide at 1µg/ml, hPAP42mer mutated peptide at 10µg/ml and CMV/EBV/FluA cocktail at 2µg/ml for each peptide. PBMCs were then incubated at 37°C, 5% CO_2. Following four days of culture, IL-2 and IL-15 were added to each well at 10IU/ml and 10ng/ml respectively. One further mL of TEXMACS media was added per well and PBMCs were incubated for a further six days at 37°C, 5% CO_2.

On Day 10, PBMCs were transferred into Falcon tubes, each well was gently rinsed with pre-warmed TexMACS media and the cell suspension was centrifuged at 300g for 10 minutes. PBMCs were resuspended in TexMACS media with 10IU/mL of IL-2, re-seeded in the 24-well plate an incubated for a further 2 days.

On day 12, cells were washed as described above, counted with the NucleoCounter and used as required for Dextramer staining and cytotoxicity assays.

2.2.3.4.Dextramer staining

1×10^6 cells were transferred into FACS tubes and washed with PBS by centrifugation at 400g for 5 minutes. Cells were then resuspended in 90µL PBS and 10µL FcR blocking agent was added for 10 minutes at 4°C in the dark. 10µl of control dextramer, ILL dextramer or CMV dextramer was added to the appropriate tubes and incubated for 10 minutes at 4°C in the dark. CD8, CD3 and CD19 antibodies were added to each tube and incubated for 30 minutes at 4°C in the dark. Cells were then washed in PBS by centrifugation at 400g for 5 minutes, resuspended in 300µl isoton and acquired on a Gallios flow cytometer. Results were analysed on Kaluza software.

Table 2.6: List of flow cytometry antibodies for dextramer staining

Antibody	Provider	Volume (µL)
Dextramers	Immudex	10
CD8 APC/Fire750	Biolegend	2.5

CD3 PE/Dazzle594	Biolegend	2.5
CD19 Brilliant violet 421	Biolegend	2.5
Live dead yellow	Invitrogen	0.5

2.2.3.5.Cytotoxicity assays

Cytotoxicity assays were performed as described section 2.2.2.8.5 using PBMCs instead of splenocytes. Two different effector:target ratio were used: 5:1 (350,000:70,000) and 1:1 (70,000:70,000).

2.2.4.Statistical analysis

Statistical analysis for all experiments were performed using GraphPad Prism 7 software. p-values were calculated using either Student's t-test with two-tailed distribution or Two-way/one-way ANOVA as stated. Values of $p < 0.05$ were considered to be statistically significant.

Chapter 3: Optimisation of the vaccination strategy to enhance the immunogenicity of the PAP42mer vaccine

3.1. Introduction

The main challenge when developing therapeutic cancer vaccines is choosing the right antigen. PAP protein as an appropriate target antigen when developing a therapeutic vaccine against PCa was discussed in the introduction. In brief, PAP expression is mainly restricted to the prostate, with some expression in other tissues, but at a much lesser magnitude than its expression within prostate tissues (Graddis, et al. 2011). The secretory form of PAP is overexpressed during PCa (Kong and Byun 2013). Finally, the strongest argument for using PAP as a target for the development of a vaccine against PCa is the FDA-approval of Sipuleucel-T in 2010 for the treatment of mCRPC patients. It confirmed the pertinence and safety of targeting PAP for the treatment of PCa.

Besides the choice of the antigen being crucial when developing a vaccine, the choice of the delivery system used also is, as it affects its capacity to generate an effective immune response. The different types of vaccine delivery systems can be divided into 4 categories: tumour cell vaccines, DC vaccines, protein/peptide-based cancer vaccines and DNA/RNA-based vaccines (Guo, et al. 2013). This study focuses strictly on peptide-based cancer vaccines and DNA vaccines. Regarding peptide-based vaccines, the other parameter to consider, other than the choice of the target, is the choice of the immunostimulatory adjuvant. This study focuses on two adjuvants that induce an innate immune response by stimulating APCs: CpG and CAF09, a poly I:C like synthetic molecule. Although no peptide-based vaccine for the treatment of cancer has yet shown sufficient efficacy to be FDA-approved, many phase I and II clinical trials are ongoing in many different type of cancers, including PCa, using either short TAA-derived peptides or synthetic long peptides (Bezu, et al. 2018).

CpG Synthetic oligonucleotides (ODN) target TLR9 (Toll like receptor 9), which are expressed by plasmacytoid DCs and B cells (Scheiermann, et al. 2014). The resulting innate immune response is characterised by the production of Th1 and pro-inflammatory cytokines. Numerous clinical trials have evaluated the use of CpG ODN as a vaccine adjuvant and showed that it could improve antigen presentation and generate vaccine-specific cellular responses.

CAF09 is a poly I:C like synthetic molecule that binds to TLR-3 receptors expressed by myeloid DCs and macrophages. Its binding induces the production of pro-inflammatory cytokines and chemokines (Korsholm, et al. 2014). CAF09 has been used in preclinical studies and is now undergoing phase I clinical with a Bcl-Xl peptide for the treatment of PCa patients with lymph node metastases (NCT03412786).

DNA vaccines have also confirmed their efficacy in cancer. Indeed, evaluation of a DNA vaccine targeting PAP has been discussed in section 1.4.2.2.

The DNA vaccine assessed in this study, ImmunoBody®, has two mechanisms of action: direct presentation by transfection of APCs and cross-presentation by uptake via the Fc Receptor (Metheringham, et al. 2009). The SCIB1 cancer vaccine uses the ImmunoBody® technology to target two antigens (TRP2 and gp100) and has been assessed in a phase I/II clinical trial for the treatment of melanoma (Patel, et al. 2018). The study showed that the DNA vaccine was well tolerated and induced T-cell responses in patients.

Previously published data have demonstrated that a 15 amino-acid sequence, PAP 114-128 HLA-DR1 peptide, containing the PAP115-123 HLA-A2 peptide, could elicit peptide-specific T cell responses after immunisation into transgenic HHDII/DR1 humanised mice. Higher avidity T cell responses in C57Bl/6 and HHDII/DR1 mice were generated by incorporating this sequence into the backbone of the ImmunoBody® DNA vaccine. Moreover, the DNA vaccine could produce an anti-tumour response against pre-established TRAMP C1 murine prostate cancer cell-derived tumours (Saif, et al. 2014).

The elongation of this 15mer peptide to a 42 amino acids sequence and the introduction of a point mutation increased the number of potential class-I and II epitopes and the immunogenicity of the peptide, rendering it foreign in order to break tolerance against PAP. The improved predicted peptide-MHC binding score towards several epitopes is shown Table 3.2.

The aim of this chapter is to evaluate the immunogenicity of the wild-type vs mutated PAP42mer vaccine and the effect of the different adjuvants (CpG, CAF09 and ImmunoBody®). This was assessed in two mouse models. It is important to point that the sequence of the PAP42mer peptide is different between human and mouse, in that there are two amino acids that differ between the 2 sequences, as shown in Table 3.1.

The C57Bl/6 model allowed to determine if the vaccine was sufficiently immunogenic to induce an effective immune response against PAP and therefore to break tolerance against PAP protein, as this self-antigen is expressed in normal prostate tissue. The HHDII/DR1 humanized model allowed the evaluation of the vaccine in an HLA-A2/ DLA-DR1 context, which is relevant and translatable to the human setting. Firstly, the vaccine approach was optimised by incorporating mutations in the PAP42mer sequence and assessing the effect of these mutations on the immunogenicity of the vaccine. The PAP-specific immune response elicited after vaccinating the animals with the mutated peptides or their WT counterpart was compared. Secondly, the PAP-specific immune response elicited when using the selected sequence in combination with different delivery systems: two peptide-based vaccines and a DNA-based vaccine (ImmunoBody®) was also assessed.

These results permitted us to select the vaccine strategy capable of inducing the most effective

immune response against PAP and to assess its potential as a PCa therapeutic vaccine.

Table 3.1: List of human and murine, WT and mutated PAP42mer peptides

HHDII/DR1 mice Human peptides	Peptide sequences	C57Bl/6 mice Murine peptides
	1 YIRSTDVDRTLMSAMTNLAALFPPEGISIWNPRLLWQPIPVH 42	WT
	1 YIRSTDVDRTLMSLMTNLAALFPPEGISIWNPRLLWQPIPVH 42	
WT	1 YIRSTDVDRTLMSAMTNLAALFPPEGVSIWNPILLWQPIPVH 42	2 mutations
1 mutation	1 YIRSTDVDRTLMSLMTNLAALFPPEGVSIWNPILLWQPIPVH 42	3 mutations

3.2. Results

3.2.1. Effect of introducing mutations in the human and murine PAP42mer peptide sequences on the immunogenicity of peptide-based vaccines

The first approach to increase the immunogenicity of the vaccine was to introduce at least one mutation in the 42 amino acids sequence.

3.2.1.1. Human PAP42mer sequences and epitope repertoire

The immunogenicity of both the WT and the mutated humanPAP42mer peptides were assessed using CpG adjuvant by vaccinating HHDII/DR1 mice, as described in 2.2.2.3. Seven days after the last immunisation, spleens of the animals were harvested to isolate the splenocytes and assess their ability to specifically recognize human PAP-derived peptides based on the IFNγ ELISpot assay. The HLA-A2 class-I and HLA-DR1 class-II peptides assessed, as determined by the SYFPEITHI algorithm/website, are listed in Table 3.2, along with their binding score. The amino acid affected by the mutation is presented in red. Only wild-type peptides were used in the *in vitro* experiments performed.

Table 3.2: List of HLA-A2 class-I and HLA-DR1 class-II peptides derived from the hPAP42mer sequence

HHDII/DR1 mice	Sequence	Haplotype	Length	SYFPEITHI score hPAP42mer WT	SYFPEITHI score hPAP42mer mut
Class-I peptides	SAMTNLAAL	HLA-A*02:01	9mer	24	30
	ILLWQPIPV		9mer	24	24
	ALFPPEGVSI	HLA-A*0201/A*03	10mer	27/25	27/25
Class-II peptides	LAALFPPEGVSIWNP	HLA-DRB1*0101	15mer	25	25
	MSAMTNLAALFPPEG		15mer	33	33
	PEGVSIWNPILLWQP		15mer	25	25
	VSIWNPILLWQPIPV		15mer	25	25
	DRTLMSAMTNLAALF		15mer	22	30

Immunisation with the WT hPAP42mer peptide induced IFNγ-secreting T-cells following stimulation with all hPAP-derived peptides, except for SAM 9mer and MSA 15mer (figure 3.1 A). The ILL 9mer class-I peptide and VSI 15mer and DRT 15mer class-II peptides induced the highest number of IFNγ-secreting T-cells. Immunisation with the mutated form of the hPAP42mer peptide increased the number of IFNγ-secreting T-cells following stimulation with all 8 PAP-derived peptides tested, although not all increases were of statistical significance. Stimulation with the ILL 9mer elicited a statistically significant increase in IFNγ-secreting and was shown to be the strongest class-I epitope, regardless of the PAP42mer peptide used for the immunisation, despite not having the highest HLA-A2 binding score. Indeed, this epitope was previously identified as an HLA-A2.1-restricted epitope for which specific CD8^{+} T-cells were present in PBMCs from PCa patients and from healthy blood donors (Olson, et al. 2010). VSI 15mer, DRT 15mer and PEG 15mer were the 3 class-II epitopes shown to induce the highest number of IFNγ-secreting T-cells, regardless of the PAP42mer peptide used for the immunisation.

The functional avidity of the TCR is defined by the T-cell responsiveness to a peptide and depends, in part, on its affinity for a peptide. T-cells having a high functional avidity are able to respond to low quantities of peptides (Viganò, et al. 2012) and are essential for establishing an effective anti-tumour immune response (Durrant, et al. 2010). Moreover, there is a direct link between the binding affinity and the immunogenicity of a potential cytotoxic T-cell epitope (Sette, et al. 1994). Following the identification of ILL 9mer peptide as the strongest class-I epitope, the functional avidity of T-cells for the ILL 9mer class-I epitope was assessed. For this, an IFNγ ELISpot assay was performed using decreasing concentrations of the ILL 9mer peptide to stimulate the splenocytes. The vaccination strategy using the mutated peptide was able to induce ILL-specific T-cells with higher functional avidity than when immunising using the WT peptide (Figure 3.1 B). Indeed, the half maximal effective concentration (EC50) of ILL peptide was 10 times lower: WT= 0.01267µg/ml and Mut = 0.00105µg/ml (Figure 3.1 B bottom). Moreover, a concentration 1000 times lower of ILL 9mer peptide than the 1µg/mL usually used (0.001µg/mL) was able to induce the same number of ILL-specific IFNγ-releasing T-cells (Figure 3.1 B top).
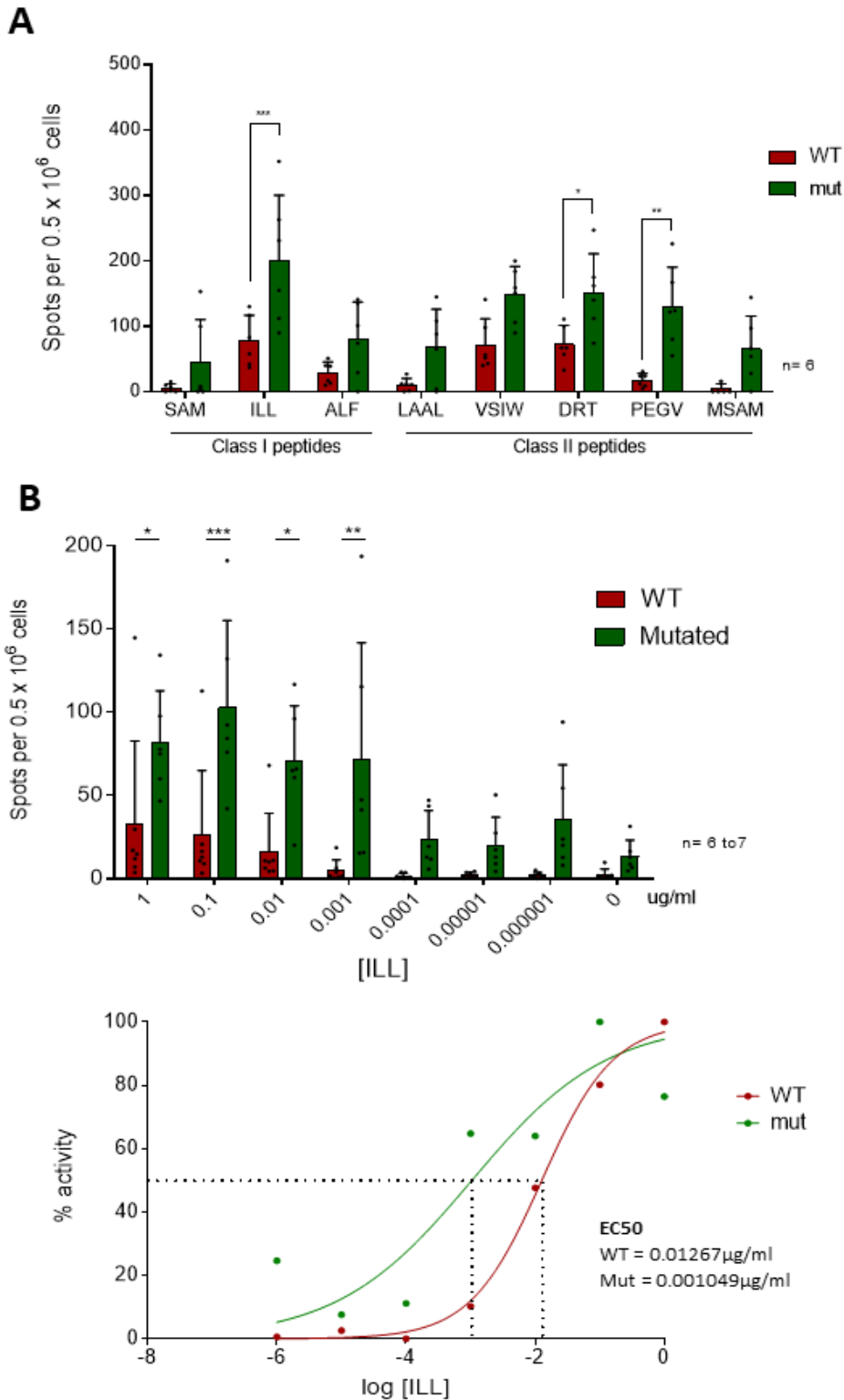
Figure 3.1: Assessment of the hPAP 42mer WT or mutated peptides with CpG adjuvant vaccination on the overall response against several hPAP-derived class I and class II epitopes and on the avidity to ILL class-I epitope. HHDII/DR1 mice were immunised on day**s** 1, 15 and 29 with either hPAP 42mer WT or mutated peptide with CpG adjuvant. Seven days after the last immunisation, splenocytes were isolated from spleens and an *in vitro* IFNγ ELISpot assay was performed. Splenocytes were stimulated with (A) hPAP-derived class I and class II peptides or (B) decreasing concentrations of ILL 9mer peptide, for 48 hours at 37°C. Immunisation with the mutated hPAP42mer peptide induced higher number**s** of peptide-specific IFNγ releasing T-cells and induced T-cells with a higher functional avidity for ILL 9mer peptide than immunisation with the WT hPAP42mer peptide. Bars represent the mean number of spots and the error bars represent the SD. Sigmoidal curve representing the functional avidity of ILL 9mer peptide (B, bottom). Two independent experiments performed (n= 6-**7** mice per test group). A significant difference in the induction of peptide-specific IFNγ releasing T-cells between immunisation groups was determined using a two-way ANOVA comparison test.

3.2.1.2.Murine PAP42mer sequences and epitope repertoire

The immunogenicities of the WT and 2 different mutated murine PAP42mer peptides in combination with the CAF09 adjuvant were assessed by vaccinating C57Bl/6 mice using a similar approach to that used for the HHDII/DR1 model. The CAF09 adjuvant was selected following a brief pilot study demonstrating that CpG adjuvant was too weak to observe differences between the different mPAP42er peptides to be assessed. The 2 mutated peptides consist of the WT hPAP42mer peptide and the mutated hPAP42mer peptide, which contain 2 and 3 mutations, respectively, in comparison to the WT mPAP42mer sequence. In this model, the ability of splenocytes to specifically recognize murine PAP-derived peptides was assessed using IFNγ ELISpot assay. The H2-Kb and H2-Db class-I and H2-IAb class-II epitopes assessed, determined by the SYFPEITHI algorithm/website, are listed in Table 3.3, along with their binding score.

Table 3.3: List of H2-Kb and H2-Db class-I and H2-IAb class-II peptides derived from the mPAP42mer sequence

C57Bl/6 mice	Sequence	Haplotype	Length	SYFPEITHI score mPAP42mer WT	SYFPEITHI score mPAP42mer 2 mutations	SYFPEITHI score mPAP42mer 3 mutations
Class-I peptides	SAMTNLAAL	H2-Db	9mer	28	28	26
	SIWNPRLL	H2-Kb	8mer	13	13	13
	GISIWNPRL	H2-Db	9mer	10	8	8
	ISIWNPRLL	H2-Db	9mer	25	26	26
Class-II peptides	ISIWNPRLLWQPIPV	H2-IAb	15mer	N/A	N/A	N/A
	PEGISIWNPRLLWQP	H2-IAb	15mer	N/A	N/A	N/A

Immunisation with the WT mPAP42mer peptide did not induce IFNγ-releasing T-cells following stimulation with the mPAP-derived peptides. However, immunisation with either the 2 or the 3 mutations mPAP42mer peptides was able to induce IFNγ-releasing T-cells following stimulation with all 3 class-I (ISI 9mer, GIS 9mer and SIW 8mer) and 2 class-II (ISI 15mer and PEG 15mer) epitopes (figure 3.2 A). The ISI9mer peptide has previously been reported as being an immunogenic H2-Db epitope, inducing lysis of peptide-pulsed RMA-S cells (Spies, et al. 2012). There was no significant difference between the 2 or the 3 mutations mPAP42mer peptides. Although exhibiting the highest binding score (28), the SAM 9mer peptide did not induce IFNγ-releasing T-cells, neither did the MSAM 15mer (data not shown).

On the basis of these results and due to its high binding score (25) ISI 9mer was further assessed. The functional avidity of T-cells towards this epitope was compared following vaccination of C57Bl/6 mice with each of the three murine PAP42mer peptides and CAF09 adjuvant. For this assay, mice were pooled per group due to practical reasons. Immunisation using both the 2 and the 3 mutations peptides induced T-cells having a higher avidity towards the two peptides. Indeed, immunising mice with both the 2 and 3 mutations peptides induced a high number of ISI-specific

IFNγ-releasing T-cells following *in vitro* stimulation with low peptide concentrations, in comparison to immunising mice with the WT peptide (Figure 3.2 B). In the group of mice immunised with the mutated peptides, a concentration 1000 times lower of ISI 9mer peptide than the 1µg/mL usually used (0.001µg/mL) was able to induce the same number of ISI-specific IFNγ-releasing T-cells. ISI was shown to generate high avidity T-cells.
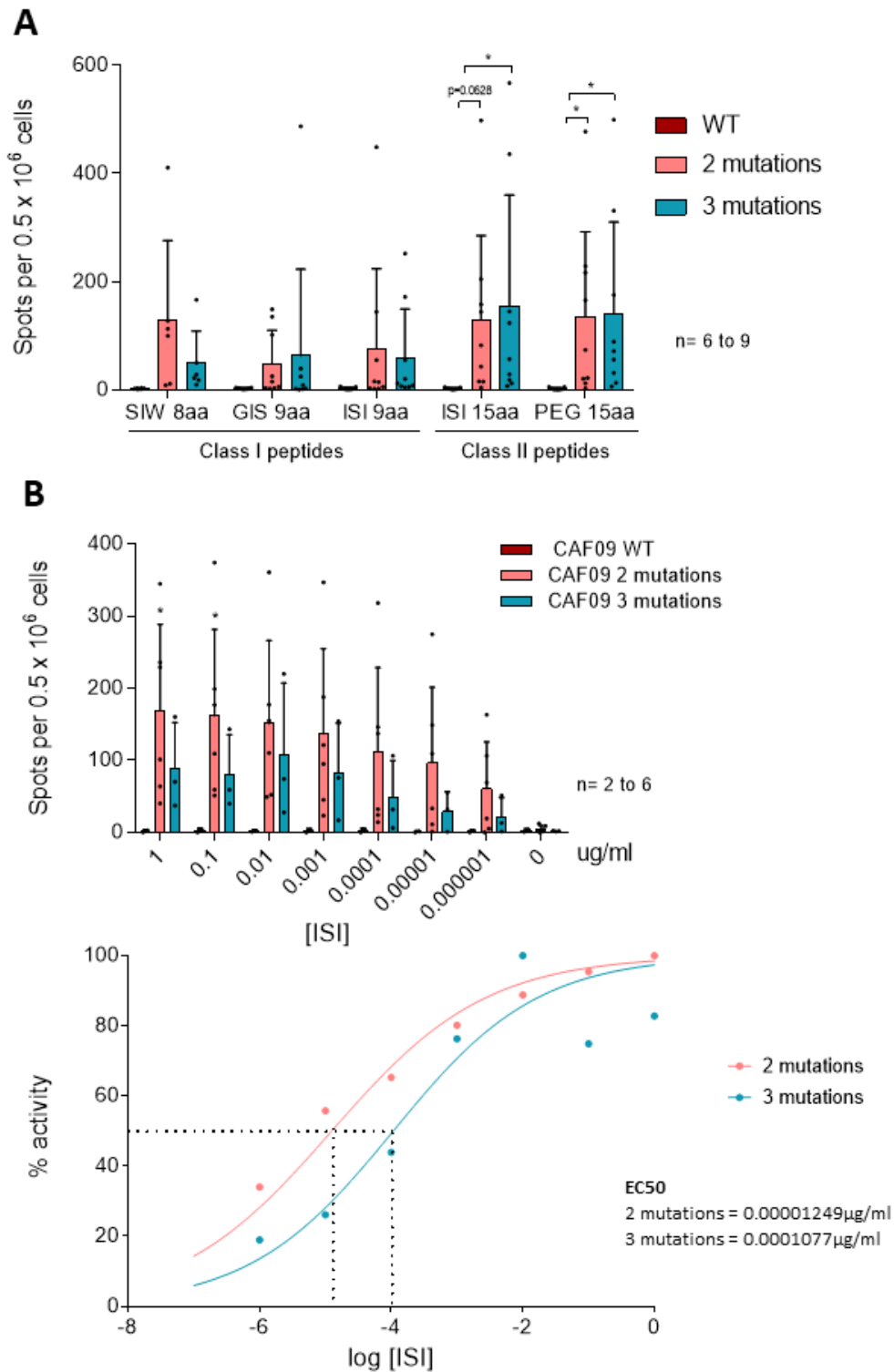
Figure 3.2: Assessment of the mPAP 42mer WT or mutated peptides with CAF09 adjuvant vaccination on the overall response against several mPAP-derived class I and class II epitopes and on the avidity to ISI class-I epitope. C57Bl/6 mice were immunised on days 1, 15 and 29 with either mPAP 42mer WT, 1 mutation or 2 mutations peptides with CAF09 adjuvant. Seven days after the last immunisation, splenocytes were isolated from spleens and an *in vitro* IFNγ ELISpot assay was performed. Splenocytes were stimulated with (A) mPAP-derived class I and class II peptides or (B) decreasing concentrations of ISI 9mer peptide, for 48 hours at 37°C to measure the immune response induced. Immunisation with both 2 mutations and 3 mutations mPAP42mer peptides induced high numbers of peptide-specific IFNγ releasing T-cells and higher avidity T-cells while immunisation with the WT mPAP42mer peptide did not induce any. Bars represent the mean number of spots and the error bars represent the SD. Sigmoidal curve representing the functional avidity of ISI class-I epitope (B bottom). Two to three independent experiments performed (n= 6 to 9 mice per test group). A significant difference in the induction of peptide-specific IFN-secreting T-cells between immunisation groups was determined using a two-way ANOVA comparison test.

3.2.2. Effect of different adjuvants and delivery system on the immunogenicity of the PAP42mer vaccine: peptide + CpG *versus* peptide + CAF09 *versus* the ImmunoBody®-PAP DNA vaccine

Following the determination of the most immunogenic PAP42mer peptide in both mouse models, the second approach to enhance the immunogenicity of the vaccine was by using different delivery systems. As described in the introduction of this chapter, 3 different vaccines were compared in each mouse model: two peptides + adjuvant-based vaccines and one DNA vaccine.

3.2.2.1. HHDII/DR1 model

3.2.2.1.1. Effect on the overall response against class-I and class-II epitopes

The human PAP42mer mutated peptide was shown to be more immunogenic than its WT counterpart (Figure 3.1). These results were obtained using the CpG adjuvant. A new adjuvant was assessed, CAF09, and a DNA vaccine, the ImmunoBody®. The DNA sequence coding for the human mutated PAP 42mer peptide sequence was inserted into the Complementarity determining regions (CDR) region of the ImmunoBody®. The immunogenicity of each delivery system was compared by vaccination of HHDII/DR1 mice, as described previously, followed by an IFNγ ELISpot assay. Vaccination using CAF09 adjuvant induced significantly (p<0.0001) higher numbers of IFNγ-secreting T-cells following stimulation with ILL 9mer peptide and VSIW 15mer peptide in comparison with CpG adjuvant and the ImmunoBody® DNA vaccine (Figure 3.3 A). As expected, immunisation with CpG adjuvant induced IFNγ-secreting T-cells, although the response to some hPAP-derived peptides was not as high as previously obtained in experiments reported in Figure 3.1 A. On the other hand, the ImmunoBody® DNA vaccine did not induce IFNγ-secreting T-cells. These results showed that CAF09 is a strong adjuvant and that the CAF09-based vaccine induces the strongest PAP-specific immune response in this model, out of the 3 vaccine strategies tested.

The functional avidity of T-cells for the ILL 9mer class-I peptide was compared following vaccination with the humanPAP42mer peptide with either CpG or CAF09 adjuvant and followed by an IFNγ ELISpot assay (Figure 3.3 B). This assay was not performed with the ImmunoBody® DNA vaccine, as it did not induce IFNγ-secreting T-cells following stimulation with the ILL 9mer peptide. CAF09 adjuvant was able to induce higher number of ILL-specific T-cells down to 0.01µg/mL of peptide, but at lower peptide concentrations, the induction of ILL-specific T-cells was only detected in the CpG adjuvant group (Figure 3.3 B). Indeed, the half maximal effective concentration (EC50) of ILL peptide was 9 times lower for the CpG adjuvant group: CpG = 0.00105µg/ml, CAF09 = 0.00937µg/ml (graph on the right).
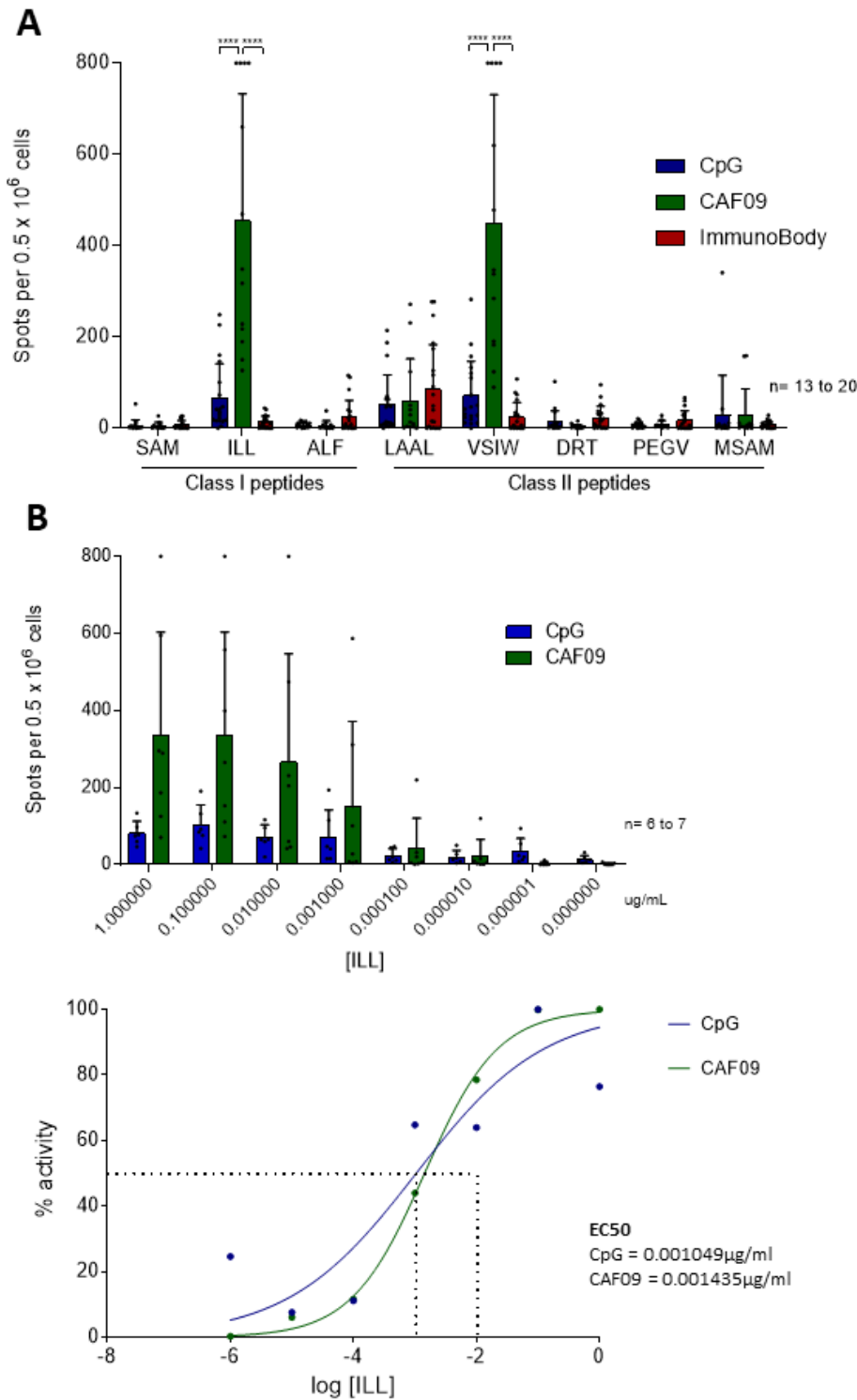
**Figure 3.3: Effect of the hPAP 42 peptide mutated form with CpG, CAF09 adjuvant or in the ImmunoBody®
DNA vaccine on the overall response against class I and class II epitopes and on the avidity to ILL class-I
epitope.** HHDII/DR1 mice were immunised on days 1, 15 and 29 with either the CpG, the CAF09 or the
ImmunoBody®-based mutated hPAP 42mer vaccine. 7 days after the last immunisation, splenocytes were
isolated from spleens and an *in vitro* IFNγ ELISpot assay was performed. Splenocytes were stimulated with (A)
hPAP-derived class I and class II peptides or (B) decreasing concentrations of ILL 9mer peptide, for 48 hours
at 37°C. Immunisation with the CAF09-based vaccine induced higher numbers of peptide-specific IFNγ-
secreting T-cells than immunisation with other vaccines. Immunisation with CpG adjuvant induced T-cells
with a higher functional avidity for ILL 9mer peptide than immunisation with the CAF09 adjuvant. Bars
represent the mean number of spots and the error bars represent the SD. Sigmoidal curve representing the
functional avidity of ILL 9mer peptide (B right). (A) 4 to 6 independent experiments performed (n= 13 to 20
mice per test group) and (B) 1 to 2 independent experiments (n= 3 to 6 mice per test group). A significant
difference in the induction of peptide-specific IFNγ releasing T-cells between immunisation groups was
determined using a two-way ANOVA comparison test.

3.2.2.1.2.Immunophenotyping of CD8+ T-cells

To assess the effect of the vaccine on T-cell subsets, the phenotype of splenocytes from vaccinated mice was investigated using flow cytometry. The gating strategy used is presented in Figure 3.4. The effect of the 3 different vaccines were compared with each other and with a baseline: naïve, non-vaccinated mice. Splenocytes were stained with antibodies to assess the proportion of T-cell subsets, the presence of memory T-cells and the presence of activation and inhibitory markers on T-cells. To determine the T-cells responsible for the IFNγ production, splenocytes were also stimulated *in vitro* with ILL 9mer alone or with VSIW 15mer peptides for 6 hours and then assessed by flow cytometry for the expression of cytokines, degranulation markers and for proliferation. Indeed, the secretion of IFNγ in response to VSIW 15mer peptide could be actually directed against the ILL9mer epitope after processing of the 15mer by APCs during the 48hrs of culture period.
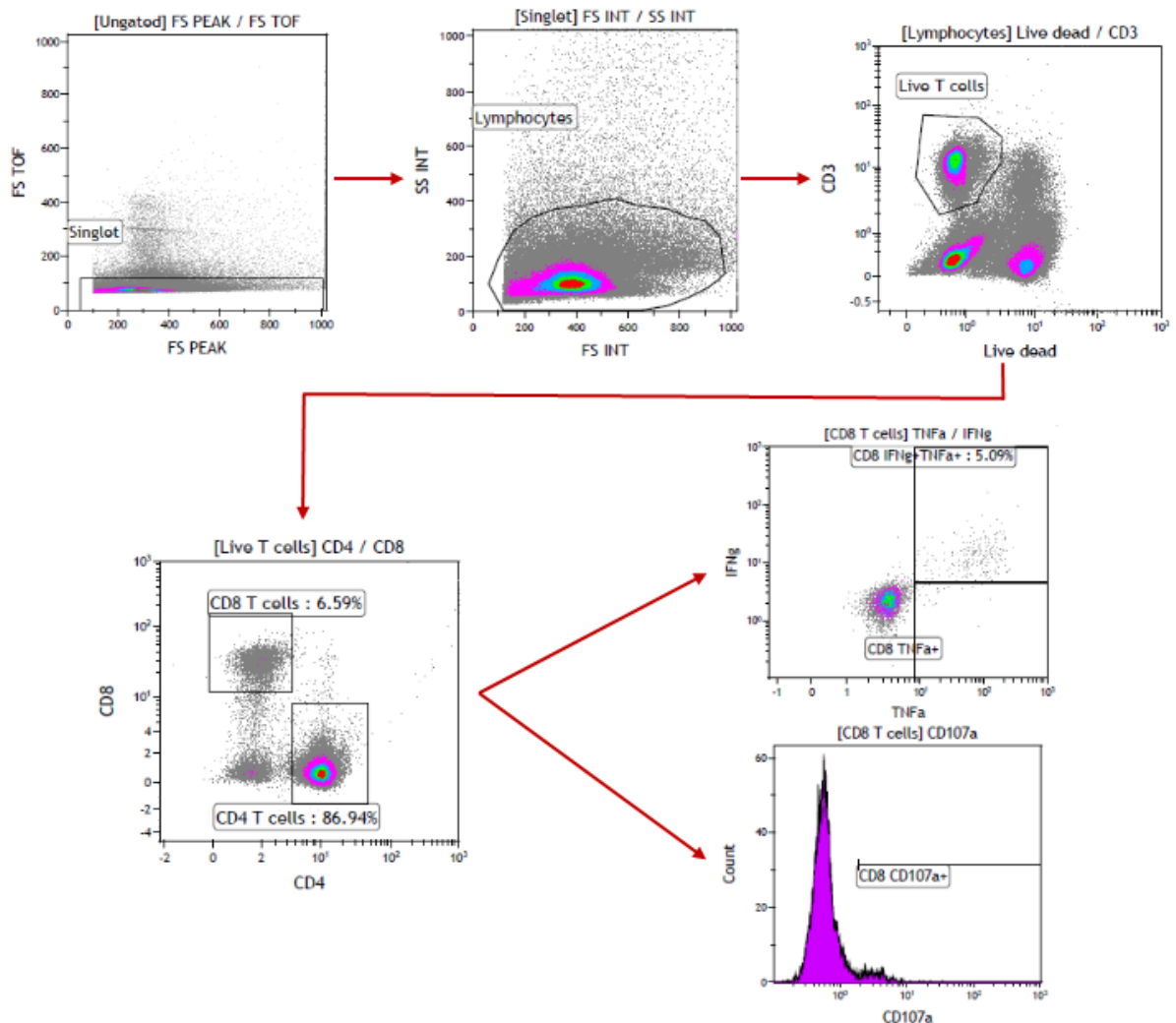
Figure 3.4: Gating strategy used for flow cytometry analysis.

Percentages of CD4+ and CD8+ T-cells within the T-cell compartment were measured. Both CAF09 and ImmunoBody® based vaccines induced an increase in the proportion of CD8+ T-cells (Figure 3.5

A). The CAF09-based vaccine induced approximately a 2-fold increase in comparison to the baseline and to the CpG-based vaccine (p<0.0005). The ImmunoBody®-based vaccine induced a lesser increase in comparison to the baseline and the CpG-based vaccine. Surprisingly, the CpG-based vaccine did not increase the proportion of CD8$^+$ T-cells. As expected, any increase in the proportion of CD8$^+$ cells was accompanied by a proportional decrease in the proportion of CD4$^+$ T-cells (Figure 3.5 A).

CD4$^+$ and CD8$^+$ T cells can be categorized into different effector, memory and naïve phenotypes based on their expression of defined markers. Naïve T-cells are CD44^{low}CD62L$^+$, central memory T-cells are CD44^{high}CD62L$^+$, and the effector and/or effector memory CD4$^+$ and CD8$^+$ T-cells are CD44^{high}CD62L^{neg} (Sckisel, et al. 2017).

The percentage of CD4$^+$ memory T-cells was not affected by the vaccination (Figure 3.5 B). On the other hand, the proportion of CD8$^+$ effector/effector memory T-cells was significantly increased (3-fold change) in the CAF09-based vaccine group in comparison to all other groups (p<0.0005), reaching an average of 60% of CD8$^+$ T-cells exhibiting a memory phenotype (Figure 3.5 B). There was no increased proportion of central memory T-cells (data not shown).

The expression of activation and inhibitory markers on CD4$^+$ and CD8$^+$ T-cells was then assessed. The expression of GITR and OX40 activation markers and of CTLA-4, LAG-3 and Tim-3 inhibitory markers in CD4$^+$ nor in CD8$^+$ T-cells was not significantly affected by vaccination (Figure 3.5 C). The expression of PD-1 inhibitory marker by CD4$^+$ T-cells was modestly increased by the CAF09-based vaccine and the ImmunoBody®-based vaccine in comparison to the baseline. However, the increased PD-1 expression by CD8$^+$ T cells was only observed in the CAF09-based vaccine group (p<0.0005), with 40% of CD8$^+$ T-cells expressing PD-1 on average.
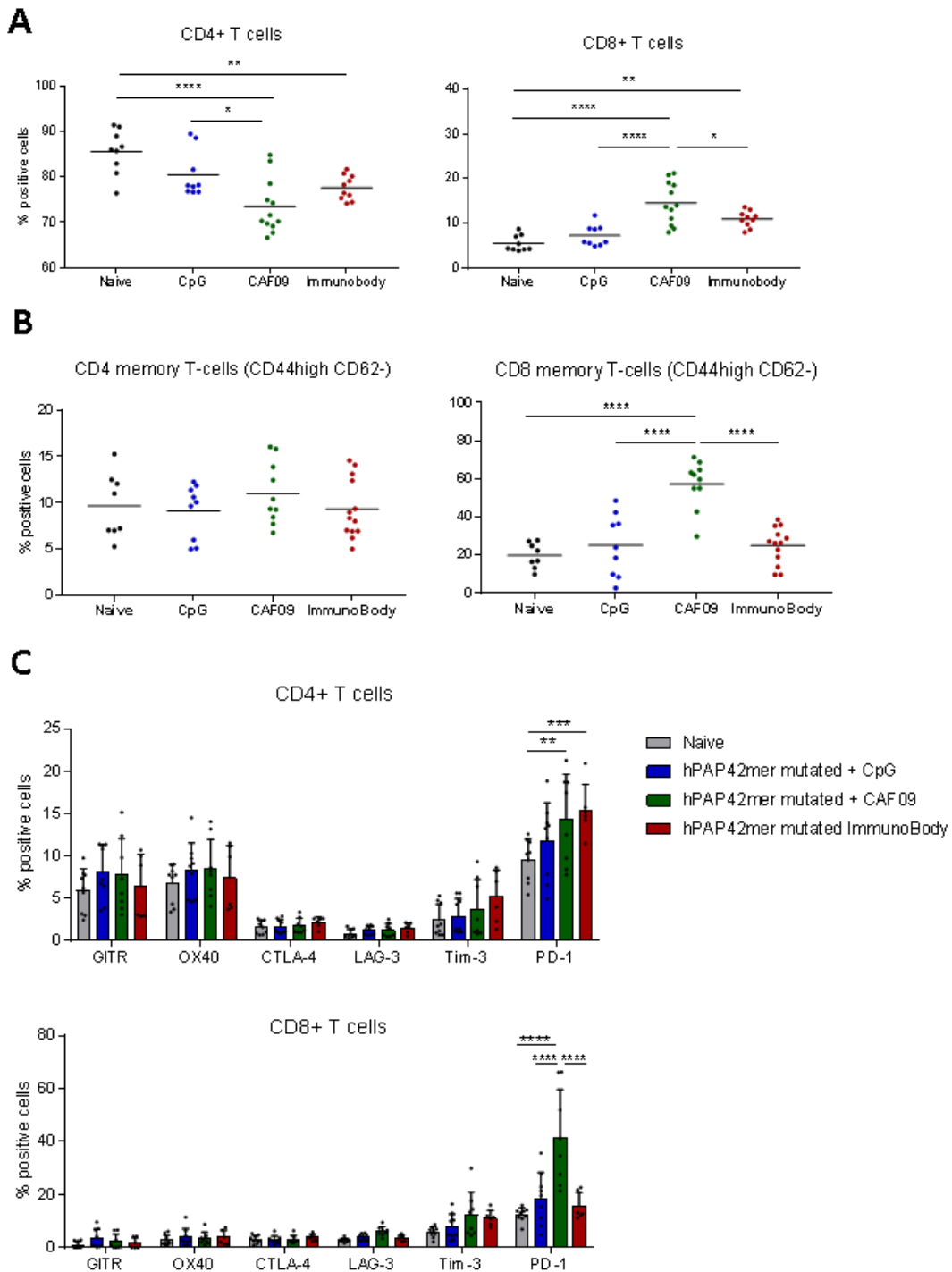
Figure 3.5: Effect of different delivery systems on the induction of a memory response and the expression of activation and inhibitory markers following immunisation with the hPAP42mer mutated sequence. HHDII/DR1 mice were immunised on days 1, 15 and 29 with either the CpG-based, the CAF09-based or the ImmunoBody®-based mutated hPAP 42mer vaccine. Seven days after the last immunisation, splenocytes were isolated from spleens, incubated with a murine FcR block and then stained with surface antibodies for flow cytometry analysis indicating (A) proportion of CD4$^+$ and CD8$^+$ T-cells, (B) proportion of memory T-cells and (C) proportion of T-cells expressing activating and inhibitory markers. The CAF09-based vaccine induced an increase of the proportion of CD8$^+$ T-cells, an increase of the proportion of CD8$^+$ memory T-cells and the expression of PD-1 on both CD4$^+$ and CD8$^+$ T-cells. Bars represent the mean percentage of positive cells and the error bars represent the SD. Two to three independent experiments performed (n= 6 to 9 mice per test group). A significant difference in the proportion of positive cells between immunisation groups was determined using a two-way ANOVA comparison test.

The functionality of splenocytes was then assessed following 6 hours of *in vitro* stimulation with relevant peptides, either ILL 9mer alone or with VSI 15mer.

The proliferation of T-cells was measured based on the expression of Ki67, which has been shown to be a maker of antigen-specific *in vitro* lymphoproliferation (Soares, et al. 2010). Both stimulating conditions induced the proliferation of CD8^{+} T-cells, with up to 7% of CD8^{+} T-cells being Ki67^{+} in the CAF09-based vaccine group (Figure 3.6 A). This result correlates with the higher percentage of CD8^{+} T-cells within the T-cell compartment (Figure 3.6 A). The proliferation of CD4^{+} T-cells was not affected (data not shown).

Then, the cytokine secreting capacity of T-cells was assessed. As revealed using the IFNγ ELISpot assay, the response of splenocytes from the CAF09 immunised mice to ILL and VSI peptides was greater than that of splenocytes from other groups, with only CD8^{+} T-cells, among T-cells, being responsible for the IFNγ secretion (Figure 3.6 B), as CD4^{+} T-cells did not secrete cytokines (data not shown). Interestingly, IFNγ and TNFα were strictly co-secreted by the same CD8^{+} T-cells. IL-2 was also secreted upon stimulation in the CAF09-based vaccine group, by a subset of IFNγ/TNFα-releasing CD8^{+} T-cells. The addition of VSI 15mer peptide to ILL9mer peptide induced a non-significant increase in the proliferation and cytokine secreting capacities of CD8^{+} T-cells. CD4^{+} T-cells did not secrete cytokines upon peptide stimulation (data not shown).

Finally, the capacity of CD8^{+} T-cells to release cytolytic granules was measured based on the expression of CD107a and Granzyme B proteins. CD107a molecule was described as a marker of degranulation, its surface expression correlates with the loss of intracellular perforin and with the production of IFNγ following activation with a peptide (Betts, et al. 2003). Betts *et al.* showed that CD8^{+} T cells expressing CD107a mediated cytolytic activity in an antigen-specific manner.

The CAF09-based vaccine induced a significant increase in the expression of CD107a degranulation marker expression upon *in vitro* peptide stimulation while no difference was observed for the expression of Granzyme B (Figure 3.6 C). Regardless of the stimulating conditions, the proportion of CD8^{+} T-cells expressing Granzyme B was the greatest for the CAF09-based vaccine group. As suggested by Tietze *et al.* Granzyme B can be released by non-antigen-specific CD8^{+} T-cells (Tietze, et al. 2012). The presence of CD8^{+} T-cells co-expressing CD107a and Granzyme B was only observed for the CAF09-based vaccine group (Figure 3.6 D). Overall, 15% to 20% of total CD8^{+} T-cells were expressing CD107a and/or Granzyme B in the CAF09-vaccine based group, *versus* up to 7% in other groups. The same analysis was made when focusing on CD8^{+} T-cells secreting IFNγ and TNFα (Figure 3.6 E). For the CAF09-based vaccine group, the majority of cytokine-secreting CD8^{+} T-cells were either CD107a^{+} or Granzyme B^{+}, or co-expressed both. Therefore, it appears that vaccine-induced

CD8$^+$ T-cells have a double functionality, being able to secrete cytokines and to degranulate at the same time.

Figure 3.6: Effect of different delivery systems with the hPAP 42 mutated sequence on the functional capacities of CD8⁺ T-cells following class-I and class-II peptides stimulation. HHDII/DR1 mice were immunised on days 1, 15 and 29 with either the CpG, the CAF09 or the ImmunoBody®-based mutated hPAP 42mer vaccine. 7 days after the last immunisation, splenocytes were isolated from spleens, stimulated with either ILL 9mer alone or with VSI 15mer for 6 hours at 37°C. Splenocytes were then incubated with a murine FcR block, stained with surface Abs, fixed and permeabilized and stained with intracellular Abs for flow cytometry analysis indicating (A) proliferation (B) cytokines secretion (C) degranulation markers single expression or (D) double expression and (E) co-expression of degranulation markers within secreting cells. The CAF09-based vaccine induced the proliferation, the cytokines secretion and the degranulation of CD8⁺ T-cells upon stimulation. Bars represent the mean percentage of positive cells and the error bars represent the SD. 1 to 3 independent experiments performed (n= 3 to 9 mice per test group). A significant difference in the proportion of positive cells between immunisation groups was determined using a two-way ANOVA comparison test.

3.2.2.2.C57Bl/6 model

3.2.2.2.1.Effect on the overall response against class-I and class-II epitopes

The murine PAP42mer 2 and 3 mutations peptides were shown to be more immunogenic than the WT peptide (Figure 3.2). The capacity of different delivery systems to further increase the immunogenicity of the mutated PAP sequence were compared, as was undertaken for the HHII/DR1 mice: CpG or CAF09 adjuvant and the ImmunoBody® DNA vaccine were assessed. The DNA sequences coding for the murine PAP42mer 2 or 3 mutations peptides were incorporated into the CDR regions of the ImmunoBody® vaccine sequence. The immunogenicity of each delivery system was compared by vaccination of C57Bl/6 mice followed by IFNγ ELISpot assay. Both the CAF09-based vaccine and the ImmunoBody® DNA vaccine were able to induce higher numbers of IFNγ-secreting T-cells following stimulation with three class-I (ISI 9mer, GSI 9mer and SIW 8mer) and two class-II (ISI 15mer and PEG 15mer) epitopes (Figure 3.7 A) in comparison to CpG adjuvant, which did not induce any IFNγ-secreting T-cells. The mPAP42mer 2 mutations sequence, either in the CAF09-based vaccine or in the ImmunoBody®-based vaccine, induced the highest number of IFNγ-secreting T-cells upon stimulation with mPAP-derived peptides, although this difference was not of statistical significance.

The functional avidity of T-cells for both the ISI 9mer and the SIW 8mer epitopes were compared following vaccination with either the 2 or the 3 mutations murine PAP42mer peptides with CAF09 or in the ImmunoBody® DNA vaccine, followed by an IFNγ ELISpot assay. For this assay, mice were again pooled per group for practical reasons. All vaccination strategies were able to induce high affinity ISI-specific IFNγ releasing T-cells, as even the lowest concentration was able to induce ISI-specific IFNγ releasing T-cells (Figure 3.7 B). On the other hand, except for the 2 mutations peptide-based vaccine administered with the CAF09 adjuvant, there was no high affinity SIW-specific T-cells generated as there was no SIW-specific IFNγ releasing T-cells at low peptide concentrations. Based on these results, the 2 mutations sequence in combination with either CAF09 adjuvant or in the ImmunoBody® DNA vaccine were the selected vaccine strategies for further experiments.
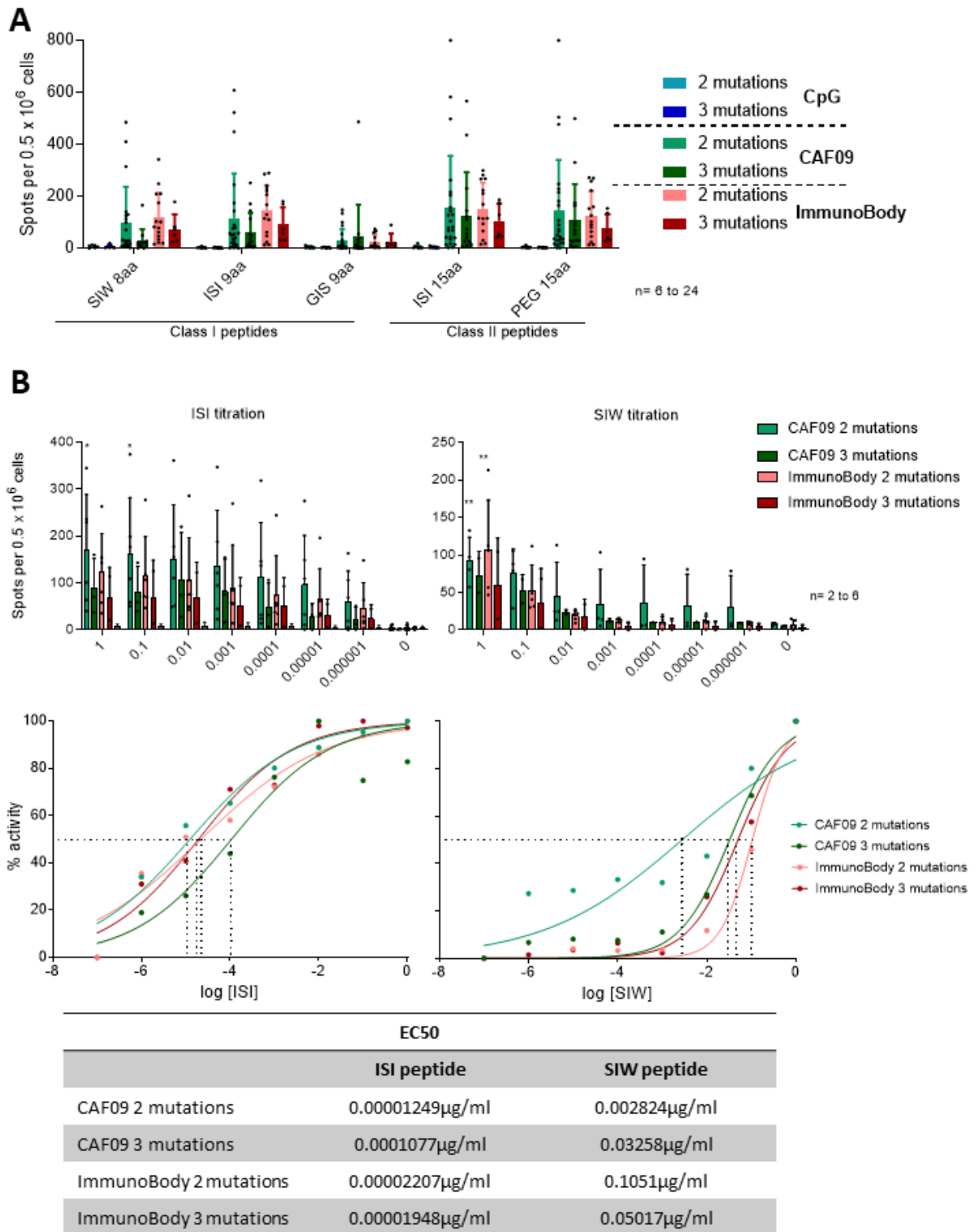
**Figure 3.7: Effect of the mPAP 42 peptide mutated forms with CpG, CAF09 adjuvant or in the ImmunoBody®
DNA vaccine on the overall response against class I and class II epitopes and on the avidity to ISI and SIW
class-I epitopes.** C57Bl/6 mice were immunised on days 1, 15 and 29 with either the CpG-based, the CAF09-
based or the ImmunoBody®-based mutated mPAP 42mer vaccine. Seven days after the last immunisation,
splenocytes were isolated from spleens and an *in vitro* IFNγ ELISpot assay was performed. Splenocytes were
stimulated with (A) mPAP-derived class I and class II peptides or (B) decreasing concentrations of ISI or SIW
peptides, for 48 hours at 37°C. Immunisation with both CAF09-based and ImmunoBody®-based vaccine
induced high numbers of peptide-specific IFNγ releasing T-cells and high functional avidity for ISI peptide,
whereas the CpG-based vaccine did not induce IFNγ-releasing T-cells. Bars represent the mean number of
spots and the error bars represent the SD. Sigmoidal curve representing the functional avidity of ISI and SIW
peptide (B right). (A) two to seven independent experiments performed (n= 6 to 24 mice per test group) and

(B) two independent experiments. A significant difference in the induction of peptide-specific IFNγ releasing T-cells between immunisation groups was determined using a two-way ANOVA comparison test.

3.2.2.2.2.Immunophenotyping of CD8+ T-cells

The effect of the vaccine strategies on T-cell subsets was assessed in this model as described for the HHDII/DR1 model. To determine the T-cells responsible for the IFNγ production, splenocytes were stimulated *in vitro* with either class-I peptides alone (ISI 9mer and SIW) or with class-II peptides (ISI 15mer and PEG) for 6 hours. Indeed, the same hypothesis can be made regarding the secretion of IFNγ in response to 15mer peptides, which could be directed against 9mer peptides after processing by APCs during the culture period.

CAF09 and ImmunoBody®-based vaccines both induced a modest increase in the proportion of CD8+ T-cells (Figure 3.8 A). The proportion of CD4+ memory T-cells did not change, however, the proportion of CD8+ effector/effector memory T-cells was slightly increased in both the CAF09-based vaccine and the ImmunoBody®-based vaccine groups in comparison to the baseline, reaching an average of 10-12% of CD8+ T-cells exhibiting an effector memory phenotype (Figure 3.8 B).

As was found in the HHDII/DR1 model, only the expression of the inhibitory PD-1 molecule was affected by the vaccines. Its expression was increased on CD4+ and in CD8+ T-cells in the CAF09-based vaccine group in comparison to the baseline and to the ImmunoBody®-based vaccine group, with a higher increase found in the CD8+ T-cell compartment (Figure 3.8 C).
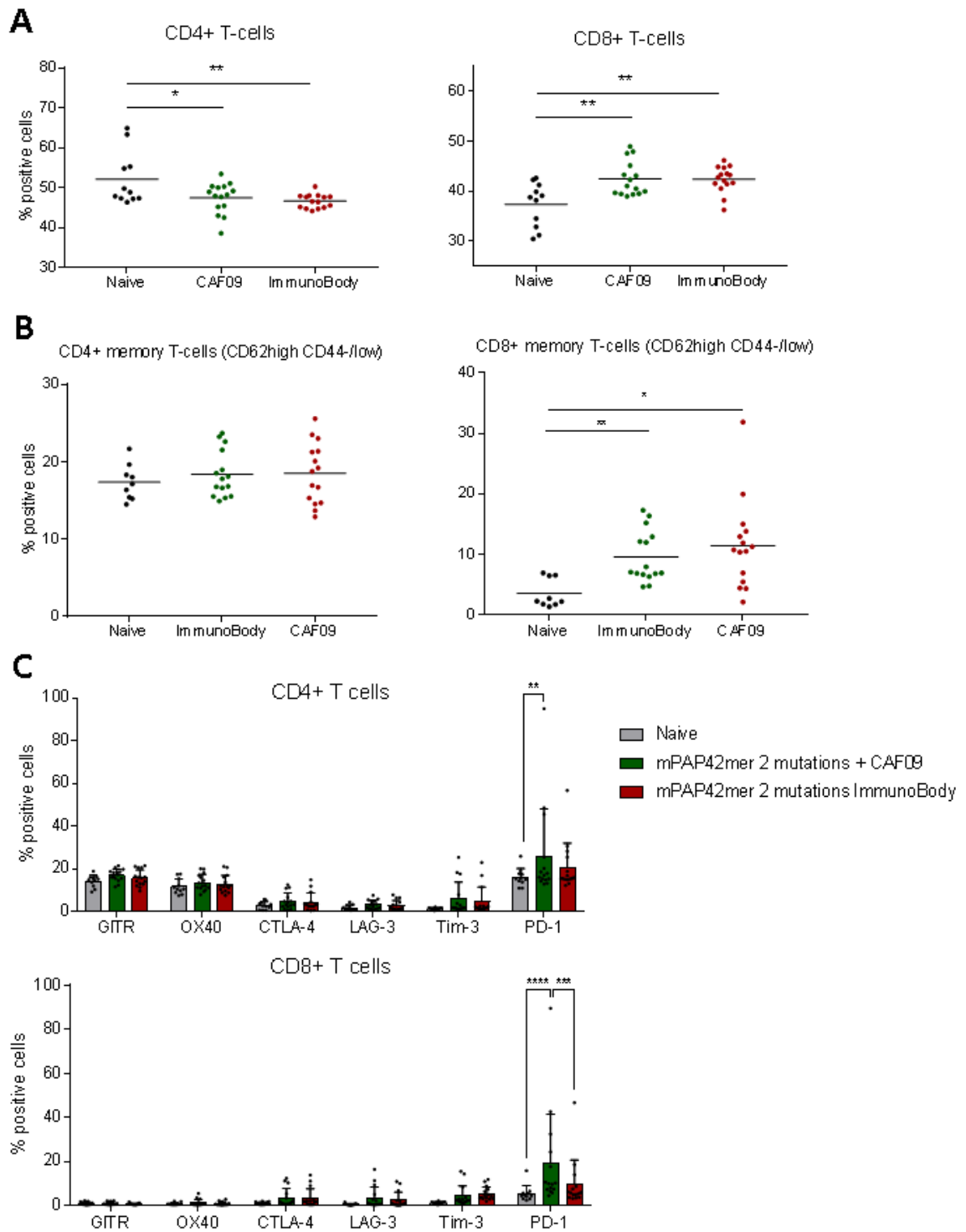
Figure 3.8: Effect of different delivery systems with the mPAP42mer mutated sequence on the induction of a memory response and the expression of activation and inhibitory markers. C57Bl/6 mice were immunised on days 1, 15 and 29 with either the CAF09-based or the ImmunoBody®-based mutated mPAP 42mer vaccine. Seven days after the last immunisation, splenocytes were isolated from spleens, incubated with a murine FcR block and then stained with surface antibodies for flow cytometry analysis indicating (A) proportion of CD4+ and CD8+ T-cells, (B) proportion of memory T-cells and (C) proportion of T-cells expressing activating and inhibitory markers. Both vaccines induced an increase of the proportion of CD8+ T-cells and an increase of the proportion of CD8+ memory T-cells, but only the CAF09-based vaccine increased the expression of PD-1 on CD4+ and CD8+ T-cells. Bars represent the mean percentage of positive cells and the error bars represent the SD. Two to three independent experiments performed (n= 6 to 9 mice per test group). A significant difference in the proportion of positive cells between immunisation groups was determined using a two-way ANOVA comparison test.

The functionality of the splenocytes was then assessed following 6 hours of *in vitro* stimulation with ISI 9mer/SIW 8mer +/- ISI 15mer/PEG 15mer. Both stimulating conditions induced the proliferation of CD8+ T-cells with up to 1.8% of CD8+ T-cells expressing Ki67 in the ImmunoBody®-based vaccine group (Figure 3.9 A). The proliferation of CD4+ T-cells was not affected (data not shown).

As was showed in the IFNγ ELISpot assay, splenocytes from both vaccine groups were able to produce class-I-specific IFNγ-releasing T-cells. Results showed that only CD8+ T-cells were responsible for the IFNγ secretion (Figure 3.9 B). In this model too, IFNγ and TNFα were strictly co-secreted by the same CD8+ T-cells. IL-2 was also secreted upon stimulation, in both vaccine groups, by a subset of IFNγ/TNFα-secreting CD8+ T-cells. The increase in IL-2 secretion was only significant when class-II peptides were added to class-I peptides for the stimulation. The addition of class-II peptides to the class-I peptides induced a non-significant increase of proliferative and secreting capacities of CD8+ T-cells. CD4+ T-cells did not secrete cytokines upon stimulation (data not shown).

Considering the degranulation capacities of CD8+ T-cells, both vaccines induced an increase of CD107a degranulation marker expression upon stimulation (non-significant for the ImmunoBody® group) (Figure 3.9 C). Regardless of the stimulating conditions, CD8+ T-cells from the CAF09-based vaccine group exhibited a higher proportion of Granzyme B+ CD8+ T-cells. The presence of CD8+ T-cells co-expressing CD107a and Granzyme B was observed in both vaccine groups, in a very small proportion (less than 0.5% of CD8+ T-cells) (Figure 3.9 D). Overall, 3-5% of CD8+ T-cells were expressing either CD107a or Granzyme B or both in vaccine groups, *versus* up to 1% for the baseline. Unlike what was observed in the HHDII/DR1 model, CD8+ secreting T-cells (IFNγ and TNFα) expressed CD107a but no expression of Granzyme B was observed (Figure 3.9 E).
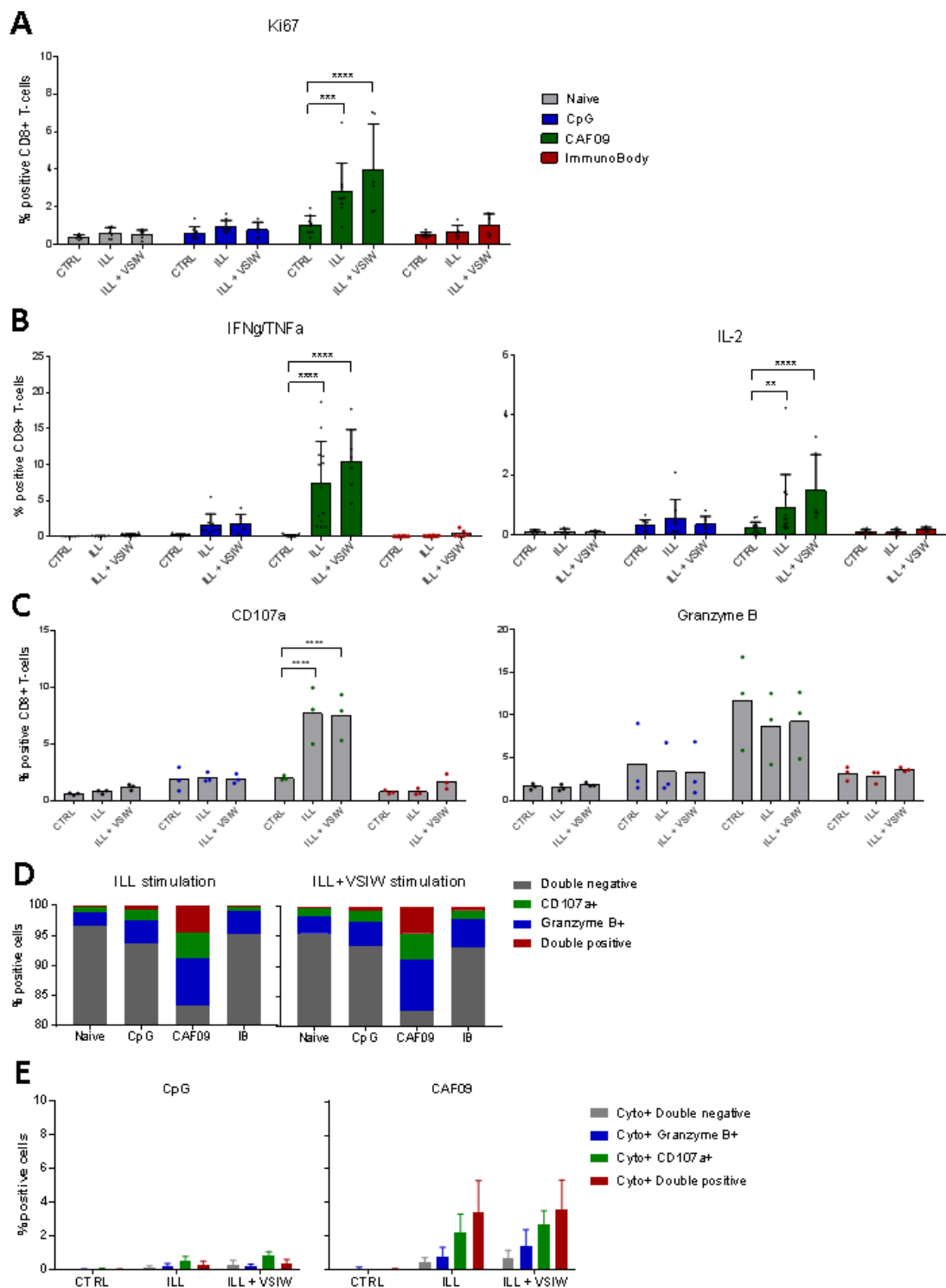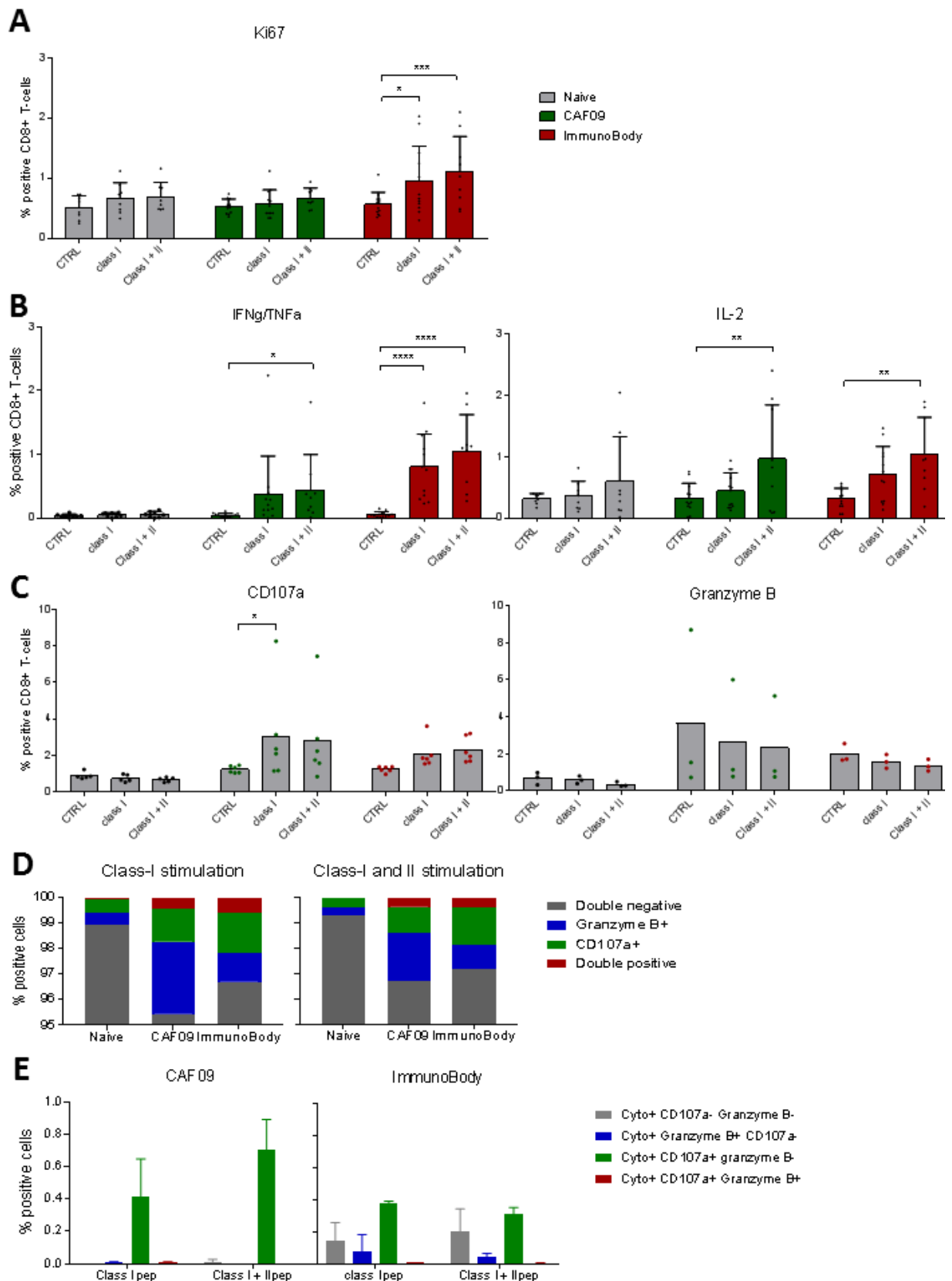
Figure 3.9: Effect of different delivery systems with the mPAP 42 mutated sequence on the functional capacities of CD8⁺ T-cells following class-I and class-II peptides stimulation. C57Bl/6 mice were immunised on days 1, 15 and 29 with either the CAF09 or the ImmunoBody®-based mutated mPAP 42mer vaccine. 7 days after the last immunisation, splenocytes were isolated from spleens, stimulated with either ISI 9mer + SIW 8mer alone or with ISI 15mer + PEG 15mer for 6 hours at 37°C. Splenocytes were then incubated with a murine FcR block, stained with surface antibodies, fixed and permeabilized and then stained with intracellular antibodies for flow cytometry analysis indicating (A) proliferation (B) cytokines secretion (C) degranulation markers single expression or (D) double expression and (E) co-expression of degranulation markers within secreting cells. Both vaccines induced the cytokines secretion and the degranulation of CD8⁺ T-cells but only

93

the ImmunoBody®-based vaccine induced the proliferation of CD8+ T-cells upon stimulation. Bars represent the mean percentage of positive cells and the error bars represent the SD. 1 to 3 independent experiments performed (n= 3 to 9 mice per test group). A significant difference in the proportion of positive cells between immunisation groups was determined using a two-way ANOVA comparison test.

3.3. Discussion

This study focussed on the use of PAP protein as a target for the development of a therapeutic vaccine against prostate cancer. PAP protein is an attractive target for prostate cancer vaccines due to its relative specific expression within the prostate and its disease-dependant overexpression. Moreover, the FDA-approval of Provenge vaccine in 2010 has demonstrated the rationale for using PAP as a target for cancer vaccines in prostate cancer.

The first goal of this study was to optimise our vaccine, in order to identify the most immunogenic vaccine strategy capable of inducing PAP-specific T cell responses that were identified with the SYFPEITHI database. In the two mouse models tested, the findings demonstrate the higher capacity of mutated 42mer PAP-derived peptides to induce a PAP-specific immune response. Higher number of IFNγ-releasing T cells was obtained following stimulation with short class-I and long class-II WT peptides and the functional avidity to short peptides was also improved.

In the humanized model, the ILL 9mer and the VSIW 15mer peptides induced the highest number of IFNγ-releasing T cells. The ILL 9mer particularly has been reported to induce anti-tumour immunity *in vitro*, through killing of HLA-A2.1+ LNCaP cells and of peptide-pulsed T2 cells by peptide-primed PBMCs, and *in vivo*, in the HHDII mice, making it a good vaccine candidate for immunotherapy of prostate cancer (Machlenkin, et al. 2005). The murine and human PAP proteins are only 81% identical, the ILL9mer murine homologue has 1AA difference: ILLLWQPIPV→RLLWQPIPV, keeping the anchor motifs at positions 2 and 9 (Rammensee, et al. 1993). It is therefore possible that the ILL9mer induces cytotoxic T lymphocytes reactive against xenoantigenic determinants, as has been suggested by Machlenkin *et al.* (Machlenkin, et al. 2005). Indeed, considering that HHDII/DR1 humanized mice naturally express the murine PAP protein, immunisation using the hPAP42mer mutated peptide is an immunisation with a peptide containing 3 mutations (two between murine and human PAP42mer sequence, plus the additional mutation). Therefore, CD8+ T-cells are recognizing a foreign antigen during vaccination. The ELISpot assay is performed with hPAP42mer-derived short sequences, human and foreign sequences. Although the assay proves that the vaccination induced ILL-specific CD8+ T-cells, the intensity of the response is probably overestimated due to the 'foreignness' of ILL 9mer.

In the C57Bl/6 model, 2 short peptides: SIW 8mer and ISI 9mer and 2 long peptides: ISI 15mer and PEGI 15mer, induced high number of IFNγ-releasing T cells.

In both models, class-I and class-II peptides displaying the highest SYFPEITHI binding score did not induce the highest number of IFNg releasing T-cells, thereby illustrating the limitations of the algorithm. Indeed, in the HHDII/DR1 model, ILL, the strongest HLA-A2 epitope has a score of 24 but induced a greater number of peptide-specific releasing T-cells than SAM and ALF which have scores of 24 and 27 respectively. As for the C57Bl/6 model, ISI which has the highest binding score, 25, was as immunogenic as SIW, with a binding score of only 13. GIS was less immunogenic, which correlates with its lower binding score: 10. However, the functional avidity assay demonstrated the much higher functional avidity of T-cells for ISI peptide, which correlates with its higher binding score.

The absence of IFNγ release following stimulation with SAM 9mer and MSAM 15mer in the two models was unexpected as these two peptides have previously been described as immunogenic (Saif, et al. 2014). This could be explained by a differential processing of the 42mer peptide in comparison to the 15mer peptide, not in favour of the SAM 9mer and MSAM 15mer peptides, as well as the potential binding competition between ILL and SAM in some way advantaging ILL.

In both models, the short peptide sequences (8 to 9mer) were part of the 15AA long peptides sequences. Since the ELISpot assay was developed 48hrs after the stimulation it is possible that 15AA long peptides were processed by APCs and cut into 8-9mer long peptides and therefore that the IFNγ secretion observed in response to the long 15mer peptides stimulation was due to CD8^{+} and not CD4^{+} T-cells. To answer this question, *in vitro* stimulation with short and long peptides followed by intra-cellular flow cytometry staining was performed. The results showed that CD8^{+} T-cells only were responsible for the secretion of IFNγ, suggesting that the vaccine induces a class-I response only. The lack of cytokine secretion by CD4^{+} T-cells was unexpected. However, the addition of long 15mer peptides did increase the intensity of the CD8^{+} T-cell response (cytokines secretion and proliferation). In particular, IL-2 secretion by CD8^{+} T-cells was increased in the presence of class-II epitopes during the stimulation, suggesting a potential helper role for CD4^{+} T-cells, however this was not investigated further.

Interestingly, although the mutation in the hPAP42mer sequence does not directly affect the ILL9mer and the VSIW15mer sequences, it appears to affect their immunogenicity. On the other hand, the mutations in the mPAP42mer sequences directly affect ISI9mer, SIW8mer, PEGI15mer and ISI15mer sequences and their immunogenicity, with the T-cells generated still able to recognise the wild-type sequences of these peptides.

The other aspect of the study was to determine whether different adjuvants or delivery systems could improve the immunogenicity of the PAP42mer vaccine. CAF09 adjuvant was identified as a stronger adjuvant than CpG in the two models studied. The ImmunoBody® DNA vaccine was able to improve the immunogenicity of the vaccine in only one of the two mouse model tested, demonstrating that the efficacy of an adjuvant/delivery system depends on the antigen of interest and in the model in which it is tested.

Overall, the immune response in the HDDII/DR1 model was stronger than that obtained with the C57Bl/6 model, probably due to the foreignness of the hPAP42mer peptide. The proportion of CD8$^+$ T-cells displaying a memory phenotype was higher in the HHDII/DR1 mice as was the proportion of proliferating, secreting and degranulating CD8$^+$ T-cells. The two-models differed in their quantitative response, but not in their qualitative response. Indeed, the pattern of cytokines produced was identical: co-secretion of IFNγ and TNFα by CD8$^+$ T-cells, and for a subset of these cells, co-secretion of IL-2 as well. The pattern of degranulation was also identical, CD107a expression was affected by the presence of antigen whereas that of granzyme B was not.

The only major difference between the two models was the incapacity of the ImmunoBody®-based vaccine to elicit a PAP-specific immune response in the HHDII/DR1 model. This result is surprising considering that the incorporation of the PAP15mer sequence into the ImmunoBody® DNA vaccine increased the immunogenicity and anti-tumour response of the vaccine (Saif, et al. 2014). Moreover, the ImmunoBody® was previously described as a strong delivery system capable of inducing high frequency helper and cytolytic responses capable of anti-tumour activity (Durrant, et al. 2010). A possibile explanation was that the PAP42mer sequence is too long, as incorporating such a long sequence had never been assessed before (maximum was 30AA). However, the ImmunoBody®-derived vaccine was able to induce a strong immune response in the C57Bl/6.

The CAF09-based vaccine induced PD-1 expression in both models in CD4$^+$ and CD8$^+$ T-cells. The ImmunoBody®-based vaccine also induced the expression of PD-1 on T-cells, albeit to a much lesser extent. The expression of PD-1 on T-cells has different implications. Its expression is the evidence that the TCR of T-cells has been activated (Simon and Labarriere 2017). In the absence of the antigen, PD-1 expression will decrease, however, in the case of persisting antigen stimulation, PD-1 expression is maintained as this inhibitory receptor has for role to maintain the peripheral immune tolerance and to limit auto-immunity. Although PD-1 has been described as a marker of dysfunction / exhaustion for T-cells, it is now accepted that its expression on its own is not sufficient to conclude on the exhausted status of T-cells. The co-expression of various other inhibitory markers has to be present. PD-1 expression has been linked to the presence of tumour-reactive CD8$^+$ T-cells (Inozume,

et al. 2010) (Gros, et al. 2014) and of high avidity CD8^{+} T-cells (Simon, et al. 2015; Gros, et al. 2016). Its expression level is related to the strength of TCR signalling, therefore to the functional avidity of peptide specific T-cells. As suggested by Simon *et al.* (Simon, et al. 2015) and correlating with the results obtained in our study, the expression of PD-1 seems to be a marker of efficient CD8^{+} T-cells. The presence of "exhausted" T-cells will be assessed in the next chapters when assessing the anti-tumour activity of T-cells, both *in vitro* and *in vivo*. Indeed, in the case of exhaustion of T-cells, their unability to secrete cytokines and to degranulate cytotoxic molecules upon PAP recognition on the surface of tumour cells would be deleterious to the anti-tumour activity of the vaccine. If this is observed, combining the vaccine with an anti-PD1 antibody might be necessary, as suggested by Rekoske *et al.* (Rekoske, et al. 2015).

Nonetheless, the fact that the CAF09-based vaccine was able to induce the expression of CD107a and granzyme B by CD8^{+} T-cells suggests that CD8^{+} T-cells from that vaccine group would have a better capacity of lysing tumour cells.

Previous studies have described a population of memory T-cells that can proliferate and exhibit effector functions in response to cytokines during viral and bacterial infections, without TCR engagement (Tough, et al. 1998) (Dhanji, et al. 2004) (Ehl, et al. 1997). TLR agonists, CpG and Poly I:C, have also been shown to induce the proliferation of these CD8^{+} CD44^{high} T-cells (Sprent, et al. 2000). These antigen-nonspecific CD44^{high} T-cells, described as the main cell type expanding following stimulatory immunotherapies, express NKG2D, release granzyme B and are induced following cytokine exposure (Tietze, et al. 2012). Further studies demonstrated a correlation between PD-1 expression and CD62L^{low} expression (corresponding to an effector/effector memory phenotype) (Sckisel, et al. 2017). Moreover, the elevated PD-1 expression on effector/effector memory cells was also observed in patients undergoing systemic high-dose IL-2 therapy. Although, this was found to be true for CD4^{+} T-cells mainly and in the peripheral organs, these results correlate with our findings regarding CD8^{+} splenocytes. Indeed, within the CD8^{+} T-cells from CAF09-vaccine immunised mice, approximately 60% displayed an effector/effector memory phenotype (20% for naïve mice), about 50% expressed PD-1 (20% for naïve mice) and about 10% expressed Granzyme B without antigen stimulation (2% for naïve mice). These findings suggest that the effector/effector memory cells could express PD-1 and that a small proportion of these cells might have cytotoxic capacities by releasing Granzyme B, although it could not be verified. Assessing the expression of NKG2D would be of interest to compare our findings with those of others and determine if the CAF09-based vaccine induces antigen non-specific CD8^{+} memory T cells with non-MHC restricted cytotoxic capacities. The induction of these cells would be of advantage when assessing the anti-

tumour effect of the vaccine, as tumour cells have the capacity to downregulate both MHC and tumour antigen expression in order to avoid recognition by CD8$^+$ T cells (Dunn, et al. 2002).

In conclusion, these results demonstrated the relevance of using a mutated peptide sequence in a vaccine in order to render it more immunogenic. The capacity of splenocytes from immunised animals to recognize WT-derived epitopes was therefore increased. Moreover, the different vaccine strategies tested have highlighted the importance of choosing the optimal delivery system in order to maximise the immunogenic potential of a vaccine. It is important to note that the optimal delivery system can differ depending on the peptide sequence length and on the mouse model used. We have shown that a strong vaccine strategy can induce a PAP-specific immune response, and generate functional PAP-specific CD8$^+$ T-cells capable of cytokine secretion and of degranulation of cytotoxic granules. In the next part of the study, the anti-tumour capacity of splenocytes from animals immunised with the optimised vaccine strategy was assessed *in vitro*. More precisely, the ability of splenocytes to kill target cells in a PAP-specific manner.

Chapter 4: Generation of relevant murine and human target cells and assessment of the anti-tumour capacity of the PAP42mer vaccine *in vitro*

4.1. Introduction

As detailed in the introduction, cytotoxic T lymphocytes (CTLs) are essential for long-term anti-tumour response. Indeed, tumours highly infiltrated in CTLs are more responsive to immunotherapy (Farhood, et al. 2019). The proliferation of intratumoral CTLs correlates with the reduction of tumour size (Tumeh, et al. 2014). The TCR of primed CD8$^+$ T-cells recognises antigenic peptides presented by MHC class-I molecules on the surface of tumour cells. Upon TCR engagement, activated CTLs secrete IFNγ and TNFα to promote cytotoxicity and induce direct cytotoxicity by two main pathways: the perforin/granzyme pathway and the death ligand pathway (section 1.3.4.1).

In the previous chapter, immunization with CAF09 adjuvant, which has previously been reported to elicit cytotoxic CD8$^+$ T-cells (Korsholm, et al. 2014), was demonstrated to induce ILL-specific CD8$^+$ T-cells capable of cytokine secretion and of degranulation of cytotoxic granules.

The aim of the studies presented in this chapter was to assess the efficacy of the selected vaccine strategies in generating CTLs capable of killing cancer cells in a PAP-specific manner *in vitro*. To this end, murine and human cancer cell lines were selected and modified to render them suitable targets. The first step was to assess the endogenous MHC class-I expression as well as the endogenous PAP expression. Secondly, to induce both the expression of the relevant MHC class-I molecule (human HLA-A2 or murine H2-K^{b}D^b) and either the murine or the human PAP protein.

Following the generation of relevant target cells, the next step was to assess the capacity of vaccine-induced T-cells to lyse these target cells. Class-I peptide specific CD8$^+$ T-cells which would then be able to recognize and lyse target cells, were expanded *in vitro* prior to proceeding with the cytotoxicity assay. Two different cytotoxicity assays were used: the ^{51}Cr release assay and a flow cytometry-based cytotoxicity assay.

These results allowed the selection of the vaccine strategy best capable of inducing PAP-specific cytotoxic T-cells, which will be used to assess its anti-tumour capacity *in vivo*.

4.2. Results

4.2.1. Generation of relevant target cells and tumour models

In order to assess the anti-tumour efficacy of the vaccine in the C57Bl/6 mouse model and in the HHDII/DR1 humanised mouse model, six cell lines were selected: three murine, two human and one humanized murine cell line. The tables below summarize the different target cells used and the changes required to assess the PAP-specific cytotoxicity.

Table 4.1: MHC class-I and PAP expression in murine cell lines

Murine cell lines					
		TRAMP-C1	**TRAMP-C2**	**RMAS**	
MHC class-I	Endogenous expression	Low H2-K^b-D^b	Low H2-K^b-D^b	H2-K^b-D^b	
	Adaptation needed	IFNγ treatment	IFNγ treatment	Optimisation of peptide-binding	
PAP expression	Endogenous expression	Murine PAP	Murine PAP	None	
	Adaptation needed	Murine PAP knock-down	Murine PAP knock-down	Optimisation of peptide-binding	

Table 4.2: MHC class-I and PAP expression in human cell lines

Human(ized) cell lines				
		B16 HHDII	**LNCaP**	**T2**
MHC class-I	Endogenous expression	Chimeric HLA-A2	HLA-A2	HLA-A2
	Adaptation needed	NONE	Chimeric HLA-A2 knock in	Optimisation of peptide-binding
PAP expression	Endogenous expression	None	Human PAP	None
	Adaptation needed	Human PAP knock in	Human PAP knock-down	Optimisation of peptide-binding

4.2.1.1. TRAMP-C1 and TRAMP-C2 murine cell lines

The TRAMP-C1 and the TRAMP-C2 prostatic murine cancer cell lines are derived from the Transgenic Adenocarcinoma Mouse Prostate (TRAMP) mouse model (Foster, et al. 1997). TRAMP males develop histological prostatic intraepithelial neoplasia (PIN) by 8 to 12 weeks of age that progresses to adenocarcinoma with distant metastases by 24-30 weeks of age. Three cell lines were established from the heterogeneous tumour of a 32-week old TRAMP mouse: TRAMP-C1, TRAMP-C2 and TRAMP-C3. Only TRAMP-C1 and TRAMP-C2 cell lines are tumorigenic when implanted into syngeneic C57Bl/6 animals (Foster, et al. 1997). All three cell lines are epithelial of origin. In this chapter, TRAMP-C1 and TRAMP-C2 cells were considered as target cells for *in vitro* killing.

4.2.1.1.1.Assessing MHC class-I expression

TRAMP-C2 cells have been described as having low MHC class-I molecules expression on their surface (Martini, et al. 2010). MHC class-I expression is required for class-I epitope presentation to CD8$^+$ T-cells, as a consequence of which, H2-K^b-D^b expression on TRAMP-C1 and TRAMP-C2 cells was assessed by flow cytometry. The analysis indicated that there was no endogenous H2-K^b-D^b expression (Figure 4.1A). Although IFNγ can induce MHC class-I expression and promote tumour-specific immune responses in TRAMP-C2-derived tumours (Martini, et al. 2010), IFNγ has also been shown to induce PD-L1 expression, an inhibitory molecule that binds to the PD-1 receptor expressed on T-cells thereby impairing the anti-tumour immunity (Abiko, et al. 2015). TRAMP-C1/C2 cells were treated with various concentrations of murine IFNγ for 24 hours and the (co-)expression of H2-K^b-D^b and of PD-L1 was measured by flow cytometry (Figure 4.1B and C). A concentration as low as 0.1ng/mL increased the percentage of H2-K^b-D^b positive cells up to 49% (~25% on average), however, ~66% of these cells also co-expressed PD-L1 (Figure 4.1B). A concentration of 1ng/mL resulted in 51% and 47% of H2-K^b-D^b positive TRAMP-C1 and TRAMP-C2 cells, respectively, with almost 100% of these cells also expressing PD-L1. A concentration of 2ng/mL or higher only slightly increased the percentage of H2-K^b-D^b positive cells.

PD-L1 was expressed on ~20% of TRAMP cells without IFNγ treatment (Figure 4.1 B). 0.1ng/mL of IFNγ induced PD-L1 expression in 50% of TRAMP cells and concentrations of 1ng/mL and over induced PD-L1 expression in 95% of TRAMP-C1 cells (Figure 4.1B).

The intensity of expression (Median Fluorescence Intensity, MFI) of H2-K^b-D^b and PD-L1 on TRAMP cells was also determined (Figure 4.1C). A concentration of 2ng/mL of IFNγ and over induced the highest H2-K^b-D^b MFI value (Figure 4.1C left), with 5ng/mL being required to induce maximal expression of PD-L1 MFI (Figure 4.1C right).

Considering these results, 1ng/mL of IFNγ was selected as the optimal concentration for pre-treating TRAMP cells prior *in vitro* killing assays. Although this concentration was shown to induce the expression of PD-L1 in most TRAMP cells, it induced the expression of H2-K^b-D^b molecules on 50% of TRAMP cells while 0.1ng/mL only induced the expression of MHC class-I molecules on 25% of TRAMP cells. This compromise was based on prioritising the expression of MHC class-I expression, despite the expression of PD-L1 molecule.
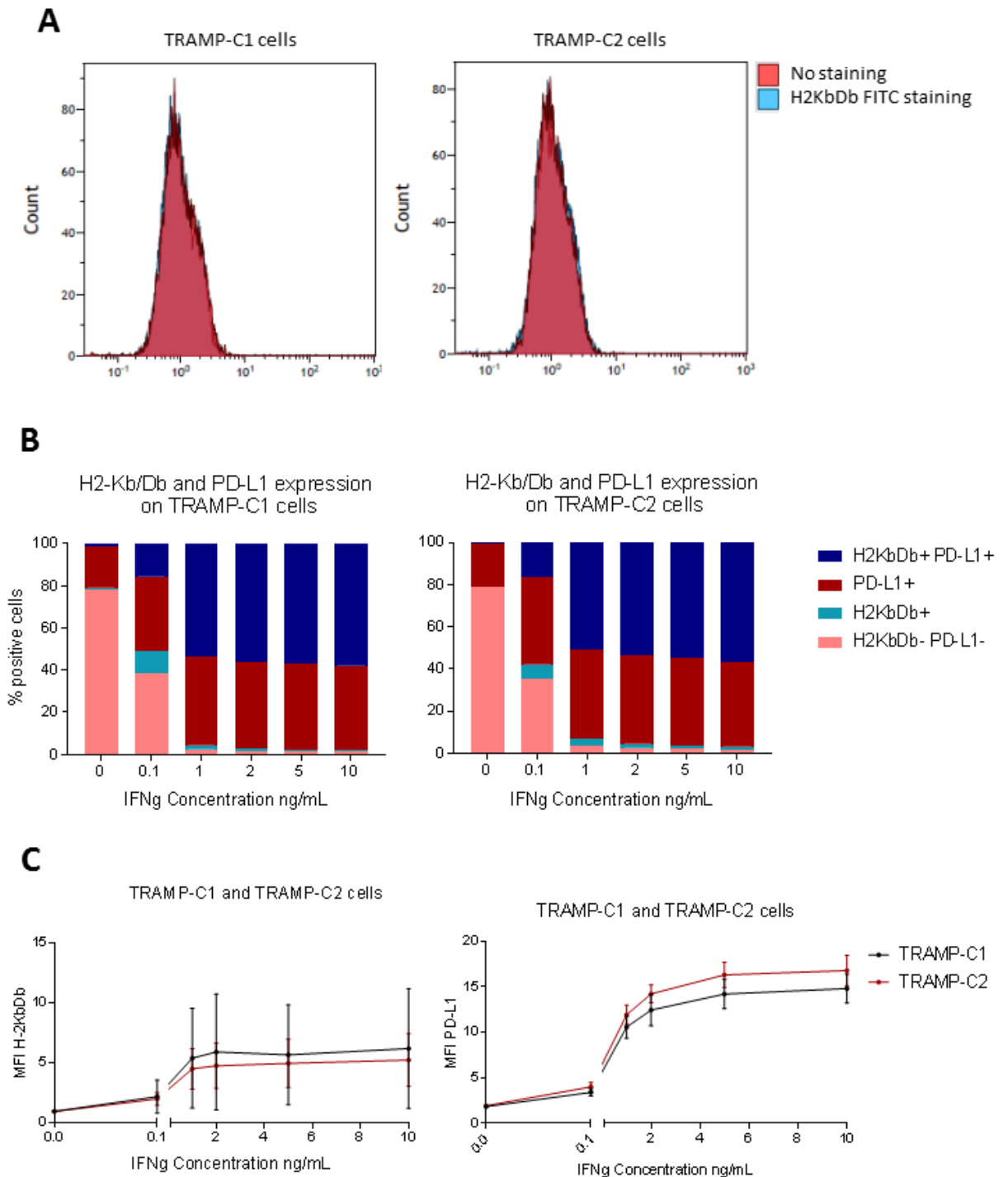
Figure 4.1: MHC class-I expression in TRAMP-C1 and TRAMP-C2 murine cancer cell lines (A) Histogram of H2Kb Db expression in TRAMP-C1 and TRAMP-C2 cells. (B) Effect of 24 hours mIFNγ treatment on the (co-) expression of MHC class-I H2Kb Db and PD-L1 molecules in TRAMP-C1 and TRAMP-C2 cells. (C) Expression by MFI of MHC class-I H2Kb Db and PD-L1 molecules. N=3 independent experiments.

4.2.1.1.2.Assessing endogenous mPAP expression and knock down of mPAP

TRAMP-C1 and TRAMP-C2 cell lines have been described as endogenously expressing PAP mRNA (Grossmann, et al. 2001). A qPCR for the murine PAP gene confirmed its expression within both TRAMP cell lines, with a higher mPAP expression in TRAMP-C2 cells (Figure 4.2 A).

In order to assess the role of mPAP expression in the killing of TRAMP cells by vaccine-induced CTLs, the mPAP gene was knocked down in TRAMP-C1 and TRAMP-C2 cell lines. The lentiviral transduction method was used (described in 2.2.1.3). mRNA from successfully transduced cells (selected in 1μg/mL of puromycin) was extracted to assess the expression of the mPAP gene. In both cell lines, there was a decrease in the mPAP expression in comparison to the empty vector control transduced cells (Figure 4.2 B). TRAMP-C1 knock down cells expressed 18% of the empty vector transfected counterpart, whereas TRAMP-C2 knock down cells expressed 47% of the empty vector transfected counterpart. In order to decrease the percentage of mPAP expression in the knock down cells, clones from single cells were selected. Empty vector transfected clones with the highest mPAP expression and shRNA knock down clones with the lowest mPAP expression were selected (Figure 4.2 C): TRAMP-C1 empty vector control clone 5, TRAMP-C1 shRNA clone 4, TRAMP-C2 empty vector clone 2 and TRAMP-C2 shRNa clone 3. These selected clones were used for subsequent *in vitro* killing assays.

The choice of clones could not be based on the protein expression of mPAP because none of the antibodies tested could recognize the mPAP protein by Western Blotting.
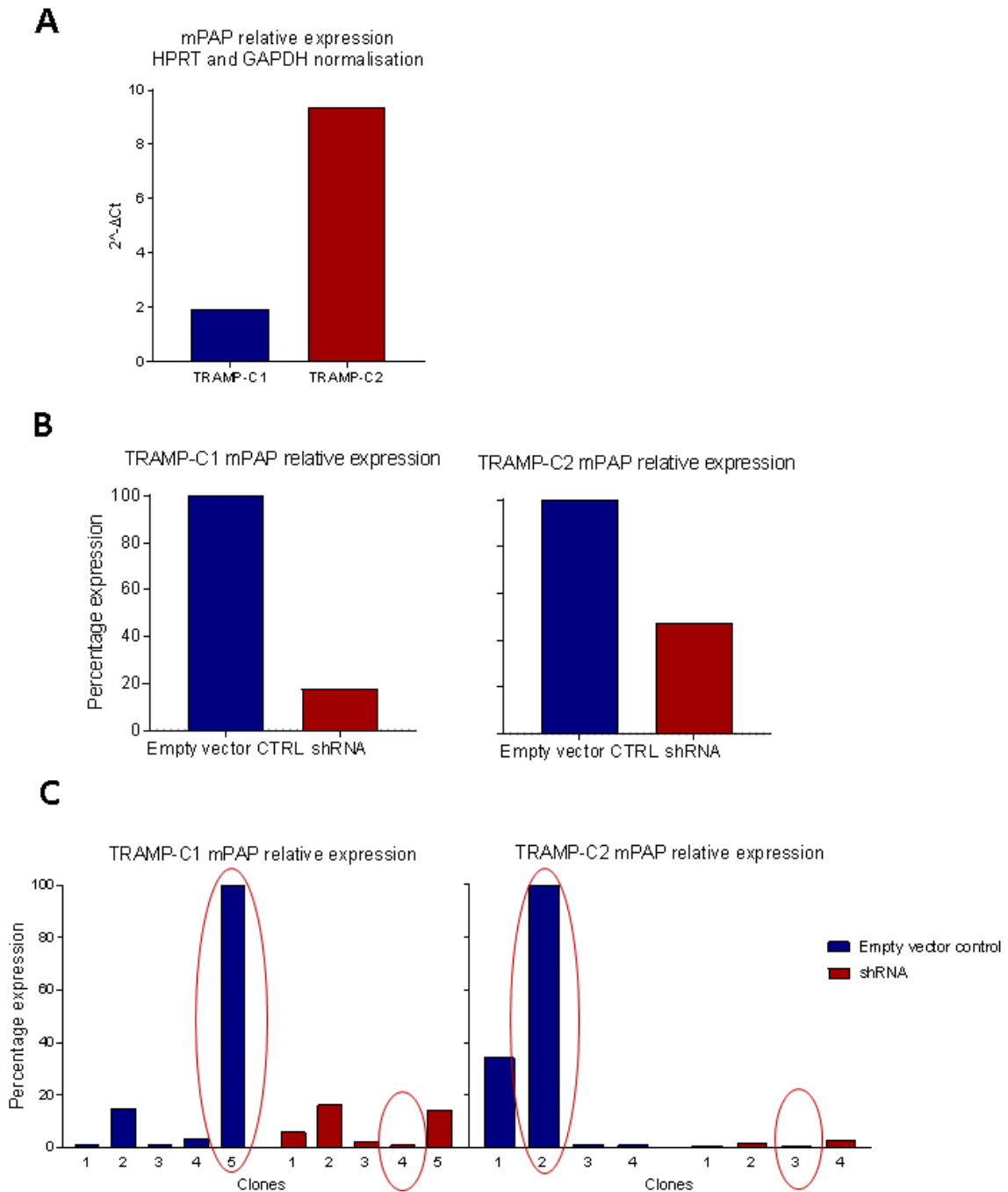
Figure 4.2: Endogenous mPAP expression and knock down of mPAP in TRAMP-C1 and TRAMP-C2 murine cancer cell lines. (A) Relative endogenous expression of mPAP. (B) Relative expression of the murine PAP gene following knock down with shRNA, before cloning (HPRT and GAPH normalisation) and (C) after cloning (HPRT normalisation). N=1 for each experiment.

4.2.1.2. LNCaP human cell line

The LNCaP cell line was isolated from a lymph node biopsy from a 50-year-old Caucasian male diagnosed with metastatic prostate carcinoma in 1977 (Horoszewicz, et al. 1980). The morphology, preservation of functional properties and conservation of tumorigenicity in athymic nude mice confirmed the human prostatic cancer tissue origin of LNCaP cells (Horoszewicz, et al. 1983). LNCaP cells were shown to be positive for the androgen receptor and for the oestrogen receptor. Moreover, their production of PAP and PSA was demonstrated *in vitro* as well as *in vivo* in tumours

and in the plasma of tumour-bearing animals (Horoszewicz, et al. 1983). The plasma level of PAP was found to increase with the size of the tumours.

4.2.1.2.1.Assessment of MHC class-I expression

The LNCaP cell line has been described as being HLA-A*0201 positive, although the HLA-A2 expression level was low and did not increase in response to IFN-gamma stimulation (Carlsson, et al. 2007). Olson *et al.* found similar results and used HLA-A2 transfected LNCaP as targets in cytotoxicity assays (Oslon, et al. 2010). However, when assessing the expression of HLA-A2 in the LNCaP cell line by flow cytometry, cells were positive (Figure 4.3 A). Thus, there was no need to increase the HLA-A2 expression of LNCaP cells in order to use them as target cells for future cytotoxicity experiments.

On the other hand, in order to use LNCaP cells as target cells for splenocytes from vaccinated HHDII/DR1 mice, cells were transfected to express a chimeric HLA-A2 gene, called HHD. The HHD molecule contains the HLA-A2.1 α1 and α2 domains, the H-2D^b α3 domain and the human β2 microglobulin. The presence of the H-2D^b α3 domain has been shown to facilitate the interaction with mouse CD8 molecules, thereby improving the CTL responses, as HHD-transfected cells are more efficiently recognized than cells transfected with the human HLA-A2.1 molecule (Pascolo, et al. 1997). The selection of successfully transfected cells was solely based on antibiotic selection (1mg/mL of G418) because the expression of the chimeric HLA-A2 cannot be distinguished from that of the wild-type HLA-A2 molecules. Hereafter, these cells will be called LNCaP HHDII cells.

4.2.1.2.2.Assessment of endogenous hPAP expression and knock down of hPAP

As stated earlier (section 4.2.1.2), LNCaP cells have been described as expressing PAP. Its expression was confirmed RT-PCR in comparison with HEK293t cells which are known to be PAP negative (Figure 4.3 B). In order to assess the role of human PAP expression in their sensitivity to killing by vaccine-induced CTLs, the humanPAP gene was knocked down in both the LNCaP WT and the LNCaP HHDII cell lines. The lentiviral transduction method was used and mRNA from successfully transduced cells (selected in 1μg/mL of puromycin) was extracted to assess the expression of the hPAP gene. In both cell lines, there was a decrease in the hPAP expression in comparison to the empty vector control transduced cells (Figure 4.3 C): 100 to 16% for LNCaP WT cells and 100 to 7% for LNCaP HHDII cells. These cells were not cloned due to their sensitivity and the difficulty to expand clones from single cells.
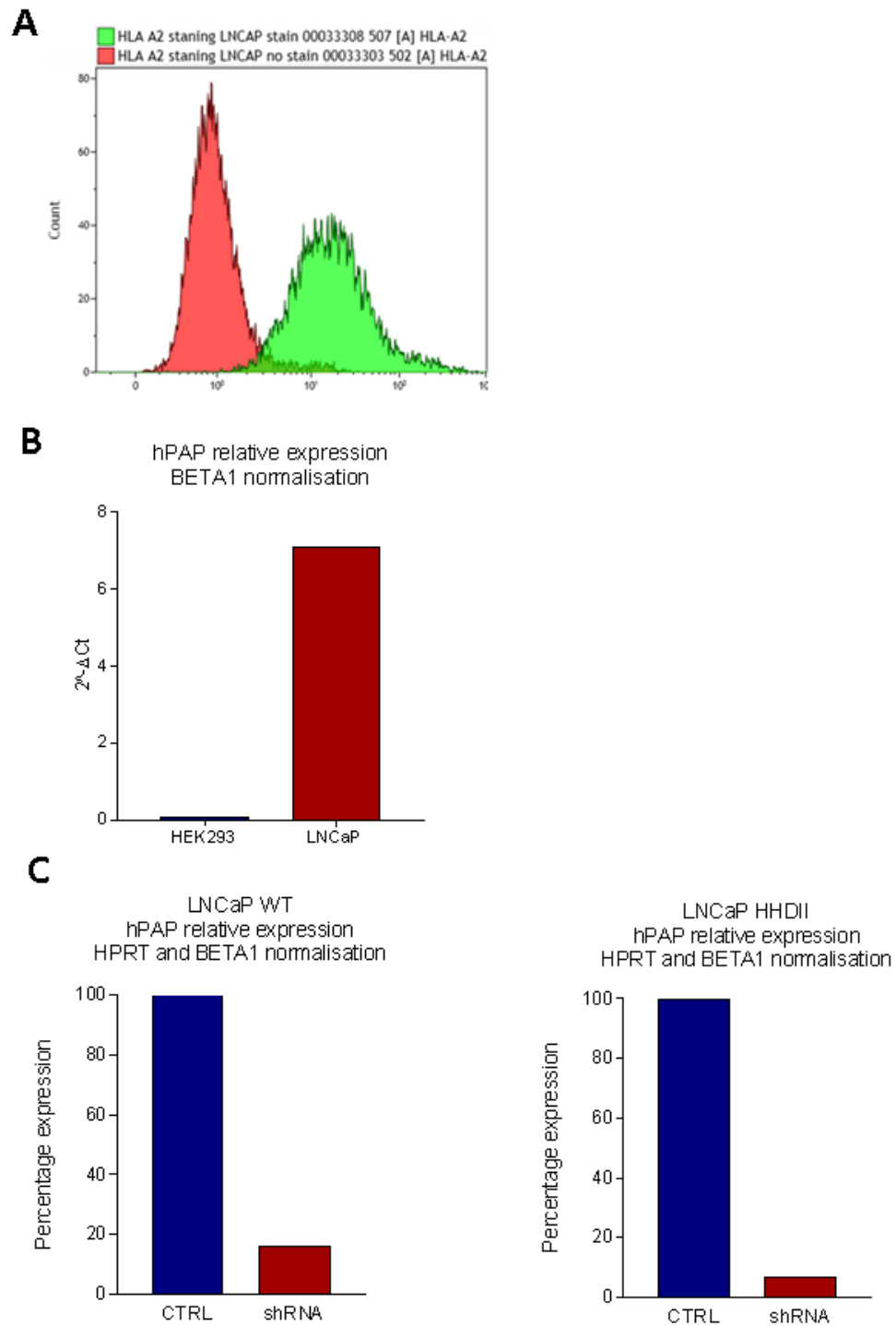
Figure 4.3: MHC class-I expression and endogenous hPAP expression and knock down of hPAP in LNCaP human cancer cell line. (A) Histogram of HLA-A2 expression. (B) Relative endogenous expression of hPAP. (C) Relative expression of the hPAP gene following knock down with shRNA. N=1 for each experiment.

4.2.1.3. B16F10 humanised murine cell line

B16F10 are melanoma cells derived from C57Bl/6 mice and were engineered by Scancell Limited to express the chimeric HLA-A2 and HLA-DR1 molecules, as described in 2.2.1.1.1. Although melanoma cells, these are the only available cell line that can be used to establish tumours in the HHDII/DR1 mice and therefore are being used as "proof of concept" in this study. Expression of the chimeric HLA-A2 and the HLA-DR1 molecules was confirmed by flow cytometry by a colleague by measuring the expression of the human β-2microglobulin and of the HLA-DR1 proteins (data not shown). As these cells do not express PAP protein, the hPAP gene was knocked-in to enable them to be used as target cells for the *in vitro* cytotoxicity assays and *in vivo* tumour studies. For this, the cell line was subjected to lentiviral transduction with both fraction 1 and 2 collected as described in 2.2.1.3.2. mRNA from the successfully transduced cells (selected in 1µg/mL of puromycin) was extracted to assess the expression of the hPAP gene by RT-PCR. Cells infected with both fractions showed a strong hPAP expression in comparison to the empty vector control transduced cells (Figure 4.4 A). Fraction 1, displaying an earlier Ct value, has a stronger expression of the hPAP gene. The expression was confirmed at the protein level by Western Blotting of supernatants from B16F10 cells, as PAP protein is mainly secreted (Figure 4.4 B). Indeed, the hPAP protein could not be detected from cell lysates (data not shown).

Clones from single cells were grown from both the empty vector control and the fraction 1 transduced cells. Six clones were expanded for each and the hPAP expression was assessed at the mRNA level. The clone number 5 displayed the highest hPAP expression (Figure 4.4 C). The expression was confirmed at the protein level by Western Blotting (Figure 4.4 D). B16F10 PAP clone 5 cells was selected for subsequent studies.
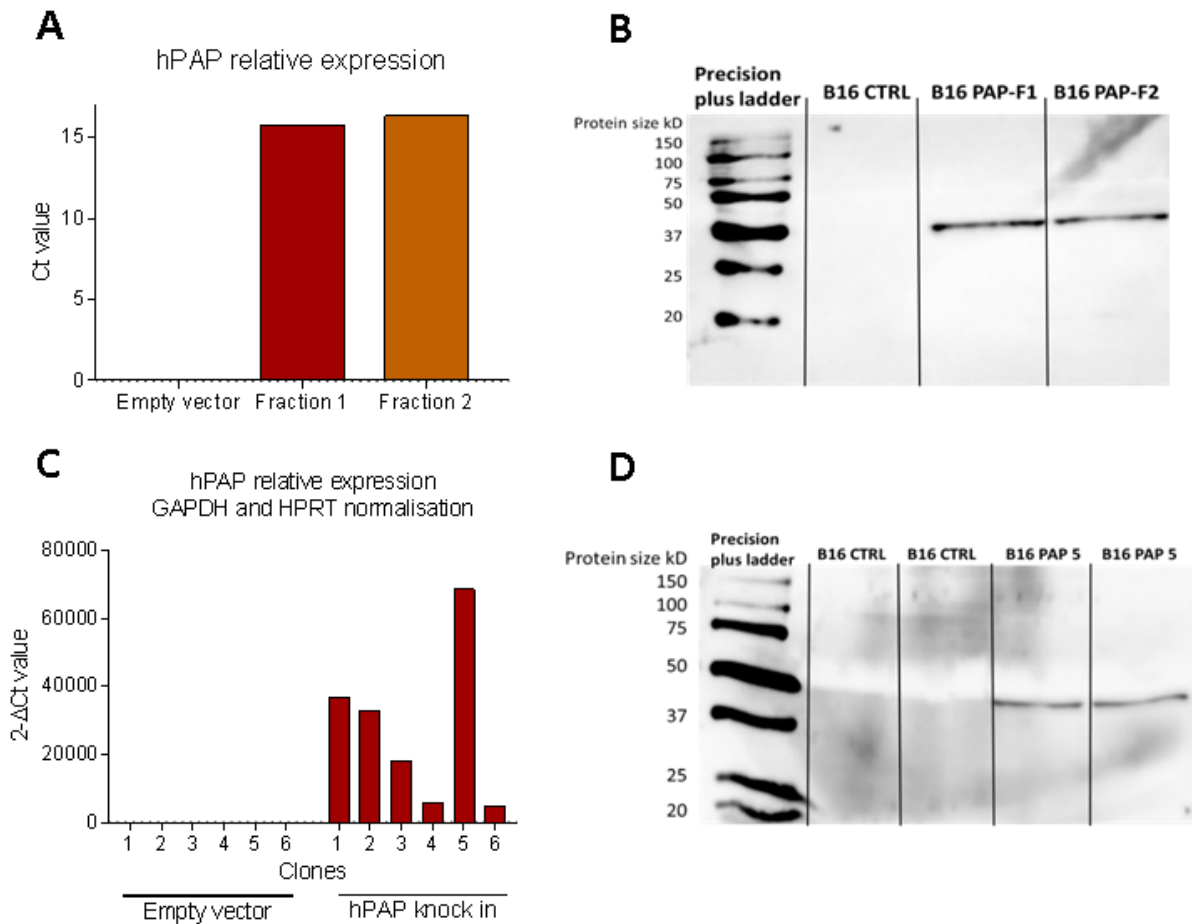
Figure 4.4: Knock in of hPAP in B16F10 humanized murine cancer cell line. (A) Relative expression of the human PAP gene following knock in in B16F10 cell line. (B) Protein expression of the human PAP from supernatants following knock in in B16F10 cell line. (C) Relative expression of the human PAP following knock in in B16 cell line and cloning. (D) Protein expression of the human PAP in B16-HHDII-PAP$^+$ clone 5 cells. N=1 for each experiment.

4.2.1.4. R-MAS and T2 cells

T2 and R-MAS cells are deficient for TAP, and therefore cannot process and present any internal peptides which are TAP-dependant (Anderson, et al. 1993). As a consequence, any empty MHC class-I/beta2 microglobulin (beta2m) molecules reaching the surface of the cells are quickly disassembled and recycled. However, an exogenous peptide with sufficient binding affinity for the MHC-Class-I molecule can stabilise the MHC class-I/beta2m complex. The stable MHC/beta2m/peptide complex can then be indirectly detected by staining for MHC-Class-I molecules. The total number of MHC Class-I molecules on the surface of the cells reflects the number of peptides bound. T2 and R-MAS cells can be pulsed with short (class-I) peptides, so that the epitopes can be presented at the surface of HLA-A2 (T2) or H-2K^{b}D^b (R-MAS) MHC class-I molecules and be used as target cells during cytotoxicity assays.

4.2.1.4.1.Effect of overnight incubation of R-MAS and T2 cells at 26°C

Incubation of R-MAS and T2 cells at 26°C increases the intensity of MHC class-I expression (Ljunggren, et al. 1990). This was confirmed by comparing the effect of overnight incubation of TAP-deficient cells at 37° and at 26°C followed by a flow cytometry staining with anti-MHC class-I antibodies (HLA-A2 for T2 cells, H-2K^b-D^b for R-MAS cells). In both cell lines, the expression of MHC class-I molecules increased by overnight incubation at 26°C (figure 4.5 A).

4.2.1.4.2.T2 and R-MAS peptide binding assay

The lowest concentration of short peptides necessary to obtain the highest number of peptide/MHC class-I stable complexes at the surface of R-MAS and T2 cells was determined by performing MHC peptide binding assays. Peptide binding assays were performed on cells which had been incubated overnight at 26°C. The assay was performed with ISI 9mer peptide for R-MAS H2-K^b-D^{b+} cells and with ILL 9mer peptide for T2 HLA-A2$^+$ cells. In both cases, 50μg/mL was found to be the concentration needed to reach a plateau in the MFI of MHC class-I molecules (Figure 4.5 B).
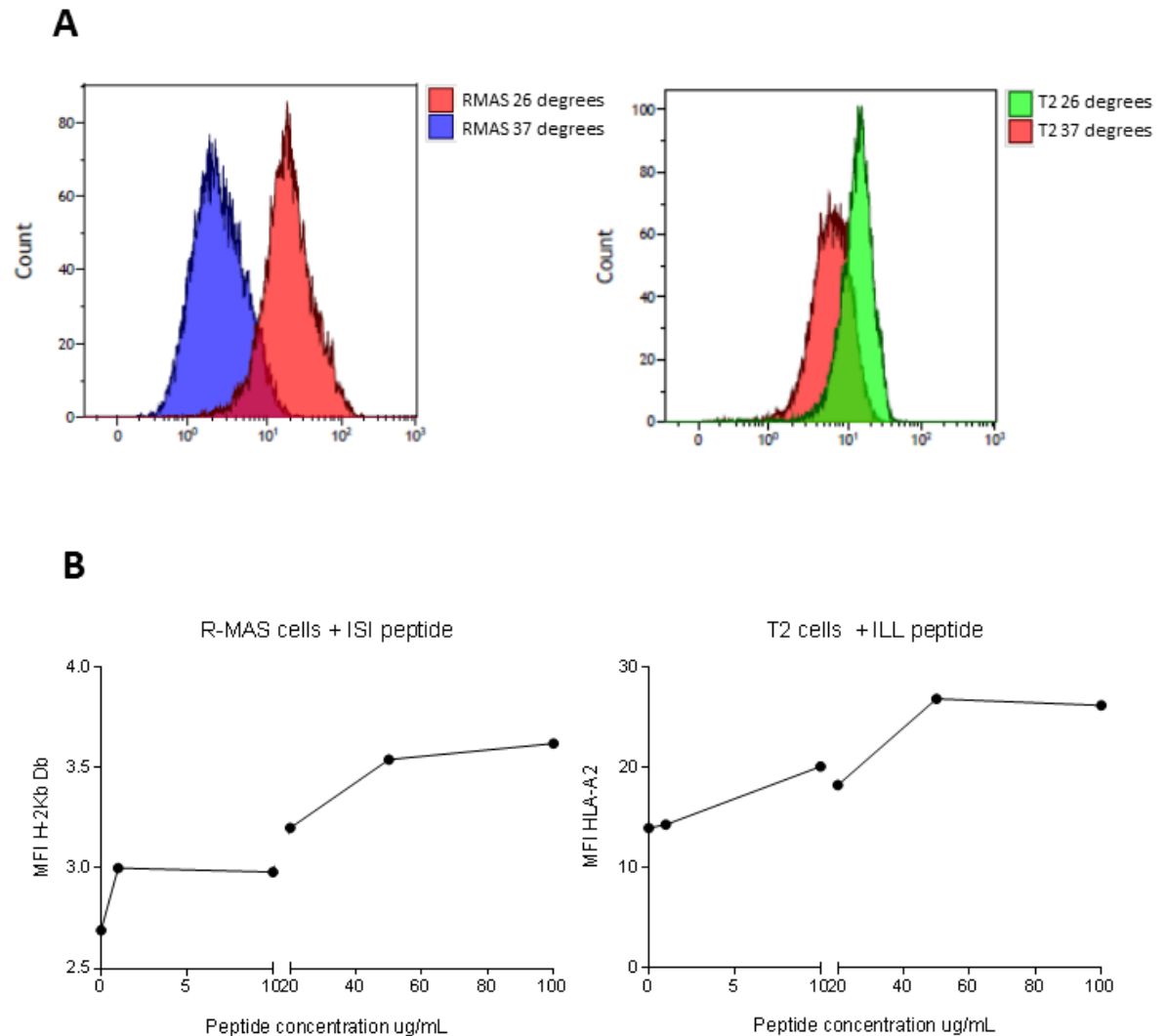
Figure 4.5: Enhancement of T2 and R-MAS cell lines as class-I peptide presenting target cells. (A) Effect of overnight incubation at 26°C on MHC class-I expression of R-MAS and T2 cells. (B) Effect of increasing quantity of 9mer peptides on MHC class-I expression in R-MAS and T2 cells. N=1 for each experiment.

4.2.2. Capacity of vaccine induced T-cells to kill relevant target cells

Following the generation of relevant target cells, the next step was to assess the capacity of vaccine-induced T-cells to kill these target cells. To expand vaccine-specific T-cells, splenocytes were stimulated *in vitro* with either mitomycin treated LPS-blast cells previously pulsed with class-I peptides or with class-I peptides directly. The use of syngeneic LPS-irradiated blasts has been shown to induce the stimulation of T-cells and to generate effector cytotoxic and helper cells (Bjorklund, et al. 1986). The goal was to expend class-I peptide specific CD8+ T-cells which would then be able to recognize and kill target cells. Because total splenocytes were used for the cytotoxicity assays, the proportion of T-cells, CD4+ and CD8+ T-cells was assessed by flow cytometry (Figure 4.6 A). In the C57Bl/6 model, the proportion of CD8+ T-cells within total T-cells in vaccinated mice was ~70-80% (Figure 4.6 A left), which was similar to the proportion of CD8+ T-cells in splenocytes from naïve mice. The proportion of CD8+ T-cells in the CAF09-based vaccine group was greater than that in the ImmunoBody®-based vaccine group.

On the other hand, the increased proportion of CD8+ T-cells and decreased proportion of CD4+ T-cells within the total T-cell population was vaccine-specific in the HHDII/DR1 model (Figure 4.6 A right). The proportion of CD8+ T-cells in the CAF09-based vaccine group was significantly higher than that in naïve and in other vaccinated groups. The CpG-based and the ImmunoBody®-based vaccines induced a non-significant increase in the proportion of CD8+ T-cells.

Given the fact that CD8+ T-cells were shown to be activated by the vaccines in both models in Chapter 3, their expression of activating and inhibitory markers was determined. In the C57Bl/6 model, both vaccines induced a significant increase of PD-1 expression and a non-significant increase in the proportion of PD-1/Tim3+ cells (Figure 4.6 B top graph). Other markers were not affected in a vaccine-specific manner, but GITR, LAG-3 and Tim-3 were increased in all groups in comparison to their expression before class-I epitope stimulation (Figure 3.5C and 3.8C versus Figure 4.6B). In the HHDII/DR1 model, the proportion of PD-1/Tim3+ cells was significantly increased in the CAF09-vaccine group (~90% of cells) and in the CpG-vaccine group (~60% of cells). GITR, LAG-3 and Tim-3 were also increased in all groups, although there was a slight decrease of GITR in the CA09-vaccine group and a slight increase of OX40 in the CpG-vaccine group. Overall, the CAF09-based vaccine induced the highest proportion of CD8+ T-cells and of PD-1/Tim3+ CD8+ T-cells in both models.

The use of mitomycin-C treated peptide-pulsed LPS blasts or of class-I peptides alone to stimulate splenocytes did not change the number or the phenotype of T-cells, neither did it change the outcome of the cytotoxicity assay (compared in the case of T2 cells killing) (data not shown).
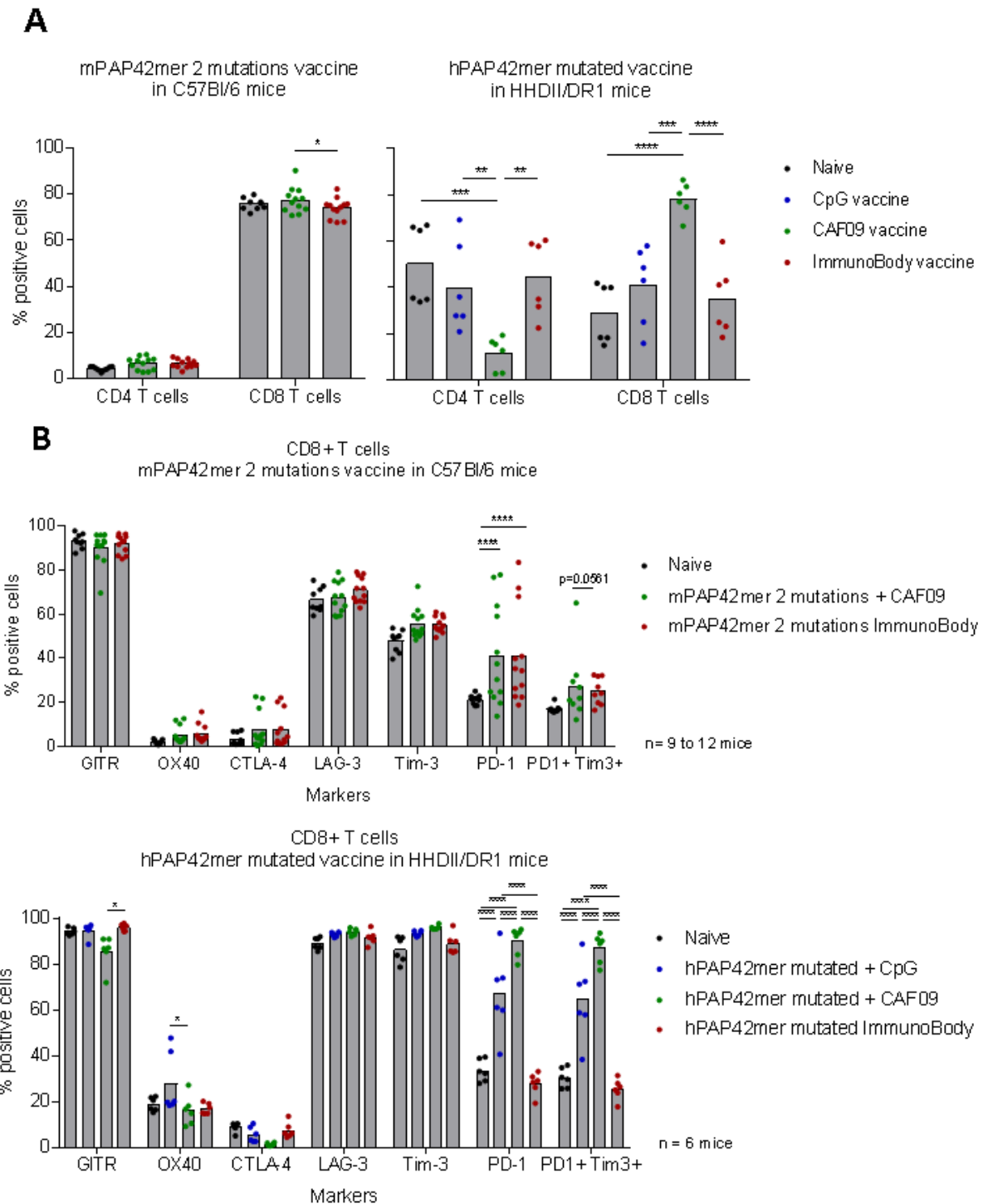
Figure 4.6: Effect of different vaccines on the proportion of CD4+ and CD8+ T-cells and on the phenotype of CD8+ T-cells following 6 days of *in vitro* stimulation in both mouse models. C57Bl/6 mice or HHDII/DR1 mice were immunised on days 1, 15 and 29 with either the CpG-based, the CAF09-based or the ImmunoBody®-based PAP 42mer vaccine. Seven days after the last immunisation, splenocytes were isolated from spleens and incubated with either pulsed LPS-blast cells or class-I peptides alone. Six days later, splenocytes were incubated with a murine FcR block and then stained with surface antibodies for flow cytometry analysis indicating (A) proportion of CD4+ and CD8+ T-cells, (B) proportion of CD8+ T-cells expressing activating and inhibitory markers. The CAF09-based vaccine induced an increase of the proportion of CD8+ T-cells, and an increase in the proportion of PD-1 +/- Tim3+ CD8+ T-cells. Bars represent the mean percentage of positive cells and the error bars represent the SD. Results are representative of two to three independent experiments (n= 6 to 9 mice per test group). A significant difference between immunisation groups was determined using a two-way ANOVA comparison test.

4.2.2.1.HHDII/DR1 model

4.2.2.1.1.Killing of ILL peptide-pulsed T2 cells

The ability of splenocytes from mice vaccinated with the hPAP42mer mutated vaccines to lyse relevant target cells was assessed *in vitro* by performing a ^{51}Cr release assay. To assess the capacity of splenocytes to specifically recognise the ILL 9mer epitope presented by an HLA-A2-expressing target cell, T2 cells previously pulsed with the ILL9mer peptide were used (Figure 4.7 A). Splenocytes from the CpG-vaccine immunised group and from the CAF09-vaccine immunised group were able to specifically lyse ILL-pulsed T2 cells, with a greater percentage of cytotoxicity against T2 ILL cells for the CAF09-vaccine group. There was no ILL-specific killing in the ImmunoBody®-vaccine nor in the naïve group. The proportion of CD8$^+$ T-cells co-expressing PD-1, LAG-3 and Tim-3 correlated positively with the capacity of splenocytes to recognize and lyse ILL-pulsed T2 cells (Figure 4.7 B).

4.2.2.1.2.Killing of B16-HHDII-PAP$^+$ cells

Similarly, the cytotoxic capacity of splenocytes from mice vaccinated with the hPAP42mer mutated vaccines against B16-HHDII-PAP$^+$ cells was assessed (Figure 4.7 C). Although the cytotoxicity observed was not PAP-specific, the cytotoxic capacity of splenocytes from both the CAF09 and the ImmunoBody®-vaccine groups was greater than that of splenocytes from the CpG-vaccine group.
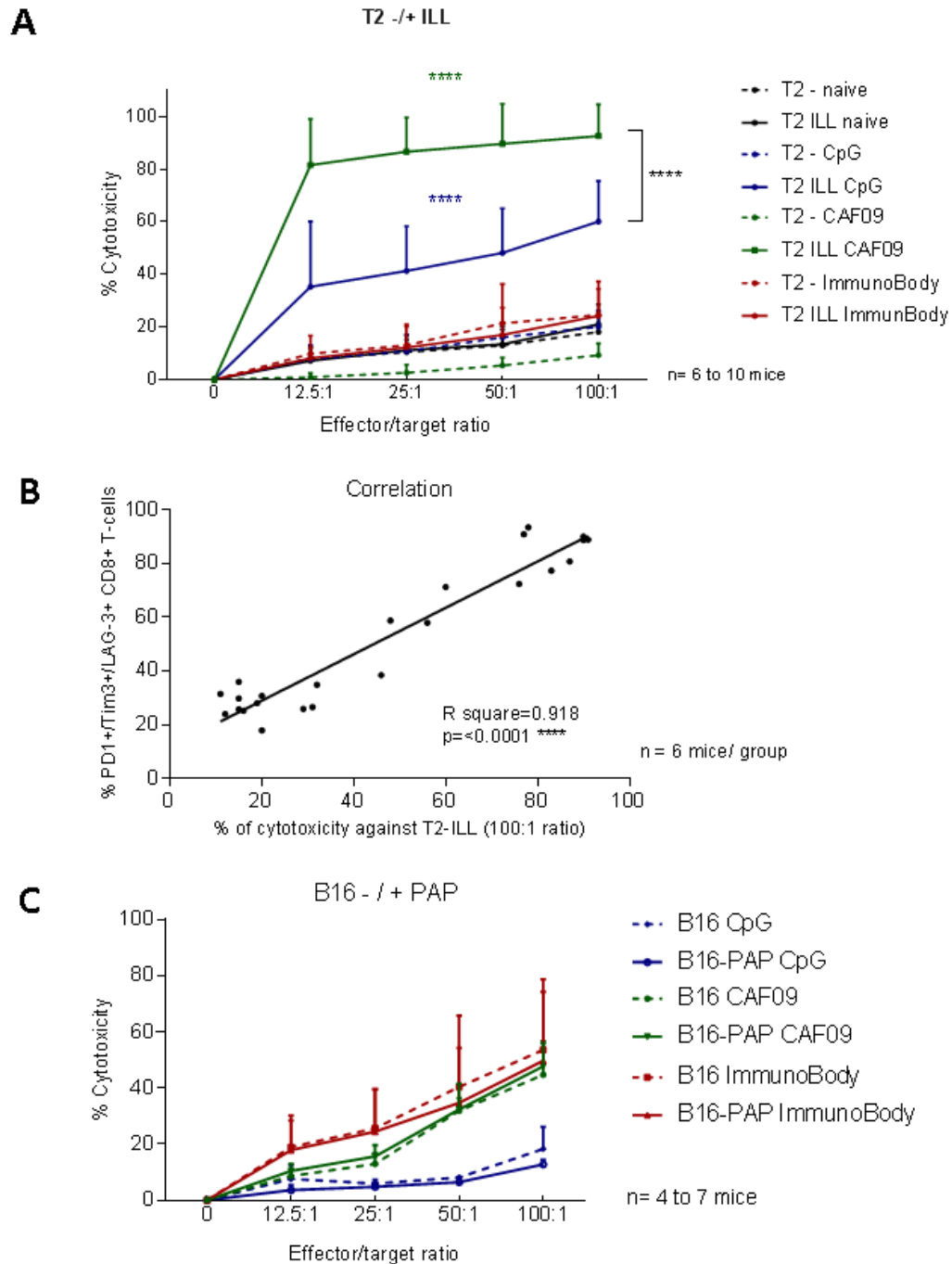
Figure 4.7: Cytotoxic capacity of splenocytes from vaccinated HHDII/DR1 mice against T2 cells -/+ ILL peptide and against B16-HHDII cells -/+ hPAP. HHDII/DR1 mice were immunised on days 1, 15 and 29 with either the CpG-based, the CAF09-based or the ImmunoBody®-based hPAP 42mer mutated vaccine. Seven days after the last immunisation, splenocytes were isolated from spleens and incubated with either pulsed LPS-blast cells or class-I peptides alone. Six days later, splenocytes were co-incubated with ^{51}Cr labelled target cells for an incubation of 4hrs to overnight, at the end of which the radioactivity was measured to determine the percentage of cytotoxicity. (A) Percentage of cytotoxicity against T2 cells pulsed or not with ILL9mer peptide and (B) correlation between the percentage of CD8^{+} T-cells co-expressing PD-1, Tim-3 and LAG-3 and the percentage of cytotoxicity against T2-ILL cells at 100:1 ratio. (C) Percentage of cytotoxicity against B16 cells -/+ hPAP. The CAF09 and the CpG-based vaccines induced ILL-specific killing against T2 cells. No PAP-specific killing was observed against B16 cells. Dots represent the mean percentage of cytotoxicity and the error bars represent the SD. Results are representative of two to three independent experiments. A significant difference between immunisation groups was determined using a two-way ANOVA comparison test.

4.2.2.1.3. Killing of LNCaP HHDII cells

The next step was to assess the capacity of vaccine-induced T-cells to lyse LNCaP cells naturally expressing the hPAP protein and transfected with the chimeric HLA-A2 molecule. This was firstly performed using a ^{51}Cr release assay, however, results were inconclusive, both after 4 hours and after overnight incubation (data not shown). LNCaP cells are highly sensitive and the spontaneous cell death was high. It was therefore decided to perform a flow cytometry-based assay, which allows the direct detection of target cell death on an individual cell basis, therefore allowing a shorter time of co-incubation (3 hours). The cytotoxic activity of total splenocytes was assessed at similar effector cell : target cell ratios (minus the 100:1 ratio). No PAP-specific killing (Figure 4.8A upper graph) and no vaccine-specific killing (Figure 4.8A lower graph) was detected. The cytotoxicity effect of isolated CD8$^+$ T-cells was measured at lower ratios: 5:1, 10:1 and 20:1. No significant PAP-specific killing (Figure 4.8 B upper graph) and no vaccine-specific killing (Figure 4.8B lower graph) was observed, although cells from the CpG-vaccine and the CAF09-vaccine groups induced a higher percentage of cytotoxicity than cells from the naive, non-immunised group.
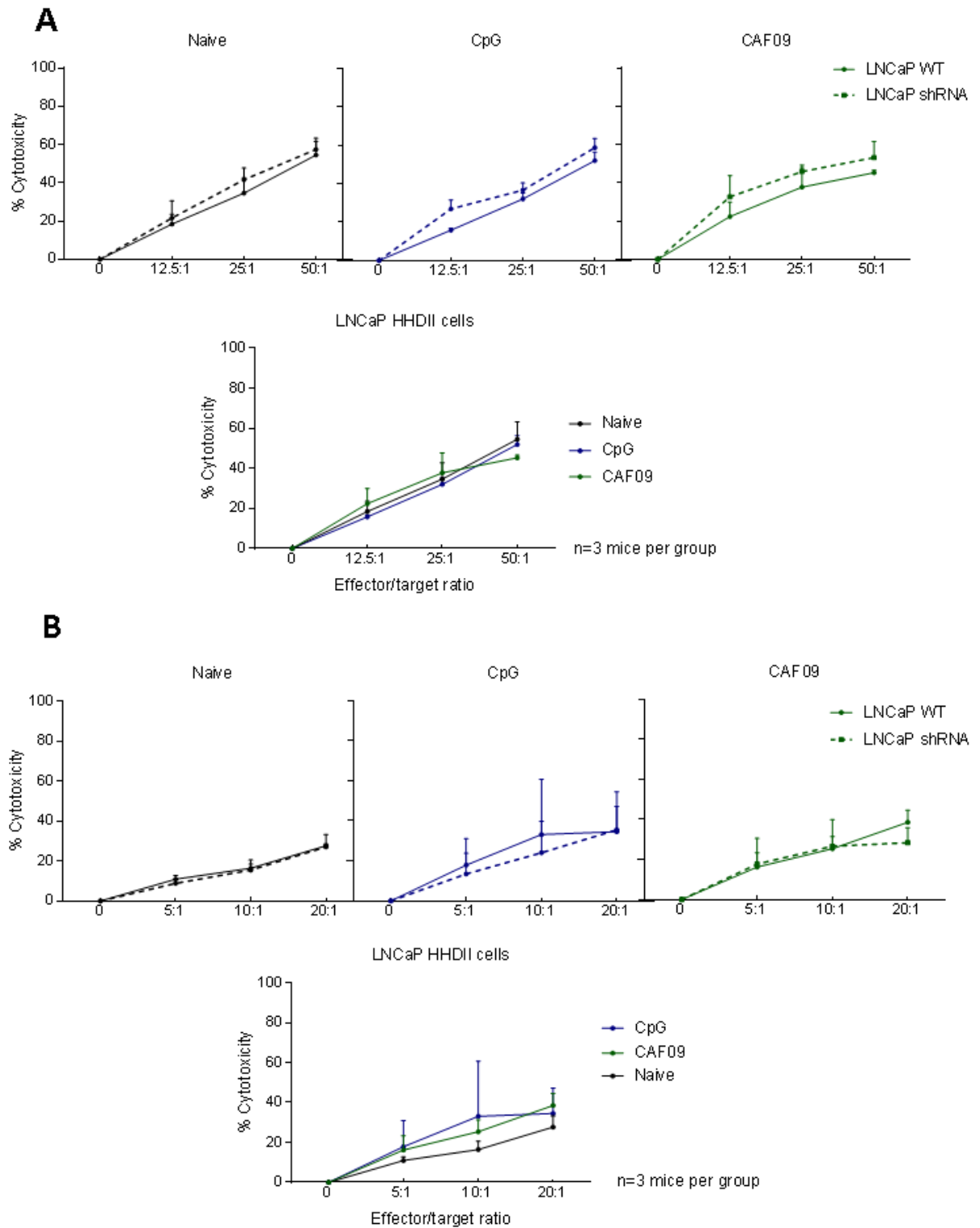
Figure 4.8: Killing of LNCaP HHDII -/+ hPAP cells by splenocytes from vaccinated HHDII/DR1 mice. HHDII/DR1 mice were immunised on days 1, 15 and 29 with either the CAF09-based or the CpG-based hPAP 42mer 1 mutation vaccine. Seven days after the last immunisation, splenocytes were isolated from spleens and incubated with either pulsed LPS-blast cells or class-I peptides alone. Six days later, splenocytes were co-incubated with PK26 fluorescent dye-labelled target cells for 3hrs, at the end of which the cytotoxicity of PK26+ cells was measured by flow cytometry. Percentage of cytotoxicity against LNCaP HHDII cells -/+ hPAP was measured when co-incubated with (A) total splenocytes or (B) isolated CD8+ T-cells. None of the vaccines induced PAP-specific killing. Dots represent the mean percentage of cytotoxicity and the error bars represent the SD. Results are representative of one experiment. A significant difference between immunisation groups was determined using a two-way ANOVA comparison test.

4.2.2.2.C57Bl/6 model

4.2.2.2.1.Killing of R-MAS cells pulsed with ISI and SIW peptides

The ability of splenocytes from mice vaccinated with the mPAP42mer 2 mutations vaccines to lyse relevant target cells was assessed *in vitro* using the ^{51}Cr release assay. To assess the capacity of splenocytes to specifically recognise ISI9mer and SIW8mer epitopes presented by H2-K^b-D^b-expressing target cell, RMAS cells were previously pulsed with each epitope (Figure 4.9). To confirm the most immunogenic mPAP42mer peptide to be used in the vaccine, the experiment was performed with splenocytes from animals immunised with either the WT, the 2 mutations or the 3 mutations mPAP42mer peptide with CAF09 adjuvant (Figure 4.9 A). As concluded in Chapter 3, the mPAP42mer 2 mutation peptide was the most immunogenic with significant specific killing achieved for all ratios with both peptide (ISI and SIW) in that group. The 3 mutations peptide also induced ISI and SIW peptides specific killing, but to a lesser extent and not in the case of the 100:1 ratio. Despite displaying a lowest binding score and being recognised by lower avidity T-cells than ISI9mer (section 3.2.2.2.1), RMAS cells pulsed with the SIW8mer peptide induced a higher percentage of cytotoxicity than those pulsed with the ISI9mer peptide.

The same experiment was performed to compare the cytotoxicity induced by the mPAP42mer 2 mutations CAF09 or ImmunoBody®-vaccine approaches (Figure 4.9 B). Splenocytes from the CAF09-vaccine group were able to induce ISI and SIW specific cytotoxicity down to an effector: target cell ratios of 12.5:1. However, the difference with the unpulsed RMAS cells was not as high as previously (Figure 4.9 A middle graph) as there is more variability due to the higher experimental (n) number. Splenocytes from the ImmunoBody®-vaccine group were able to induce ISI specific killing at the 12.5:1 ratio, but there was no SIW specific killing (Figure 4.9 B right).

To assess vaccine-specific induced killing, the percentage of RMAS ISI and RMAS SIW cytotoxicity induced by vaccines was compared with that induced using splenocytes from naïve mice (Figure 4.9 C). In the case of ISI9mer epitope, only cells from the ImmunoBody®-vaccine group induced a significantly higher percentage of killing at ratios 12.5:1 and 50:1. In the case of SIW8mer epitope, both CAF09 and ImmunoBody® vaccines induced a significantly higher percentage of cytotoxicity at all ratios (except for ImmunoBody® group at 12.5:1 ratio). Overall, the SIW8mer epitope appears to be recognised better than ISI9mer epitope.
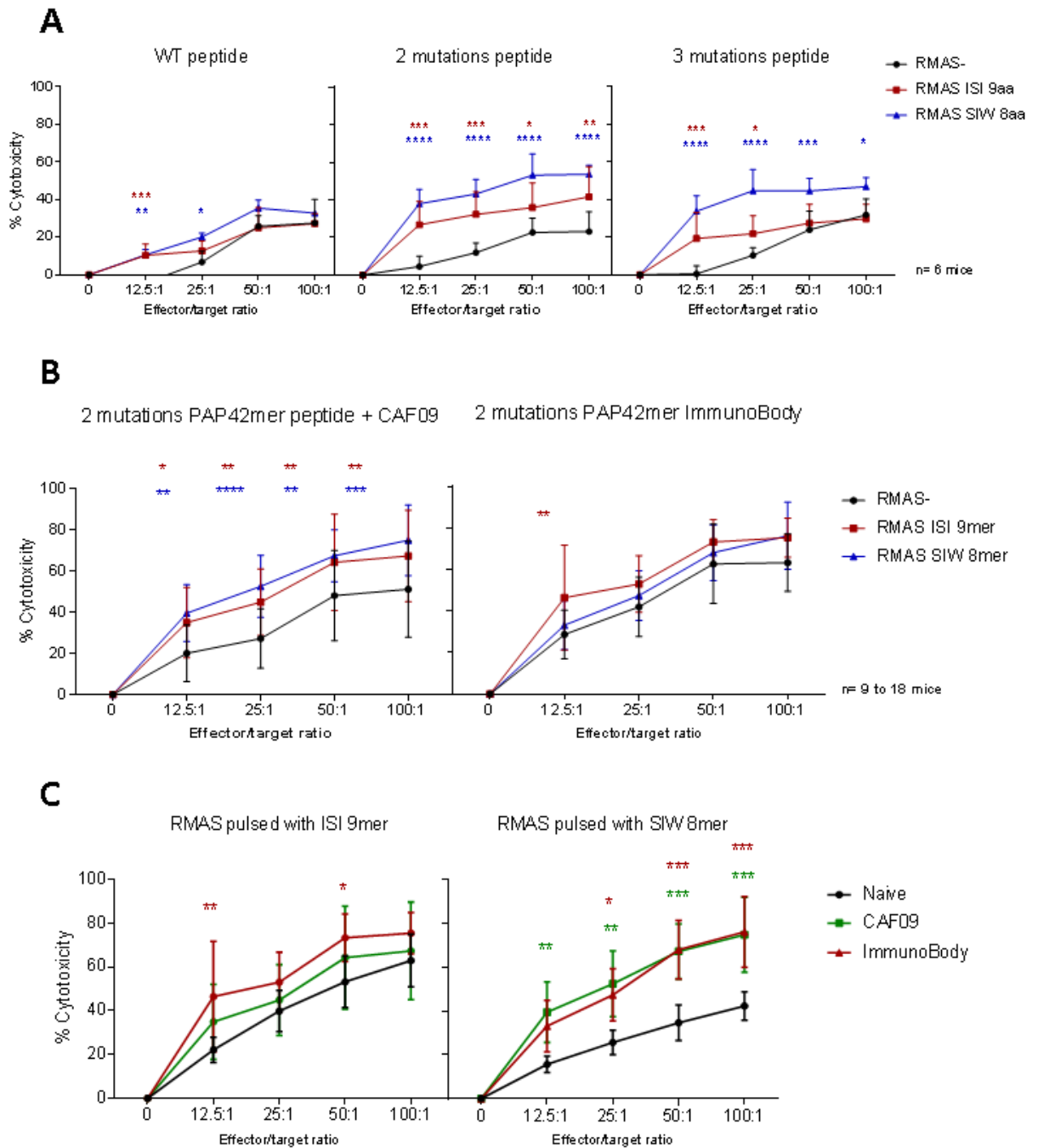
Figure 4.9: Killing of R-MAS cells pulsed with ISI / SIW peptides by splenocytes from vaccinated C57Bl/6 mice. C57Bl/6 mice were immunised on days 1, 15 and 29 with either the CAF09-based or the ImmunoBody®-based mPAP 42mer 2 mutations vaccine. Seven days after the last immunisation, splenocytes were isolated from spleens and incubated with either pulsed LPS-blast cells or class-I peptides alone. Six days later, splenocytes were co-incubated with ^{51}Cr labelled target cells for 4hrs, at the end of which the radioactivity was measured to determine the percentage of cytotoxicity. Percentage of cytotoxicity against RMAS cells un-pulsed or pulsed with ISI9mer or SIW8mer was measured according to (A) the mPAP42mer peptide sequence used for vaccination, (B) the delivery system and (C) in comparison to splenocytes from naive mice. The 2 mutation mPAP42mer peptide induced more ISI and SIW-specific killing than other peptides. The CAF09-based vaccine induced ISI and SIW-specific killing against RMAS cells. Dots represent the mean percentage of cytotoxicity and the error bars represent the SD. Results are representative of one to six independent experiments. A significant difference between immunisation groups was determined using a two-way ANOVA comparison test.

4.2.2.2.2.Killing of TRAMP-C1 and TRAMP-C2 cell lines

The same experiment was performed with TRAMP-C1 and TRAMP-C2 cell lines as target cells, naturally expressing the mPAP. The cells knocked down for the mPAP gene were used as controls to assess the PAP-specificity of the cytotoxicity.

As mentioned in section 4.2.1.1.1, the effect of IFNγ pre-treatment of TRAMP cells on their susceptibility to be killed *in vitro* was assessed. To this end, the capacity of splenocytes from mice immunised with either the CAF09 or the ImmunoBody®-based vaccine to kill TRAMP-C1 cells was tested. Regardless of the vaccine used, IFNγ pre-treatment of TRAMP-C1 cells lead to a higher percentage of cytotoxicity (Figure 4.10 A). Without IFNγ pre-treatment, splenocytes from the ImmunoBody®-vaccine group induced more killing, whereas with IFNγ pre-treatment, splenocytes from the CAF09-vaccine group induced a higher percentage of cytotoxicity.

The observation that IFNγ pre-treatment of TRAMP-C1 renders them more susceptible to killing by splenocytes can be explained by the induction of immunoproteasome (Tanaka et Kasahara, 1998) in TRAMP-C1 cells which renders them more immunogenic through the presentation of different epitopes by MHC class-I molecules.

To understand if the cytotoxicity observed was PAP-specific, the same experiment was performed using both the WT and the mPAP knocked down TRAMP-C1 cells. PAP-specific killing was observed in the CAF09-vaccine group at ratios 50:1 and 100:1, whereas it was only observed at the ratio 100:1 in the ImmunoBody®-vaccine group (Figure 4.10 B). Surprisingly, the PAP-specific killing was almost exclusively observed when cells had not been pre-treated with IFNγ. These results led us to perform subsequent cytotoxicity assays without IFNγ pre-treatment.
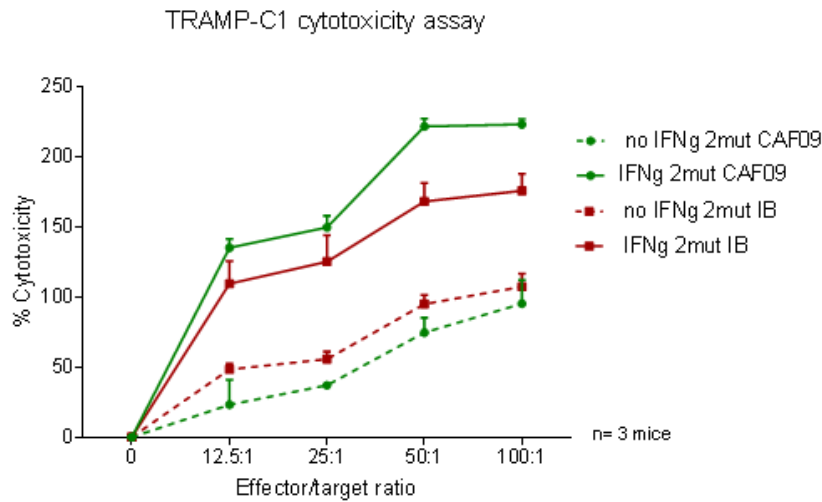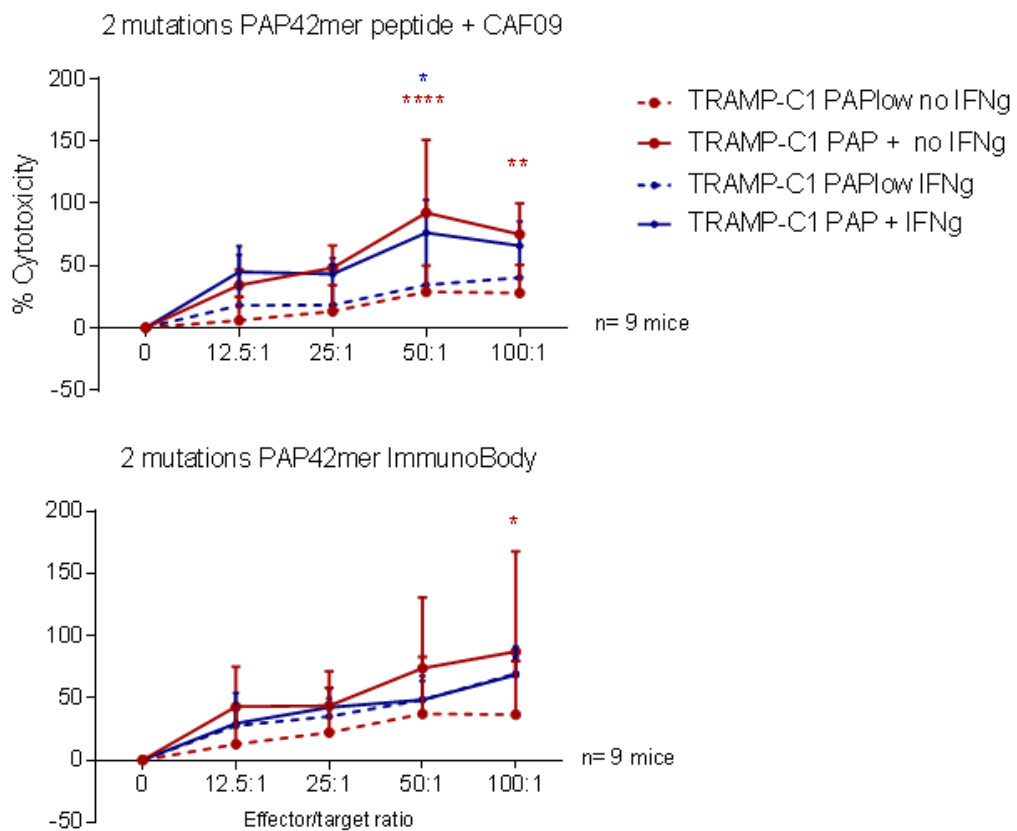
Figure 4.10: Optimisation of killing assay using TRAMP-C1 cells -/+ mPAP and -/+ IFNg pretreatment, with splenocytes from vaccinated C57Bl/6 mice. C57Bl/6 mice were immunised on days 1, 15 and 29 with either the CAF09-based or the ImmunoBody®-based mPAP 42mer 2 mutations vaccine. Seven days after the last immunisation, splenocytes were isolated from spleens and incubated with either pulsed LPS-blast cells or class-I peptides alone. Six days later, splenocytes were co-incubated with ^{51}Cr labelled target cells for an overnight incubation, at the end of which the radioactivity was measured to determine the percentage of cytotoxicity. Percentage of cytotoxicity against TRAMP-C1 cells was measured according to (A) IFNγ pre-treatment and (B) PAP-specific killing. IFNγ pre-treatment increased the percentage of cytotoxicity. The CAF09-based vaccine induced PAP-specific killing against TRAMP-C1 cells without IFNγ pre-treatment. Dots represent the mean percentage of cytotoxicity and the error bars represent the SD. Results are representative of one to three independent experiments. A significant difference between immunisation groups was determined using a two-way ANOVA comparison test.

To determine if the PAP-specific TRAMP-C1 killing observed was due to the vaccine itself, the killing assay was also performed with splenocytes from unvaccinated naïve mice. Splenocytes from all three groups induced a higher percentage of cytotoxicity against the WT TRAMP-C1 cells in comparison to their knocked down counterpart (Figure 4.11 A), albeit non-significantly in the case of the ImmunoBody®-vaccine group. The same experiment performed on TRAMP-C2 cells demonstrated that only splenocytes from the CAF09-vaccine group lysed these cells in a PAP-specific manner (Figure 4.11 B). However, there was a non-significant increase in the percentage of cytotoxicity against the WT TRAMP-C2 cells in the ImmunoBody®-vaccine group. Finally, the percentage of cytotoxicity against the WT TRAMP cells between the three groups was compared. There was no vaccine-specific killing against TRAMP-C1 cells, whereas in the case of TRAMP-C2 cells, the CAF09-vaccine induced a significantly higher percentage of cytotoxicity than the ImmunoBody®-vaccine or no vaccination (Figure 4.11 C).
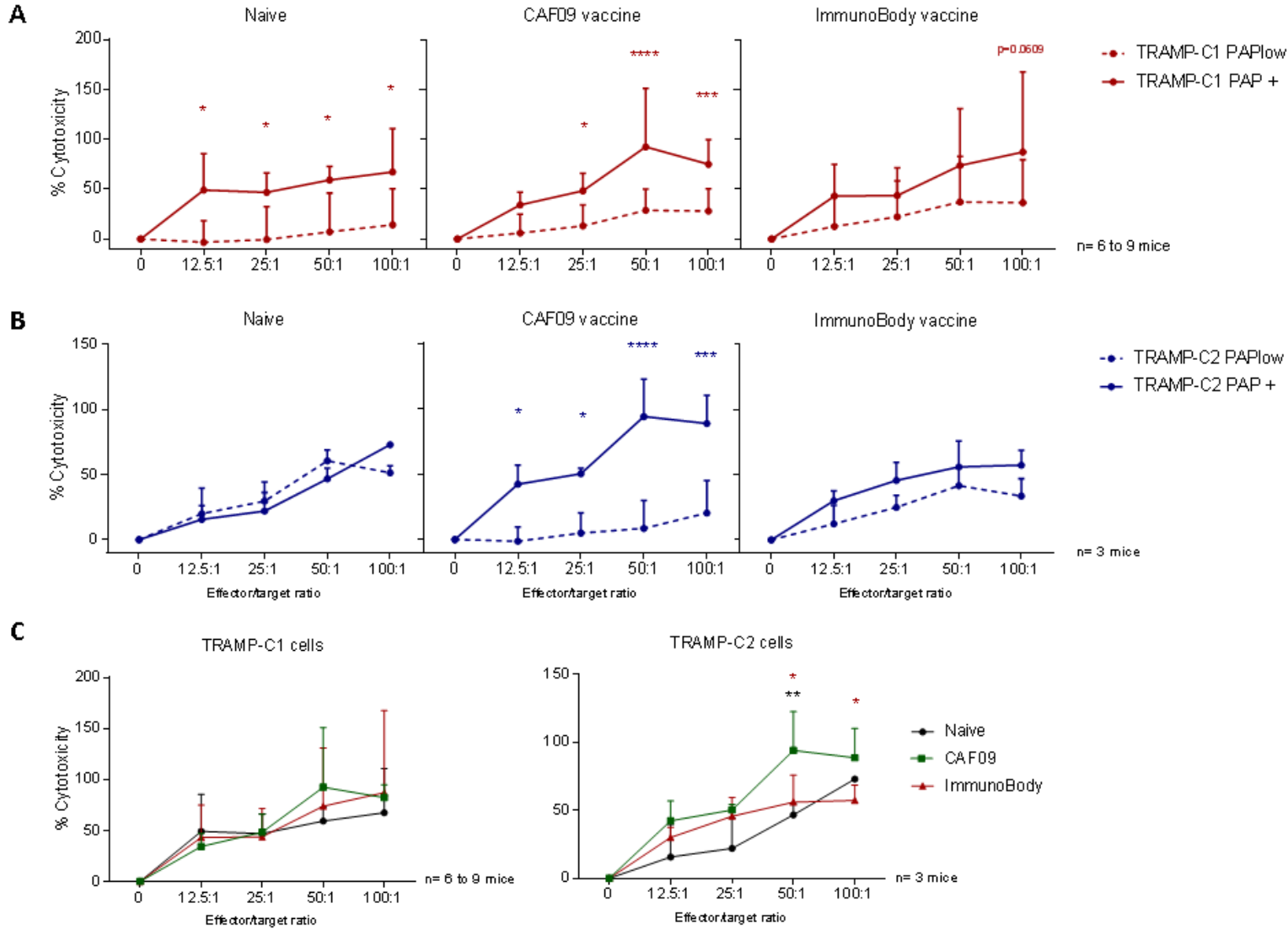
Figure 4.11: Killing of TRAMP-C1 and TRAMP-C2 cells -/+ mPAP by splenocytes from vaccinated C57Bl/6 mice. C57Bl/6 mice were immunised on days 1, 15 and 29 with either the CAF09-based or the ImmunoBody®-based mPAP 42mer 2 mutations vaccine. Seven days after the last immunisation, splenocytes were isolated from spleens and incubated with either pulsed LPS-blast cells or class-I peptides alone. Six days later, splenocytes were co-incubated with ^{51}Cr labelled target cells for an overnight incubation, at the end of which the radioactivity was measured to determine the percentage of cytotoxicity. (A) Percentage of cytotoxicity against TRAMP-C1 cells (A) and (B) TRAMP-C2 cells according to mPAP expression. (C) Percentage of cytotoxicity against WT TRAMP-C1 cells or WT TRAMP-C2 cells according to the vaccination. Both the CAF09-based vaccine and no vaccination were sufficient to induce PAP-specific killing against TRAMP-C1 cells. Only the CAF09-based vaccine induced PAP-specific killing against TRAMP-C2 cells. Dots represent the mean percentage of cytotoxicity and the error bars represent the SD. Results are representative of one to three independent experiments. A significant difference between immunisation groups was determined using a two-way ANOVA comparison test.

121

4.3. Discussion

The aim of this part of the project was to select the vaccine strategies inducing the strongest cytotoxicity against target cells in a PAP-specific manner. To achieve this, suitable target cells were prepared. The expression of MHC class-I molecules matching those of the mouse model was assessed qualitatively and quantitatively and modified when required. The expression of either the mPAP or the hPAP gene was assessed and modified through genetic modifications as per required.

Prior to performing cytotoxicity assays, total splenocytes were enriched in class-I peptide specific CD8$^+$ T-cells by 6 days of *in vitro* stimulation in the presence of class-I peptides and of IL-2. IL-2 cytokine has been shown to control the proliferation and differentiation of T-cells (Ross, et al. 2018) and to promote the expansion of CD8$^+$ CTLs (Ross, et al. 2016). Although the peptide-specificity of CD8$^+$ T-cells was not assessed, their proportion and phenotype were. The *in vitro* stimulation led to an overall increase of CD8$^+$ T-cells in both models, in comparison to their proportion in freshly isolated splenocytes. However, this increase was only vaccine-induced in the HHDII/DR1 model, in which the percentage of CD8$^+$ T-cells within T-cells in naive mice went from 6% (freshly isolated splenocytes) to 29% (after 6 days *in vitro* stimulation), whereas it went from 15% to 78% in the case of cells from CAF09-vaccine immunised mice. In the C57Bl/6 model, the proportion of CD8$^+$ T-cells in naïve mice went from 37% to 76%, from 43% to 78% in CAF09-vaccine immunised mice and from 42% to 74% for ImmunoBody®-vaccine immunised mice, reaching approximately the same proportion after 6 days of stimulation. These results suggest that the presence of IL-2 in the culture had a major role in inducing the proliferation of CD8$^+$ T-cells. Indeed, IL-2 has been shown to induce the proliferation of CD8$^+$ T-cells in an antigen-independent manner (Wong, et al. 2001; Wong, et al. 2004). An overall increase in the proportion of CD44^{high}CD62L^{neg} effector memory CD8$^+$ T-cells was observed after the *in vitro* expansion, in all groups (data not shown), reinforcing the fact that the IL-2 induced an antigen-independent proliferation of CD8$^+$ T-cells. However, the proportion was higher in the vaccinated groups (mainly CAF09-based vaccine in the HHDII/DR1 model), suggesting a clonal expansion and differentiation of ILL-specific CD8$^+$ T-cells. These results correlate with the hypothesis made in the previous chapter, that the CAF09-based vaccine induces antigen-nonspecific CD8$^+$ memory T cells with non-MHC restricted cytotoxic capacities. Dhanji *et al.* described a subset of IL-2-activated CD8$^+$ CD44^{high} cells displaying significant levels of activating NK receptors (2B4 and NKG2D) that are capable of specifically killing syngeneic tumour cells in a NKG2D-dependant manner (Dhanji, et al. 2003). These cells expressed receptors of both the innate and the adaptive immune system. Therefore, it would have been of interest to assess by flow cytometry whether the proportion of innate cells had increased as a result of the *in-vitro* stimulation.

Regarding the phenotype of expanded CD8^{+} T-cells, the main difference observed between the groups in both models was the induction of PD-1 expression. As discussed in the previous chapter (Section 3.3), the meaning of PD-1 expression is controversial, being described as an activation marker and as a marker of dysfunction/exhaustion. However, its co-expression with other inhibitory markers such as LAG-3 and Tim-3 is a sign of exhaustion (He, et al. 2019). In the HHDII/DR1 model, PD-1 was co-expressed with Tim-3 and LAG-3: 64% for CpG group and 87% for CAF09 group. In the C57Bl/6 group, only 27% of CD8^{+} T-cells exhibited this exhausted phenotype in the CAF09 group and 25% in the ImmunoBody® group, with some CD8^{+} T-cells expressing PD-1 on its own. Unlike others (Wang, et al. 2019), we did not observe the expression of CTLA-4 molecule.

It would have been of interest to assess the expression of exhaustion markers after resting of T-cells, to determine if the exhausted phenotype observed is reversible or permanent.

These results suggest that the CAF09-vaccine in the HHDII/DR1 model mainly induces CD8^{+} T-cells displaying an exhausted phenotype. Exhausted T-cells are commonly described as dysfunctional T-cells having lost their proliferative potential, their capacity to secrete cytokines, their memory phenotype, their cytotoxic capacities and expressing inhibitory receptors (Wherry, et al. 2015) (Maimela, et al. 2019). Tim-3 in particular has been described as a negative regulator of CD8^{+} T-cell induced cytotoxicity in the context of HIV infection, despite the fact that Tim-3-expressing CD8^{+} T-cells still contained high levels of perforin (Sakhdari, et al. 2012). Others have shown that "exhausted" T-cells from patients with Chronic Lymphoid Leukaemia (CLL) retained their ability to secrete cytokines (Riches, et al. 2013). On the other hand, in the context hepatocellular carcinoma, "exhausted" T-cells displayed lower secretory capacities (Wang, et al. 2019).

The present findings show that vaccine-induced CD8^{+} T-cells co-expressing inhibitory markers displayed a memory phenotype and were capable of cytotoxicity in an antigen-dependant manner, although cytotoxicity assays were performed on total splenocytes (except for LNCaP killing). The proliferative and secretory functions of CD8^{+} T-cells upon ILL recognition were not studied.

As stated above, splenocytes from the CAF09-vaccine group lysed ILL-presenting cells in a highly specific manner, far better than splenocytes from CpG-vaccinated mice, whereas splenocytes from naïve or ImmunoBody®-vaccinated mice did not induce any cytotoxicity. The positive correlation between the presence of exhausted CD8^{+} T-cells and the cytotoxicity against T2-ILL cells demonstrate the cytotoxic capacities of vaccine-induced CD8^{+} T-cells. Taken together, these results suggest that CD8^{+} T-cells are responsible for the cytotoxicity observed and confirm the findings presented in the last chapter demonstrating that the CAF09-vaccine induced CD8^{+} T-cells express both CD107a and Granzyme B (markers of degranulation) and display cytotoxic capacities.

Although lysis of B16 cells observed was not influenced by the expression of the hPAP protein, the cytotoxicity appeared to be enhanced by vaccination. The CpG-vaccine induced almost no cytotoxicity, whereas the ImmunoBody®-vaccine and the CAF09-vaccine induced similar levels of cytotoxicity. The cytotoxicity of cells from non-immunised animals would be required to confirm this.

As discussed earlier, the CAF09-based vaccine might induce antigen non-specific CD8^{+} memory T cells displaying non-MHC restricted cytotoxic capacities. Although this could be responsible for the killing of B16 cells -/+ hPAP, it does not explain the induction of cytotoxicity against B16 cells in the ImmunoBody®-vaccine group. These results suggest the possibility that ILL epitope is not presented at the surface of B16-HHDII-PAP cells. Considering that these cells do not naturally express PAP, its processing might be different and lead to different epitopes being presented, epitopes that are not contained in the 42mer sequences and therefore that T-cells from vaccinated animals have not yet encountered.

One can also hypothesise that the cytotoxicity observed is due to another cell type, for example NK cells. These cells do not induce cytotoxicity in an antigen-dependant manner (Topham, et al. 2009) and their proliferation is also induced by IL-2 (Sharma, et al. 2018). However, their presence within splenocytes was not assessed following the *in vitro* stimulation.

The cytotoxicity of LNCaP cells was neither PAP- nor vaccine-dependant. The isolation of CD8^{+} T-cells reduced the percentage of cytotoxicity suggesting that cells other than CD8^{+} T-cells were responsible for the killing when performed with total splenocytes. In that context, results observed suggest that the toxicity might be vaccine-dependant although there was no significant difference. Olson *et al.* (Olson, et al. 2010) demonstrated that ILL epitope is not a naturally processed epitope specific for PAP and that ILL-specific CTLs cannot lyse LNCaP cells in an HLA-A2 restricted manner. However, Machlenkin *et al.* showed that ILL-specific CTLs could kill LNCaP cells and concluded that ILL was naturally processed and presented by LNCaP cells (Machlenkin, et al. 2005). Unlike for B16 cells, PAP protein is naturally expressed in LNCaP cells, however we cannot conclude with our results if the ILL epitope is presented at their surface. It is important to remember that these LNCaP cells express the HLA-A2 and the chimeric HLA-A2 molecules.

The absence of significant differences between the killing of two LNCap cell types (PAP[+] and PAP[low]) could be explained by the fact that the cells were 'knocked down' rather than 'knocked out' for PAP and therefore still express PAP. The qPCR data showed there is still 6.65% of PAP mRNA in

comparison to the cells transfected with the empty vector plasmid. Therefore, the expression at the protein level could be high enough for a similar number of ILL-HLA-A2 complexes to be presented at their surface. A knockout of PAP within LNCaP cells would answer this question and an HLA-A2 blocking antibody would be needed to conclude if the lysis was HLA-A2 restricted.

In the C57Bl/6 model, both vaccine strategies induced class-I peptide-specific killing, but the CAF09-vaccine induced a higher peptide-specific killing with both ISI9mer and SIW8mer peptides. Similarly, the CAF09-vaccine induced the highest percentage of PAP-specific killing of TRAMP-C1 and TRAMP-C2 cells in comparison to the ImmunoBody®-vaccine or to the "no vaccine" control. These results corroborate findings from the last chapter demonstrating that CAF09-vaccine induced a higher percentage of CD8$^+$ T-cells expressing both CD107a and Granzyme B, in comparison to the ImmunoBody®-vaccine.

One can therefore hypothesize that in this model, the CAF09-vaccine induces CD8$^+$ T-cells with higher cytotoxic capacities, whereas the ImmunoBody®-vaccine induces CD8$^+$ T-cells with higher capacity to proliferate and secrete cytokines. It would be worth assessing what would happen if one was to immunise mice first with ImmunoBody®-based vaccine and then boost with CAF09-based vaccine.

As for the LNCaP cells, TRAMP cells were only knocked down for the mPAP gene. This need to be taken into consideration as the TRAMP-PAP^{low} cells could still present some class-I epitopes-MHC class-I complexes on their surface and be recognized and lysed specifically.

TRAMP-C1 and TRAMP-C2 cells, do not express naturally detectable H2-K^{b}D^b MHC class-I molecules on their surface, which limits the capacity of CD8$^+$ T-cell's TCR to bind to peptide-loaded MHC class-I molecules and to induce cytotoxicity in these cells. IFNγ pre-treatment of TRAMP cells increased the number of H2-K^{b}D^b MHC class-I molecules on their surface which increased the cytotoxicity of these cells, despite the concomitant expression of PD-L1 molecule. However, these conditions did not demonstrate PAP-specific killing.

The fact that cytotoxicity against TRAMP cells could be observed without IFNγ pre-treatment suggests that CD8$^+$ T-cells secreted IFNγ during the overnight co-culture of TRAMP-cells and splenocytes, leading to the upregulation of H2-K^{b}D^b MHC class-I molecules. Indeed, in the previous chapter, CD8$^+$ T-cells were shown to secrete IFNγ within 6 hours of class-I peptide stimulation, and although it was not quantified, the level of IFNγ secreted might be sufficient. In order to confirm this, the level of MHC class-I expression on TRAMP cells should have been assessed after *in vitro* co-culture with splenocytes.

One can hypothesize that ISI9mer and SIW8mer epitopes are presented by TRAMP-C1 and TRAMP-C2 cells and that there are more epitope/MHC-complexes present at the surface of TRAMP-C2 cells, as these cells express higher levels of PAP mRNA than TRAMP-C1 cells. This could explain the observed PAP-specific and vaccine-specific lysis against TRAMP-C2 but not TRAMP-C1 cells.

ISI-specific CTLs capable of killing ISI-pulsed RMAS cells as well as TRAMP-C1 have been described by Spies *et. al* (Spies, et al. 2012), In these studies, a PAP-based DNA vaccine could induce ISI-CTLs capable of IFNγ secretion and detectable by pentamers, and had the capacity to induce the regression of TRAMP-C1 tumours and to inhibit the growth of spontaneous tumours in TRAMP mice.

It has been reported that the knockdown of PAP expression allows androgen-sensitive prostate cancer cells to develop the castration-resistant phenotype having the capacity to proliferate under an androgen-reduced condition (Muniyan, et al. 2013). Hence, PAP has a major role in the growth of prostate cancer cells. Although we did not observe differences in the proliferation of WT *versus* knock down cells (LNCaP, TRAMP-C1 and TRAMP-C2 cells), this should be taken into consideration.

In conclusion, these results demonstrated that the vaccine was able to induce the PAP-specific lysis of target cells *in vitro*. The mPAP42mer and the hPAP42mer CAF09-based vaccines induced splenocytes capable of recognising PAP42mer-derived class-I epitopes presented by T2 and RMAS cells, respectively. Moreover, these splenocytes were also able to recognise and kill TRAMP-C1 and TRAMP-C2 cells in a PAP-specific manner. On the other hand, the mPAP42mer ImmunoBody®-based vaccine induced splenocytes much weaker in term of cytotoxicity. These results, together with the results obtained from the previous chapter, justified the assessment of the CAF09-based vaccine in the HHDII/DR1 tumour model and with both the CAF09 and the ImmunoBody®-based vaccine in the C57Bl/6 tumour model. In the next chapter, the effect of the vaccines on the *in vivo* anti-tumour capacity of immune cells was assessed in prophylactic and in therapeutic settings.

Chapter 5: Assessment of the anti-tumour capacity of the PAP42mer vaccine *in vivo*

5.1. Introduction

The fact that a vaccine is capable of inducing a strong PAP-specific immune response in non-tumour bearing animals does not necessarily mean that the same proportion of PAP-specific T-cells can be induced in tumour-bearing animals and that the vaccine can elicit protective anti-tumour immunity. Indeed, even if cells migrate to the TME, they might face immuno-suppressive mechanisms that would render them non-functional/exhausted, incapable of recognizing their cognate antigen or incapable of initiating CTL functions when they do.

The prostate cancer TME has been described as predominantly immunosuppressive. Indeed, an abundance of TGF-β in PCa tumours has been reported and shown to inhibit NK cell-mediated cytotoxicity (Pasero, et al. 2016). Moreover, overexpression of TGF-β in comparison to benign prostates correlates with Gleason scores ≥7 of poor prognosis (Reis, et al. 2011) and metastatic stages (Adler, et al. 1999). The presence of Tregs (Miller, et al. 2006), Th17 cells (Sfanos, et al. 2008), MDSCs (Garcia, et al. 2014) and of PD-L1/PD-L2-expressing DCs (Bishop, et al. 2015) has been observed in tumours from patients with prostate cancer. The dysfunction of T-cells has also widely been described in prostate cancer (Ness, et al. 2014; Sfanos, et al. 2009; Ebelt, et al. 2008) as has a linkage between the presence of TILs and poor prognosis (Ness, et al. 2014; Leclerc, et al. 2016). These facts illustrate the main challenge when developing a cancer vaccine for PCa: inducing an immune response sufficiently strong to outperform the immunosuppressive mechanisms put in place in the TME.

Murine tumour models are therefore essential to assess the anti-tumour efficacy of a cancer vaccine. The anti-tumour efficacy can be assessed in two different setting: prophylactic or therapeutic. Although prophylactic studies can determine if a vaccine can elicit vaccine-specific T-cells capable of recognising and lysing tumour cells *in vivo* and prevent tumour growth, they do not mimic the clinical situation of patients presenting established tumours.

On the contrary, although more challenging, therapeutic models better mimic the clinical situation of cancer patients. Two situations could indicate an efficient anti-tumour response, either the slowing down of tumour growth or the regression of tumours. However, the most crucial outcome when performing these studies is survival. Assessing the TILs present in tumours helps understanding the efficacy of a vaccine, by measuring the functionality and exhaustion status of these cells.

In the previous chapters, both ImmunoBody® and CAF09 PAP-derived vaccine strategies were shown to induce functional PAP-specific CD8+ T-cells and PAP-specific killing of target cells. The aim of the work presented in this chapter was to develop tumour models in which the anti-tumour efficacy of selected vaccine strategies could be assessed. Moreover, the vaccine-specific immune response was evaluated by studying the presence and the phenotype of T-cells from the spleen as well as TILs.

Two established tumour models were chosen for the C57Bl/6 mouse model - implantation of tumorigenic TRAMP-C1 or TRAMP-C2 cells. The HHDII/DR1 model involved the implantation of the engineered B16 cells (humanised and expressing hPAP). In each model, the anti-tumour efficacy of the most potent vaccine strategies, identified in the previous chapter, were assessed both in the prophylactic and therapeutic settings. Findings from these studies provide insight into whether the PAP42mer vaccine can slow down or eradicate PAP-expressing tumours. This information is crucial for understanding whether the vaccine has therapeutic and translational potential for patients with prostate cancer.

Tumour studies were conducted according to the Home Office regulations. The endpoint was based on the tumour size and animals were culled when tumours reached the maximum size permitted under the Home Office PPL Licence (1.2cm mean diameter for prophylactic studies and 1.5cm mean diameter for therapeutic studies). Besides tumour growth, the effect of each vaccine strategies on the survival of animals was compared. Survival was however directly related to the tumour growth.

5.2. Results

5.2.1. B16F10 model in HHDII/DR1 mice

The first step to establish the B16-HHDII-PAP tumour model was to assess the number of cells required to obtain tumour growth in 100% of mice. Injecting 0.25×10^6 cells per animal resulted in 13% of animals not developing tumours while doubling this number (0.5×10^6 cells/animal) led to an overly rapid tumour growth which would allow insufficient time to assess the anti-tumour efficacy of the vaccine (data not shown). The optimal number was found to be 0.3×10^6 cells per animal and was used for subsequent experiments.

5.2.1.1. Prophylactic setting

The anti-tumour efficacy of the hPAP42mer mutated peptide vaccine was firstly assessed in a prophylactic setting (Figure 5.1). For this, animals were immunised three times according to the immunisation protocol shown Figure 5.1 A and challenged a week later with 0.3×10^6 B16-HHDII-PAP$^+$ cells per mouse. The first group of animals did not receive any immunisation to assess the effect of the CAF09 adjuvant on its own. The effect of the CAF09 vaccine (CAF09 adjuvant with the hPAP42mer mutated peptide) on tumour growth was compared to that in a group which was not immunised and the group receiving CAF09 alone. All animals ultimately had to be culled due to tumour size. The tumour growth showed that animals developed tumours between day 11 and day 25, regardless of the group (Figure 5.1 A). One animal from the CAF09 alone group (6%) and 3 animals from the CAF09 vaccine group (16%) developed tumours after day 25. However, once tumours were measurable, the growth rate was similar. There was a non-significant increased survival of 3 days in the CAF09 alone treated group in comparison to the control group (figure 5.1 B). The survival of the CAF09 vaccine treated group was prolonged by 10 days in comparison to the control group and by 7 days in the CAF09 alone group, although none of the two were significant. Overall, 16% of vaccine-treated animals displayed a tumour growth delay.
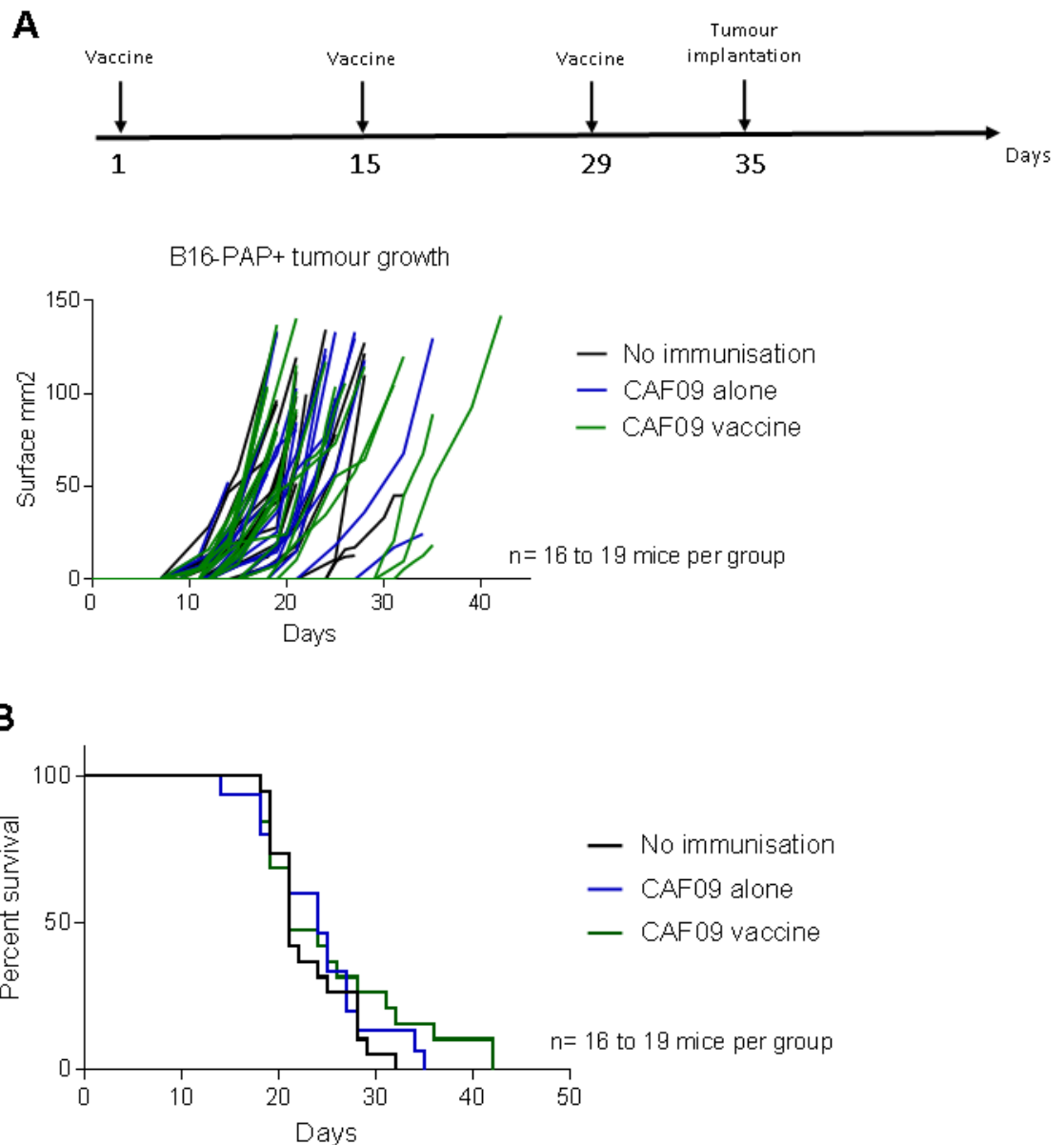
Figure 5.1: Effect of the hPAP 42 mutated sequence with CAF09 adjuvant on B16-HHDII-PAP+ tumour growth in a prophylactic setting in HHDII/DR1 mice. HHDII/DR1 mice were immunised on days 1, 15 and 29 with the CAF09 adjuvant alone or with the CAF09-based hPAP 42mer mutated vaccine. Seven days after the last immunisation, 0.3x10^{6} B16-HHDII-PAP+ cells were implanted into the right flank of animals and tumour growth followed. (A) Individual tumour growth monitored by callipers measurements and (B) Kaplan-Meier curve of OS. The CAF09 vaccine prolonged the survival of animals in comparison to control groups, although this was not of statistical significance. Three independent experiments performed.

When tumours reached the maximum size permitted under the Home Office PPL Licence, spleens and tumours were taken to study the status and function of CD4$^+$ and of CD8$^+$ T-cells. As demonstrated Chapter 3, the CAF09 vaccine induced a CD8$^+$ T-cell driven immune response (Figure 5.2). CD4$^+$ T-cells were not affected by the vaccine (data not shown). The vaccine induced an increase in the proportion of CD8$^+$ T-cells within the peripheral T-cell compartment and an increase of effector memory CD8$^+$ T-cells (Figure 5.2 A). Although immunisation also induced high levels of PD-1 expression on CD8$^+$ T-cells (Figure 5.2 B), it had no effect on the expression of other inhibitory markers. A proportion of CD8$^+$ T-cells secreted IL-2, IFNγ and TNFα and degranulated (CD107a) in response to ILL peptide stimulation (Figure 5.2 C). Increased expression of Granzyme B by CD8$^+$ T-cells in a peptide-independent manner was also observed in the CAF09 vaccine group.
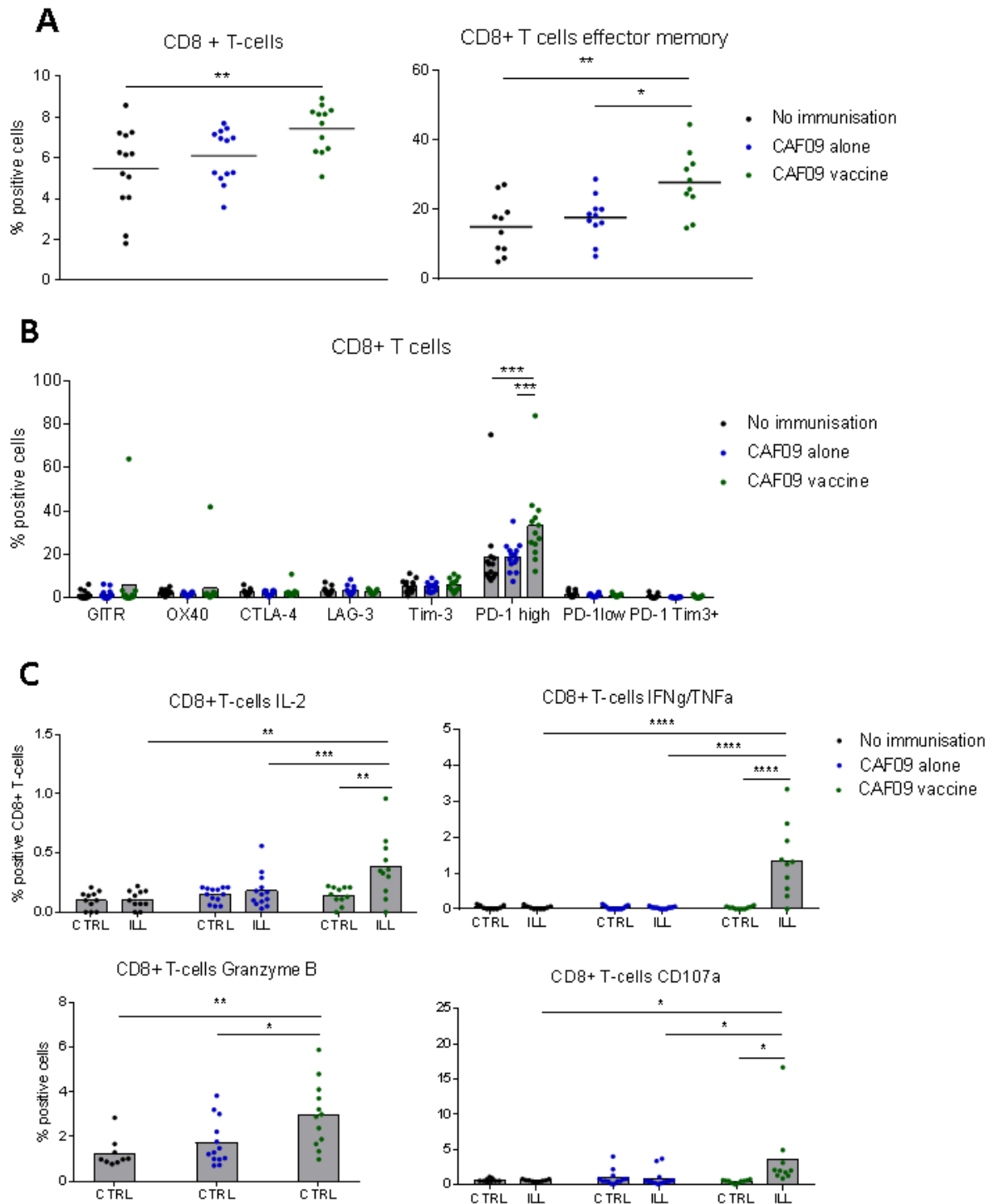
Figure 5.2: Effect of the hPAP42mer mutated CAF09-based vaccine on the phenotype of splenocytes from HHDII/DR1 mice bearing B16-HHDII-PAP+ tumours in a prophylactic setting. HHDII/DR1 mice were immunised on days 1, 15 and 29 with the CAF09 adjuvant alone or with the CAF09-based hPAP 42mer mutated vaccine. Seven days after the last immunisation, 0.3×10^6 B16-HHDII-PAP+ cells were implanted into the right flank of animals and tumour growth followed. Once the tumour size limit was reached, spleens were taken, dissociated, incubated with a murine FcR block and then stained with surface antibodies for flow cytometry analysis indicating (A) proportion of CD8+ T-cells and proportion of effector memory CD8+ T-cells, (B) proportion of CD8+ T-cells expressing activating and inhibitory markers or (C) proportion of CD8+ T-cells secreting cytokines and degranulating after ILL stimulation for 6 hours. The CAF09 vaccine induced a CD8+ T-cell driven immune response with cytokines secretion and degranulation of CD8+ T-cells upon stimulation. Bars represent the mean percentage of positive cells and the error bars represent the SD. Two to three independent experiments performed (n= 9 to 15 mice per test group). A significant difference in the proportion of positive cells between immunisation groups was determined using a two-way ANOVA comparison test.

To understand if the vaccine was responsible for the delay observed, the status and function of TILs was studied. The results observed were different from those observed in splenic CD8$^+$ T-cells. A higher proportion of CD8$^+$ T-cells was found in the tumour (approximately 40% on average), inversing the CD4/CD8 ratio: the proportion of CD8$^+$ T-cells was higher than that of CD4$^+$ T-cells. Moreover, the proportion of CD8$^+$ T-cells was increased in the CAF09 vaccine group, although this difference was not of statistical significance (Figure 5.3 A). CD8$^+$ TILs from the CAF09 vaccine group displayed a slightly less exhausted phenotype, in that a lower proportion of cells expressed LAG-3, Tim-3 and PD-1 at high levels (Figure 5.3 B). Inversely, there were more PD-1^{low} CD8$^+$ T-cells in the CAF09 vaccine group. Unexpectedly, expression of the activation markers GITR and OX-40 was also slightly decreased in the CAF09-vaccine group. There was an increase in the proportion of CD8$^+$ T-cells secreting IFNγ and TNFα, particularly in 2 mice, but no IL-2 secretion (Figure 5.3 C). A higher proportion of CD8$^+$ T-cells expressed CD107a in response to ILL in comparison to the control group, but there was no increase of Granzyme B expression. Overall, there were less cytokines-secreting CD8$^+$ T-cells in the tumour than in the spleen.
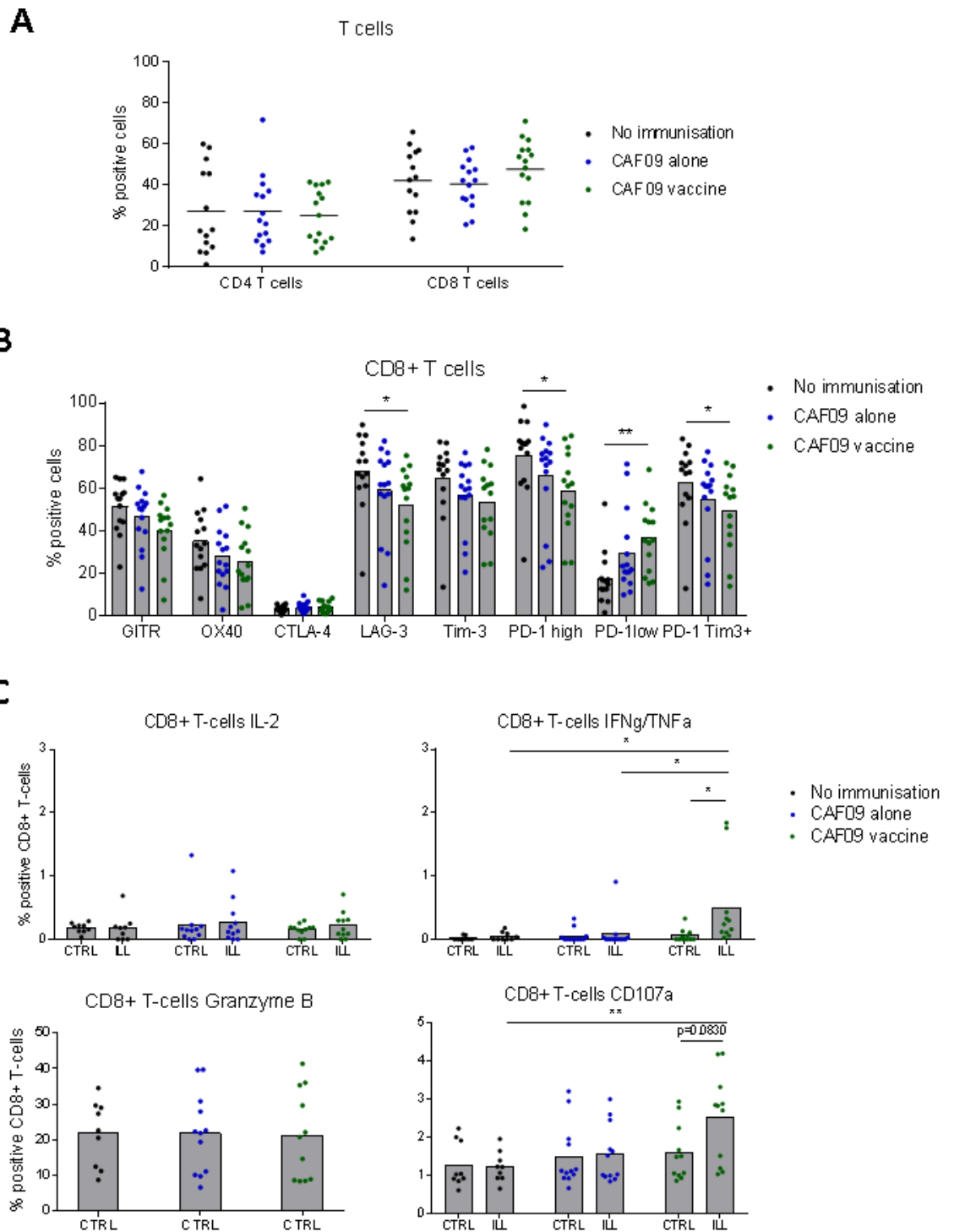
Figure 5.3: Effect of the hPAP42mer mutated CAF09-based vaccine on the phenotype of tumour infiltrating lymphocytes in B16-HHDII-PAP⁺ tumours in HHDII/DR1 in a prophylactic setting. HHDII/DR1 mice were immunised on days 1, 15 and 29 with the CAF09 adjuvant alone or with the CAF09-based hPAP 42mer mutated vaccine. Seven days after the last immunisation, 0.3×10^6 B16-HHDII-PAP⁺ cells were implanted into the right flank of animals and tumour growth followed. Once the tumour size limit was reached, tumours were taken, dissociated, incubated with a murine FcR block and then stained with surface antibodies for flow cytometry analysis indicating (A) proportion of CD4⁺ and CD8⁺ T-cells and proportion of effector memory CD8⁺ T-cells, (B) proportion of CD8⁺ T-cells expressing activating and inhibitory markers or (C) proportion of CD8⁺ T-cells secreting cytokines and degranulating after ILL stimulation for 6 hours. The CAF09 vaccine induced a CD8⁺ T-cell driven immune response with cytokine secretion and degranulation of CD8⁺ T-cells upon stimulation. Bars represent the mean percentage of positive cells and the error bars represent the SD. Two to three independent experiments performed (n= 9 to 15 mice per test group). A significant difference in the proportion of positive cells between immunisation groups was determined using a two-way ANOVA comparison test.

5.2.1.2.Therapeutic setting

Considering the unclear effect of the CAF09 vaccine on the growth of B16-HHDII-PAP$^+$ tumours in a prophylactic setting and the large proportion of CD8$^+$ T-cells expressing PD-1 in the spleen and in the tumour, its effect was assessed in a therapeutic setting in combination with an anti-PD-1 antibody. Treatment started at day 4 post tumour implantation, before tumours were palpable, due to the rapid and aggressive phenotype of the B16 tumour model.

Tumour growth showed that animals developed tumours between day 14 and day 18, regardless of the group (Figure 5.4 A). One animal from the CAF09 alone + anti-PD-1 antibody group and 1 animal from the CAF09 vaccine group developed tumours after day 31. The growth rate was similar in all test groups. There was no significant difference in survival between any groups (Figure 5.4 B). However, in comparison to the control group (CAF09 alone and isotype control) the anti-PD1 antibody increased the survival of 8 days, the vaccine alone of 11 days and the combination of the two increased the survival of 4 days. There was no combinatorial effect of the vaccine with the anti-PD-1 antibody.

The proportion of CD8$^+$ T-cells within the spleen and the tumour was assessed, but no difference was observed between the groups (Figure 5.4 C). Also, due to technical difficulties, the flow cytometry could not be performed on all animals rendering the results less reliable.
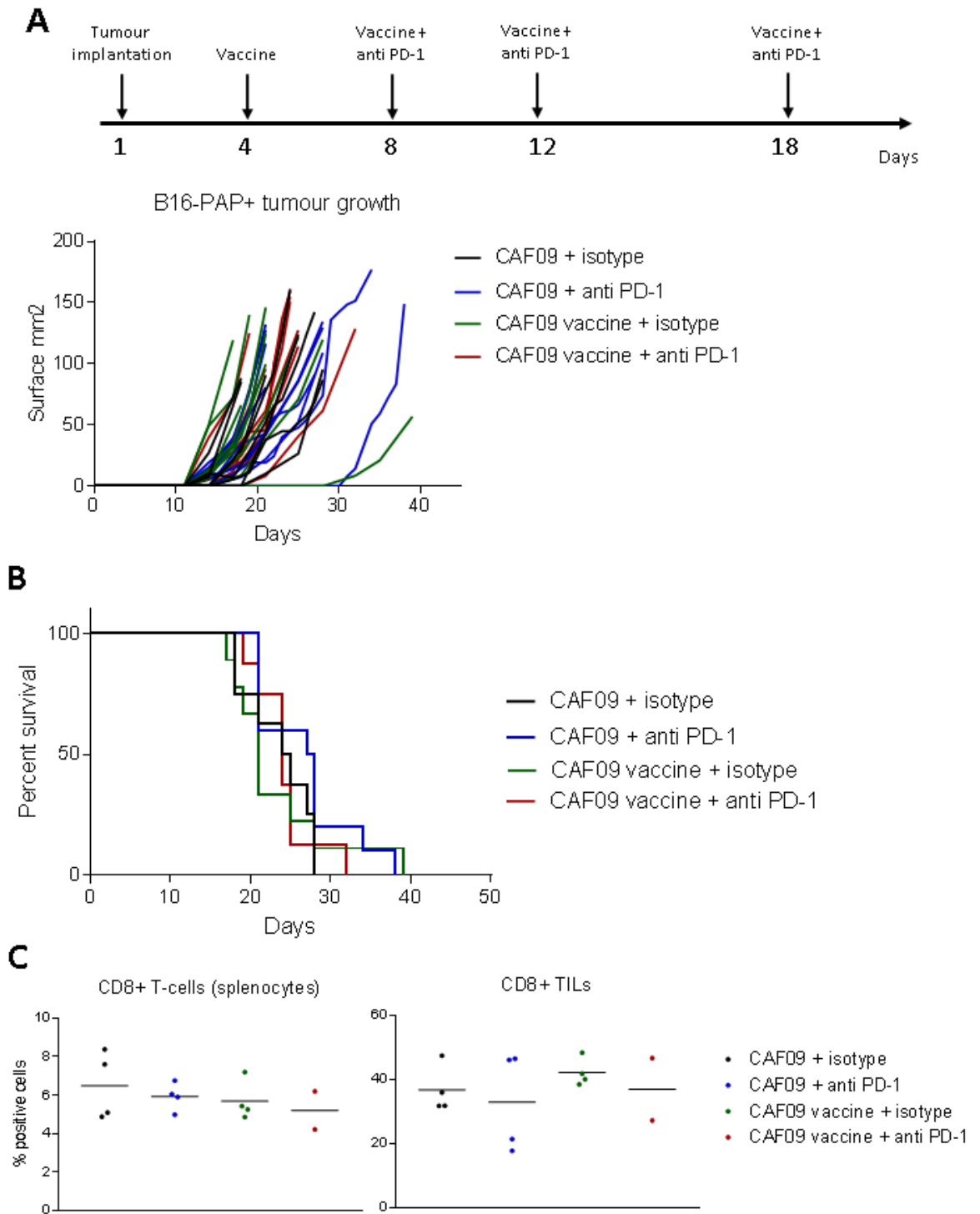
Figure 5.4: Effect of the hPAP42mer mutated CAF09-based vaccine in combination with an anti PD-1 antibody on tumour growth and immune responses in HHDII/DR1 bearing B16-HHDII-PAP+ tumours in a therapeutic setting. HHDII/DR1 mice were injected with 0.3x10^6 B16-HHDII-PAP+ cells into their right flank, then immunised on days 4, 8, 12 and 18 with the CAF09 adjuvant alone or with the CAF09-based hPAP 42mer mutated vaccine and with the isotype control or with anti-PD-1 antibody while the tumour growth was followed. (A) Individual tumour growth monitored by calliper measurements, (B) Kaplan -Meier curve of OS and (C) proportion of splenic CD8+ T-cells and of CD8+ TILs at the time of culling of each an-Meier curve of OS and (C) proportion of splenic CD8+ T-cells and of CD8+ TILs at the time of culling of each animal. The CAF09 vaccine alone and the anti-PD1 antibody alone prolonged the survival of animals in comparison to other groups, but no statistical difference was observed. Two independent experiments performed.

5.2.2. TRAMP-C1 and TRAMP-C2 tumour model in C57Bl/6 mice

5.2.2.1.TRAMP-C1 and TRAMP-C2 tumour model establishment

Several issues were encountered when establishing both the TRAMP-C1 and the TRAMP-C2 tumour models. TRAMP-C1 cells were obtained from a collaborator (Matteo Bellone). These cells were isolated from TRAMP-C1 tumours and grown in culture to render them more tumorigenic and to facilitate tumour implantations. The number of cells needed to obtain tumour growth in 100% of mice was assessed. Three concentrations were tested: 1, 2 and 5×10^6 cells per animal, with 5×10^6 cells being found to be the optimal number of cells required. Although not 100% of mice developed tumours, this cell number was used for subsequent experiments. However, after a short time, cells ceased developing tumours. Thus, TRAMP-C1 and TRAMP-C2 cells were obtained from the ATCC. Both cell lines were transfected with the Luciferase2 gene to follow the tumour growth with more accuracy, as well as to potentially develop an orthotopic model by injecting the TRAMP cells directly into the prostate of C57Bl/6 males. The expression of the LUC2 gene was confirmed (data not shown). However, tumour implantation with 5×10^6 cells per animal did not result in tumour development. Animals were imaged a day after tumour implantation and the signal was followed weekly. The Luciferin signal decreased from the tumour implantation until becoming undetectable (data not shown). This can be explained by the immunogenicity of the Luciferase2 protein, inducing an immune reponse against that foreign antigen and resulting in tumour rejection.

Various parameters were modified to increase the tumorigenicity of TRAMP cells: cells were implanted 1) into old (immuno-depressed) animals, 2) into immuno-suppressed NOD/SCID mice and 3) with 10 and 50% Matrigel™ to facilitate the attachment of the cells.

Nonetheless, all these attempts were unsuccessful. Therefore, our collaborator (Matteo Bellone) kindly gave us TRAMP-C1 cells which had been obtained from TRAMP-C1 tumours, grown in culture and then implanted back into C57Bl/6 animals multiple times. Tumours were obtained from these cells and cells were isolated from these tumours, grown in culture and stored for future use. Unfortunately, the TRAMP-C2 tumour model could never be established, restricting our tumour studies to the TRAMP-C1 tumour model.

5.2.2.2.Therapeutic setting

A first pilot study assessed the anti-tumour effect of mPAP42mer vaccines against established TRAMP-C1 tumours. Treatment started when 33% of animals had tumours measurable by callipers (4 out of 12 animals), on day 17 post tumour implantation. Mice that did not receive any treatment were used as a control for the CAF09-based vaccine and for the ImmunoBody®-based vaccine. The tumour growth rate was similar in all groups (Figure 5.5 A). One animal in the CAF09 vaccine group started developing a tumour at day 46 post tumour-implantation and exhibited a slower growth

rate. Its survival was prolonged by 29 days in comparison to the last animal of the control group (day 48 *versus* day 77) and by 27 days in comparison to the last animal of the ImmunoBody® vaccine group (day 50 *versus* day 77) (Figure 5.5 B).

Although there was no statistically significant difference between groups, 25% (1 out of 4 animals) of the animals immunised with the CAF09 vaccine had a tumour growth delay and therefore an increased survival, while none responded to the ImmunoBody® vaccine. The proportion of splenic CD8$^+$ T-cells was unchanged between groups, neither was the proportion of CD8$^+$ TILs. However, the proportions of CD8$^+$ T-cells in the CAF09 vaccine treated animal which had a delay in tumour growth was also unchanged. Moreover, splenic CD8$^+$ T-cells and CD8$^+$ TILs from this animal did not secrete cytokines or degranulate in response to ISI9mer and SIW8mer peptides stimulation *in vitro* (data not shown). These results suggest that the vaccine was not responsible for the tumour growth delay; however, the delay in tumour growth might be explained by an incorrect subcutaneous injection of tumour cells at the day of tumour implantation or by the heterogenous tumour growth pattern observed with TRAMP-C1 as discussed section 5.2.2.1.
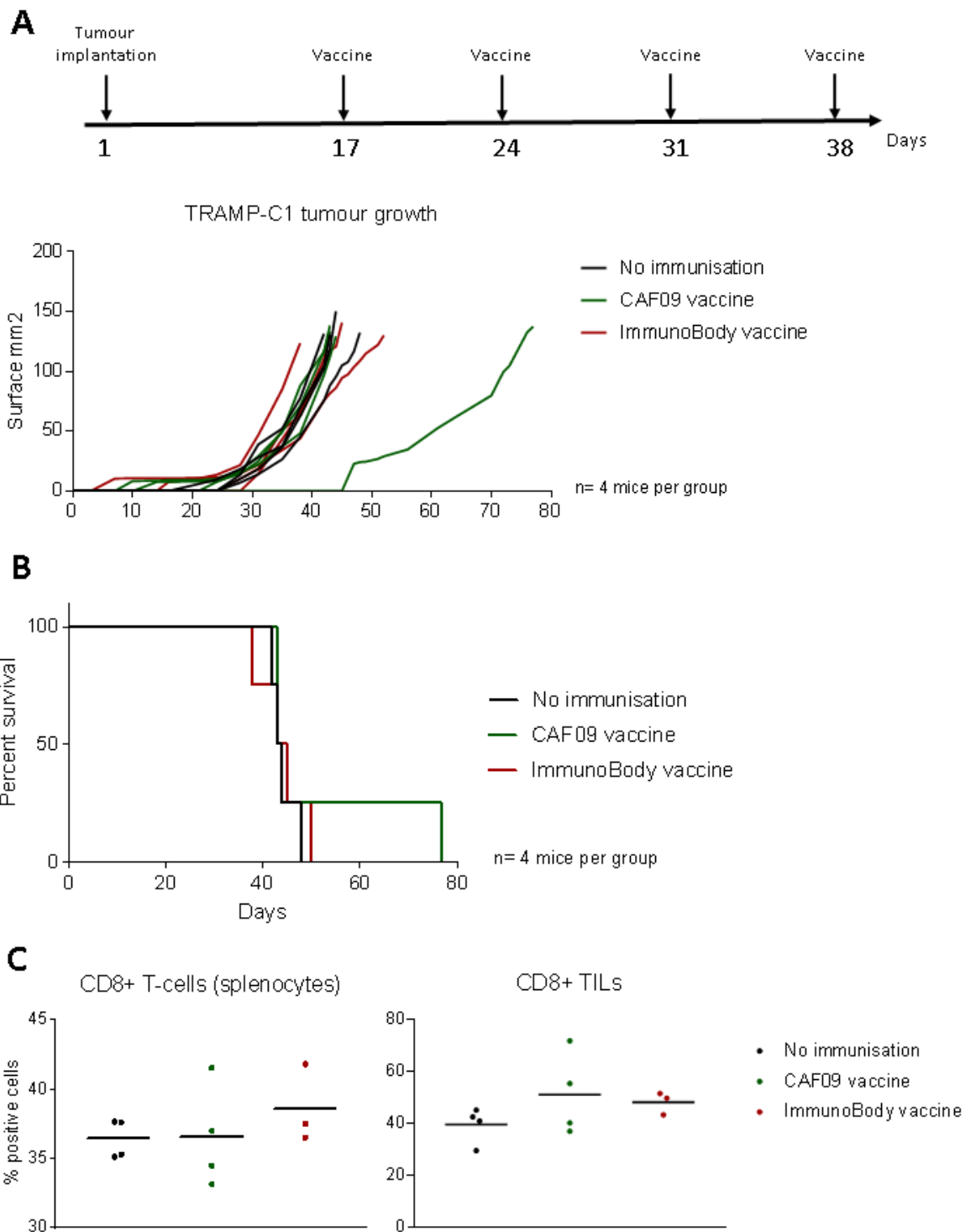
Figure 5.5: Pilot study: effect of the mPAP42mer mutated CAF09 and ImmunoBody®-based vaccines on tumour growth and immune parameters in C57Bl/6 mice bearing TRAMP-C1 tumours in a therapeutic setting. C57Bl/6 mice were injected with $5x10^6$ TRAMP-C1 cells into their right flank, immunised on days 17, 24, 31 and 38 with the CAF09-based or the ImmunoBody®-based mPAP 42mer mutated vaccine while the tumour growth was followed. (A) Individual tumour growth monitored by callipers measurements, (B) Kaplan-Meier curve of OS and (C) proportion of splenic CD8+ T-cells and of CD8+ TILs at the time of culling of each animal. The CAF09 vaccine prolonged the survival of one animal in comparison to other groups, but no statistical difference was observed. One experiment performed.

The immunisation regimen was slightly modified in order to leave a similar prime-boost gap as the one when assessing the vaccine in Chapter 3, by treating animals every 14 days. Due to the length of this regimen, it was decided that animals would only receive prime and boost immunisations. However, when the experiment was performed, there was no tumour growth in any group (data not shown). The next experiment was conducted using the frozen cells from untreated tumours from another study. This experiment contained two extra groups. A group of mice immunised with the CAF09 adjuvant alone, to assess the effect of the adjuvant alone and to be used as a control group for the CAF09 vaccine group and another group of mice receiving only a prime of the CAF09 vaccine, as it was suggested that booster immunisations might be detrimental in the therapeutic setting (Ricupito, et al. 2013).

Due to a faster tumour growth rate observed, animals received the 'prime' immunisation 8 days post tumour-implantation instead of 17 days in the case of the pilot study. Nonetheless, none of the treatment strategies induced a delay in the tumour growth (Figure 5.6 A). Tumours appeared between day 7 and day 45, regardless of the treatment received. As a result, none of the vaccine induced a prolonged survival (Figure 5.5 B). The proportions of splenic CD8^{+} T-cells and of CD8^{+} TILs were similar in all groups (Figure 5.5C).
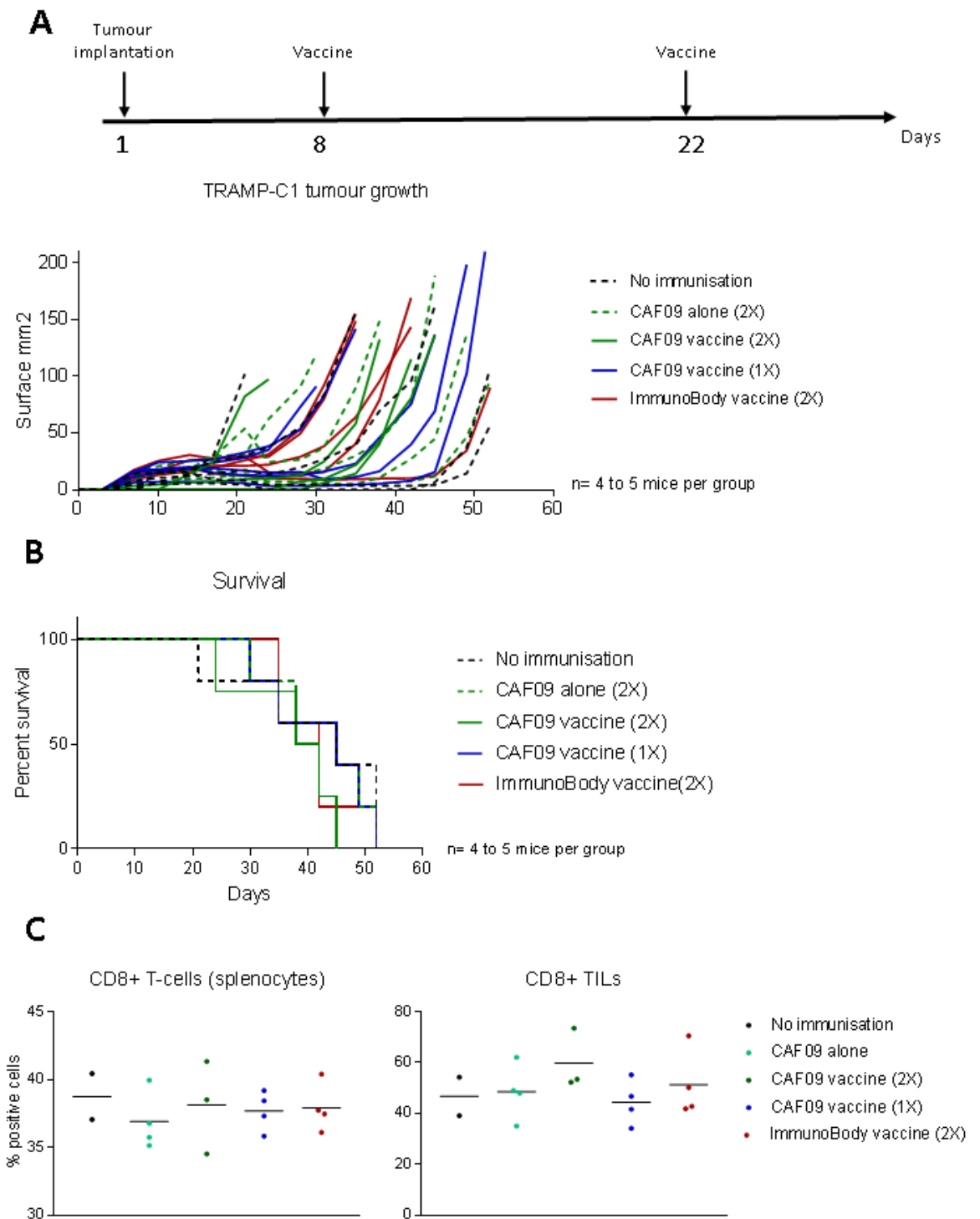
Figure 5.6: Effect of the mPAP42mer mutated CAF09 and ImmunoBody®-based vaccines on tumour growth and immune parameters in C57Bl/6 mice bearing TRAMP-C1 tumours in a therapeutic setting. C57Bl/6 mice were injected with 5×10^6 TRAMP-C1 cells into their right flank, immunised on days 8 and 22 with the CAF09 adjuvant alone, the CAF09-based or the ImmunoBody®-based mPAP 42mer mutated vaccine while the tumour growth was followed. (A) Individual tumour growth monitored by callipers measurements, (B) Kaplan-Meier curve of OS and (C) proportion of splenic CD8+ T-cells and of CD8+ TILs at the time of culling of each animal. No difference was observed in between groups. One experiment performed.

5.2.2.3. Prophylactic setting

In parallel to the therapeutic study, a prophylactic study was performed to understand if any of the vaccines could prevent the growth of TRAMP-C1 tumours. Animals were immunised three times according to the immunisation regimen shown in Figure 5.7 A and challenged a week later with TRAMP-C1 cells. Animals developed tumours between days 7 and 33 regardless of the group (Figure 5.7A). None of the treatments induced a change in the tumour growth rate. However, the 2 animals left in the study on day 42, were not culled due to tumour size: one from the CAF09 alone group and one from the CAF09 vaccine group. The animal from the CAF09 alone group had a tumour of 56mm^2. The animal from the CAF09 vaccine group had no measurable tumour and no raised area. We can extrapolate that even if this animal developed a tumour, it would have survived a minimum of an extra two weeks. We therefore cannot make any conclusions about the effect of the CAF09 vaccine on the growth of TRAMP-C1 tumours, however, this experiment suggests that 20% (1 out of 5 animals) of the animals responded to the CAF09 vaccine, whereas none responded to the ImmunoBody® vaccine.

However, the effect of the vaccine on T-cells was not investigated in this study, therefore, the delay in tumour growth might be explained by an incorrect subcutaneous injection of tumour cells at the day of tumour implantation or by the heteregenous tumour growth pattern observed with TRAMP-C1 as discussed section 5.2.2.1.
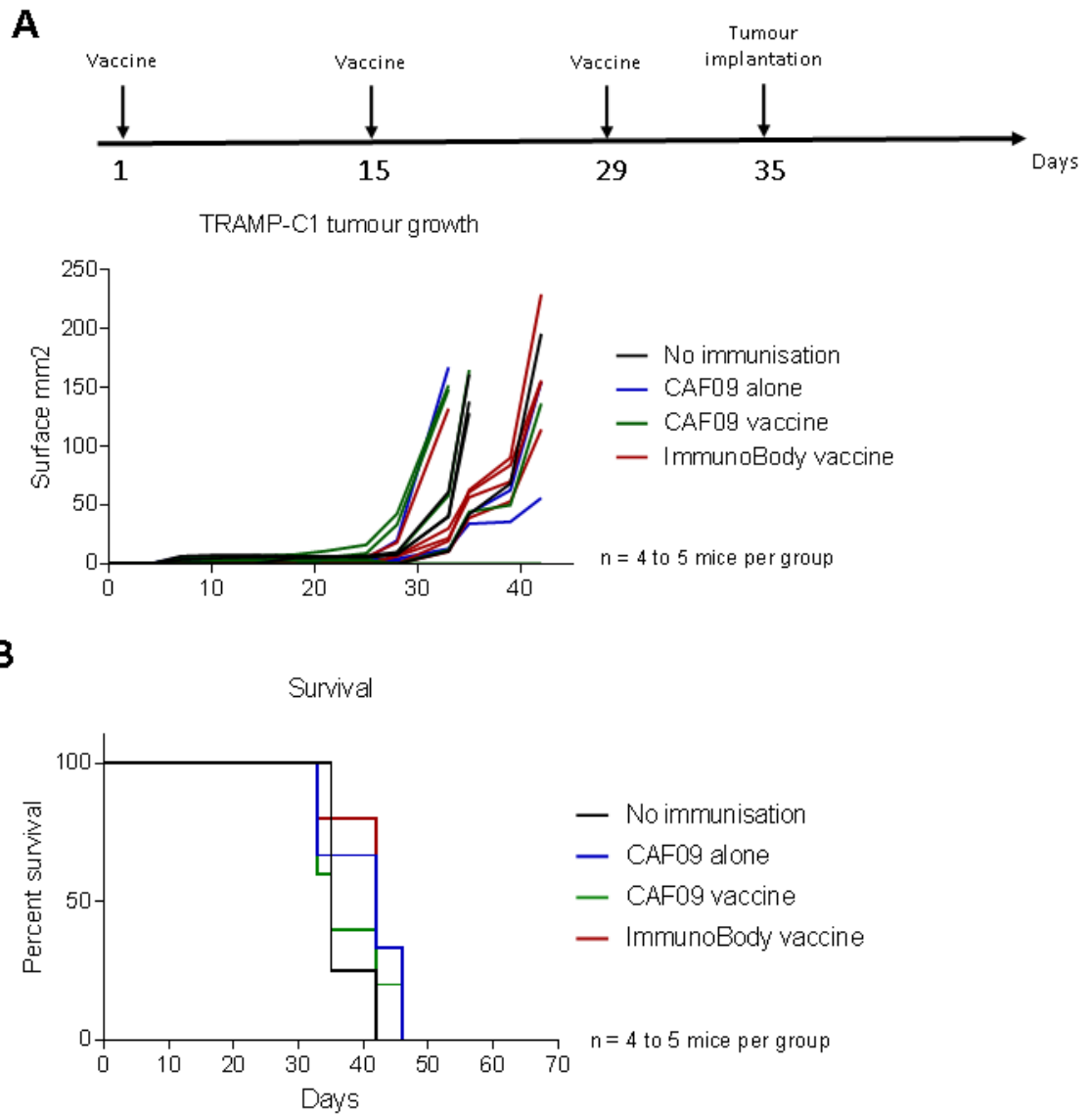
Figure 5.7: Effect of the mPAP42mer mutated CAF09 and ImmunoBody®-based vaccines on tumour growth in C57Bl/6 mice bearing TRAMP-C1 tumours in a prophylactic setting. C57Bl/6 mice were immunised on days 1, 15 and 29 with the CAF09 adjuvant alone, the CAF09-based or the ImmunoBody®-based mPAP 42mer mutated vaccine. Six days after the last immunisation, 5×10^6 TRAMP-C1 cells were injected into their right flank, while the tumour growth was followed. (A) Individual tumour growth monitored by callipers measurements, and (B) Kaplan-Meier curve of OS. The CAF09 vaccine induced 20% of tumour-free animals at day 42 post tumour-implantation. One experiment performed.

5.3. Discussion

Results obtained in the previous chapters demonstrated that the vaccines used induced a CD8^{+} T-cell immune response. Moreover, the vaccine-induced CD8^{+} T-cells displayed characteristics of CTLs, as well as the ability to kill target cells in a PAP-specific manner.

However, the *in vivo* anti-tumour effect of the vaccines in the prophylactic and therapeutic settings in both mouse models used did not reflect these.

In the HHDII/DR1 mouse model, the B16-HHDII-PAP tumour model was used to assess the efficacy of the hPAP/CAF09-based vaccine. The prophylactic study led to a delay of tumour growth in 16% of the animals with a small survival increase despite no effect on the growth rate of the tumour. The analysis of splenic T-cells and TILs showed that the vaccine induced a PAP-specific immune response weaker than in non-tumour bearing vaccinated animals (Chapter 3). The proportion of CD8^{+} T-cells, of memory CD8^{+} T-cells and of ILL-specific CD8^{+} T-cells was diminished. Indeed, a smaller proportion of CD8^{+} T-cells had the capacity to proliferate (data not shown), to secrete cytokines and to degranulate in response to ILL stimulation. Interestingly though, the proportion of PD-1-expressing CD8^{+} T-cells was not increased and no other inhibitory marker was expressed.

In the tumour, there were more CD8^{+} TILs than CD4^{+} TILs, which could explain the lower proportion than expected of splenic CD8^{+} T-cells. The majority of CD8^{+} TILs displayed an "exhausted" phenotype, as characterised by the co-expression of PD-1, Tim-3, LAG-3, but no CTLA-4. The vaccine increased the proportion of PD-1^{low} CD8^{+} TILs and decreased the proportion of exhausted CD8^{+} TILs. CD4^{+} T-cells has a similar phenotype, co-expressing all inhibitory markers apart from CTLA-4, with no differences between groups (data not shown). ILL-specific CD8^{+} T-cells secreting IFNγ and TNFα were detected at a lower frequency than in the spleen. Interestingly, the animal that survived the longest had CD8^{+} TILs displaying an "exhausted" phenotype: high GITR, higher PD-1^{+}Tim3^{+}, and fewer PD-1^{low}. Despite the exhausted phenotype, their functional capacity was retained as these cells displayed the highest percentage of IFNγ/TNFα secreting CD8^{+} T-cells.

Although results from the previous chapter suggested that ILL epitope is not presented by B16 cells, the CAF09-based vaccine induced splenocytes capable of lysing B16 cells, which could be explained by the presence of NK cells. The low proportion of ILL-specific CTLs at the tumour site suggests that ILL epitope is indeed not presented by B16 cells, otherwise these cells would have been recruited in higher number at the tumour site. Yet, the observation that the longest survival correlated with the highest proportion of IFNγ/TNFα secreting CD8^{+} T-cells in response to ILL suggests the opposite. However, this could be a random event as it was observed in one animal only. It is possible that the

delay in tumour growth observed is due to the cytokine secretion of CD8+ T-cells activating other cell types, such as NK cells, responsible for the anti-tumour response observed.

The activation of NK cells following vaccination has been described and depends on myeloid accessory cell-derived cytokines such as IL-12, IL-18 and type I interferons (Wagstaffe, et al. 2018). In particular, the activation of APC by the use of adjuvants was found to enhance and sustain NK cell activity, thereafter, contributing to T cell recruitment and memory cell formation. In particular, a subset of cytokine-induced memory-like (CIML) NK cells characterised by enhanced IFNγ production and cytotoxicity have been described to be induced by IL-2 secreting CD4$^+$ T-cells (Fehniger, et al. 2003; Goodier, et al. 2016) and myeloid cell-derived IL-12 and type I interferons. Although the enhanced NK immune response following vaccination has mainly been described in the context of infectious disease (Blohmke, et al. 2017; Darboe, et al. 2017) and in a CD4$^+$ T-cells-dependant manner (Horowitz, et al. 2010; Jost, et al. 2014), CIML NK cells have been shown to exhibit enhanced responses against myeloid leukaemia in a pre-clinical mouse model and in a first-in-human phase 1 clinical trial (Romee, et al. 2016). Administration of poly ICLC adjuvant on its own was shown to activate DCs and NK cells (Martins, et al. 2014). Although IL-2 secretion by CD4$^+$ T-cells following vaccination was not demonstrated, IL-2 secretion by CD8$^+$ T-cells was observed and could have led to NK activation.

Despite the unclear effect of the CAF09-based vaccine in preventing the growth of B16-HHDII-PAP tumours, the anti-tumour efficacy of the vaccine against established B16 tumour was assessed. Considering the results obtained in the prophylactic setting, an anti-PD-1 antibody was used in combination with the vaccine. No anti-tumour effect was observed. One animal treated with the anti-PD1 alone and one treated with the vaccine alone had a prolonged survival due to tumour developing more than 10 days later. However, one can argue about the role of the treatments in tumour growth delay since the treatment started before the observation of measurable tumours. Moreover, two animals in the prophylactic study who did not receive treatment developed tumours after day 20 post tumour implantation. Another important point to take into consideration is that the treatment schedule was different, with a 4 days gap in between immunisation instead of two weeks, due to the aggressiveness of the B16 tumour model. However, this immunisation schedule is not as efficient in inducing a PAP-specific immune response (data not shown). Although the immunophenotyping of T-cells was not performed, this was confirmed by the absence of increased proportion of splenic CD8$^+$ T-cells in the therapeutic study.

The presence of established tumours has been shown to suppress the clonal expansion of CD8$^+$ T-cells *in vivo*, following vaccination in comparison to tumour-free animals (Oizumi, et al. 2008). Schreiber *et al.* described a potential mechanism by which tumours escape immunosurveillance by

preventing the clonal expansion of tumour-specific CTLs without inducing anergy (Schreiber, et al. 2009). This mechanism can explain the reduction of the vaccine-induced immune response observed in our model. These results demonstrate the difficulty of breaking tolerance in tumour-bearing animals in comparison to tumour-free animals.

The same observations can be made about the TRAMP-C1 therapeutic studies. In the pilot study, the therapeutic treatment started at day 17 post tumour implantation, when only 33% of animals had developed tumours. One can again question the effect of the vaccine on the tumour growth delay observed in one animal. Moreover, immunisations were one week apart instead of two. The PAP-specific immune response induced using this treatment schedule was not assessed. The unchanged proportion of splenic and TIL CD8$^+$ T-cells suggest that the schedule was not optimal for mounting a vaccine-induced PAP-specific immune response.

In the other therapeutic study performed with faster growing TRAMP-C1 cells, no effect was observed on the tumour growth nor on the proportion of splenic and TIL CD8$^+$ T-cells in vaccinated animals. No conclusion can be drawn out of the prophylactic study, although it appears that one animal responded to the CAF09 vaccine.

Overall, the CAF09 vaccine delayed tumour growth in 20-25% of animals in 2/3 of the experiments whereas the ImmunoBody® vaccine had no anti-tumour effects. A higher number of animals per group is required to be able to reach a definite conclusion on the anti-tumour effect of the CAF09 vaccine.

Although others have shown that PAP-specific vaccines could break tolerance and induce anti-tumour responses against TRAMP-C1 tumour (Silva, et al. 2015; Spies, et al. 2012), treatment started at day 2 and day 6-8 post tumour implantation respectively. Cytotoxicity assay results (Chapter 4) showed PAP-specific killing against TRAMP-C1 and TRAMP-C2 cells, but vaccine-specific killing only against TRAMP-C2 cells. This could be explained by the fact that TRAMP-C2 express 5 times more PAP mRNA than TRAMP-C1 cells (Figure 4.2 A). The TRAMP-C2 tumour model would therefore have been a better choice, but could not be established.

Established tumours induce immunosuppression and tolerance (Mapara, et al. 2004). As mentioned in the context of B16 tumours, TRAMP-C1 tumours may have had a deleterious impact on the induction of a strong PAP-specific immune response. The presence of PAP-specific CD8$^+$ CTL should be assessed in further tumour studies to answer this hypothesis.

As mentioned earlier, the induction of a CD4$^+$ helper T-cell response was not demonstrated by the vaccine strategies studied here. However, CD4$^+$ T-cells are required for inducing CD8$^+$ CTL responses (Bennet, et al. 1998). In particular, the induction of CD8$^+$ memory T-cells is dependent on CD4$^+$ T-cells (Janssen, et al. 2003). CD4$^+$ T-cells have also been described as capable of displaying cytotoxic activity against established tumours (Quezada, et al. 2010). For these reasons, tumour-specific T helper epitopes should be included in the design of epitope-based vaccines (Ossendorp, et al. 1998).

As concluded by Melief "Therapeutic cancer vaccines cannot be expected to act as a monotherapy" (Melief, et al. 2015). The CAF09-based vaccine will need to be assessed in combination with other immuno-modulatory drugs to compensate for the immunosuppression induced by TRAMP-C1 tumours.

To conclude, despite a vaccine strategy inducing PAP-specific CD8$^+$ CTLs, the anti-tumour response elicited was too weak to prevent the tumour growth or to observe regression of established tumours. These results can be explained for several reasons. Firstly, the treatment scheduling was not optimal. Secondly, another immuno-modulatory treatment is likely to be required to counteract the immunosuppression induced by the tumour. Lastly, the tumour models used might not be the most adequate.

In the final part of this study, the relevance of this work for patients with prostate cancer was studied using PBMCs from patients with prostate cancer and healthy individuals. The presence of ILL-specific T-cells and their capacity to lyse ILL-presenting and PAP-expressing human prostatic cancer cell lines was assessed.

Chapter 6: Assessing the presence of PAP-specific immune responses in healthy individuals and patients with prostate cancer

6.1. Introduction

PAP protein is naturally expressed by the prostate and is therefore not foreign to the immune system of patients with prostate cancer. The expression of both PAP variants, cellular and secreted has been observed in mouse (Quintero, et al. 2007) and human thymus (Kong and Byun 2013), meaning that T-cells with high avidity TCRs towards PAP epitopes would have been eliminated when undergoing negative selection by the process of central tolerance. This mechanism is necessary to protect organs, such as the prostate, from auto-immune responses. Peripheral tolerance mechanisms further regulate auto-reactive T-cells that might have escaped central tolerance. These mechanisms include suppression of T cells by 1) expression of checkpoints (PD-1, Tim-3, LAG-3,...), 2) immuno-suppressive cells (Treg cells, MDSCs), 3) immunosuppressive cytokines and enzymes (TGF-β, IL-10, IDO), 4) poor T cell infiltration in tumours and 5) improper inflammation (Melief, et al. 2015).

Voutsas *et al.* demonstrated that high pre-existing immunity in patients with prostate cancer towards the native HER-2 peptide, AE36, correlated with longer PFS following vaccination with a HER-2/neu hybrid peptide in a phase I clinical trial (Voutsas, et al. 2016).

We can therefore assume that the efficacy of a prostate cancer vaccine targeting PAP is likely to be higher if the patient has pre-existing PAP-specific T-cells that could be boosted by the vaccine, or pre-existing naïve T-cells that express TCRs recognizing PAP-derived epitopes and could be primed by DCs after vaccination. However, although the presence of PAP-specific T-cells can be detected, proving the existence of naïve T-cell expressing PAP peptide-specific TCRs is much more difficult due to their low frequency.

The presence of circulating PAP-specific T-cells in patients with prostate cancer has previously been reported and generating insight into this might constitute a valuable tool to predict the potential efficacy of a PAP vaccine.

The presence of PAP-specific T-cells has been particularly evaluated in HLA-A2$^+$ individuals given their high frequency in the population. HLA-A2 is a large and diverse allele family as it is composed of 31 alleles, and is common in all ethnicities (Ellis, et al. 2000). Ellis *et al.* reported HLA-A2 frequencies in 5 US ethnic groups: Caucasian (49.6%), African-American (34.6%), Asian/Pacific Islander (36%), Hispanic (46.9%) and Native Americans (49.7%), with an average of 47.6% of all individuals tested (82,979) being HLA-A2$^+$. Moreover, a Swedish study has demonstrated a higher

HLA-A2 frequency in patients with prostate cancer (69%) than in healthy individuals (58%), thereby suggesting the negative prognostic correlation with HLA-A2 (Masucci, et al. 2006).

Studies have demonstrated the presence of PAP-specific T-cells that could secrete IFNγ in response to *in vitro* stimulation with PAP-derived peptides and/or lyse peptide pulsed T2 cells in healthy individuals (Peshwa, et al. 1998) and in patients with prostate cancer (Olson, et al. 2010). Several epitopes were identified, one of which was PAP 135-143 (ILL), for which specific T-cells were found in 40% of patients with prostate cancer (6 of 15) (Olson, et al. 2010). In that study, ILL-specific cells were shown to lyse ILL-pulsed T2 cells, but not LNCaP cells. However, these findings were distinct to those of Machlenkin *et al.* who had previously demonstrated that LNCaP cells were lysed by ILL-specific T-cells from patients with prostate cancer in an HLA-A2 specific manner (Machlenkin, et al. 2005).

Although the presence of PAP-specific CTLs is relevant given their involvement in tumour cell cytotoxicity, the presence and function of PAP-specific CD4^{+} helper T-cells is of interest given their role in promoting CTL responses and inducing long-term memory CD8^{+} T-cells.

McNeel *et al.* observed PAP-specific T-cells with a Th1 phenotype (as characterised by proliferation and IFNγ secretion in response to PAP whole protein stimulation) in 11% of patients with prostate cancer (McNeel, et al. 2001) and later identified two MHC class-II epitopes (15AA) that were capable of inducing PAP-specific proliferation in patients with prostate cancer (McNeel, et al. 2001). Klyushnenkova *et al.* then identified two PAP-derived HLA-DRB1*1501-restricted T-cell epitopes of 20AA (PAP (133-152) and PAP (173-192)) capable of stimulating CD4^{+} T-cells in healthy individuals and patients with prostate cancer (Klyushnenkova, et al. 2007). Johnson *et al.* subsequently identified four HLA-DRB1*0101 epitopes of 15AA (PAP (161-175), PAP (181-195), PAP (191-205), and PAP (351-365)) in HLA-A2.01/HLA-DRB1*0101 transgenic mice, along with one epitope which could elicit specific T-cells following immunisation with the pTVG-HP DNA vaccine (Johnson and McNeel 2012). Although this study does not refer to naturally occurring PAP-specific CD4^{+} helper T-cells, it reinforces the findings of Klyushnenkova *et al.* that MHC class-II PAP-derived epitopes can be present in patients with prostate cancer.

The aim of the studies presented in this chapter was to compare the presence and functionality of ILL-specific CTLs in the blood of HLA-A2[+] patients with prostate cancer and HLA-A2[+] healthy individuals.

Responsiveness was assessed following a 12-day protocol to expand the potential ILL-specific CTLs within the PBMC compartment of each individual. Two stimulating conditions were employed: using the ILL 9mer peptide itself or the hPAP42mut peptide.

Firstly, the pre-existence of ILL-specific CTLs was measured by dextramer-based flow cytometric analysis. Dextramers were shown to be better at assessing the presence of antigen-specific T-cells than tetramers for several reasons: brighter staining, stronger binding for TCR-pMHC complexes of low affinity and enhanced sensitivity (Dolton, et al. 2014). Then, the capacity of PBMCs to recognize and lyse ILL-presenting cells and human prostatic cell lines was measured.

6.2. Results

6.2.1.Patients information

PBMCs were obtained from three HLA-A2$^+$ groups:

- **Healthy individuals:** 40+ years old males (**3 individuals**);

- **Men with benign disease**: males with benign prostate tumours (**5 individuals**);

- **Patients with prostate cancer** (**16 individuals**).

Samples from patients with prostate cancer and men with benign disease were obtained from Leicester Hospital.

Clinical information available included:

- Presence of Lower Urinary Tract Symptoms (LUTS)

- Serum PSA concentration and PSA density

- Two different type of biopsy information: TRUS and TPTPB, which was shown to improve diagnostic accuracy in men with elevated PSA and previous negative TRUS biopsies (Nafie, et al. 2014)

- Gleason score, TNM pathological stage and D'Amico classification.

Regarding patients LE097 to LE113, only pathology information from the TRUS biopsy was available, whereas the TRUS pathology + TPTP pathology was available for LE309 to LE325 patients.

Table 6.1: Clinical information for patients with prostate cancer

Patient	Age	Diagnosis	LUTS	PSA (ng/mL)	PSAD (ng/mL/cc)	TRUS pathology	TPTP pathology	Gleason score	TNM pathological stage	D'Amico classification
LE097	75	Benign	YES	11	0.22	N/A		-	N/A	-
LE100	68	Benign	YES	0.25	0.01	N/A		-	T2	-
LE103	65	Benign	YES	12	0.10	N/A		-	Benign	-
LE112	60	Benign	NO	5.7	0.14	N/A		-	N/A	-
LE312	67	Benign	NO	12	0.13	N/A		-	N/A	-
LE317	73	Cancer	YES	11	0.16	N/A	3+3	6	T1c	Low
LE098	74	Cancer	NO	8.3	0.18	3+3		6		Intermediate
LE101	51	Cancer	YES	4.2	0.16	3+4		7	Benign	Intermediate
LE111	83	Cancer	YES	11	0.11				Flat	Intermediate
LE319	69	Cancer	YES	7.2	15.00	N/A	3+4	7	T1c	Intermediate
LE320	71	Cancer	NO	7.5	0.18	N/A	3+4	7	T1c	Intermediate
LE322	71	Cancer	NO	21	0.16	N/A	3+3	6	T1c	Intermediate
LE102	74	Cancer	YES	75	2.72	4+5		9	T3	High
LE104	78	Cancer	YES	82	2.68	5+5		10	T4	High
LE105	80	Cancer	YES	40	1.90	5+4		9	T3	High
LE109	65	Cancer	YES	31	1.53	4+5		9	T2	High
LE113	79	Cancer	NO	29	1	4+5		9	T2	High
LE309	56	Cancer	YES	10	0.19	N/A	4+3	7	T2	High
LE311	64	Cancer	YES	47	1.09	4+3	Mets	7	Bone metastasis	High
LE313	76	Cancer	YES	66	0.05	Neg	4+5	9	T1c	High
LE325	75	Cancer	NO	21	0.18	N/A	3+5	8	T1c	High

Samples from patients LE097, 101, 102, 103, 104, 105, 111, 112 and 113 (9 patients) and one healthy control were processed and analysed by Dr Stéphanie McArdle and Holly Nicholls (Masters student). These experiments were performed in 2017 and the dextramer data obtained pooled with the data generated by myself (LE309 to LE325 patients).

Due to the number of PBMCs available after expansion protocol, not all assays could be performed on all samples, and this limitation needs to be considered when interpreting results.

6.2.2. Validation of the method for expanding antigen-specific CD8$^+$ T-cells from PBMCs

In order to validate the 12-day expansion protocol (see Figure 6.1), PBMCs of patients LE309 to LE325 were stimulated with a cocktail of 3 HLA-A2 class-I viral epitopes: Influenza A virus (FLuA), Epstein-Barr virus (EBV) and Cytomegalovirus (CMV). IL-2 and IL-15 cytokines were used as they have been shown to promote the expansion of antigen-specific CD8$^+$ T-cells (Montes, et al. 2005). The high frequency of these viruses means that most individuals of the population would have encountered at least one of these viruses during their life. FLuA, which causes the common Flu, affects 20% of the population every year (Klein, et al. 2016), EBV herpes virus infects more than 90% of adults (Lünemann, et al. 2008) and CMV infects between 60 to 70% of the adult population in developed countries and almost 100% of adults in emerging countries (Gupta and Shorman 2019). These were therefore used as positive controls to assess the presence of antigen specific T-cells by dextramer analysis and recognition and lysis of epitope-pulsed T2 cells.
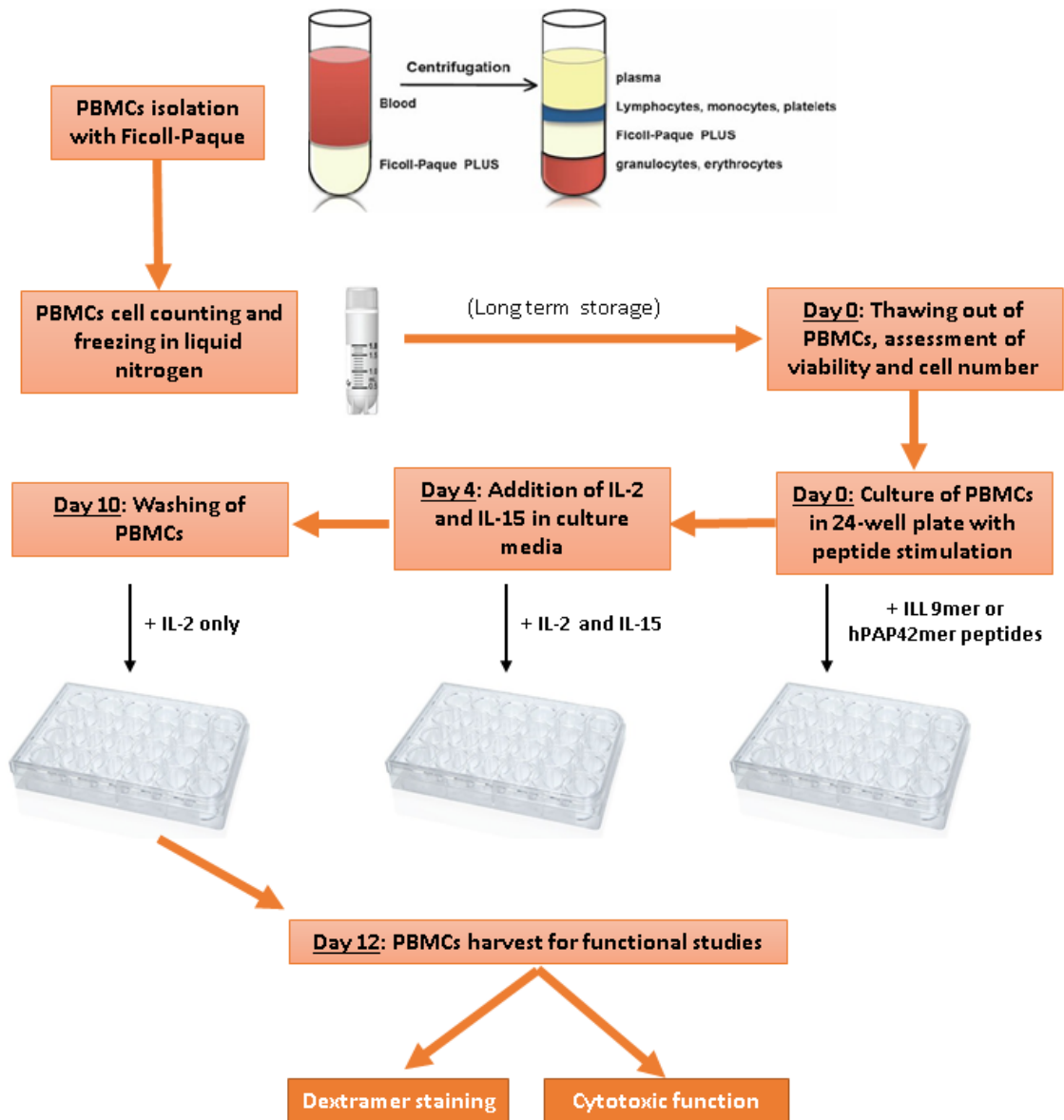
Figure 6.1: Workflow of the protocol for the expansion of antigen-specific CD8$^+$ T-cells from PBMCs.

Given their cost, the assessment of antigen-specific cells by dextramer analysis was only performed for the CMV epitope. Others have previously confirmed the accuracy of fluorescently-labelled TCR-specific dextramers for quantifying CMV antigen-specific T-cells in blood samples (Tario, et al. 2015). To this end, CMV-specific dextramer fluorescence of CD8$^+$ T-cells was determined according to the gating strategy showed Figure 6.2A.

One of two healthy individuals and 4 of 8 patients with prostate cancer exhibited CMV-specific CTLs (Figure 6.2B), which is just below the 60 to 70% of positive individuals previously reported (Gupta and Shorman 2019). To evaluate the enrichment in CMV-specific T-cells after 12 days of culture, the proportion of circulating *versus in vitro* expanded CMV-specific T-cells was compared for one patient. 0.06% of dextramer positive cells were detected on day 0, whereas 1.92% was observed

on day 12, thereby demonstrating the capacity of the protocol to expand antigen-specific CD8^{+} T-cells (data not shown).

The healthy individual and two of the patients had between 1.92 and 4.52% of CMV-specific CTLs. The other two patients had a surprisingly high percentage of CMV-specific T-cells of 34.8 and 56.11%. However, these represent the proportion of CMV-specific T-cells within total CD8^{+} T-cells after *in vitro* expansion and not the proportion of circulating CMV-specific CTLs. We can speculate that these two patients had an ongoing CMV infection.

Results from dextramer analysis are summarized in Table 6.2 below.

Table 6.2: Positive cells for dextramer negative control and dextramer CMV (red= patients exhibiting CMV-specific CTLs)

Individual	% Dextramer negative CTRL	% Dextramer CMV
Healthy 1	0.13	1.92
Healthy 2	0.05	0.09
LE309	0.01	0
LE311	0.04	4.52
LE313	0	3.39
LE317	0.01	34.84
LE319	0.02	0.04
LE320	0.03	0.01
LE322	0.02	0.03
LE325	0	56.11
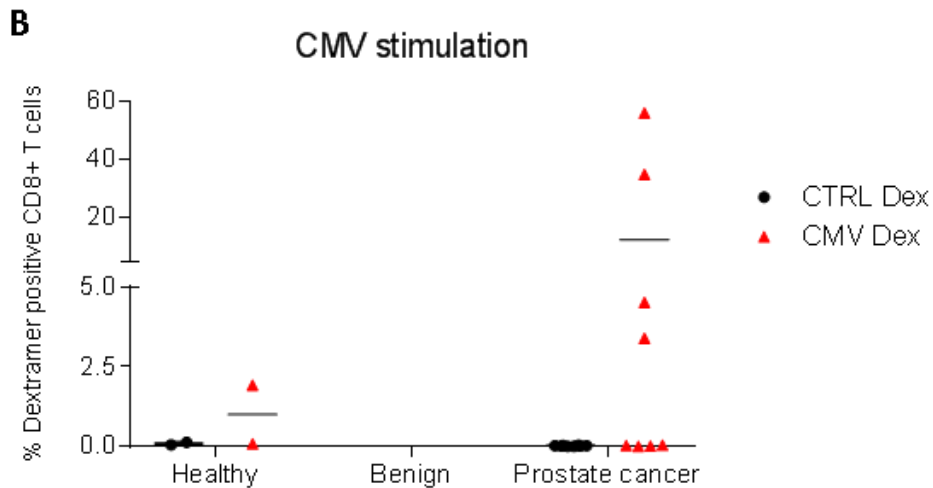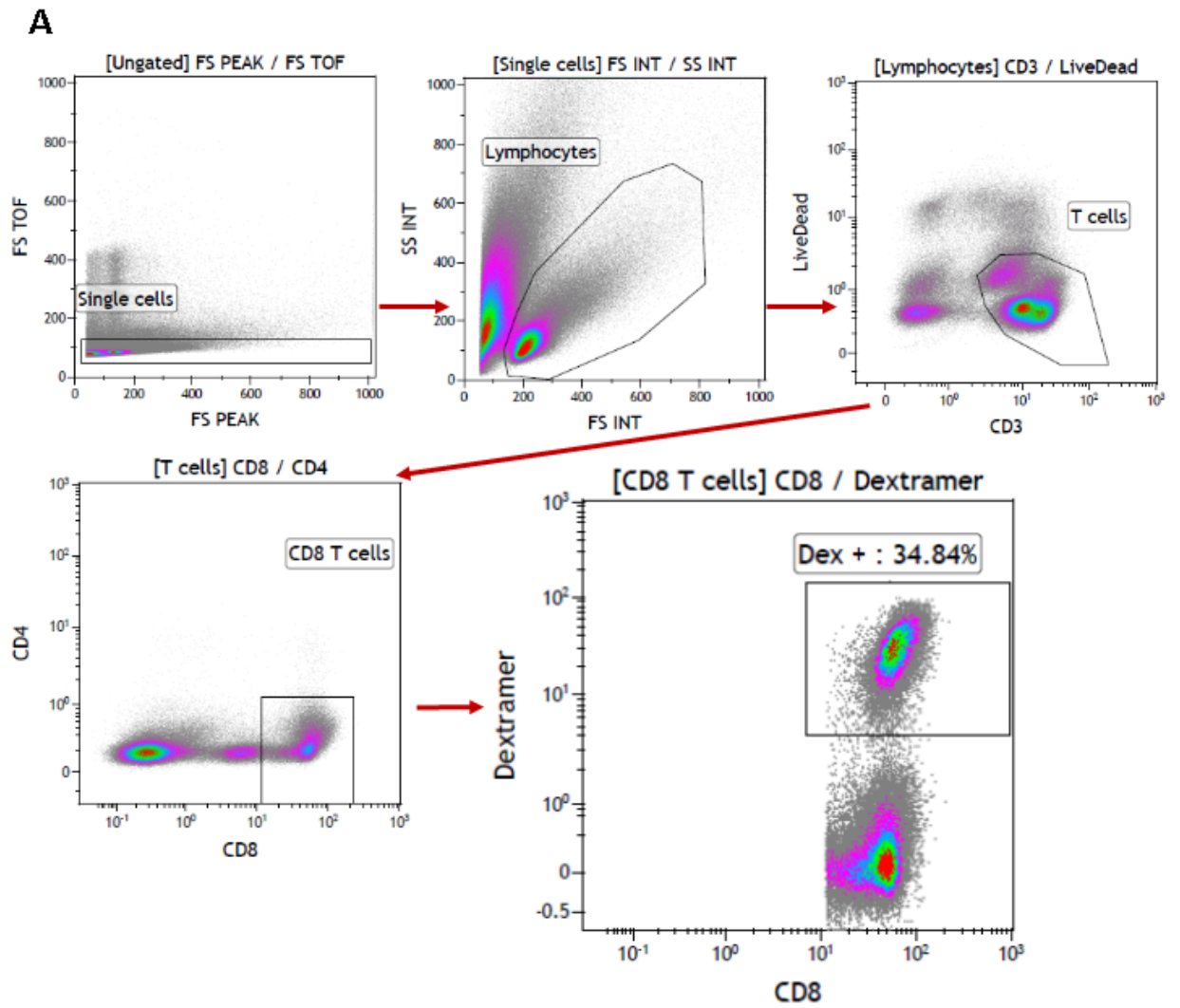
Figure 6.2: Gating strategy and results for CMV dextramer analysis. Cryopreserved PBMCs from HLA-A2[+] healthy individuals and patients with prostate cancer were cultured for 12 days in the presence of IL-2, IL-15 and an HLA-A2-restricted CMV epitope. At the end of the stimulation, PBMCs were incubated with a human FcR block and then stained with surface antibodies and the CMV dextramer. (A) Represents the gating strategy used and (B) represents the proportion of dextramer positive cells within CD8^{+} T-cells. CMV-specific CTLs were detected in 5 of 10 individuals.

Subsequently, expanded virus-specific CTLs were tested for their capacity to recognise and lyse epitope-pulsed T2 cells. The gating strategy used to analyse results is shown Figure 6.3A. Gating of PKH26^{+} target cells was purposely stringent in order to avoid contamination of PBMCs.

Evidently, this experiment was not only relevant for CMV dextramer[+] patients as PBMCs had been stimulated with the cocktail of viral epitopes. Three conditions were compared, PBMCs were co-incubated with either T2 cells, T2 cells pulsed with all three epitopes used for the expansion or T2 cells pulsed with the CMV epitope only. This last condition was used for only four patients (LE317, 319, 322 and 325). Table 6.3 summarizes the assays that were performed.

Table 6.3: Summary of assays performed for CMV stimulated PBMCs (orange = assay done)

Patient	Dextramer		Cytotoxicity					
			T2 cells					
	CTRL	CMV	T2-		T2 cocktail		T2 CMV	
			1:1	5:1	1:1	5:1	1:1	5:1
Healthy 3	orange	orange	orange	orange	orange	orange	grey	grey
LE309	orange	orange	orange	orange	orange	orange	grey	grey
LE311	orange	orange	grey	orange	orange	grey	grey	grey
LE312	grey	grey	grey	grey	grey	grey	grey	grey
LE313	orange	orange	orange	orange	orange	orange	grey	grey
LE317	orange	orange	orange	grey	orange	grey	orange	grey
LE319	orange	orange	orange	orange	orange	orange	orange	grey
LE320	orange	orange	grey	grey	grey	grey	grey	grey
LE322	orange	orange	orange	orange	orange	orange	orange	orange
LE325	orange	orange	orange	orange	orange	orange	orange	orange

On average, cytotoxicity towards peptide-pulsed T2 cells was higher than that towards un-pulsed T2 cells (Figure 6.3B top). As expected, PBMCs from CMV dextramer[+] patients induced cytotoxicity against both CMV-pulsed and cocktail pulsed-T2 cells (Figure 6.3.B bottom right), whereas PBMCs from CMV dextramer[-] patients only induced cytotoxicity against cocktail pulsed-T2 cells (Figure 6.3.B bottom left). These results suggest that CMV dextramer[-] patients probably had encountered EBV and/or FluA, and if dextramer analysis for CTLs specific for these epitopes was performed, EBV/FluA-specific CTLs would have been found.

For LE325, which had 56.11% of CMV dextramer^{+} CD8^{+} T-cells, the killing of CMV peptide- and cocktail pulsed-T2 cells was similar (60.02% *versus* 54.17%, respectively), thereby suggesting that LE325 did not have FluA or EBV CTLs. These results also suggest the possibility that CMV epitope had a higher affinity for HLA-A2 molecules at the surface of T2 cells, although this was not tested. If this was the case, results assessing the capacity of PBMCs to lyse FluA or EBV-pulsed T2 cells

would not be optimal and the assay should have been performed with single epitope-pulsed T2 cells. Nonetheless, dextramer analysis and cytotoxicity assays performed on viral epitope-specific CTLs demonstrated the efficacy of each technique and the correlation between the presence of epitope-specific CD8$^+$ T-cells and the capability of these cells to lyse specifically epitope-pulsed target cells.

Although planned, the secretory function and the activated status of CD4$^+$ and CD8$^+$ T-cells could not be assessed due to the shortage of PBMCs. Despite the 30-fold increase in CMV-specific CTLs observed, the recovery of PBMCs following 12 days of *in vitro* culture was consistently reduced by 33-50% (data not shown). This was also observed for ILL and PAP42mut stimulated cells.
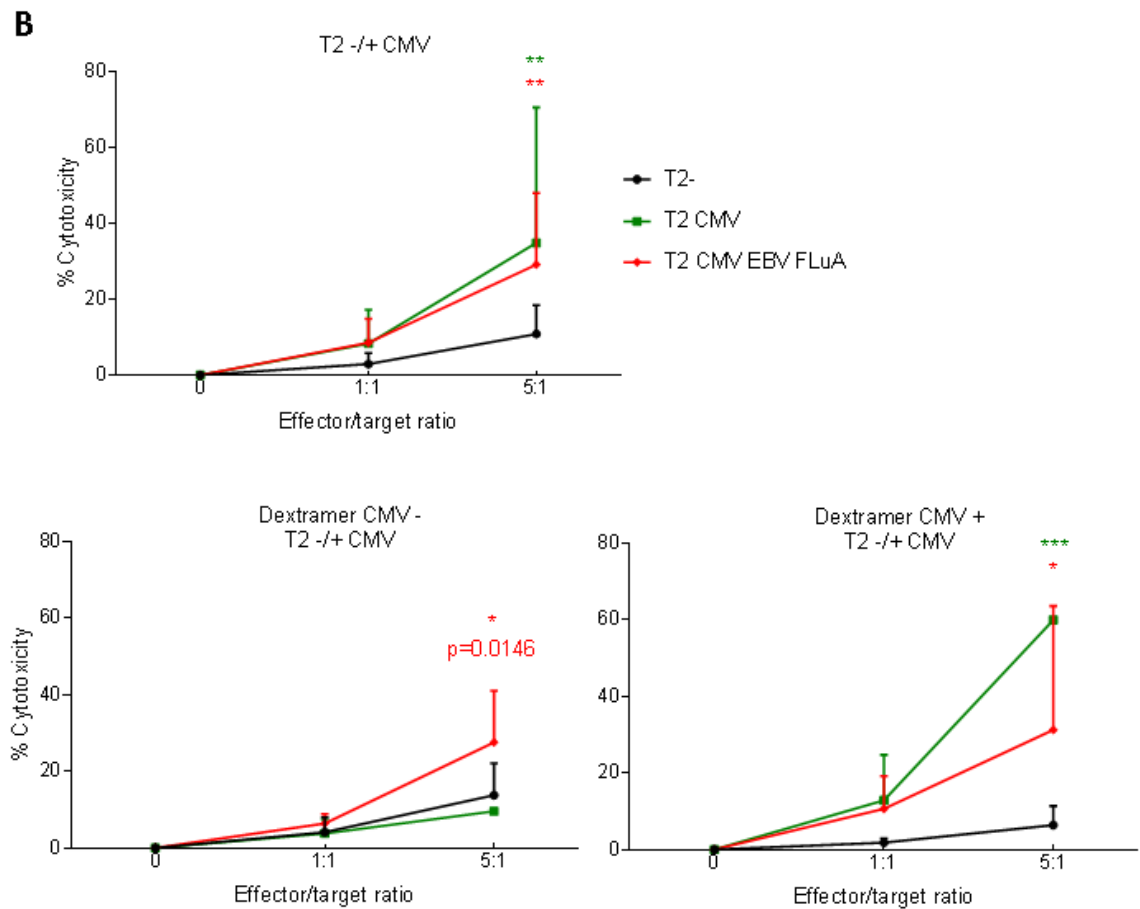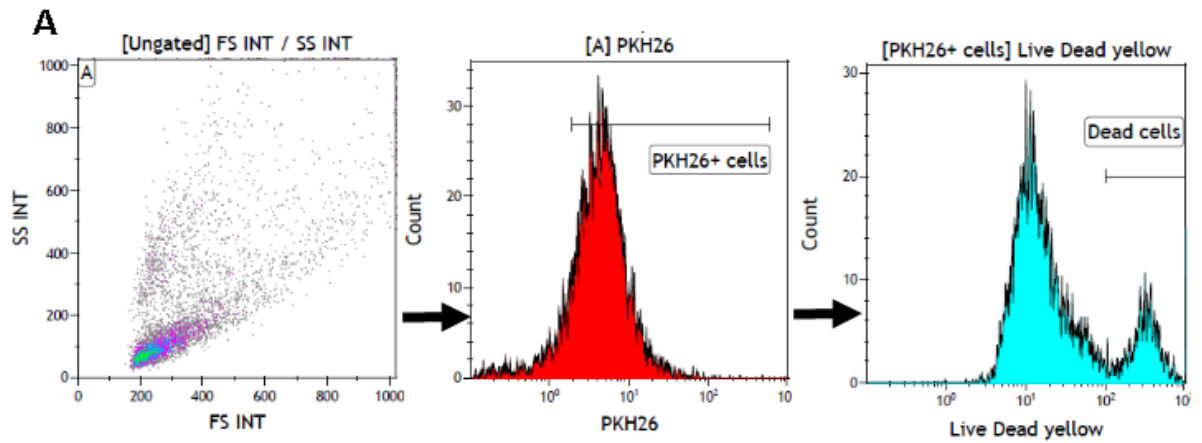
Figure 6.3: Gating strategy for cytotoxicity assay analysis and cytotoxicity against CMV-presenting T2 cells. Cryopreserved PBMCs from HLA-A2[+] healthy individuals and patients with prostate cancer were cultured for 12 days in the presence of IL-2, IL-15 and an HLA-A2-restricted CMV epitope. At the end of the stimulation, PBMCs were co-incubated with PKH26 stained target cells for 3 hours, at the end of which cells were stained with LIVE/DEAD™ Yellow Dead Cell Stain to measure the percentage of dead target cells. (A) Gating strategy used and (B) percentage of cytotoxicity against PK26^{+} (target) cells. PBMCs from patients with CMV-specific CTLs induced CMV-specific cytotoxicity. Bars represent the mean percentage of positive cells and the error bars represent the SD (n= 1 to 8 patients). Differences in the cytotoxicity between groups were determined using a two-way ANOVA comparison test.

6.2.3.Presence of HLA-A2 ILL-specific CD8^{+} T-cells

The presence of ILL-restricted HLA-A2 CD8^{+} T-cells was assessed using the dextramer technology. Two stimulating conditions were compared to expand the ILL-specific CTLs population: stimulation with the ILL 9mer epitope or with the human PAP42mer mutated peptide. Neither stimulation influenced the proportion of CD8^{+} T-cells within the CD3^{+} T-cell population (Figure 6.4A). Moreover, the proportion of CD8^{+} T-cells in healthy individuals, men with benign disease and patients with prostate cancer were similar (Figure 6.4A).

Following ILL stimulation, ILL-specific CTLs were detected in patients with prostate cancer (Figure 6.4B). Of the 16 patients with prostate cancer, 6 had ILL-specific CTLs, ranging from 0.29 to 1.6% with only one patient having a percentage higher than 1%. Although, a small cohort, 37.5% of patients with prostate cancer had detectable circulating ILL-specific CTLs, whereas only one individual (out of 5 tested i.e 20%) with benign disease exhibited ILL-specific CTLs (0.92%).

Following stimulation with the PAP42mut peptide, ILL-specific CTLs were also detected in patients with prostate cancer (Figure 6.4B), however, the proportion was systematically lower than when PBMCs where stimulated with the ILL9mer (Figure 6.4B). Moreover, for LE109, 111 and 312, only ILL stimulation could induce ILL-specific CTLs. We can conclude that 4 of 15 (26.7%) patients with prostate cancer and 1 of 5 (20%) individuals with benign disease had detectable ILL-specific CTLs after stimulation with the hPAP42mut peptide.
None of the 3 healthy individuals tested had detectable ILL-specific CTLs, although the cohort is too small to conclude.

In conclusion, stimulation with the ILL 9mer peptide is more efficient than stimulation with the whole PAP42mut peptide to expand the pre-existing population of circulating ILL-specific CTLs from PBMCs. Results from dextramer analysis are summarized in Table 6.4.

Table 6.4: Positive cells for dextramer negative control and dextramer ILL (red= patients exhibiting ILL-specific CTLs)

Individual	ILL stimulation		PAP42mut stimulation	
	% Dextramer negative CTRL	% Dextramer ILL	% Dextramer negative CTRL	% Dextramer ILL
Healthy 1	0.1	0.12	0.09	0.11
Healthy 2	0.02	0.02	0.02	0.02
Healthy 3	0.03	0.06	0.03	0.07
LE097	0.18	0.1	0.16	0.2
LE098	0.1	0.11	0.09	0.12
LE100	0.14	0.14	0.09	0.15
LE101	0.04	0.37	0.01	0.39
LE102	0.05	0.29		
LE103	0.12	0.19	0.01	0.48
LE104	0.02	0.8	0.08	0.3
LE105	0.03	1.6	0.08	1.09
LE109	0.1	0.42	0.12	0.17
LE111	0.13	0.46	0.18	0.21
LE112	0.11	0.26	0.11	0.13
LE113	0.11	0.23	0.11	0.31
LE309	0	0	0.01	0.01
LE311	0	0.01	0	0.03
LE312	0.01	0.92	0.03	0.01
LE313	0	0	0	0
LE317	0.01	0.02	0	0.01
LE319	0.06	0.04	0.03	0.09
LE320	0.01	0.01	0.02	0.04
LE322	0.05	0.04	0.03	0.03
LE325	0.01	0.01	0.01	0.01
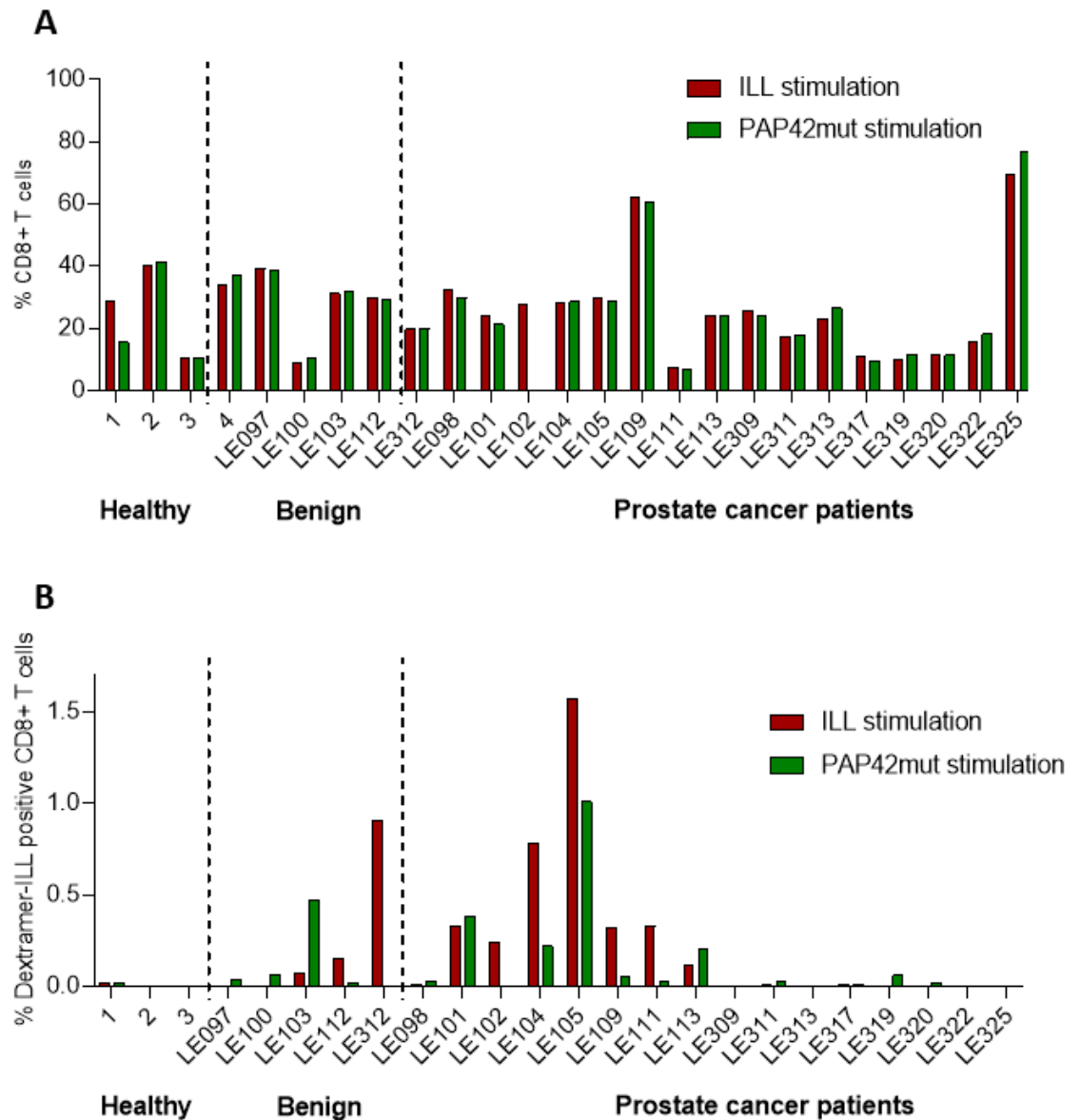
Figure 6.4: Presence of ILL-specific CD8+ T-cells within the blood of patients with prostate cancer. Cryopreserved PBMCs from HLA-A2+ healthy individuals, individuals with benign disease and patients with prostate cancer were cultured for 12 days in the presence of IL-2, IL-15 and either the HLA-A2-restricted ILL epitope or the hPAP42mer mutated peptide. At the end of the stimulation, PBMCs were incubated with a human FcR block and then stained with surface antibodies and the ILL dextramer. (A) proportion of CD8+ T-cells within total T-cells, (B) proportion of ILL dextramer positive cells within CD8+ T-cells following ILL peptide or hPAP42mut peptide stimulation (normalised on dextramer control). There was no difference in the proportion of CD8+ T-cells among groups. ILL-specific CTLs were detected following ILL stimulation (benign disease: 1/5, prostate cancer: 6/16) and after hPAP42mut peptide stimulation (benign disease: 1/5, prostate cancer: 4/16). N= 3 to 16 patients.

6.2.4. Cytotoxic function of PBMCs against ILL-presenting cells and the human prostatic cell line LNCaP

The capacity of PBMCs to recognize and lyse target cells in a PAP-dependant manner was assessed by performing cytotoxicity assays, as detailed in Section 6.2.2. Firstly, cytotoxicity against ILL-pulsed T2 cells was measured to assess the correlation between the presence of ILL-specific CTLs and the lysis of ILL-pulsed cells. Due to shortage of PBMCs, the assay could only be performed on PBMCs from individuals who did not have ILL-specific CTLs detectable with the dextramer, therefore, no ILL-specific killing was observed regardless of the stimulating condition (Figure 6.5A, B and C).

The LNcaP cell line was shown in Chapter 4 to be HLA-A2$^+$ and to express the hPAP (Figure 4.3). 'Knocking out' the hPAP gene reduced PAP expression by 84%, relative to LNCaP WT cells (Figure 4.3) and these cells (LNCaP PAP^{low}) were used to evaluate the capacity of PBMCs to lyse LNCaP cells in a PAP-specific manner. To further test the presence of ILL-specific CTLs, LNCaP WT cells were also pulsed with the ILL 9mer peptide prior to performing cytotoxicity assays.

Results demonstrated a slight, but non-significant higher cytotoxicity against LNCaP WT cells than against LNCaP PAP^{low} for both stimulating conditions (Figure 6.6B), with cytotoxicity against LNCaP cells being higher after PAP42mut peptide stimulation (Figure 6.6C). However, the only significant difference between the 2 stimulating conditions was observed for ILL-pulsed LNCaP WT target cells. This result is surprising as no ILL-specific CTLs were detected in these patients. These results suggest the possibility that these patients have PAP-specific CTLs for epitope(s) other than ILL, that are contained within the hPAP42mer sequence and that these were expanded during the 12 days *in vitro* culture. There is also the possibility that because the method used was initially developed for expanding CTLs of higher frequencies, such as those against viruses, it might not be optimal for expanding low frequency TAA-specific CTLs such as ILL-specific CTLs.
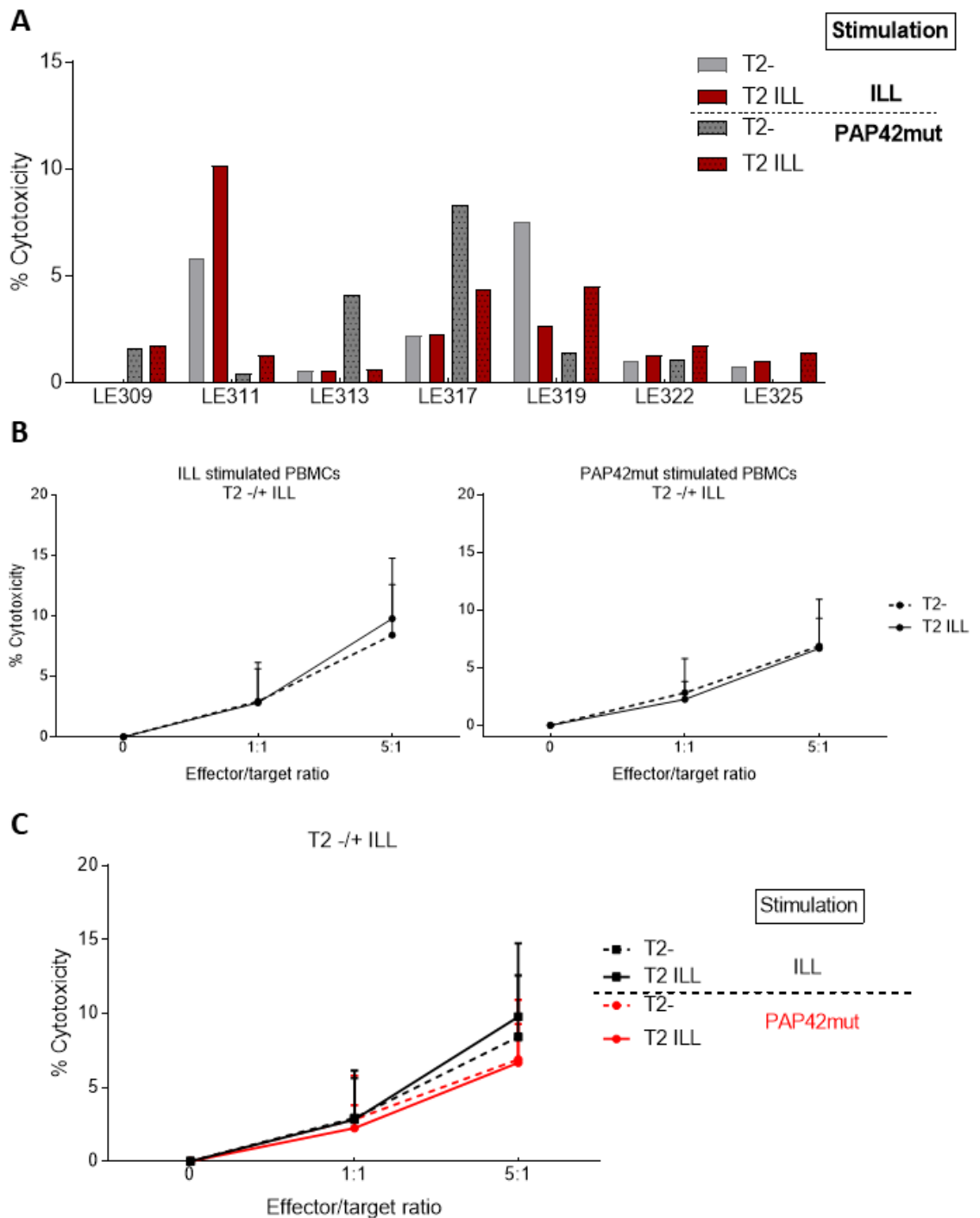
Figure 6.5: Cytotoxicity of PBMCs from patients with prostate cancer against ILL-presenting T2 cells. Cryopreserved PBMCs from HLA-A2[+] patients with prostate cancer were cultured for 12 days in the presence of IL-2, IL-15 and either the HLA-A2-restricted ILL epitope or the hPAP42mer mutated peptide. At the end of the stimulation, PBMCs were co-incubated with PKH26 stained target cells for 3 hours, at the end of which cells were stained with LIVE/DEAD™ Yellow Dead Cell Stain to measure the percentage of dead target cells. Percentage of cytotoxicity against PK26^{+} (target) cells was compared per patient (A) between T2 unpulsed and pulsed cells (B) and between stimulating condition (C). No ILL-specific lysis was observed. Bars represent the mean percentage of positive cells and the error bars represent the SD (n= 3 to 7 patients). Differences in the cytotoxicity between groups were determined using a two-way ANOVA comparison test.
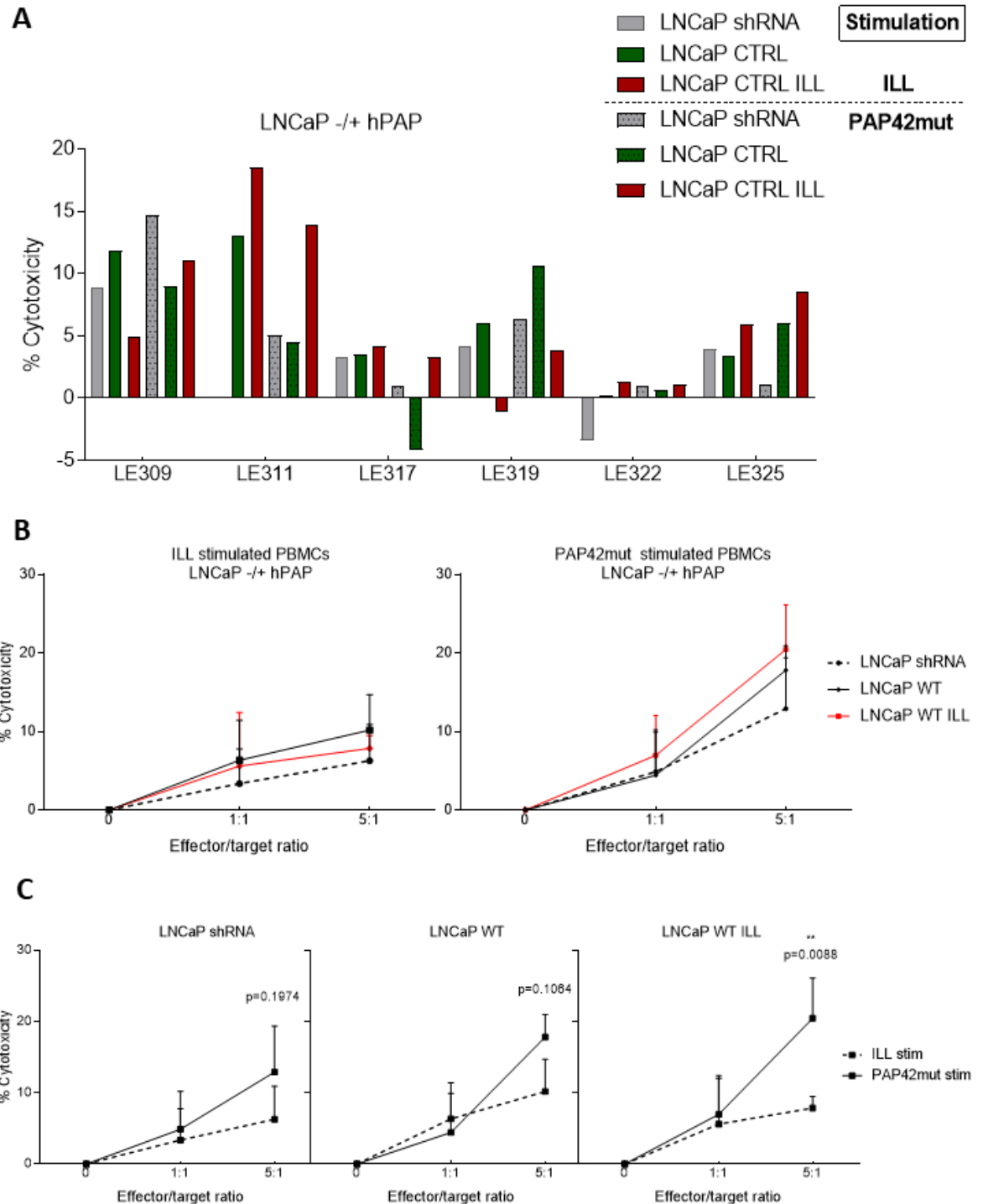
Figure 6.6: Cytotoxicity of PBMCs from patients with prostate cancer the human prostatic cell line LNCaP. Cryopreserved PBMCs from HLA-A2[+] patients with prostate cancer were cultured for 12 days in the presence of IL-2, IL-15 and either the HLA-A2-restricted ILL epitope or the hPAP42mer mutated peptide. At the end of the stimulation, PBMCs were co-incubated with PKH26 stained target cells for 3 hours, at the end of which cells were stained with LIVE/DEAD™ Yellow Dead Cell Stain to measure the percentage of dead target cells. Percentage of cytotoxicity against PK26^{+} (target) cells was compared per patient (A) between LNCaP shRNA, WT and WT ILL cells (B) and between stimulating condition (C). No significant PAP-specific lysis was observed. PAP42mut peptide stimulated PBMCs induced higher percentage of cytotoxicity against LNCaP cells. Bars represent the mean percentage of positive cells and the error bars represent the SD (n= 2 to 6 patients). Differences in the cytotoxicity between groups were determined using a two-way ANOVA comparison test.

Table 6.4: Summary of assays performed per patients for ILL and PAP42mut peptides stimulated PBMCs (orange = assay done)

Patient	Stimulation	Dextramer		Cytotoxicity									
				T2 cells				LNCaP cells					
				T2-		T2 ILL		shRNA		WT		WT ILL	
		CTRL	ILL	1:1	5:1	1:1	5:1	1:1	5:1	1:1	5:1	1:1	5:1
Healthy 2	ILL	O	O										
	PAP42mut	O	O										
Healthy 3	ILL	O	O	O				O	O	O	O	O	O
	PAP42mut	O	O	O				O	O	O	O	O	O
LE309	ILL	O	O	O		O		O		O		O	
	PAP42mut	O	O		O	O	O	O	O	O	O	O	O
LE311	ILL	O	O	O		O		O		O		O	
	PAP42mut	O	O	O		O		O		O		O	
LE312	ILL	O	O										
	PAP42mut	O	O										
LE313	ILL	O	O	O	O	O	O						
	PAP42mut	O	O	O	O	O	O						
LE317	ILL	O	O	O	O	O	O	O		O		O	
	PAP42mut	O	O	O		O	O	O		O			
LE319	ILL	O	O	O	O	O	O	O	O	O	O	O	
	PAP42mut	O	O	O	O	O	O	O		O		O	
LE320	ILL	O	O										
	PAP42mut	O	O										
LE322	ILL	O	O	O	O	O	O	O	O	O	O	O	O
	PAP42mut			O		O		O	O	O		O	
LE325	ILL	O	O	O	O	O	O	O	O	O	O	O	O
	PAP42mut	O	O	O	O	O	O	O	O	O	O	O	O

6.3. Discussion

Results presented in this chapter illustrate the heterogeneity of each individual's immune system. Evidently, the incapacity or capacity of patients with prostate cancer to develop an ILL-specific immune response depends on diversity in central and peripheral tolerance mechanisms which can vary between individuals. The expression of peripheral tissue antigens in the thymus varies among individuals, suggesting that the level of expression of a specific antigen determines the susceptibility to autoimmunity against that antigen (Takase, et al. 2005). Although PAP has been shown to be expressed in the thymus (Kong and Byun 2013), no investigation has assessed the differential expression of this protein among individuals. Based on the study by Takase *et al.*, one can speculate that PAP expression in thymic cells varies among individuals (Takase, et al. 2005), providing a possible explanation for the disparity in circulating ILL-specific T-cells in patients with prostate cancer.

Stimulation with the PAP42mut was less efficient at inducing ILL-specific CTLs, which could be due to the length of the peptide. Indeed, although 9mer epitopes can bind directly to MHC class-I molecules and be presented to T-cells, longer peptides such as the hPAP42mut peptide are required to be taken up and processed by APCs in order for these cells to break down the peptide into class-I and class-II epitopes that can be presented to T-cells (Melief 2008). Although monocytes and B cells present in PBMCs can act as APCs, they are not as efficient at stimulating antigen-experienced T cells as DCs. The *in vitro* generation of DCs would have allowed a more efficient processing of the hPAP42mut peptide and possibility not only improve the generation of ILL-specific CTLs, but also allow for other/additional peptide(s) to be presented.

Johnson *et al.* demonstrated that 80% of patients with prostate cancer had PAP-specific IFNγ-releasing T-cells (Johnson, et al. 2017). Although this percentage is much higher than 37.5%, the current study was highly restrictive and only assessed the presence of CTLs specific to a single HLA-A2 epitope, in a few patients. The study of other HLA-A2 epitopes contained within the hPAP42mer sequence would be of interest. Indeed, the higher cytotoxicity induced against LNCaP cells following stimulation with the hPAP42mut peptide suggests the presence of PAP-specific CTLs other than ILL-specific CTLs.

The aim of this study assumed that patients with prostate cancer exhibiting pre-existing PAP-specific immunity, in particular of ILL-specific CTLs, which were highly increased following vaccination with the CAF09-based vaccine in Chapter 3, would respond better to immunisation with this new and patented mutated-PAP derived 42mer peptide vaccine.

However, whether pre-existing immunity towards a class-I epitope can predict an improved OS in vaccinated patients is not clear. Voutsas *et al.*, assessed a therapeutic peptide-based vaccine targeting the oncogene HER-2 in a phase I clinical trial for the treatment of patients with prostate cancer (Voutsas, et al. 2016). Pre-existence of reactivity to 2 PSA-derived epitopes at high frequencies was detected and a further enhancement was observed after vaccination. However, while pre-existing immunity towards the HLA-A24 restricted epitope correlated with longer PFS, high pre-existing and vaccine-induced immunity towards the HLA-A2 restricted epitope showed a trend towards a shorter PFS.

In the context of pTVG-HP PAP DNA vaccine, two predictive parameters of the development of vaccine-induced PAP-specific effector responses have been described. Johnson *et al.* investigated baseline immune parameters that were predictive of the establishment of a PAP-specific immune response following vaccination with the pTVG-HP PAP DNA vaccine (Johnson, et al. 2017). Although T-cell responses towards HLA-restricted epitopes was not assessed, cytokine secretion following PAP stimulation was. Both responders and non-responders exhibited PAP-specific Th1 responses before vaccination, however non-responders displayed a higher PAP-specific secretion of IL-10 (p=0.09) which was secreted by both $CD4^+$ and $CD8^+$ T-cells. It therefore appears that pre-existing regulatory-type antigen-specific T-cell immunity is a negative predictive parameter of responsiveness to a PAP DNA vaccine. These results suggest that vaccination should be combined with anti-IL-10 treatment.

Another potential negative predictive marker for the development of PAP-specific immunity after vaccination is the presence PAP-specific $CD8^+$ regulatory T-cells expressing CTLA-4 and secreting IL-35 (Olson, et al. 2012). The presence of these cells was detected in 33% (7/21) of patients with prostate cancer before vaccination and it has been suggested that they inhibit the detection of PAP-specific effector responses after vaccination. Unlike IL-10 or TGF-β blockade, CTLA-4 and IL-35 blockade could reverse their suppressive phenotype. However, none of these studies correlated the presence of these negative predictive markers with OS.

Other than assessing the presence of antigen-specific T-cells prior to vaccination, Farsaci *et al*. have calculated a "peripheral immunoscore" that can predict the OS benefit of prostate cancer before receiving PROSTVAC vaccine, which is characterised by the presence of specific immune cell subsets prior vaccination, (Farsaci, et al. 2016). High frequencies of $PD-1^+$ and $CTLA-4^+$ $CD4^+$ T-cells and of differentiated $CD8^+$ T-cells and low frequencies of Treg cells and differentiated $CD4^+$ T-cells were shown to correlate with improved OS following combination of GVAX vaccine with Ippilimumab (Santegoets, et al. 2013). Moreover, high frequencies of MDSCs pre-treatment were associated with shorter OS (Santegoets, et al. 2014). These studies demonstrate the feasibility and utility of

determining pre-vaccine immune subsets that can predict the efficacy of a therapeutic prostate cancer vaccine and enable the selection of individuals that are most likely to benefit from it.

In conclusion, 37.5% of the patients with prostate cancer evaluated had circulating ILL-specific T-cells. Moreover, PBMCs from most patients were able to lyse the LNCaP prostatic cancer cell line. Although it was not significant, cytotoxicity towards LNCaP was lower in LNCaP PAP^{low} cells, suggesting that cytotoxicity was driven by recognition of PAP epitopes. However, this study was conducted on only 16 patients. Moreover, control groups (healthy individuals and individuals with benign disease) were too small to assess if the proportion of individuals with circulating ILL-specific CTLs is higher in patients. Further studies are required to assess not only the presence, but also the functionality of ILL-specific CTLs. PBMCs from additional patients would allow the cytotoxic function of ILL-CTLs to be assessed. Additionally, as suggested by studies mentioned above, it is essential to assess the regulatory function of PAP-specific T-cells.

Chapter 7: Discussion

Prostate cancer is a slow evolving disease, however, for patients who become resistant to androgen-deprivation therapy, there is currently no curative treatment. The five therapies currently FDA-approved for mCRPC only improve the OS of patients by few months, testifying of the need for developing new therapies.

Despite the breakthrough in immunotherapeutic treatments for cancer in the last decade, only one of the therapies for mCRPC is an immunotherapy: Provenge vaccine.

The limitations of Provenge vaccine include 1) its limited efficacy (improved OS of 4.1 months) 2) its autologous aspect, requiring PBMCs from each patient to be taken prior to reinfusion and 3) its cost, in order to isolate and cultivate CD54$^+$ DCs in the presence of the PAP/GM-CSF fusion protein per patient.

The current study focused on a vaccine more restrictive in terms of potential PAP-derived epitope CTLs that can be elicited, as it encompasses 42AA of the PAP protein, while Provenge covers the whole PAP protein (354AA). However, this vaccine would be non-invasive and its production easier and less costly.

The rationale behind the current study was therefore to develop a PAP-derived vaccine for the treatment of mCRPC.

This study demonstrated the ability of our vaccine to 1) elicit HLA-A2 restricted CTLs with secretory and cytolytic functions in a humanized mouse model, 2) break tolerance towards PAP in the C57Bl/6 mouse model by eliciting mPAP-specific CTLs with secretory and cytolytic functions and 3) the pre-existence of HLA-A2 restricted CTLs in PCa.

7.1. Optimisation of the vaccine strategy

The study began with the optimisation of the vaccine strategy. Two parameters of the vaccine were altered: the sequence of the PAP42mer peptide and the vehicle/adjuvant used.

The alteration of the PAP sequence was based on a previously characterised 15AA sequence, PAP 114-128 (MSAM), validated as an immunogenic HLA-DR1 peptide, containing the PAP115-123 HLA-A2 peptide (SAM) (Saif, et al. 2013). A mutation was introduced to increase the predicting binding affinity of SAM class-I epitope to HLA-A*02:01, according to the SYFPEITHI algorithm, which was confirmed by IFNγ ELISpot assays (data not shown). The 15mer was subsequently elongated to a 42mer sequence to include several class-I and class-II epitopes.

However, elongating the sequence to 42AA lead to the loss of SAM-specific IFNγ release and the preeminence of ILL class-I epitope (PAP135-143). Although this peptide was not affected by the mutation, its immunogenicity increased following immunisation with the mutated PAP42mer. Regarding the C57Bl/6 model, all class-I epitopes with an improved IFNγ response following

immunisation with mutated mPAP42mer peptides (2 or 3 mutations sequences), were altered by the mutation. In both models, the functional avidity towards immunogenic epitopes was improved by immunising with mutated PAP42mer peptides. Therefore, immunisation with a mutated sequence improved the CTL response towards WT epitopes following *in vitro* stimulation, whether these epitopes were altered or not by the mutation.

This phenomenon has not been studied well but was described by other groups as a mean to overcome tolerance towards self-antigens. In melanoma, DNA vaccines targeting two mouse antigens (gp100 and tyrosinase) demonstrated safety and immunogenicity in phase I clinical trials (Yuan, et al. 2009) (Wolchok, et al. 2007). Moreover, peptide analogues to a NY-ESO-1 epitope were more efficient than the wild-type peptide in expanding NY-ESO-1-specific CTLs from melanoma patients PBMCs (Chen, et al. 2000).

One phase I clinical trial assessed the capacity of a dendritic cell-based xenoantigen vaccine to break tolerance towards PAP (Fong, et al. 2001). All 21 PCa patients developed Th1 T-cell responses towards the murine PAP and 11 out of 21 towards the human PAP. Moreover, 6 of these patients had a stable disease.

These examples demonstrate the feasibility in human clinical trials of vaccines using modified antigens capable of breaking tolerance towards self-antigens.

The second parameter modified was the delivery system. Two peptide-based strategies and one DNA vaccine were tested. CpG adjuvant was able to induce PAP responses in the HHDII/DR1 model but could not break tolerance in the C57B/6 model. The ImmunoBody® DNA vaccine could elicit strong immune responses in the C57Bl/6 model but none in the HHDII/DR1 model. The CAF09 adjuvant, however, was able to induce strong PAP-specific immune responses in both mouse models.

It should be noted that the route of administration was different for each vaccine strategies, rendering the results obtained not directly comparable. The CpG vaccine was injected via intramuscular route while the CAF09 vaccine and the ImmunoBody® vaccine were administered as per recommended by collaborators providing these vaccines (intraperitoneal route for CAF09 and via a gold coated bullet fired with a gene gun for the ImmunoBody®).

The intraperitoneal route aims at targeting the mucosal lymphatic system and was shown to induce stronger splenic CD8$^+$ T-cell response in comparison to intramuscular or subcutaneous administration in the context of the CAF09 vaccine (Schimdt. et al, 2016). However, it does not translate to human subjects as the intramuscular route is generally used. It would have been of interest to compare the CpG and CAF09 vaccines using the same route of administration, both intramuscular and intraperitoneal for each.

7.2. Characterisation of the vaccine-induced immune response

Subsequent to the optimisation of the vaccination strategy, selected optimal vaccine strategies were further assessed. Beyond the IFNγ release response, the phenotype and function of vaccine-induced T-cells was evaluated.

Overall, the immune response observed in both mouse models was defined by a CD8-driven immune response characterised by 1) an increased functional avidity towards class-I epitopes, 2) induction of PD-1 expression on both CD4$^+$ and CD8$^+$ T-cells, 3) induction of effector memory but not central memory CD8$^+$ T-cells, 4) cytokine release, proliferation (Ki67) and degranulation (CD107a and granzyme B) by CD8$^+$ T-cells following 6hrs of class-I epitope(s) stimulation, 5) induction of an exhausted phenotype on CD8$^+$ T-cells (co-expression of PD-1, TIM-3 and LAG-3) following 6 days stimulation with class-I epitopes and 6) epitope and/or PAP-specific cytotoxicity.

As mentioned in section 1.3.4.1, the functional avidity relates to the overall clonal T-cell response towards its antigen and usually correlates with TCR affinity and avidity, both of which are crucial in the context of TAAs such as PAP. High avidity T-cells are highly cytotoxic (Dutoit, et al. 2001) (Pudney, et al. 2010) and T-cells with high TCR affinity are required for efficient tumour eradication as they allow efficient antigen cross-presentation and cytokines secretion by CTLs (Engels, et al. 2013). Moreover, PD-1 expression defines CTLs clonotypes of high avidity (Simon, et al. 2015). Altogether, these data suggest the highly cytotoxic potential of vaccine-elicited CTLs in this study.

The goal of vaccination is to produce a long-term immunological memory response which, in the case of cancer, can contribute to tumour eradication and prevent relapse. Our vaccine strategy generated effector memory CD8$^+$ T-cells. In fact, the CD44^{high}CD62L$^{neg/low}$ population could be effector and/or effector memory cells. Considering that the vaccine-induced immune response was found to be CD8 driven, it is not surprising that no memory CD4$^+$ T-cells response was elicited. However, the lack of central memory T-cells (CD44^{high}CD62L$^+$) could be deleterious as these cells are less differentiated than effector memory cells, persist longer *in vivo* and have a higher proliferative potential conferring a more efficient capacity to generate protective immunity (Wherry, et al. 2003). Seaman *et al.* suggested that in the case of vaccines inducing CTLs responses, central memory rather than effector memory T-cell responses were essential as effector memory T-cells were unable to expand efficiently *in vivo* following a secondary antigen exposure (Seaman, et al. 2004). Recently, the indispensable role of tissue resident memory T-cells in mediating anti-cancer immunity was illustrated. These long-lived memory T-cells, that do not recirculate once established in tissue, were shown to enhance the efficacy of a cancer vaccine in a preclinical model (Nizard, et al. 2017). Moreover, the study demonstrated a correlation between the number of tissue resident memory T-cells and the improved survival of patients in lung cancer, suggesting the

importance of designing vaccine strategies eliciting tissue resident memory T-cells. In the current study, the presence of these cells following vaccination was not assessed but would be of interest. The lack of central memory T-cells could be due to the timing. Indeed, Roberts *et al.* suggested that there is a progressive loss of effector memory T cell pools over time, and a subsequent establishment of a stable pool of central memory T cells (Roberts, et al. 2005). The presence of effector memory T-cells *versus* central memory T-cells could therefore be followed over time following vaccination (e.g. at months 1, 6, 12, and 20 after vaccination, as performed by Roberts *et al.*).

The functional capacity of vaccine-elicited CD8$^+$ T-cells following short stimulation (6 hours) with class-I epitopes was assessed and revealed the presence of ILL (HHDII/DR1 model) or ISI/SIW (C57Bl/6 model)-specific CTLs with secretory, proliferative and cytotoxic functions. A small proportion of secretory CTLs released IFNγ, TNFα and IL-2 while the rest released IFNγ and TNFα. The release of Granzyme B and perforin molecules constitutes the main cytolytic TCR-triggered pathway. However, only the release of Granzyme B was assessed in CTLs. Granzyme B has been shown to function in a perforin-independent manner, entering target cells by endocytosis. Granzyme B expression was vaccine-dependant but was not altered by ILL stimulation, while CD107a expression was vaccine and ILL stimulation-dependant. CD107a is a marker of degranulation and was shown to correlate with the loss of intracellular perforin (Betts, et al. 2003). The fact that CD107a expression did not correlate with Granzyme B release suggests that CD107a expression correlated with the release of perforin or of other cytotoxic molecules, such as other Granzymes molecules, although this was not assessed. It would also have been of interest to assess the death ligands pathways by measuring the expression of TRAIL and FAS-ligand on CTLs.

To confirm the cytolytic potential of vaccine-elicited CTLs, cytotoxicity assays were performed following 6 days of stimulation in the presence of class-I epitopes and IL-2. In both mouse models, the proportion of CD8$^+$ T-cells exhibiting an exhausted phenotype (co-expression of PD-1, Tim-3 and LAG-3) was increased in splenocytes from vaccinated mice. Class-I epitope specific lysis was confirmed, although it was performed on total splenocytes. Performing cytotoxicity assays on isolated CD8$^+$ T-cells would have been advantageous to confirm that CTLs were responsible for the lysis observed. Moreover, it would enable to remove potential immunosuppressive cells that could dampen the cytolytic activity of CTLs, such as Tregs, whose development and expansion is promoted by IL-2 (Nelson 2004).

In regard to PAP-specific cytotoxicity, results were disparate between mouse models.

In the HHDII/DR1 model, the hPAP-specific lysis could not be confirmed. No hPAP-specific cytotoxicity was observed when using total splenocytes with B16 cells or LNCaP cells. However, when performing the assay with isolated CD8+ T-cells, there was a slight increased cytotoxicity against LNCaP WT cells in comparison to LNCaP-PAP^{low} cells (still expressing 7% of hPAP mRNA) in the CpG and CAF09-vaccine groups. It should be noted that LNCaP cells express less hPAP protein than B16-HHDII-PAP+ cells (data not shown).

B16-HHDII -/+ hPAP provided a perfect model to assess the hPAP-specific cytotoxicity, however, results suggest that these cells might not present ILL-HLA-A2 complexes at their surface. Cytotoxicity assays were performed following 6 days of *in vitro* stimulation in the presence of the HLA-A2 restricted epitope ILL. Therefore, only ILL-specific CTLs were expected to be expanded, although it was not verified. As a result, potential CTLs specific for other epitopes, induced by vaccination with the hPAP42mer mutated peptide would not have been expanded. If B16-HHDII-PAP+ cells presented at their surface these epitopes, they would not have been recognized. To answer this question, the hPAP42mer mutated peptide should be used for *in vitro* stimulation of splenocytes.

Several factors might have induced a different processing of the hPAP protein in B16-HHDII-PAP+ cells. Firstly, the expression of PAP was induced via transfection of the gene encoding for the human PAP rather than naturally expressed as in LNCaP cells. Secondly, B16-HHDII cells express chimeric and not WT HLA-A2 molecules. The consequence of chimeric HHDII molecules expression by B16 cells could have been investigated by exogenous loading of ILL synthetic peptide onto these cells. Finally, murine cells probably have a different machinery for processing proteins. All these factors might have led to a different pool of epitopes being produced in B16-HHDII-PAP+ cells. Peptide-elution followed by mass-spectrometry analysis could have answered this question.

In the C57Bl/6 model, the CAF09-based vaccine induced mPAP-specific lysis of TRAMP-C1 and TRAMP-C2 cells. However, the cytotoxicity was only vaccine-specific against TRAMP-C2 cells. The *in vitro* expansion of epitope-specific CTLs might have induced ISI or SIW-specific CTLs from splenocytes from naive animals. However, it is unlikely considering that TRAMP-C2 cells naturally express 5 times more mPAP mRNA than TRAMP-C1, suggesting that mPAP protein expression is higher in TRAMP-C2 cells. If PAP-derived CTLs had been induced from naive animals, they would have lysed TRAMP-C2 cells more efficiently than TRAMP-C1 cells.

One major criticism that can be made against the methods used to assess the cytotoxicity towards PCa cell lines is that both techniques (Cr51 release assay and flow cytometry-based assay) constrained target cells being in suspension. However, all cell lines used: B16, LNCaP, TRAMP-C1 and TRAMP-C2 cells, are adherent cells. In the future, alternative cytotoxicity assays allowing the

use of adherent cells could be used. For example, the Xcelligence real time monitoring system measures the electrical impedance at the bottom of plates providing information on adherent cells including viability, cell numbers and morphology.

Optimal vaccination strategies should induce not only CD8 but also CD4 antigen-specific immune responses in order to optimise the magnitude and quality of the CD8^{+} immune response. In particular, CD4^{+} T-cells provide help signals to CD8^{+} T-cells via DCs during the priming phase (Borst, et al. 2018) and have a major role in generating CD8^{+} T-cells memory cells (Laidlaw, et al. 2016). Moreover, the help provided by CD4^{+} T-cells was shown to rescue exhausted CD8^{+} T-cells, allowing them to regain functional capacities such as cytokines secretion and proliferation, in the context of chronic viral infection (Aubert et al. 2011). Recently, CD4^{+} T-cell help was shown to improve the CTL response by increasing the expression of cytotoxic effector molecules and decreasing the expression of inhibitory receptors (Ahrends, et al. 2017).

The 15mer PAP-derived peptide previously described contained both class-I and a class-II restricted epitopes. In this study, the PAP42mer peptide was predicted to contain several class-I and class-II restricted epitopes in order to generate CD4 and CD8 PAP-specific T-cells.

However, in spite of CAF09 adjuvant being described as inducing CD4^{+} T-cell responses, especially Th1 and Th17 immune responses (Pedersen, et al. 2018), no cytokine release and no memory response was detected by CD4^{+} T-cells in this study.

The possibility that the CAF09 vaccine (in both models) and the ImmunoBody® DNA vaccine (in the C57Bl/6 model only) induced a CD4 helper immune response was suggested in section 3.3 due to higher IL-2 secretion by CD8^{+} T-cells when the stimulation was in the presence of 15mer epitopes, although it was not confirmed. The lack of helper immune response in our study might explain the absence of central memory CD8^{+} T-cells.

Circulating neoantigen-specific CD8^{+} T-cells expressing PD-1 in melanoma patients (Gros, et al. 2016) were proposed to be primed in the absence of help (Borst, et al. 2018) as CTLs primed with CD4 help downregulated PD-1 (Ahrends, et al. 2017). This theory provides another argument supporting the absence of a CD4 helper response in the current study as CD8^{+} T-cells from vaccinated animals upregulated PD-1.

Borst *et al.* also suggest that the inclusion of helper epitopes in therapeutic vaccines design does not ensure the delivery of the help signal as these epitopes require to reach specific DC subtypes (Borst, et al. 2018).

Studies suggested the use of CD27 and CD40 agonist antibodies in order to mimic help to provide co-stimulatory signals to CD8^{+} T-cells (Ahrends, et al. 2016; Vonderheide, et al. 2013), this could be considered to improve the current vaccine strategy.

The possibility that our vaccine induces antigen non-specific CD8 T-cells was mentioned in section 3.3. This theory was supported by the fact that others described antigen non-specific CD8^{+} T-cells with an effector/effector memory phenotype (CD44^{high}, CD62L^{low}) expressing PD-1, releasing Granzyme B and displaying cytotoxic functions without TCR engagement, that could proliferate following cytokines stimulation and could be induced by TLR agonists such as CpG and Poly I:C. In our model, CAF09 adjuvant could therefore induce these cells.

CD8^{+} T-cells with some of these features were describes both in preclinical models and in humans following high dose IL-2 therapy.

Tietze *et al.* described the antigen-independent expansion of memory CD8^{+} T-cells capable of antigen-specific tumour cell killing through TCRs with upregulation of PD-1 and CD25, as well as the presence of cytokine-induced memory CD8^{+} T-cells expressing NKG2D, Granzyme B, with an NKG2D-dependant anti-tumour effect. TCR-transgenic mice bearing non-antigen expressing tumours still benefited from the immunotherapy treatment. Their results demonstrated the innate and adaptive capacities of memory CD8^{+} T-cells depending on the stimuli (Tietze, et al. 2012).

Another study described CD8^{+} T-cells with a memory phenotype capable of both MHC-restricted and non-MHC-restricted cytotoxicity (Dhanji, et al. 2004).

These cells might have an advantage against immunosuppressive mechanisms such as antigen loss and down-regulation of MHC class-I molecules and it would therefore be of interest to perform further experiments to evaluate their presence in our model.

7.3. *In vivo* tumour studies

The next stage of the study was naturally to test the cytotoxic capacities of vaccine-induced PAP-specific CTLs *in vivo* against PAP-expressing tumours.

The B16-HHDII-PAP[+] cell line was used to establish a tumour model allowing to assess the anti-tumour efficacy of the hPAP42mer mutated vaccine (with CAF09 adjuvant). Although no PAP-specific lysis of B16-HHDII cells was observed *in vitro*, both CAF09 and ImmunoBody®-based vaccine induced higher percentage of cytotoxicity towards B16-HHDII cells than the CpG-based vaccine.

In a prophylactic setting, the CAF09 vaccine induced a slight delay in tumour growth and therefore prolonged survival, while the ImmunoBody® vaccine had no effect (data not shown). The immunophenotyping of splenocytes and TILs confirmed that the CAF09 vaccine induced ILL-specific CTLs, which mainly remained in the spleen with a small proportion migrating to the tumour site. TILs in vaccinated animals displayed a less exhausted phenotype which could explain the anti-tumour effect observed. However, the therapeutic experiment with or without an anti-PD-1 antibody did not show any anti-tumour effect. These results confirmed that ILL epitope might not

be presented at the surface of B16-HHDII-PAP$^+$ cells and therefore was not the correct model to use to assess the anti-tumour efficacy of the vaccine.

One point to consider is that hPAP expression was assessed in B16-HHDII-PAP$^+$ cells prior tumour implantation but hPAP expression was not assessed in tumours.

A more suitable tumour model would consist in establishing LNCaP/HHDII tumours into NOD/SCID immuno-deficient animals which would receive isolated T-cells from immunised HHDII/DR1 animals by adoptive transfer. However, this could not be performed due to the complexity, duration and cost of this type of experiment.

The anti-tumour efficacy of the mPAP42mer mutated vaccines (both CAF09 and ImmunoBody®-based vaccines) were evaluated against TRAMP-C1 tumours.

TRAMP-C2 cells were believed to be a more suitable cell line to establish a tumour model as these cells express 5 times more mPAP mRNA than TRAMP-C1 cells, however, they were not enough tumorigenic to generate tumours. We can hypothesize that the higher PAP expression renders these cells more immunogenic. This hypothesis could have been investigated by assessing the presence of ISI of SIW-specific CTLs in the animals, following tumour rejection, and by rechallenging with TRAMP-C1 tumour cells and looking for protection.

The results of these experiments showed that with the exception of one animal in the first therapeutic pilot study, no treated animals experienced tumour growth delay with either mPAP42mer mutated vaccines in prophylactic or therapeutic settings. The presence of PAP-specific CTLs and the phenotype of splenocytes and TILs were not assessed in these TRAMP-C1 studies, therefore, we cannot speculate on the presentation of ISI or SIW epitopes at the surface of TRAMP-C1 cells. However, an ongoing study demonstrated that similarly to the B16 tumour model, animals treated with the CAF09 vaccine display less exhausted TILs (data not shown).

These results demonstrate that the CAF09 vaccine can decrease the exhaustion of CTLs at the tumour site. Nevertheless, tumour cells employ numerous immunosuppressive mechanisms that can counteract an efficient vaccine strategy. For example, the presence of MDSCs within the tumour, as well as in other lymphoid compartments (spleen, tumour draining lymph node), in the blood and the bone marrow was observed in the ongoing TRAMP-C1 study (data not shown). This information provides one possible immunosuppressive mechanism adopted by TRAMP-C1 tumours that could be targeted to improve the anti-tumour efficacy of the CAF09 vaccine. Assessing the presence of other immuno-suppressive cells in the TME such as Tregs or TAMs would be of interest as well. Indeed, it was suggested that multiple vaccinations can induce Tregs, therefore dampening the anti-tumour immunity (LaCelle, et al. 2009).

One interesting observation worth noting is the fact that *in vitro*, the CAF09 vaccine induced CTLs exhibiting an exhausted phenotype, which had retained their cytotoxic functions as their presence correlated strongly with high cytotoxicity towards ILL-pulsed T2 cells. On the other hand, *in vivo*, animals treated with the CAF09 vaccine displayed a smaller proportion of exhausted CD8$^+$ TILs. However, in the prophylactic B16 study, the animal with the longest survival displayed exhausted CD8$^+$ TILs (high proportion of PD-1$^+$/Tim3$^+$ and small proportion of PD-1^{low}) and CD8$^+$ TILS with the highest percentage of IFNγ/TNFα secretion. These results suggest that *in vivo* as well, the exhausted phenotype correlates with functional CTLs. The meaning of co-expression of markers such as PD-1, Tim-3 and LAG-3 should be further studied. Other makers such as 4-1BB or CD38 could further distinguish between non-functional and functional CTLs. Indeed, one study reported that co-expression of LAG-3 and 4-1BB on CTLs characterised dysfunctional antigen-specific CD8$^+$ TILs deficient in IL-2 and TNFα production but retaining the expression of IFNγ, *in vitro* (Williams, et al. 2017). Another study described the presence of circulating PSA-specific CD8$^+$ T-cells in healthy individuals and in PCa patients, with cells from PCa patients expressing higher levels of Tim-3 and CD38, suggesting exhaustion, although their function was not assessed (Japp, et al. 2015).

The lack of CD4$^+$ T-cells helper response could play a major role in the weak anti-tumour effect of the CAF09 vaccine. As discussed above, CD4 helper T-cells are essential for an optimal CD8 response. In the case of antigen persistence, the generation of a CD8 memory response cannot be achieved and CD8$^+$ T-cells are ultimately eliminated (Bevan 2004). The ability of CD4$^+$ T-cells to promote the survival of CTLs in that case is unclear.

Accessing tumours samples from PCa patients is difficult, impeding the possibility to compare the phenotype of TILs induced in preclinical experiments from this study with the phenotype of TILs in PCa patients. However, although the data available in the literature is limited, some studies have assessed TILs from patients with PCa prior immunotherapy.

Fong *et al.* compared the tumour infiltrate of prostate tumours before and after Sipuleucel-T treatment and observed a 3-fold increase in infiltrating CD4$^+$ and CD8$^+$ T-cells at the tumour interface, which was not observed in the control group (Fong, et al. 2014). Most of infiltrating T-cells expressed PD-1 and Ki67, but these were the only surface markers assessed which are not sufficient to determine whether T-cells have an exhausted phenotype. No information was available on the correlation between increased expression of PD-1$^+$ CD8$^+$ TILs following Sipuleucel-T treatment and survival of patients.

Sfanos *et al.* demonstrated that CD8$^+$ TILs from PCa patients were oligo-clonal and PD-1$^+$, but did not assess their function (Sfanos et al. 2009).

In melanoma, PD-1/Tim-3/LAG-3-expressing CD8^{+} TILs were described as autologous tumour-reactive CTLs, and were capable of secreting IFNγ and lysing tumour cells *in vitro* following IL-2 expansion, suggesting that the dysfunction of "exhausted" T-cells can be reversed (Gros, et al. 2014). Another study assessing TILs from melanoma cancer patients determined that PD-1-expressing CD8^{+} T-cells were tumour specific, however, these cells exhibit impaired effector functions as shown by a reduced IFNγ secretion (Ahmadzadeh, et al. 2009). Expression of PD-1 on CD8^{+} TILs from melanoma determined clones of low functional avidity and *in vitro* PD-1 blockade could select high avidity T-cell clonotypes (Simon, et al. 2015).

TILs from gastric cancer patients co-expressing PD-1 and Tim-3 or Tim-3 alone also exhibited impaired functions characterised by a decreased secretion of IFNγ, TNF-α and IL-2 (Lu, et al. 2017).

These results indicate that antigen persistence in tumour induce PD-1-expression on tumour-specific T-cells. Moreover, 20% of TRAMP-C1 and TRAMP-C2 cells express a basal level of PD-L1 which increases to almost 100% in the presence of IFNγ as showed in figure 4.1. Even though it might be reversible *in vitro*, T-cells require blockade of the PD-1/PD-L1/L2 axis to be functional *in vivo*. The efficacy of the vaccine in the TRAMP-C1 model should therefore be considered in combination with an anti-PD-1 antibody.

7.4. Pre-existence of PAP-specific immunity in PCa patients

The assumption that a pre-existing immunity towards a tumour antigen can be enhanced by immunisation with a vaccine targeting that specific antigen seems evident.

Considering that CTLs specific for ILL9mer HLA-A*02:01-restricted epitope were previously described in HLA-A*02:01[+] healthy individuals and PCa patients (Machlenkin, et al. 2005) and that the hPAP42mer mutated peptide vaccine with CAF09 adjuvant can elicit functional ILL-specific CTLs in HHDII/DR1 mice, dextramer technology was used to assess the presence of ILL-specific CD8^{+} T-cells in PCa patients.

In a cohort of 16 patients, 37.5% had detectable circulating ILL-specific CTLs. 1 out of 5 individuals with benign tumours and none of the 3 healthy individuals had detectable ILL-specific CTLs. The number of healthy individuals and benign tumour bearing individuals was too low to conclude if patients with PCa do have an increased proportion of circulating ILL-specific CTLs in their blood. Nonetheless, our results demonstrate the existence of a pre-existing immunity towards ILL epitope in PCa patients, which might be boosted with a vaccine targeting PAP. It would be of interest to assess the proportion of ILL-specific CTLs in PCa patients prior to and after vaccination with Provenge or with the pTVG-HP DNA vaccine as these two vaccines target the PAP protein.

Preliminary results from ongoing experiments confirmed the specificity of vaccine-elicited CD8^{+} T-cells towards ILL epitope in the HHDII/DR1 model that can be detected by the same dextramer used

in human studies, further reinforcing the potential of the CAF09-based vaccine for patients with prostate cancer.

As discussed in section 6.3, the correlation between pre-existing immunity prior vaccination and improved OS or PFS post vaccination has not been demonstrated in a sufficient number of studies in order to conclude.

A study assessing a vaccine in myeloid malignancies compared the percentage of HLA-A2-restricted epitope tetramer[+] CTLs before and after vaccination (Qazilbash, et al. 2017). Out of 66 patients, 85% had pre-existing antigen-specific CTLs, independently of disease type and status. 53% of patients had at least a 2-fold increase in the percentage of tetramer[+] CTLs. However, there was no association between the percentage of antigen-specific CTL prior and after vaccination. Interestingly, they demonstrated that TCR avidity of epitope-specific CTLs increased following vaccination and that the increase was higher in clinical responders.

This study demonstrates that not only the percentage of epitope-specific CTLs is of importance but also the quality of these CTLs.

The study mentioned above by Japp *et al.* demonstrated that PSA-CTLs from PCa patients expressed higher levels of Tim-3 and CD38 that those from healthy individuals, suggesting that these cells were exhausted, and reinforces the requirement for estimating the quality of antigen-specific CTLs (Japp, et al. 2015).

It would therefore be of interest to further assess the phenotype and function of ILL-CTLs by evaluating their TCR avidity, their "exhausted" phenotype (PD-1, CTLA-4, Tim-3, …) , their cytokines secretory pattern (IFNγ, TNFα, IL-2) and the presence of ILL-specific Tregs (secretion of IL-10). Moreover, although, the capacity of ILL-CTLs to lyse ILL-pulsed T2 cells and LNCaP cells could not be performed in the current study, assessing the cytolytic capacity of ILL-CTLs cells is essential and should be performed in the future.

Hadaschik *et al.* found a correlation between the proportion of ILL-CTLs (characterised as ILL-specific IFNγ-secreting CTLs) and the stage of the disease, with a higher proportion of mCRPC patients displaying ILL-CTLs in comparison to low, intermediate or high risk PCa patients (Hadaschik, et al. 2012). In the current study, no correlation was found between the presence of circulating ILL-CTLs and the stage of the disease (low, intermediate or high risk) (data not shown), although only one patient out of 16 was known to have metastasis.

The study by Hadaschik *et al.* also determined that removal of Tregs in the culture highly increased the number of ILL-specific IFNγ-secreting T-cells.

Another study demonstrated that *in vitro* blockade of PD-L1 with a monoclonal antibody could enhance the frequency of activated antigen-specific CTLs and induced a switch from Th2 to Th1 cytokines (Grenga, et al. 2016). These two studies suggest that immuno-suppressive cells present in the blood can dampen the antigen-specific response to an antigen *in vitro*, therefore underestimating the full potential of antigen-specific CTLs. This observation reinforces the fact that cancer vaccines require to be combined with other immunotherapies than can counteract mechanisms of peripheral tolerance employed by the tumour.

The most important question to render this study more relevant to PCa patients is "is ILL epitope presented by HLA-A2 molecules at the surface of prostate tumours of HLA-A2$^+$ patients?" Indeed, ILL-presenting tumour cells could have been deleted during immunoediting, via antigen loss variant. Ostroumov *et al.* suggests that epitopes with high affinity for MHC class-I molecules have undergone high selection pressure during the phase of immunoediting (Ostroumov, et al. 2018). Moreover, CTLs with high TCR affinity towards their epitope probably generated escape variants by the tumour. It has been proposed that low to medium avidity polyclonal rather than high avidity monoclonal immune responses could provide better anti-tumour responses (Ostroumov, et al. 2018).

Besides boosting a pre-existent PAP-specific immune response, the current vaccine strategy could induce antigen spreading and generating immune responses against other PAP epitopes or against other prostate specific antigens such as PSA or PSMA.

7.5. Conclusion and future work

The development of new immunotherapies for the treatment of cancer constitutes a major challenge. Most preclinical studies are never translated into human studies. The few, most successful, tested in clinical trials, do not achieve the same level of anti-tumour response in cancer patients. This is partly due to the heterogeneity of cancer patients, whereas preclinical studies are performed on few mouse models with identical genetic background. Therefore, there is no possibility to predict the success of a preclinical treatment once translated in human clinical trials.

This study demonstrated the therapeutic potential of a newly developed vaccine targeting PAP antigen for the treatment of PCa.
This research lead to the development of an immunogenic vaccine strategy targeting 42AA of the PAP protein optimised by rendering its sequence more foreign and by selecting a strong adjuvant. Two mouse models allowed to demonstrate both the potential translation of this work for human HLA-A2$^+$ patients and the capacity of the PAP vaccine to break tolerance towards a self-antigen. In

both models, selected vaccine strategies induced strong PAP-specific CD8 responses. The CAF09 + peptide-based vaccine rather than the ImmunoBody® DNA vaccine was shown to induce highly cytotoxic antigen-specific CTLs *in vitro*, capable of lysing target cells in a PAP-specific manner.

Regarding the *in vivo* anti-tumour effect of the PAP vaccine, further studies are required to conclude. In the HHDII/DR1 model, the B16 tumour model was not adequate to assess the efficacy of the hPAP42mer mutated peptide + CAF09 adjuvant vaccine.

In the C57Bl/6 model, the mPAP42mer mutated vaccine did not induce sufficient anti-tumour immunity to break tolerance in the presence of a tumour. Results obtained strongly suggest the necessity of combining the vaccine with other immunomodulatory treatments such as immunotherapies or conventional therapies as these were shown to impact the immune system.

Although ICB have had a limited efficacy in PCa patients so far, they have shown some effects in subsets of patients as well as in combination with therapeutic vaccines. Until now, studies have concentrated mainly on anti CTLA-4 and anti PD-1/PD-L1 monoclonal antibodies, yet, there is an abundance of ICB antibodies with a therapeutic potential for PCa patients. For example, LAG-3 and TIM-3 molecules were co-expressed with PD-1 on T-cells in our model and could be targeted. The expression of VISTA molecule was not assessed but could a potential target as it was shown to be increased following Ipilimumab treatment in PCa patients (Gao, et al. 2017).

MDSCs might also be a suitable target to improve the vaccine efficacy as these cells were found in TRAMP-C1 tumours (data not shown), have been observed in the blood of PCa patients (Idorn, et al. 2014), with an increased proportion in patients with visceral metastases (Autio, et al. 2015) and their blockade was shown to sensitize PCa patients to ICB therapies (Lu, et al. 2017).

In order to render this work more relevant to the pathophysiology of PCa, an ongoing collaboration is assessing the anti-tumour efficacy of the mPAP42mer mutated peptide with the CAF09 adjuvant vaccine against spontaneous prostate tumours in TRAMP mice. These tumours grow spontaneously and slowly in the prostates of mice which will make these results highly informative.

Finally, the potential of the hPAP42mer mutated vaccine to elicit PAP-specific responses in PCa patients was reinforced by the fact that 37.5% of the 16 PCa patients tested had pre-existing circulating ILL-specific CTLs. However, the questions of whether or not ILL epitope is a naturally processed epitope specific for PAP and if ILL-specific CTLs can lyse prostate tumour cells remain unanswered. Our findings neither corroborate Machlenkin et al. findings that ILL-CTLs could lyse LNCaP cells (Machlenkin, et al. 2005) nor contradict Olson et al. observations that ILL-CTLs from prostate cancer patients could not lyse prostate cancer cells (Olson, et al. 2015). Further studies are therefore required to conclude.

References

Abel, A.M., Yang, C., Thakar, M.S. and Malarkannan, S., 2018. Natural Killer Cells: Development, Maturation, and Clinical Utilization. *Frontiers in Immunology,* 9, 1869.

Abiko, K., Matsumura, N., Hamanishi, J., Horikawa, N., Murakami, R., Yamaguchi, K., Yoshioka, Y., Baba, T., Konishi, I. and Mandai, M., 2015. IFN-gamma from lymphocytes induces PD-L1 expression and promotes progression of ovarian cancer. *British Journal of Cancer,* 112 (9), 1501-1509.

Adler, H.L., McCurdy, M.A., Kattan, M.W., Timme, T.L., Scardino, P.T. and Thompson, T.C., 1999. Elevated levels of circulating interleukin-6 and transforming growth factor-beta1 in patients with metastatic prostatic carcinoma. *The Journal of Urology,* 161 (1), 182-187.

Agaugue, S., Carosella, E.D. and Rouas-Freiss, N., 2011. Role of HLA-G in tumor escape through expansion of myeloid-derived suppressor cells and cytokinic balance in favor of Th2 versus Th1/Th17. *Blood,* 117 (26), 7021-7031.

Aguilar, L.K., Teh, B., Mai, W., Caillouet, J., Ayala, G., Aguilar-Cordova, E. and Butler, E., 2006. Five year follow up of a phase II study of cytotoxic immunotherapy combined with radiation in newly diagnosed prostate cancer. *Jco,* 24 (18), 4635-4635.

Ahmadzadeh, M., Johnson, L.A., Heemskerk, B., Wunderlich, J.R., Dudley, M.E., White, D.E. and Rosenberg, S.A., 2009. Tumor antigen-specific CD8 T cells infiltrating the tumor express high levels of PD-1 and are functionally impaired. *Blood,* 114 (8), 1537-1544.

Ahmann, F.R., and Schifman, R.B., 1987. Prospective comparison between serum monoclonal prostate specific antigen and acid phosphatase measurements in metastatic prostatic cancer. *The Journal of Urology,* 137 (3), 431-434.

Ahrends, T., Babala, N., Xiao, Y., Yagita, H., van Eenennaam, H. and Borst, J., 2016. CD27 Agonism Plus PD-1 Blockade Recapitulates CD4+ T-cell Help in Therapeutic Anticancer Vaccination. *Cancer Research,* 76 (10), 2921-2931.

Ahrends, T., Spanjaard, A., Pilzecker, B., Babala, N., Bovens, A., Xiao, Y., Jacobs, H. and Borst, J., 2017. CD4(+) T Cell Help Confers a Cytotoxic T Cell Effector Program Including Coinhibitory Receptor Downregulation and Increased Tissue Invasiveness. *Immunity,* 47 (5), 848-861.e5.

Albini, A., Bruno, A., Noonan, D.M. and Mortara, L., 2018. Contribution to Tumor Angiogenesis From Innate Immune Cells Within the Tumor Microenvironment: Implications for Immunotherapy. *Frontiers in Immunology,* 9, 527.

Ammirante, M., Luo, J.L., Grivennikov, S., Nedospasov, S. and Karin, M., 2010. B-cell-derived lymphotoxin promotes castration-resistant prostate cancer. *Nature,* 464 (7286), 302-305.

Anderson, K.S., Alexander, J., Wei, M. and Cresswell, P., 1993. Intracellular transport of class I MHC molecules in antigen processing mutant cell lines. *Journal of Immunology (Baltimore, Md.: 1950),* 151 (7), 3407-3419.

Antonarakis, E.S., Kibel, A.S., Yu, E.Y., Karsh, L.I., Elfiky, A., Shore, N.D., Vogelzang, N.J., Corman, J.M., Millard, F.E., Maher, J.C., Chang, N.N., DeVries, T., Sheikh, N.A., Drake, C.G. and STAND Investigators, 2017. Sequencing of Sipuleucel-T and Androgen Deprivation Therapy in Men with Hormone-Sensitive Biochemically Recurrent Prostate Cancer: A Phase II Randomized Trial. *Clinical*

Cancer Research: An Official Journal of the American Association for Cancer Research, 23 (10), 2451-2459.

Antonarakis, E.S., Small, E.J., Petrylak, D.P., AUID, Q.D., Kibel, A.S., Chang, N.N., Dearstyne, E., Harmon, M., Campogan, D., Haynes, H., Vu, T., Sheikh, N.A. and Drake, C.G., *Antigen-Specific CD8 Lytic Phenotype Induced by Sipuleucel-T in Hormone-Sensitive or Castration-Resistant Prostate Cancer and Association with Overall Survival.*

Antonarakis, E.S., Kibel, A.S., Adams, G., Karsh, L.I., Elfiky, A., Shore, N.D., Vogelzang, N.J., Corman, J.M., Tyler, R.C., McCoy, C., Wang, Y., Sheikh, N.A. and Drake, C.G., 2013. A randomized phase II study evaluating the optimal sequencing of sipuleucel-T and androgen deprivation therapy (ADT) in biochemically recurrent prostate cancer (BRPC): Immune results. *Jco,* 31 (15), 5016-5016.

Arstila, T.P., Casrouge, A., Baron, V., Even, J., Kanellopoulos, J. and Kourilsky, P., 1999. A direct estimate of the human alphabeta T cell receptor diversity. *Science (New York, N.Y.),* 286 (5441), 958-961.

Aubert, R.D., Kamphorst, A.O., Sarkar, S., Vezys, V., Ha, S.J., Barber, D.L., Ye, L., Sharpe, A.H., Freeman, G.J. and Ahmed, R., 2011. Antigen-specific CD4 T-cell help rescues exhausted CD8 T cells during chronic viral infection. *Proceedings of the National Academy of Sciences of the United States of America,* 108 (52), 21182-21187.

Autio, K.A., Wong, P., Rabinowitz, A., Yuan, J., Slavin, L.M., Brennan, R., DerSarkissian, M., Mu, Z., Scher, H.I. and Lesokhin, A.M., 2015. Presence of myeloid-derived suppressor cells (MDSC) in patients with metastatic castration-sensitive and castration-resistant prostate cancer. *Jco,* 33 (7), 222-222.

Bahl, A., Oudard, S., Tombal, B., Ozguroglu, M., Hansen, S., Kocak, I., Gravis, G., Devin, J., Shen, L., de Bono, J.S., Sartor, A.O. and TROPIC Investigators, 2013. Impact of cabazitaxel on 2-year survival and palliation of tumour-related pain in men with metastatic castration-resistant prostate cancer treated in the TROPIC trial. *Annals of Oncology: Official Journal of the European Society for Medical Oncology,* 24 (9), 2402-2408.

Baitsch, L., Baumgaertner, P., Devevre, E., Raghav, S.K., Legat, A., Barba, L., Wieckowski, S., Bouzourene, H., Deplancke, B., Romero, P., Rufer, N. and Speiser, D.E., 2011. Exhaustion of tumor-specific CD8 (+) T cells in metastases from melanoma patients. *The Journal of Clinical Investigation,* 121 (6), 2350-2360.

Balkwill, F., 2009. Tumour necrosis factor and cancer. *Nature Reviews.Cancer,* 9 (5), 361-371.

Becker, J.T., Olson, B.M., Johnson, L.E., Davies, J.G., Dunphy, E.J. and McNeel, D.G., 2010. DNA vaccine encoding prostatic acid phosphatase (PAP) elicits long-term T-cell responses in patients with recurrent prostate cancer. *Journal of Immunotherapy (Hagerstown, Md.: 1997),* 33 (6), 639-647.

Beer, T.M., Kwon, E.D., Drake, C.G., Fizazi, K., Logothetis, C., Gravis, G., Ganju, V., Polikoff, J., Saad, F., Humanski, P., Piulats, J.M., Gonzalez Mella, P., Ng, S.S., Jaeger, D., Parnis, F.X., Franke, F.A., Puente, J., Carvajal, R., Sengelov, L., McHenry, M.B., Varma, A., van den Eertwegh, A.J. and Gerritsen, W., 2017. Randomized, Double-Blind, Phase III Trial of Ipilimumab Versus Placebo in Asymptomatic or Minimally Symptomatic Patients With Metastatic Chemotherapy-Naive Castration-Resistant Prostate Cancer. *Journal of Clinical Oncology: Official Journal of the American Society of Clinical Oncology,* 35 (1), 40-47.

Bennett, S.R., Carbone, F.R., Karamalis, F., Flavell, R.A., Miller, J.F. and Heath, W.R., 1998. Help for cytotoxic-T-cell responses is mediated by CD40 signalling. *Nature,* 393 (6684), 478-480.

Berthold, D.R., Pond, G.R., Soban, F., de Wit, R., Eisenberger, M. and Tannock, I.F., 2008. Docetaxel plus prednisone or mitoxantrone plus prednisone for advanced prostate cancer: updated survival in the TAX 327 study. *Journal of Clinical Oncology: Official Journal of the American Society of Clinical Oncology,* 26 (2), 242-245.

Bertrand, F., Montfort, A., Marcheteau, E., Imbert, C., Gilhodes, J., Filleron, T., Rochaix, P., Andrieu-Abadie, N., Levade, T., Meyer, N., Colacios, C. and Segui, B., 2017. TNFalpha blockade overcomes resistance to anti-PD-1 in experimental melanoma. *Nature Communications,* 8 (1), 2256-017-02358-7.

Betts, M.R., Brenchley, J.M., Price, D.A., De Rosa, S.C., Douek, D.C., Roederer, M. and Koup, R.A., 2003. Sensitive and viable identification of antigen-specific CD8+ T cells by a flow cytometric assay for degranulation. *Journal of Immunological Methods,* 281 (1-2), 65-78.

Bevan, M.J., 2004. Helping the CD8 (+) T-cell response. *Nature Reviews.Immunology,* 4 (8), 595-602.

Bezu, L., Kepp, O., Cerrato, G., Pol, J., Fucikova, J., Spisek, R., Zitvogel, L., Kroemer, G. and Galluzzi, L., 2018. Trial watch: Peptide-based vaccines in anticancer therapy. *Oncoimmunology,* 7 (12), e1511506.

Bhat, P., Leggatt, G., Waterhouse, N. and Frazer, I.H., 2017. Interferon-gamma derived from cytotoxic lymphocytes directly enhances their motility and cytotoxicity. *Cell Death & Disease,* 8 (6), e2836.

Bijker, M.S., van den Eeden, S.J., Franken, K.L., Melief, C.J., Offringa, R. and van der Burg, S.H., 2007. CD8+ CTL priming by exact peptide epitopes in incomplete Freund's adjuvant induces a vanishing CTL response, whereas long peptides induce sustained CTL reactivity. *Journal of Immunology (Baltimore, Md.: 1950),* 179 (8), 5033-5040.

Bishop, J.L., Sio, A., Angeles, A., Roberts, M.E., Azad, A.A., Chi, K.N. and Zoubeidi, A., 2015. PD-L1 is highly expressed in Enzalutamide resistant prostate cancer. *Oncotarget,* 6 (1), 234-242.

Bjorklund, M., Beretta, A., Coutinho, A. and Gullberg, M., 1986. Effector functions and specificities of normal murine T cells stimulated by syngeneic blasts. *European Journal of Immunology,* 16 (5), 471-477.

Blohmke, C.J., Hill, J., Darton, T.C., Carvalho-Burger, M., Eustace, A., Jones, C., Schreiber, F., Goodier, M.R., Dougan, G., Nakaya, H.I. and Pollard, A.J., 2017. Induction of Cell Cycle and NK Cell Responses by Live-Attenuated Oral Vaccines against Typhoid Fever. *Frontiers in Immunology,* 8, 1276.

Blum, J.S., Wearsch, P.A. and Cresswell, P., 2013. Pathways of antigen processing. *Annual Review of Immunology,* 31, 443-473.

Borley, N., and Feneley, M.R., 2009. Prostate cancer: diagnosis and staging. *Asian Journal of Andrology,* 11 (1), 74-80.

Borst, J., Ahrends, T., Babala, N., Melief, C.J.M. and Kastenmuller, W., 2018. CD4 (+) T cell help in cancer immunology and immunotherapy. *Nature Reviews.Immunology,* 18 (10), 635-647.

Boudadi, K., Suzman, D.L., Luber, B., Wang, H., Silberstein, J., Sullivan, R., Dowling, D., Harb, R., Nirschl, T., Dittamore, R.V., Carducci, M.A., Eisenberger, M.A., Haffner, M., Meeker, A., Eshleman,

J.R., Luo, J., Drake, C.G. and Antonarakis, E.S., 2017. Phase 2 biomarker-driven study of ipilimumab plus nivolumab (Ipi/Nivo) for ARV7-positive metastatic castrate-resistant prostate cancer (mCRPC). *Jco,* 35 (15), 5035-5035.

Brandt, A., Sundquist, J. and Hemminki, K., 2012. Risk for incident and fatal prostate cancer in men with a family history of any incident and fatal cancer. *Annals of Oncology: Official Journal of the European Society for Medical Oncology,* 23 (1), 251-256.

Braumuller, H., Wieder, T., Brenner, E., Assmann, S., Hahn, M., Alkhaled, M., Schilbach, K., Essmann, F., Kneilling, M., Griessinger, C., Ranta, F., Ullrich, S., Mocikat, R., Braungart, K., Mehra, T., Fehrenbacher, B., Berdel, J., Niessner, H., Meier, F., van den Broek, M., Haring, H.U., Handgretinger, R., Quintanilla-Martinez, L., Fend, F., Pesic, M., Bauer, J., Zender, L., Schaller, M., Schulze-Osthoff, K. and Rocken, M., 2013. T-helper-1-cell cytokines drive cancer into senescence. *Nature,* 494 (7437), 361-365.

Brentville, V.A., Metheringham, R.L., Gunn, B. and Durrant, L.G., 2012. High avidity cytotoxic T lymphocytes can be selected into the memory pool but they are exquisitely sensitive to functional impairment. *PloS One,* 7 (7), e41112.

Budhwani M, Mazzieri R, Dolcetti R. Plasticity of Type I Interferon-Mediated Responses in Cancer Therapy: From Anti-tumor Immunity to Resistance. Front Oncol. 2018 Aug 21;8:322.

Burnet, F.M., 1970. The concept of immunological surveillance. *Progress in Experimental Tumor Research,* 13, 1-27.

Buyyounouski, M.K., Choyke, P.L., McKenney, J.K., Sartor, O., Sandler, H.M., Amin, M.B., Kattan, M.W. and Lin, D.W., 2017. Prostate cancer - major changes in the American Joint Committee on Cancer eighth edition cancer staging manual. *CA: A Cancer Journal for Clinicians,* 67 (3), 245-253.

Calcinotto, A., Spataro, C., Zagato, E., Di Mitri, D., Gil, V., Crespo, M., De Bernardis, G., Losa, M., Mirenda, M., Pasquini, E., Rinaldi, A., Sumanasuriya, S., Lambros, M.B., Neeb, A., Luciano, R., Bravi, C.A., Nava-Rodrigues, D., Dolling, D., Prayer-Galetti, T., Ferreira, A., Briganti, A., Esposito, A., Barry, S., Yuan, W., Sharp, A., de Bono, J. and Alimonti, A., 2018. IL-23 secreted by myeloid cells drives castration-resistant prostate cancer. *Nature,* 559 (7714), 363-369.

Carlsson, B., Forsberg, O., Bengtsson, M., Totterman, T.H. and Essand, M., 2007. Characterization of human prostate and breast cancer cell lines for experimental T cell-based immunotherapy. *The Prostate,* 67 (4), 389-395.

Caza, T., and Landas, S., 2015. Functional and Phenotypic Plasticity of CD4 (+) T Cell Subsets. *BioMed Research International,* 2015, 521957.

Chaplin, D.D., 2010. Overview of the immune response. *The Journal of Allergy and Clinical Immunology,* 125 (2 Suppl 2), S3-23.

Chen, D.S., and Mellman, I., 2017. Elements of cancer immunity and the cancer-immune set point. *Nature,* 541 (7637), 321-330.

Chen, J.L., Dunbar, P.R., Gileadi, U., Jager, E., Gnjatic, S., Nagata, Y., Stockert, E., Panicali, D.L., Chen, Y.T., Knuth, A., Old, L.J. and Cerundolo, V., 2000. Identification of NY-ESO-1 peptide analogues capable of improved stimulation of tumor-reactive CTL. *Journal of Immunology (Baltimore, Md.: 1950),* 165 (2), 948-955.

Chen, L., and Flies, D.B., 2013. Molecular mechanisms of T cell co-stimulation and co-inhibition. *Nature Reviews.Immunology,* 13 (4), 227-242.

Chen, N., and Zhou, Q., 2016. The evolving Gleason grading system. *Chinese Journal of Cancer Research = Chung-Kuo Yen Cheng Yen Chiu,* 28 (1), 58-64.

Cheon H, Borden EC, Stark GR. Interferons and their stimulated genes in the tumor microenvironment. Semin Oncol. (2014) 41:156–73. 10.1053/j.seminoncol.2014.02.002

Comiskey, M.C., Dallos, M.C. and Drake, C.G., 2018. Immunotherapy in Prostate Cancer: Teaching an Old Dog New Tricks. *Current Oncology Reports,* 20 (9), 75-018-0712-z.

Condotta, S.A., and Richer, M.J., 2017. The immune battlefield: The impact of inflammatory cytokines on CD8+ T-cell immunity. *PLoS Pathogens,* 13 (10), e1006618.

Conry, R.M., Westbrook, B., McKee, S. and Norwood, T.G., 2018. Talimogene laherparepvec: First in class oncolytic virotherapy. *Human Vaccines & Immunotherapeutics,* 14 (4), 839-846.

D'Amico, A.V., Whittington, R., Malkowicz, S.B., Fondurulia, J., Chen, M.H., Kaplan, I., Beard, C.J., Tomaszewski, J.E., Renshaw, A.A., Wein, A. and Coleman, C.N., 1999. Pretreatment nomogram for prostate-specific antigen recurrence after radical prostatectomy or external-beam radiation therapy for clinically localized prostate cancer. *Journal of Clinical Oncology: Official Journal of the American Society of Clinical Oncology,* 17 (1), 168-172.

Dapito DH, Mencin A, Gwak GY, Pradere JP, Jang MK, Mederacke I, Caviglia JM, Khiabanian H, Adeyemi A, Bataller R, Lefkowitch JH, Bower M, Friedman R, Sartor RB, Rabadan R, Schwabe RF. Promotion of hepatocellular carcinoma by the intestinal microbiota and TLR4. Cancer Cell. 2012;21:504–516.

Darboe, A., Danso, E., Clarke, E., Umesi, A., Touray, E., Wegmuller, R., Moore, S.E., Riley, E.M. and Goodier, M.R., 2017. Enhancement of cytokine-driven NK cell IFN-gamma production after vaccination of HCMV infected Africans. *European Journal of Immunology,* 47 (6), 1040-1050.

Davidsson, S., Ohlson, A.L., Andersson, S.O., Fall, K., Meisner, A., Fiorentino, M., Andren, O. and Rider, J.R., 2013. CD4 helper T cells, CD8 cytotoxic T cells, and FOXP3 (+) regulatory T cells with respect to lethal prostate cancer. *Modern Pathology: An Official Journal of the United States and Canadian Academy of Pathology, Inc,* 26 (3), 448-455.

De Angelis, R., Sant, M., Coleman, M.P., Francisci, S., Baili, P., Pierannunzio, D., Trama, A., Visser, O., Brenner, H., Ardanaz, E., Bielska-Lasota, M., Engholm, G., Nennecke, A., Siesling, S., Berrino, F., Capocaccia, R. and EUROCARE-5 Working Group, 2014. Cancer survival in Europe 1999-2007 by country and age: results of EUROCARE--5-a population-based study. *The Lancet.Oncology,* 15 (1), 23-34.

De Bono, J.S., Goh, J.C.H., Ojamaa, K., Piulats Rodriguez, J.M., Drake, C.G., Hoimes, C.J., Wu, H., Poehlein, C.H. and Antonarakis, E.S., 2018. KEYNOTE-199: Pembrolizumab (pembro) for docetaxel-refractory metastatic castration-resistant prostate cancer (mCRPC). *Jco,* 36 (15), 5007-5007.

de Jong, E.C., Smits, H.H. and Kapsenberg, M.L., 2005. Dendritic cell-mediated T cell polarization. *Springer Seminars in Immunopathology,* 26 (3), 289-307.

De Maeseneer, D.J., Van Praet, C., Lumen, N. and Rottey, S., 2015. Battling resistance mechanisms in antihormonal prostate cancer treatment: Novel agents and combinations. *Urologic Oncology,* 33 (7), 310-321.

Derre, L., Corvaisier, M., Charreau, B., Moreau, A., Godefroy, E., Moreau-Aubry, A., Jotereau, F. and Gervois, N., 2006. Expression and release of HLA-E by melanoma cells and melanocytes: potential impact on the response of cytotoxic effector cells. *Journal of Immunology (Baltimore, Md.: 1950),* 177 (5), 3100-3107.

Descotes, J.L., 2019. Diagnosis of prostate cancer. *Asian Journal of Urology,* 6 (2), 129-136.

Dhanji, S., and Teh, H.S., 2003. IL-2-activated CD8+CD44high cells express both adaptive and innate immune system receptors and demonstrate specificity for syngeneic tumor cells. *Journal of Immunology (Baltimore, Md.: 1950),* 171 (7), 3442-3450.

Dhanji, S., Teh, S.J., Oble, D., Priatel, J.J. and Teh, H.S., 2004. Self-reactive memory-phenotype CD8 T cells exhibit both MHC-restricted and non-MHC-restricted cytotoxicity: a role for the T-cell receptor and natural killer cell receptors. *Blood,* 104 (7), 2116-2123.

Dokka, S., Shi, X., Leonard, S., Wang, L., Castranova, V. and Rojanasakul, Y., 2001. Interleukin-10-mediated inhibition of free radical generation in macrophages. *American Journal of Physiology.Lung Cellular and Molecular Physiology,* 280 (6), L1196-202.

Dolton, G., Lissina, A., Skowera, A., Ladell, K., Tungatt, K., Jones, E., Kronenberg-Versteeg, D., Akpovwa, H., Pentier, J.M., Holland, C.J., Godkin, A.J., Cole, D.K., Neller, M.A., Miles, J.J., Price, D.A., Peakman, M. and Sewell, A.K., 2014. Comparison of peptide-major histocompatibility complex tetramers and dextramers for the identification of antigen-specific T cells. *Clinical and Experimental Immunology,* 177 (1), 47-63.

Dong, H., Strome, S.E., Salomao, D.R., Tamura, H., Hirano, F., Flies, D.B., Roche, P.C., Lu, J., Zhu, G., Tamada, K., Lennon, V.A., Celis, E. and Chen, L., 2002. Tumor-associated B7-H1 promotes T-cell apoptosis: a potential mechanism of immune evasion. *Nature Medicine,* 8 (8), 793-800.

Dulos, G.J., and Bagchus, W.M., 2001. Androgens indirectly accelerate thymocyte apoptosis. *International Immunopharmacology,* 1 (2), 321-328.

Dunn, G.P., Bruce, A.T., Ikeda, H., Old, L.J. and Schreiber, R.D., 2002. Cancer immunoediting: from immunosurveillance to tumor escape. *Nature Immunology,* 3 (11), 991-998.

Durrant, L.G., Pudney, V., Spendlove, I. and Metheringham, R.L., 2010. Vaccines as early therapeutic interventions for cancer therapy: neutralising the immunosuppressive tumour environment and increasing T cell avidity may lead to improved responses. *Expert Opinion on Biological Therapy,* 10 (5), 735-748.

Dutoit, V., Rubio-Godoy, V., Dietrich, P.Y., Quiqueres, A.L., Schnuriger, V., Rimoldi, D., Lienard, D., Speiser, D., Guillaume, P., Batard, P., Cerottini, J.C., Romero, P. and Valmori, D., 2001. Heterogeneous T-cell response to MAGE-A10(254-262): high avidity-specific cytolytic T lymphocytes show superior antitumor activity. *Cancer Research,* 61 (15), 5850-5856.

Ebelt, K., Babaryka, G., Figel, A.M., Pohla, H., Buchner, A., Stief, C.G., Eisenmenger, W., Kirchner, T., Schendel, D.J. and Noessner, E., 2008. Dominance of CD4+ lymphocytic infiltrates with disturbed effector cell characteristics in the tumor microenvironment of prostate carcinoma. *The Prostate,* 68 (1), 1-10.

Ehl, S., Hombach, J., Aichele, P., Hengartner, H. and Zinkernagel, R.M., 1997. Bystander activation of cytotoxic T cells: studies on the mechanism and evaluation of *in vivo* significance in a transgenic mouse model. *The Journal of Experimental Medicine,* 185 (7), 1241-1251.

Ehrlich P. Ueber den jetzigen Stand der Karzinomforschung. *Ned Tijdschr Geneeskd.* 1909;5:273–290.

Eickhoff, S., Brewitz, A., Gerner, M.Y., Klauschen, F., Komander, K., Hemmi, H., Garbi, N., Kaisho, T., Germain, R.N. and Kastenmuller, W., 2015. Robust Anti-viral Immunity Requires Multiple Distinct T Cell-Dendritic Cell Interactions. *Cell,* 162 (6), 1322-1337.

Ellis, J.M., Henson, V., Slack, R., Ng, J., Hartzman, R.J. and Katovich Hurley, C., 2000. Frequencies of HLA-A2 alleles in five U.S. population groups. Predominance Of A*02011 and identification of HLA-A*0231. *Human Immunology,* 61 (3), 334-340.

Engels, B., Engelhard, V.H., Sidney, J., Sette, A., Binder, D.C., Liu, R.B., Kranz, D.M., Meredith, S.C., Rowley, D.A. and Schreiber, H., 2013. Relapse or eradication of cancer is predicted by peptide-major histocompatibility complex affinity. *Cancer Cell,* 23 (4), 516-526.

Etzioni, R., Gulati, R., Falcon, S. and Penson, D.F., 2008. Impact of PSA screening on the incidence of advanced stage prostate cancer in the United States: a surveillance modeling approach. *Medical Decision Making: An International Journal of the Society for Medical Decision Making,* 28 (3), 323-331.

Fakhrejahani, F., Madan, R.A., Dahut, W.L., Karzai, F., Cordes, L.M., Schlom, J. and Gulley, J.L., 2017. Avelumab in metastatic castration-resistant prostate cancer (mCRPC). *Jco,* 35 (6), 159-159.

Farhood, B., Najafi, M. and Mortezaee, K., 2019. CD8 (+) cytotoxic T lymphocytes in cancer immunotherapy: A review. *Journal of Cellular Physiology,* 234 (6), 8509-8521.

Farsaci, B., Donahue, R.N., Grenga, I., Lepone, L.M., Kim, P.S., Dempsey, B., Siebert, J.C., Ibrahim, N.K., Madan, R.A., Heery, C.R., Gulley, J.L. and Schlom, J., 2016. Analyses of Pretherapy Peripheral Immunoscore and Response to Vaccine Therapy. *Cancer Immunology Research,* 4 (9), 755-765.

Favier, B., Lemaoult, J., Lesport, E. and Carosella, E.D., 2010. ILT2/HLA-G interaction impairs NK-cell functions through the inhibition of the late but not the early events of the NK-cell activating synapse. *FASEB Journal: Official Publication of the Federation of American Societies for Experimental Biology,* 24 (3), 689-699.

Feau, S., Garcia, Z., Arens, R., Yagita, H., Borst, J. and Schoenberger, S.P., 2012. The CD4 (+) T-cell help signal is transmitted from APC to CD8 (+) T-cells via CD27-CD70 interactions. *Nature Communications,* 3, 948.

Fehniger, T.A., Cooper, M.A., Nuovo, G.J., Cella, M., Facchetti, F., Colonna, M. and Caligiuri, M.A., 2003. CD56bright natural killer cells are present in human lymph nodes and are activated by T cell-derived IL-2: a potential new link between adaptive and innate immunity. *Blood,* 101 (8), 3052-3057.

Ferlay, J., Soerjomataram, I., Dikshit, R., Eser, S., Mathers, C., Rebelo, M., Parkin, D.M., Forman, D. and Bray, F., 2015. Cancer incidence and mortality worldwide: sources, methods and major patterns in GLOBOCAN 2012. *International Journal of Cancer,* 136 (5), E359-86.

Fiorentino, D.F., Zlotnik, A., Mosmann, T.R., Howard, M. and O'Garra, A., 1991. IL-10 inhibits cytokine production by activated macrophages. *Journal of Immunology (Baltimore, Md.: 1950),* 147 (11), 3815-3822.

Fizazi, K., Scher, H.I., Molina, A., Logothetis, C.J., Chi, K.N., Jones, R.J., Staffurth, J.N., North, S., Vogelzang, N.J., Saad, F., Mainwaring, P., Harland, S., Goodman, O.B.,Jr, Sternberg, C.N., Li, J.H., Kheoh, T., Haqq, C.M., de Bono, J.S. and COU-AA-301 Investigators, 2012. Abiraterone acetate for

treatment of metastatic castration-resistant prostate cancer: final overall survival analysis of the COU-AA-301 randomised, double-blind, placebo-controlled phase 3 study. *The Lancet.Oncology,* 13 (10), 983-992.

Fong, L., Brockstedt, D., Benike, C., Breen, J.K., Strang, G., Ruegg, C.L. and Engleman, E.G., 2001. Dendritic cell-based xenoantigen vaccination for prostate cancer immunotherapy. *Journal of Immunology (Baltimore, Md.: 1950),* 167 (12), 7150-7156.

Fong, L., Carroll, P., Weinberg, V., Chan, S., Lewis, J., Corman, J., Amling, C.L., Stephenson, R.A., Simko, J., Sheikh, N.A., Sims, R.B., Frohlich, M.W. and Small, E.J., 2014. Activated lymphocyte recruitment into the tumor microenvironment following preoperative sipuleucel-T for localized prostate cancer. *Journal of the National Cancer Institute,* 106 (11), 10.1093/jnci/dju268. Print 2014 Nov.

Foster, B.A., Gingrich, J.R., Kwon, E.D., Madias, C. and Greenberg, N.M., 1997. Characterization of prostatic epithelial cell lines derived from transgenic adenocarcinoma of the mouse prostate (TRAMP) model. *Cancer Research,* 57 (16), 3325-3330.

Fridman, W.H., Zitvogel, L., Sautes-Fridman, C. and Kroemer, G., 2017. The immune contexture in cancer prognosis and treatment. *Nature Reviews.Clinical Oncology,* 14 (12), 717-734.

Friedman, E.J., 2002. Immune modulation by ionizing radiation and its implications for cancer immunotherapy. *Current Pharmaceutical Design,* 8 (19), 1765-1780.

Gabrilovich, D.I., Chen, H.L., Girgis, K.R., Cunningham, H.T., Meny, G.M., Nadaf, S., Kavanaugh, D. and Carbone, D.P., 1996. Production of vascular endothelial growth factor by human tumors inhibits the functional maturation of dendritic cells. *Nature Medicine,* 2 (10), 1096-1103.

Galletti, G., Leach, B.I., Lam, L. and Tagawa, S.T., 2017. Mechanisms of resistance to systemic therapy in metastatic castration-resistant prostate cancer. *Cancer Treatment Reviews,* 57, 16-27.

Galluzzi, L., Vacchelli, E., Bravo-San Pedro, J.M., Buque, A., Senovilla, L., Baracco, E.E., Bloy, N., Castoldi, F., Abastado, J.P., Agostinis, P., Apte, R.N., Aranda, F., Ayyoub, M., Beckhove, P., Blay, J.Y., Bracci, L., Caignard, A., Castelli, C., Cavallo, F., Celis, E., Cerundolo, V., Clayton, A., Colombo, M.P., Coussens, L., Dhodapkar, M.V., Eggermont, A.M., Fearon, D.T., Fridman, W.H., Fucikova, J., Gabrilovich, D.I., Galon, J., Garg, A., Ghiringhelli, F., Giaccone, G., Gilboa, E., Gnjatic, S., Hoos, A., Hosmalin, A., Jager, D., Kalinski, P., Karre, K., Kepp, O., Kiessling, R., Kirkwood, J.M., Klein, E., Knuth, A., Lewis, C.E., Liblau, R., Lotze, M.T., Lugli, E., Mach, J.P., Mattei, F., Mavilio, D., Melero, I., Melief, C.J., Mittendorf, E.A., Moretta, L., Odunsi, A., Okada, H., Palucka, A.K., Peter, M.E., Pienta, K.J., Porgador, A., Prendergast, G.C., Rabinovich, G.A., Restifo, N.P., Rizvi, N., Sautes-Fridman, C., Schreiber, H., Seliger, B., Shiku, H., Silva-Santos, B., Smyth, M.J., Speiser, D.E., Spisek, R., Srivastava, P.K., Talmadge, J.E., Tartour, E., Van Der Burg, S.H., Van Den Eynde, B.J., Vile, R., Wagner, H., Weber, J.S., Whiteside, T.L., Wolchok, J.D., Zitvogel, L., Zou, W. and Kroemer, G., 2014. Classification of current anticancer immunotherapies. *Oncotarget,* 5 (24), 12472-12508.

Galon, J., Costes, A., Sanchez-Cabo, F., Kirilovsky, A., Mlecnik, B., Lagorce-Pages, C., Tosolini, M., Camus, M., Berger, A., Wind, P., Zinzindohoue, F., Bruneval, P., Cugnenc, P.H., Trajanoski, Z., Fridman, W.H. and Pages, F., 2006. Type, density, and location of immune cells within human colorectal tumors predict clinical outcome. *Science (New York, N.Y.),* 313 (5795), 1960-1964.

Gannon, P.O., Poisson, A.O., Delvoye, N., Lapointe, R., Mes-Masson, A.M. and Saad, F., 2009. Characterization of the intra-prostatic immune cell infiltration in androgen-deprived prostate cancer patients. *Journal of Immunological Methods,* 348 (1-2), 9-17.

Gao, J., Ward, J.F., Pettaway, C.A., Shi, L.Z., Subudhi, S.K., Vence, L.M., Zhao, H., Chen, J., Chen, H., Efstathiou, E., Troncoso, P., Allison, J.P., Logothetis, C.J., Wistuba, I.I., Sepulveda, M.A., Sun, J., Wargo, J., Blando, J. and Sharma, P., 2017. VISTA is an inhibitory immune checkpoint that is increased after ipilimumab therapy in patients with prostate cancer. *Nature Medicine,* 23 (5), 551-555.

Garcia, A.J., Ruscetti, M., Arenzana, T.L., Tran, L.M., Bianci-Frias, D., Sybert, E., Priceman, S.J., Wu, L., Nelson, P.S., Smale, S.T. and Wu, H., 2014. Pten null prostate epithelium promotes localized myeloid-derived suppressor cell expansion and immune suppression during tumor initiation and progression. *Molecular and Cellular Biology,* 34 (11), 2017-2028.

Gattinoni, L., Lugli, E., Ji, Y., Pos, Z., Paulos, C.M., Quigley, M.F., Almeida, J.R., Gostick, E., Yu, Z., Carpenito, C., Wang, E., Douek, D.C., Price, D.A., June, C.H., Marincola, F.M., Roederer, M. and Restifo, N.P., 2011. A human memory T cell subset with stem cell-like properties. *Nature Medicine,* 17 (10), 1290-1297.

Gaudino, S.J., and Kumar, P., 2019. Cross-Talk Between Antigen Presenting Cells and T Cells Impacts Intestinal Homeostasis, Bacterial Infections, and Tumorigenesis. *Frontiers in Immunology,* 10, 360.

Gebhardt, T., Wakim, L.M., Eidsmo, L., Reading, P.C., Heath, W.R. and Carbone, F.R., 2009. Memory T cells in nonlymphoid tissue that provide enhanced local immunity during infection with herpes simplex virus. *Nature Immunology,* 10 (5), 524-530.

Gleason, D.F., and Mellinger, G.T., 1974. Prediction of prognosis for prostatic adenocarcinoma by combined histological grading and clinical staging. *The Journal of Urology,* 111 (1), 58-64.

Global Burden of Disease Cancer Collaboration, Fitzmaurice, C., Allen, C., Barber, R.M., Barregard, L., Bhutta, Z.A., Brenner, H., Dicker, D.J., Chimed-Orchir, O., Dandona, R., Dandona, L., Fleming, T., Forouzanfar, M.H., Hancock, J., Hay, R.J., Hunter-Merrill, R., Huynh, C., Hosgood, H.D., Johnson, C.O., Jonas, J.B., Khubchandani, J., Kumar, G.A., Kutz, M., Lan, Q., Larson, H.J., Liang, X., Lim, S.S., Lopez, A.D., MacIntyre, M.F., Marczak, L., Marquez, N., Mokdad, A.H., Pinho, C., Pourmalek, F., Salomon, J.A., Sanabria, J.R., Sandar, L., Sartorius, B., Schwartz, S.M., Shackelford, K.A., Shibuya, K., Stanaway, J., Steiner, C., Sun, J., Takahashi, K., Vollset, S.E., Vos, T., Wagner, J.A., Wang, H., Westerman, R., Zeeb, H., Zoeckler, L., Abd-Allah, F., Ahmed, M.B., Alabed, S., Alam, N.K., Aldhahri, S.F., Alem, G., Alemayohu, M.A., Ali, R., Al-Raddadi, R., Amare, A., Amoako, Y., Artaman, A., Asayesh, H., Atnafu, N., Awasthi, A., Saleem, H.B., Barac, A., Bedi, N., Bensenor, I., Berhane, A., Bernabe, E., Betsu, B., Binagwaho, A., Boneya, D., Campos-Nonato, I., Castaneda-Orjuela, C., Catala-Lopez, F., Chiang, P., Chibueze, C., Chitheer, A., Choi, J.Y., Cowie, B., Damtew, S., das Neves, J., Dey, S., Dharmaratne, S., Dhillon, P., Ding, E., Driscoll, T., Ekwueme, D., Endries, A.Y., Farvid, M., Farzadfar, F., Fernandes, J., Fischer, F., G/Hiwot, T.T., Gebru, A., Gopalani, S., Hailu, A., Horino, M., Horita, N., Husseini, A., Huybrechts, I., Inoue, M., Islami, F., Jakovljevic, M., James, S., Javanbakht, M., Jee, S.H., Kasaeian, A., Kedir, M.S., Khader, Y.S., Khang, Y.H., Kim, D., Leigh, J., Linn, S., Lunevicius, R., El Razek, H.M.A., Malekzadeh, R., Malta, D.C., Marcenes, W., Markos, D., Melaku, Y.A., Meles, K.G., Mendoza, W., Mengiste, D.T., Meretoja, T.J., Miller, T.R., Mohammad, K.A., Mohammadi, A., Mohammed, S., Moradi-Lakeh, M., Nagel, G., Nand, D., Le Nguyen, Q., Nolte, S., Ogbo, F.A., Oladimeji, K.E., Oren, E., Pa, M., Park, E.K., Pereira, D.M., Plass, D., Qorbani, M., Radfar, A., Rafay, A., Rahman, M., Rana, S.M., Soreide, K., Satpathy, M., Sawhney, M., Sepanlou, S.G., Shaikh, M.A., She, J., Shiue, I., Shore, H.R., Shrime, M.G., So, S., Soneji, S., Stathopoulou, V., Stroumpoulis, K., Sufiyan, M.B., Sykes, B.L., Tabares-Seisdedos, R., Tadese, F., Tedla, B.A., Tessema, G.A., Thakur, J.S., Tran, B.X., Ukwaja, K.N., Uzochukwu, B.S.C., Vlassov, V.V., Weiderpass, E., Wubshet Terefe, M., Yebyo, H.G., Yimam, H.H., Yonemoto, N., Younis, M.Z., Yu, C., Zaidi, Z., Zaki, M.E.S., Zenebe, Z.M., Murray, C.J.L. and Naghavi, M., 2017. Global, Regional, and National Cancer Incidence, Mortality, Years of Life Lost, Years Lived With Disability, and Disability-Adjusted Life-years for 32 Cancer Groups, 1990 to 2015: A Systematic Analysis for the Global Burden of Disease Study. *JAMA Oncology,* 3 (4), 524-548.

Goding, S.R., Wilson, K.A., Xie, Y., Harris, K.M., Baxi, A., Akpinarli, A., Fulton, A., Tamada, K., Strome, S.E. and Antony, P.A., 2013. Restoring immune function of tumor-specific CD4+ T cells during recurrence of melanoma. *Journal of Immunology (Baltimore, Md.: 1950),* 190 (9), 4899-4909.

Gok Yavuz, B., Gunaydin, G., Gedik, M.E., Kosemehmetoglu, K., Karakoc, D., Ozgur, F. and Guc, D., 2019. Cancer associated fibroblasts sculpt tumour microenvironment by recruiting monocytes and inducing immunosuppressive PD-1(+) TAMs. *Scientific Reports,* 9 (1), 3172-019-39553-z.

Golubovskaya, V., and Wu, L., 2016. Different Subsets of T Cells, Memory, Effector Functions, and CAR-T Immunotherapy. *Cancers,* 8 (3), 10.3390/cancers8030036.

Goodier, M.R., Rodriguez-Galan, A., Lusa, C., Nielsen, C.M., Darboe, A., Moldoveanu, A.L., White, M.J., Behrens, R. and Riley, E.M., 2016. Influenza Vaccination Generates Cytokine-Induced Memory-like NK Cells: Impact of Human Cytomegalovirus Infection. *Journal of Immunology (Baltimore, Md.: 1950),* 197 (1), 313-325.

Gosselaar, C., Roobol, M.J., Roemeling, S. and Schroder, F.H., 2008. The role of the digital rectal examination in subsequent screening visits in the European randomized study of screening for prostate cancer (ERSPC), Rotterdam. *European Urology,* 54 (3), 581-588.

Graddis, T.J., McMahan, C.J., Tamman, J., Page, K.J. and Trager, J.B., 2011. Prostatic acid phosphatase expression in human tissues. *International Journal of Clinical and Experimental Pathology,* 4 (3), 295-306.

Graff, J.N., Alumkal, J.J., Drake, C.G., Thomas, G.V., Redmond, W.L., Farhad, M., Cetnar, J.P., Ey, F.S., Bergan, R.C., Slottke, R. and Beer, T.M., 2016. Early evidence of anti-PD-1 activity in enzalutamide-resistant prostate cancer. *Oncotarget,* 7 (33), 52810-52817.

Grenga, I., Donahue, R.N., Lepone, L.M., Richards, J. and Schlom, J., 2016. A fully human IgG1 anti-PD-L1 MAb in an in vitro assay enhances antigen-specific T-cell responses. *Clinical & Translational Immunology,* 5 (5), e83.

Gros, A., Parkhurst, M.R., Tran, E., Pasetto, A., Robbins, P.F., Ilyas, S., Prickett, T.D., Gartner, J.J., Crystal, J.S., Roberts, I.M., Trebska-McGowan, K., Wunderlich, J.R., Yang, J.C. and Rosenberg, S.A., 2016. Prospective identification of neoantigen-specific lymphocytes in the peripheral blood of melanoma patients. *Nature Medicine,* 22 (4), 433-438.

Gros, A., Robbins, P.F., Yao, X., Li, Y.F., Turcotte, S., Tran, E., Wunderlich, J.R., Mixon, A., Farid, S., Dudley, M.E., Hanada, K., Almeida, J.R., Darko, S., Douek, D.C., Yang, J.C. and Rosenberg, S.A., 2014. PD-1 identifies the patient-specific CD8 (+) tumor-reactive repertoire infiltrating human tumors. *The Journal of Clinical Investigation,* 124 (5), 2246-2259.

Grossmann, M.E., Wood, M. and Celis, E., 2001. Expression, specificity and immunotherapy potential of prostate-associated genes in murine cell lines. *World Journal of Urology,* 19 (5), 365-370.

Grunberg, E., Eckert, K. and Maurer, H.R., 1998. Docetaxel treatment of HT-29 colon carcinoma cells reinforces the adhesion and immunocytotoxicity of peripheral blood lymphocytes in vitro. *International Journal of Oncology,* 12 (4), 957-963.

GuhaThakurta, D., Sheikh, N.A., Fan, L.Q., Kandadi, H., Meagher, T.C., Hall, S.J., Kantoff, P.W., Higano, C.S., Small, E.J., Gardner, T.A., Bailey, K., Vu, T., DeVries, T., Whitmore, J.B., Frohlich, M.W., Trager, J.B. and Drake, C.G., 2015. Humoral Immune Response against Nontargeted Tumor Antigens after Treatment with Sipuleucel-T and Its Association with Improved Clinical Outcome. *Clinical*

Cancer Research: An Official Journal of the American Association for Cancer Research, 21 (16), 3619-3630.

Gulley, J.L., FAU, M.R., FAU, T.K., Jochems C FAU - Marte, Jennifer,L., FAU, M.J., Farsaci B FAU - Tucker, Jo,A., FAU, T.J., FAU, H.J., FAU, L.D., FAU, S.S., FAU, H.C. and Schlom, J., *Immune impact induced by PROSTVAC (PSA-TRICOM), a therapeutic vaccine for prostate cancer.*

Gulley, J.L., Giacchino, J.L., Breitmeyer, J.B., Franzusoff, A.J., Panicali, D., Schlom, J. and Kantoff, P.W., 2015. Prospect: A randomized double-blind phase 3 efficacy study of PROSTVAC-VF immunotherapy in men with asymptomatic/minimally symptomatic metastatic castration-resistant prostate cancer. *Jco,* 33 (15), TPS5081-TPS5081.

Guo, C., Manjili, M.H., Subjeck, J.R., Sarkar, D., Fisher, P.B. and Wang, X.Y., 2013. Therapeutic cancer vaccines: past, present, and future. *Advances in Cancer Research,* 119, 421-475.

Gupta, M., and Shorman, M., 2019. Cytomegalovirus. *In:* Cytomegalovirus. *StatPearls.* Treasure Island (FL): StatPearls Publishing LLC, 2019.

Hadaschik, B., Su, Y., Huter, E., Ge, Y., Hohenfellner, M. and Beckhove, P., 2012. Antigen specific T-cell responses against tumor antigens are controlled by regulatory T cells in patients with prostate cancer. *The Journal of Urology,* 187 (4), 1458-1465.

Haiman, C.A., Chen, G.K., Blot, W.J., Strom, S.S., Berndt, S.I., Kittles, R.A., Rybicki, B.A., Isaacs, W.B., Ingles, S.A., Stanford, J.L., Diver, W.R., Witte, J.S., Chanock, S.J., Kolb, S., Signorello, L.B., Yamamura, Y., Neslund-Dudas, C., Thun, M.J., Murphy, A., Casey, G., Sheng, X., Wan, P., Pooler, L.C., Monroe, K.R., Waters, K.M., Le Marchand, L., Kolonel, L.N., Stram, D.O. and Henderson, B.E., 2011. Characterizing genetic risk at known prostate cancer susceptibility loci in African Americans. *PLoS Genetics,* 7 (5), e1001387.

Hansen, A.R., Massard, C., Ott, P.A., Haas, N.B., Lopez, J.S., Ejadi, S., Wallmark, J.M., Keam, B., Delord, J.P., Aggarwal, R., Gould, M., Yang, P., Keefe, S.M. and Piha-Paul, S.A., 2018. Pembrolizumab for advanced prostate adenocarcinoma: findings of the KEYNOTE-028 study. *Annals of Oncology: Official Journal of the European Society for Medical Oncology,* 29 (8), 1807-1813.

Harari, A., Cellerai, C., Bellutti Enders, F., Kostler, J., Codarri, L., Tapia, G., Boyman, O., Castro, E., Gaudieri, S., James, I., John, M., Wagner, R., Mallal, S. and Pantaleo, G., 2007. Skewed association of polyfunctional antigen-specific CD8 T cell populations with HLA-B genotype. *Proceedings of the National Academy of Sciences of the United States of America,* 104 (41), 16233-16238.

Hassanipour-Azgomi, S., Mohammadian-Hafshejani, A., Ghoncheh, M., Towhidi, F., Jamehshorani, S. and Salehiniya, H., 2016. Incidence and mortality of prostate cancer and their relationship with the Human Development Index worldwide. *Prostate International,* 4 (3), 118-124.

Hayakawa, Y., Takeda, K., Yagita, H., Smyth, M.J., Van Kaer, L., Okumura, K. and Saiki, I., 2002. IFN-gamma-mediated inhibition of tumor angiogenesis by natural killer T-cell ligand, alpha-galactosylceramide. *Blood,* 100 (5), 1728-1733.

He, Q.F., Xu, Y., Li, J., Huang, Z.M., Li, X.H. and Wang, X., 2019. CD8+ T-cell exhaustion in cancer: mechanisms and new area for cancer immunotherapy. *Briefings in Functional Genomics,* 18 (2), 99-106.

Hemminki, K., and Czene, K., 2002. Attributable risks of familial cancer from the Family-Cancer Database. *Cancer Epidemiology, Biomarkers & Prevention: A Publication of the American*

Association for Cancer Research, Cosponsored by the American Society of Preventive Oncology, 11 (12), 1638-1644.

Hinz, S., Trauzold, A., Boenicke, L., Sandberg, C., Beckmann, S., Bayer, E., Walczak, H., Kalthoff, H. and Ungefroren, H., 2000. Bcl-XL protects pancreatic adenocarcinoma cells against CD95- and TRAIL-receptor-mediated apoptosis. *Oncogene,* 19 (48), 5477-5486.

Hodge, J.W., Ardiani, A., Farsaci, B., Kwilas, A.R. and Gameiro, S.R., 2012. The tipping point for combination therapy: cancer vaccines with radiation, chemotherapy, or targeted small molecule inhibitors. *Seminars in Oncology,* 39 (3), 323-339.

Hodge, K.K., McNeal, J.E., Terris, M.K. and Stamey, T.A., 1989. Random systematic versus directed ultrasound guided transrectal core biopsies of the prostate. *The Journal of Urology,* 142 (1), 71-4; discussion 74-5.

Hoffmann, T.J., Van Den Eeden, S.K., Sakoda, L.C., Jorgenson, E., Habel, L.A., Graff, R.E., Passarelli, M.N., Cario, C.L., Emami, N.C., Chao, C.R., Ghai, N.R., Shan, J., Ranatunga, D.K., Quesenberry, C.P., Aaronson, D., Presti, J., Wang, Z., Berndt, S.I., Chanock, S.J., McDonnell, S.K., French, A.J., Schaid, D.J., Thibodeau, S.N., Li, Q., Freedman, M.L., Penney, K.L., Mucci, L.A., Haiman, C.A., Henderson, B.E., Seminara, D., Kvale, M.N., Kwok, P.Y., Schaefer, C., Risch, N. and Witte, J.S., 2015. A large multiethnic genome-wide association study of prostate cancer identifies novel risk variants and substantial ethnic differences. *Cancer Discovery,* 5 (8), 878-891.

Hor, J.L., Whitney, P.G., Zaid, A., Brooks, A.G., Heath, W.R. and Mueller, S.N., 2015. Spatiotemporally Distinct Interactions with Dendritic Cell Subsets Facilitates CD4+ and CD8+ T Cell Activation to Localized Viral Infection. *Immunity,* 43 (3), 554-565.

Horoszewicz, J.S., Leong, S.S., Chu, T.M., Wajsman, Z.L., Friedman, M., Papsidero, L., Kim, U., Chai, L.S., Kakati, S., Arya, S.K. and Sandberg, A.A., 1980. The LNCaP cell line--a new model for studies on human prostatic carcinoma. *Progress in Clinical and Biological Research,* 37, 115-132.

Horoszewicz, J.S., Leong, S.S., Kawinski, E., Karr, J.P., Rosenthal, H., Chu, T.M., Mirand, E.A. and Murphy, G.P., 1983. LNCaP model of human prostatic carcinoma. *Cancer Research,* 43 (4), 1809-1818.

Horowitz, A., Behrens, R.H., Okell, L., Fooks, A.R. and Riley, E.M., 2010. NK cells as effectors of acquired immune responses: effector CD4+ T cell-dependent activation of NK cells following vaccination. *Journal of Immunology (Baltimore, Md.: 1950),* 185 (5), 2808-2818.

Howlader N, Noone AM, Krapcho M, Miller D, Bishop K, Altekruse SF, Kosary CL, Yu M, Ruhl J, Tatalovich Z, Mariotto A, Lewis DR, Chen HS, Feuer EJ, Cronin KA (eds). SEER Cancer Statistics Review, 1975-2013, National Cancer Institute. Bethesda, MD, https://seer.cancer.gov/archive/csr/1975_2013/, based on November 2015 SEER data submission, posted to the SEER web site, April 2016

Humphrey, P.A., 2004. Gleason grading and prognostic factors in carcinoma of the prostate. *Modern Pathology: An Official Journal of the United States and Canadian Academy of Pathology, Inc,* 17 (3), 292-306.

Huse, M., 2009. The T-cell-receptor signaling network. *Journal of Cell Science,* 122 (Pt 9), 1269-1273.

Idorn, M., Kollgaard, T., Kongsted, P., Sengelov, L. and Thor Straten, P., 2014. Correlation between frequencies of blood monocytic myeloid-derived suppressor cells, regulatory T cells and negative

prognostic markers in patients with castration-resistant metastatic prostate cancer. *Cancer Immunology, Immunotherapy: CII,* 63 (11), 1177-1187.

Inozume, T., Hanada, K., Wang, Q.J., Ahmadzadeh, M., Wunderlich, J.R., Rosenberg, S.A. and Yang, J.C., 2010. Selection of CD8+PD-1+ lymphocytes in fresh human melanomas enriches for tumor-reactive T cells. *Journal of Immunotherapy (Hagerstown, Md.: 1997),* 33 (9), 956-964.

Janeway CA Jr, Travers P, Walport M, et al. Immunobiology: The Immune System in Health and Disease. 5th edition. New York: Garland Science; 2001.

Janicki, C.N., Jenkinson, S.R., Williams, N.A. and Morgan, D.J., 2008. Loss of CTL function among high-avidity tumor-specific CD8+ T cells following tumor infiltration. *Cancer Research,* 68 (8), 2993-3000.

Janssen, E.M., Droin, N.M., Lemmens, E.E., Pinkoski, M.J., Bensinger, S.J., Ehst, B.D., Griffith, T.S., Green, D.R. and Schoenberger, S.P., 2005. CD4+ T-cell help controls CD8+ T-cell memory via TRAIL-mediated activation-induced cell death. *Nature,* 434 (7029), 88-93.

Janssen, E.M., Lemmens, E.E., Wolfe, T., Christen, U., von Herrath, M.G. and Schoenberger, S.P., 2003. CD4+ T cells are required for secondary expansion and memory in CD8+ T lymphocytes. *Nature,* 421 (6925), 852-856.

Japp, A.S., Kursunel, M.A., Meier, S., Malzer, J.N., Li, X., Rahman, N.A., Jekabsons, W., Krause, H., Magheli, A., Klopf, C., Thiel, A. and Frentsch, M., 2015. Dysfunction of PSA-specific CD8+ T cells in prostate cancer patients correlates with CD38 and Tim-3 expression. *Cancer Immunology, Immunotherapy: CII,* 64 (11), 1487-1494.

Jeske, S.J., Milowsky, M.I., Smith, C.R., Smith, K.A., Bander, N.H. and Nanus, D.M., 2007. Phase II trial of the anti-prostate specific membrane antigen (PSMA) monoclonal antibody (mAb) J591 plus low-dose interleukin-2 (IL-2) in patients (pts) with recurrent prostate cancer (PC). *Jco,* 25 (18), 15558-15558.

Jiang, T., Zhou, C. and Ren, S., 2016. Role of IL-2 in cancer immunotherapy. *Oncoimmunology,* 5 (6), e1163462.

Jochems, C., Tucker, J.A., Tsang, K.Y., Madan, R.A., Dahut, W.L., Liewehr, D.J., Steinberg, S.M., Gulley, J.L. and Schlom, J., 2014. A combination trial of vaccine plus ipilimumab in metastatic castration-resistant prostate cancer patients: immune correlates. *Cancer Immunology, Immunotherapy: CII,* 63 (4), 407-418.

Johnson, L.E., and McNeel, D.G., 2012. Identification of prostatic acid phosphatase (PAP) specific HLA-DR1-restricted T-cell epitopes. *The Prostate,* 72 (7), 730-740.

Johnson, L.E., Olson, B.M. and McNeel, D.G., 2017. Pretreatment antigen-specific immunity and regulation - association with subsequent immune response to anti-tumor DNA vaccination. *Journal for Immunotherapy of Cancer,* 5 (1), 56-017-0260-3.

Josefowicz, S.Z., Lu, L.F. and Rudensky, A.Y., 2012. Regulatory T cells: mechanisms of differentiation and function. *Annual Review of Immunology,* 30, 531-564.

Jost, S., Tomezsko, P.J., Rands, K., Toth, I., Lichterfeld, M., Gandhi, R.T. and Altfeld, M., 2014. CD4+ T-cell help enhances NK cell function following therapeutic HIV-1 vaccination. *Journal of Virology,* 88 (15), 8349-8354.

Kantoff, P.W., Higano, C.S., Shore, N.D., Berger, E.R., Small, E.J., Penson, D.F., Redfern, C.H., Ferrari, A.C., Dreicer, R., Sims, R.B., Xu, Y., Frohlich, M.W., Schellhammer, P.F. and IMPACT Study Investigators, 2010. Sipuleucel-T immunotherapy for castration-resistant prostate cancer. *The New England Journal of Medicine,* 363 (5), 411-422.

Kantoff, P.W., Schuetz, T.J., Blumenstein, B.A., Glode, L.M., Bilhartz, D.L., Wyand, M., Manson, K., Panicali, D.L., Laus, R., Schlom, J., Dahut, W.L., Arlen, P.M., Gulley, J.L. and Godfrey, W.R., 2010. Overall survival analysis of a phase II randomized controlled trial of a Poxviral-based PSA-targeted immunotherapy in metastatic castration-resistant prostate cancer. *Journal of Clinical Oncology: Official Journal of the American Society of Clinical Oncology,* 28 (7), 1099-1105.

Kaur, H.B., Guedes, L.B., Lu, J., Maldonado, L., Reitz, L., Barber, J.R., De Marzo, A.M., Tosoian, J.J., Tomlins, S.A., Schaeffer, E.M., Joshu, C.E., Sfanos, K.S. and Lotan, T.L., 2018. Association of tumor-infiltrating T-cell density with molecular subtype, racial ancestry and clinical outcomes in prostate cancer. *Modern Pathology: An Official Journal of the United States and Canadian Academy of Pathology, Inc,* 31 (10), 1539-1552.

Khan, K.A., and Kerbel, R.S., 2018. Improving immunotherapy outcomes with anti-angiogenic treatments and vice versa. *Nature Reviews.Clinical Oncology,* 15 (5), 310-324.

Kim, H.J., and Cantor, H., 2014. CD4 T-cell subsets and tumor immunity: the helpful and the not-so-helpful. *Cancer Immunology Research,* 2 (2), 91-98.

Kiniwa, Y., Miyahara, Y., Wang, H.Y., Peng, W., Peng, G., Wheeler, T.M., Thompson, T.C., Old, L.J. and Wang, R.F., 2007. CD8+ Foxp3+ regulatory T cells mediate immunosuppression in prostate cancer. *Clinical Cancer Research: An Official Journal of the American Association for Cancer Research,* 13 (23), 6947-6958.

Kirby, M., Hirst, C. and Crawford, E.D., 2011. Characterising the castration-resistant prostate cancer population: a systematic review. *International Journal of Clinical Practice,* 65 (11), 1180-1192.

Klein, E.Y., Monteforte, B., Gupta, A., Jiang, W., May, L., Hsieh, Y.H. and Dugas, A., 2016. The frequency of influenza and bacterial coinfection: a systematic review and meta-analysis. *Influenza and Other Respiratory Viruses,* 10 (5), 394-403.

Klyushnenkova, E.N., Kouiavskaia, D.V., Kodak, J.A., Vandenbark, A.A. and Alexander, R.B., 2007. Identification of HLA-DRB1*1501-restricted T-cell epitopes from human prostatic acid phosphatase. *The Prostate,* 67 (10), 1019-1028.

Koch, U., and Radtke, F., 2011. Mechanisms of T cell development and transformation. *Annual Review of Cell and Developmental Biology,* 27, 539-562.

Kolonel, L.N., Altshuler, D. and Henderson, B.E., 2004. The multiethnic cohort study: exploring genes, lifestyle and cancer risk. *Nature Reviews.Cancer,* 4 (7), 519-527.

Kong, H.Y., and Byun, J., 2013. Emerging roles of human prostatic Acid phosphatase. *Biomolecules & Therapeutics,* 21 (1), 10-20.

Korsholm, K.S., Hansen, J., Karlsen, K., Filskov, J., Mikkelsen, M., Lindenstrom, T., Schmidt, S.T., Andersen, P. and Christensen, D., 2014. Induction of CD8+ T-cell responses against subunit antigens by the novel cationic liposomal CAF09 adjuvant. *Vaccine,* 32 (31), 3927-3935.

Ku, J., Wilenius, K., Larsen, C., De Guzman, K., Yoshinaga, S., Turner, J.S., Lam, R.Y. and Scholz, M.C., 2018. Survival after sipuleucel-T (SIP-T) and low-dose ipilimumab (IPI) in men with metastatic, progressive, castrate-resistant prostate cancer (M-CRPC). *Jco,* 36 (6), 368-368.

Kumar, B.V., Connors, T.J. and Farber, D.L., 2018. Human T Cell Development, Localization, and Function throughout Life. *Immunity,* 48 (2), 202-213.

Kvale, R., Moller, B., Wahlqvist, R., Fossa, S.D., Berner, A., Busch, C., Kyrdalen, A.E., Svindland, A., Viset, T. and Halvorsen, O.J., 2009. Concordance between Gleason scores of needle biopsies and radical prostatectomy specimens: a population-based study. *BJU International,* 103 (12), 1647-1654.

Kwon, E.D., Drake, C.G., Scher, H.I., Fizazi, K., Bossi, A., van den Eertwegh, A.J., Krainer, M., Houede, N., Santos, R., Mahammedi, H., Ng, S., Maio, M., Franke, F.A., Sundar, S., Agarwal, N., Bergman, A.M., Ciuleanu, T.E., Korbenfeld, E., Sengelov, L., Hansen, S., Logothetis, C., Beer, T.M., McHenry, M.B., Gagnier, P., Liu, D., Gerritsen, W.R. and CA184-043 Investigators, 2014. Ipilimumab versus placebo after radiotherapy in patients with metastatic castration-resistant prostate cancer that had progressed after docetaxel chemotherapy (CA184-043): a multicentre, randomised, double-blind, phase 3 trial. *The Lancet.Oncology,* 15 (7), 700-712.

Kyewski, B., and Klein, L., 2006. A central role for central tolerance. *Annual Review of Immunology,* 24, 571-606.

L.H. Sobin, C.W., 2002. **TNM Classification of Malignant Tumours**. 6th edition ed. 2002: Wiley-Liss.

Labadie, B.W., Bao, R. and Luke, J.J., 2019. Reimagining IDO Pathway Inhibition in Cancer Immunotherapy via Downstream Focus on the Tryptophan-Kynurenine-Aryl Hydrocarbon Axis. *Clinical Cancer Research: An Official Journal of the American Association for Cancer Research,* 25 (5), 1462-1471.

LaCelle, M.G., Jensen, S.M. and Fox, B.A., 2009. Partial CD4 depletion reduces regulatory T cells induced by multiple vaccinations and restores therapeutic efficacy. *Clinical Cancer Research: An Official Journal of the American Association for Cancer Research,* 15 (22), 6881-6890.

Laidlaw, B.J., Craft, J.E. and Kaech, S.M., 2016. The multifaceted role of CD4 (+) T cells in CD8 (+) T cell memory. *Nature Reviews.Immunology,* 16 (2), 102-111.

Le, D.T., Durham, J.N., Smith, K.N., Wang, H., Bartlett, B.R., Aulakh, L.K., Lu, S., Kemberling, H., Wilt, C., Luber, B.S., Wong, F., Azad, N.S., Rucki, A.A., Laheru, D., Donehower, R., Zaheer, A., Fisher, G.A., Crocenzi, T.S., Lee, J.J., Greten, T.F., Duffy, A.G., Ciombor, K.K., Eyring, A.D., Lam, B.H., Joe, A., Kang, S.P., Holdhoff, M., Danilova, L., Cope, L., Meyer, C., Zhou, S., Goldberg, R.M., Armstrong, D.K., Bever, K.M., Fader, A.N., Taube, J., Housseau, F., Spetzler, D., Xiao, N., Pardoll, D.M., Papadopoulos, N., Kinzler, K.W., Eshleman, J.R., Vogelstein, B., Anders, R.A. and Diaz, L.A.,Jr, 2017. Mismatch repair deficiency predicts response of solid tumors to PD-1 blockade. *Science (New York, N.Y.),* 357 (6349), 409-413.

Leclerc, B.G., Charlebois, R., Chouinard, G., Allard, B., Pommey, S., Saad, F. and Stagg, J., 2016. CD73 Expression Is an Independent Prognostic Factor in Prostate Cancer. *Clinical Cancer Research: An Official Journal of the American Association for Cancer Research,* 22 (1), 158-166.

Li, H., Fan, X. and Houghton, J., 2007. Tumor microenvironment: the role of the tumor stroma in cancer. *Journal of Cellular Biochemistry,* 101 (4), 805-815.

Lim, T.S., Goh, J.K., Mortellaro, A., Lim, C.T., Hammerling, G.J. and Ricciardi-Castagnoli, P., 2012. CD80 and CD86 differentially regulate mechanical interactions of T-cells with antigen-presenting dendritic cells and B-cells. *PloS One,* 7 (9), e45185.

Liu, F.T., and Rabinovich, G.A., 2005. Galectins as modulators of tumour progression. *Nature Reviews.Cancer,* 5 (1), 29-41.

Liu, Y., Saeter, T., Vlatkovic, L., Servoll, E., Waaler, G., Axcrona, U., Giercksky, K.E., Nesland, J.M., Suo, Z.H. and Axcrona, K., 2013. Dendritic and lymphocytic cell infiltration in prostate carcinoma. *Histology and Histopathology,* 28 (12), 1621-1628.

Ljunggren, H.G., Stam, N.J., Ohlen, C., Neefjes, J.J., Hoglund, P., Heemels, M.T., Bastin, J., Schumacher, T.N., Townsend, A. and Karre, K., 1990. Empty MHC class I molecules come out in the cold. *Nature,* 346 (6283), 476-480.

Loeb, S., Bjurlin, M.A., Nicholson, J., Tammela, T.L., Penson, D.F., Carter, H.B., Carroll, P. and Etzioni, R., 2014. Overdiagnosis and overtreatment of prostate cancer. *European Urology,* 65 (6), 1046-1055.

Loeb, S., Folkvaljon, Y., Bratt, O., Robinson, D. and Stattin, P., 2019. Defining Intermediate Risk Prostate Cancer Suitable for Active Surveillance. *The Journal of Urology,* 201 (2), 292-299.

Lorente, D., Mateo, J., Perez-Lopez, R., de Bono, J.S. and Attard, G., 2015. Sequencing of agents in castration-resistant prostate cancer. *The Lancet.Oncology,* 16 (6), e279-92.

Lu, X., Horner, J.W., Paul, E., Shang, X., Troncoso, P., Deng, P., Jiang, S., Chang, Q., Spring, D.J., Sharma, P., Zebala, J.A., Maeda, D.Y., Wang, Y.A. and DePinho, R.A., 2017. Effective combinatorial immunotherapy for castration-resistant prostate cancer. *Nature,* 543 (7647), 728-732.

Lu, X., Yang, L., Yao, D., Wu, X., Li, J., Liu, X., Deng, L., Huang, C., Wang, Y., Li, D. and Liu, J., 2017. Tumor antigen-specific CD8 (+) T cells are negatively regulated by PD-1 and Tim-3 in human gastric cancer. *Cellular Immunology,* 313, 43-51.

Lucia, M.S., Darke, A.K., Goodman, P.J., La Rosa, F.G., Parnes, H.L., Ford, L.G., Coltman, C.A.,Jr and Thompson, I.M., 2008. Pathologic characteristics of cancers detected in The Prostate Cancer Prevention Trial: implications for prostate cancer detection and chemoprevention. *Cancer Prevention Research (Philadelphia, Pa.),* 1 (3), 167-173.

Lundholm, M., Hagglof, C., Wikberg, M.L., Stattin, P., Egevad, L., Bergh, A., Wikstrom, P., Palmqvist, R. and Edin, S., 2015. Secreted Factors from Colorectal and Prostate Cancer Cells Skew the Immune Response in Opposite Directions. *Scientific Reports,* 5, 15651.

Lunemann, J.D., Frey, O., Eidner, T., Baier, M., Roberts, S., Sashihara, J., Volkmer, R., Cohen, J.I., Hein, G., Kamradt, T. and Munz, C., 2008. Increased frequency of EBV-specific effector memory CD8+ T cells correlates with higher viral load in rheumatoid arthritis. *Journal of Immunology (Baltimore, Md.: 1950),* 181 (2), 991-1000.

Luo, J.L., Tan, W., Ricono, J.M., Korchynskyi, O., Zhang, M., Gonias, S.L., Cheresh, D.A. and Karin, M., 2007. Nuclear cytokine-activated IKKalpha controls prostate cancer metastasis by repressing Maspin. *Nature,* 446 (7136), 690-694.

Machlenkin, A., Paz, A., Bar Haim, E., Goldberger, O., Finkel, E., Tirosh, B., Volovitz, I., Vadai, E., Lugassy, G., Cytron, S., Lemonnier, F., Tzehoval, E. and Eisenbach, L., 2005. Human CTL epitopes prostatic acid phosphatase-3 and six-transmembrane epithelial antigen of prostate-3 as candidates for prostate cancer immunotherapy. *Cancer Research,* 65 (14), 6435-6442.

Madan, R.A., Gulley, J.L., Schlom, J., Steinberg, S.M., Liewehr, D.J., Dahut, W.L. and Arlen, P.M., 2008. Analysis of overall survival in patients with nonmetastatic castration-resistant prostate cancer treated with vaccine, nilutamide, and combination therapy. *Clinical Cancer Research: An Official Journal of the American Association for Cancer Research,* 14 (14), 4526-4531.

Madan, R.A., Mohebtash, M., Arlen, P.M., Vergati, M., Rauckhorst, M., Steinberg, S.M., Tsang, K.Y., Poole, D.J., Parnes, H.L., Wright, J.J., Dahut, W.L., Schlom, J. and Gulley, J.L., 2012. Ipilimumab and a poxviral vaccine targeting prostate-specific antigen in metastatic castration-resistant prostate cancer: a phase 1 dose-escalation trial. *The Lancet.Oncology,* 13 (5), 501-508.

Maimela, N.R., Liu, S. and Zhang, Y., 2018. Fates of CD8+ T cells in Tumor Microenvironment. *Computational and Structural Biotechnology Journal,* 17, 1-13.

Malamas, A.S., Gameiro, S.R., Knudson, K.M. and Hodge, J.W., 2016. Sublethal exposure to alpha radiation (223Ra dichloride) enhances various carcinomas' sensitivity to lysis by antigen-specific cytotoxic T lymphocytes through calreticulin-mediated immunogenic modulation. *Oncotarget,* 7 (52), 86937-86947.

Mapara, M.Y., and Sykes, M., 2004. Tolerance and cancer: mechanisms of tumor evasion and strategies for breaking tolerance. *Journal of Clinical Oncology: Official Journal of the American Society of Clinical Oncology,* 22 (6), 1136-1151.

Mariathasan, S., Turley, S.J., Nickles, D., Castiglioni, A., Yuen, K., Wang, Y., Kadel, E.E.,III, Koeppen, H., Astarita, J.L., Cubas, R., Jhunjhunwala, S., Banchereau, R., Yang, Y., Guan, Y., Chalouni, C., Ziai, J., Senbabaoglu, Y., Santoro, S., Sheinson, D., Hung, J., Giltnane, J.M., Pierce, A.A., Mesh, K., Lianoglou, S., Riegler, J., Carano, R.A.D., Eriksson, P., Hoglund, M., Somarriba, L., Halligan, D.L., van der Heijden, M.S., Loriot, Y., Rosenberg, J.E., Fong, L., Mellman, I., Chen, D.S., Green, M., Derleth, C., Fine, G.D., Hegde, P.S., Bourgon, R. and Powles, T., 2018. TGFbeta attenuates tumour response to PD-L1 blockade by contributing to exclusion of T cells. *Nature,* 554 (7693), 544-548.

Marincola, F.M., Jaffee, E.M., Hicklin, D.J. and Ferrone, S., 2000. Escape of human solid tumors from T-cell recognition: molecular mechanisms and functional significance. *Advances in Immunology,* 74, 181-273.

Martin, A.M., Nirschl, T.R., Nirschl, C.J., Francica, B.J., Kochel, C.M., van Bokhoven, A., Meeker, A.K., Lucia, M.S., Anders, R.A., DeMarzo, A.M. and Drake, C.G., 2015. Paucity of PD-L1 expression in prostate cancer: innate and adaptive immune resistance. *Prostate Cancer and Prostatic Diseases,* 18 (4), 325-332.

Martinez-Lostao, L., Anel, A. and Pardo, J., 2015. How Do Cytotoxic Lymphocytes Kill Cancer Cells? *Clinical Cancer Research: An Official Journal of the American Association for Cancer Research,* 21 (22), 5047-5056.

Martini, M., Testi, M.G., Pasetto, M., Picchio, M.C., Innamorati, G., Mazzocco, M., Ugel, S., Cingarlini, S., Bronte, V., Zanovello, P., Krampera, M., Mosna, F., Cestari, T., Riviera, A.P., Brutti, N., Barbieri, O., Matera, L., Tridente, G., Colombatti, M. and Sartoris, S., 2010. IFN-gamma-mediated upmodulation of MHC class I expression activates tumor-specific immune response in a mouse model of prostate cancer. *Vaccine,* 28 (20), 3548-3557.

Martins, K.A., Steffens, J.T., van Tongeren, S.A., Wells, J.B., Bergeron, A.A., Dickson, S.P., Dye, J.M., Salazar, A.M. and Bavari, S., 2014. Toll-like receptor agonist augments virus-like particle-mediated protection from Ebola virus with transient immune activation. *PloS One,* 9 (2), e89735.

Massari, F., Ciccarese, C., Calio, A., Munari, E., Cima, L., Porcaro, A.B., Novella, G., Artibani, W., Sava, T., Eccher, A., Ghimenton, C., Bertoldo, F., Scarpa, A., Sperandio, N., Porta, C., Bronte, V., Chilosi, M., Bogina, G., Zamboni, G., Tortora, G., Samaratunga, H., Martignoni, G. and Brunelli, M., 2016. Magnitude of PD-1, PD-L1 and T Lymphocyte Expression on Tissue from Castration-Resistant Prostate Adenocarcinoma: An Exploratory Analysis. *Targeted Oncology,* 11 (3), 345-351.

Masucci, G.V., Andersson, E., Egevad, L., Kälkner, K., Harmenberg, U., Ryberg, M., Nilsson, S. and Pisa, P., 2006. High frequency of human leucocyte antigen (HLA) A2 and HLA-B7, -B44, -B15 and -DRB1–4 haplotypes in Swedish prostate cancer patients. *Jco,* 24 (18), 14543-14543.

McNeal, J.E., 1988. Normal histology of the prostate. *The American Journal of Surgical Pathology,* 12 (8), 619-633.

McNeel, D.G., Bander, N.H., Beer, T.M., Drake, C.G., Fong, L., Harrelson, S., Kantoff, P.W., Madan, R.A., Oh, W.K., Peace, D.J., Petrylak, D.P., Porterfield, H., Sartor, O., Shore, N.D., Slovin, S.F., Stein, M.N., Vieweg, J. and Gulley, J.L., 2016. The Society for Immunotherapy of Cancer consensus statement on immunotherapy for the treatment of prostate carcinoma. *Journal for Immunotherapy of Cancer,* 4, 92-016-0198-x. eCollection 2016.

McNeel, D.G., Becker, J.T., Eickhoff, J.C., Johnson, L.E., Bradley, E., Pohlkamp, I., Staab, M.J., Liu, G., Wilding, G. and Olson, B.M., 2014. Real-time immune monitoring to guide plasmid DNA vaccination schedule targeting prostatic acid phosphatase in patients with castration-resistant prostate cancer. *Clinical Cancer Research: An Official Journal of the American Association for Cancer Research,* 20 (14), 3692-3704.

McNeel, D.G., Dunphy, E.J., Davies, J.G., Frye, T.P., Johnson, L.E., Staab, M.J., Horvath, D.L., Straus, J., Alberti, D., Marnocha, R., Liu, G., Eickhoff, J.C. and Wilding, G., 2009. Safety and immunological efficacy of a DNA vaccine encoding prostatic acid phosphatase in patients with stage D0 prostate cancer. *Journal of Clinical Oncology: Official Journal of the American Society of Clinical Oncology,* 27 (25), 4047-4054.

McNeel, D.G., Eickhoff, J.C., Wargowski, E., Zahm, C., Staab, M.J., Straus, J. and Liu, G., 2018. Concurrent, but not sequential, PD-1 blockade with a DNA vaccine elicits anti-tumor responses in patients with metastatic, castration-resistant prostate cancer. *Oncotarget,* 9 (39), 25586-25596.

McNeel, D.G., Gardner, T.A., Higano, C.S., Kantoff, P.W., Small, E.J., Wener, M.H., Sims, R.B., DeVries, T., Sheikh, N.A. and Dreicer, R., 2014. A transient increase in eosinophils is associated with prolonged survival in men with metastatic castration-resistant prostate cancer who receive sipuleucel-T. *Cancer Immunology Research,* 2 (10), 988-999.

McNeel, D.G., Nguyen, L.D. and Disis, M.L., 2001. Identification of T helper epitopes from prostatic acid phosphatase. *Cancer Research,* 61 (13), 5161-5167.

McNeel, D.G., Nguyen, L.D., Ellis, W.J., Higano, C.S., Lange, P.H. and Disis, M.L., 2001. Naturally occurring prostate cancer antigen-specific T cell responses of a Th1 phenotype can be detected in patients with prostate cancer. *The Prostate,* 47 (3), 222-229.

McNeel, D.G., Eickhoff, J.C., Jeraj, R., Staab, M.J., Straus, J., Rekoske, B. and Liu, G., 2017. DNA vaccine with pembrolizumab to elicit antitumor responses in patients with metastatic, castration-resistant prostate cancer (mCRPC). *Jco,* 35 (7), 168-168.

Mehta, A.K., Gracias, D.T. and Croft, M., 2018. TNF activity and T cells. *Cytokine,* 101, 14-18.

Melero, I., Gaudernack, G., Gerritsen, W., Huber, C., Parmiani, G., Scholl, S., Thatcher, N., Wagstaff, J., Zielinski, C., Faulkner, I. and Mellstedt, H., 2014. Therapeutic vaccines for cancer: an overview of clinical trials. *Nature Reviews.Clinical Oncology,* 11 (9), 509-524.

Melief, C.J., and van der Burg, S.H., 2008. Immunotherapy of established (pre)malignant disease by synthetic long peptide vaccines. *Nature Reviews.Cancer,* 8 (5), 351-360.

Melief, C.J., van Hall, T., Arens, R., Ossendorp, F. and van der Burg, S.H., 2015. Therapeutic cancer vaccines. *The Journal of Clinical Investigation,* 125 (9), 3401-3412.

Mellor, A.L., Chandler, P., Baban, B., Hansen, A.M., Marshall, B., Pihkala, J., Waldmann, H., Cobbold, S., Adams, E. and Munn, D.H., 2004. Specific subsets of murine dendritic cells acquire potent T cell regulatory functions following CTLA4-mediated induction of indoleamine 2,3 dioxygenase. *International Immunology,* 16 (10), 1391-1401.

Meng, S., Li, L., Zhou, M., Jiang, W., Niu, H. and Yang, K., 2018. Distribution and prognostic value of tumorinfiltrating T cells in breast cancer. *Molecular Medicine Reports,* 18 (5), 4247-4258.

Mercader, M., Bodner, B.K., Moser, M.T., Kwon, P.S., Park, E.S., Manecke, R.G., Ellis, T.M., Wojcik, E.M., Yang, D., Flanigan, R.C., Waters, W.B., Kast, W.M. and Kwon, E.D., 2001. T cell infiltration of the prostate induced by androgen withdrawal in patients with prostate cancer. *Proceedings of the National Academy of Sciences of the United States of America,* 98 (25), 14565-14570.

Metheringham, R.L., Pudney, V.A., Gunn, B., Towey, M., Spendlove, I. and Durrant, L.G., 2009. Antibodies designed as effective cancer vaccines. *Mabs,* 1 (1), 71-85.

Miller, A.M., Lundberg, K., Ozenci, V., Banham, A.H., Hellstrom, M., Egevad, L. and Pisa, P., 2006. CD4+CD25high T cells are enriched in the tumor and peripheral blood of prostate cancer patients. *Journal of Immunology (Baltimore, Md.: 1950),* 177 (10), 7398-7405.

Minn AJ. Interferons and the immunogenic effects of cancer therapy. Trends Immunol. (2015) 36:725–37. 10.1016/j.it.2015.09.007

Montes, M., Rufer, N., Appay, V., Reynard, S., Pittet, M.J., Speiser, D.E., Guillaume, P., Cerottini, J.C., Romero, P. and Leyvraz, S., 2005. Optimum in vitro expansion of human antigen-specific CD8 T cells for adoptive transfer therapy. *Clinical and Experimental Immunology,* 142 (2), 292-302.

Muniyan, S., Chaturvedi, N.K., Dwyer, J.G., Lagrange, C.A., Chaney, W.G. and Lin, M.F., 2013. Human prostatic acid phosphatase: structure, function and regulation. *International Journal of Molecular Sciences,* 14 (5), 10438-10464.

Nafie, S., Mellon, J.K., Dormer, J.P. and Khan, M.A., 2014. The role of transperineal template prostate biopsies in prostate cancer diagnosis in biopsy naive men with PSA less than 20 ng ml(-1.). *Prostate Cancer and Prostatic Diseases,* 17 (2), 170-173.

Naito, Y., Saito, K., Shiiba, K., Ohuchi, A., Saigenji, K., Nagura, H. and Ohtani, H., 1998. CD8+ T cells infiltrated within cancer cell nests as a prognostic factor in human colorectal cancer. *Cancer Research,* 58 (16), 3491-3494.

Nardone, V., Botta, C., Caraglia, M., Martino, E.C., Ambrosio, M.R., Carfagno, T., Tini, P., Semeraro, L., Misso, G., Grimaldi, A., Boccellino, M., Facchini, G., Berretta, M., Vischi, G., Rocca, B.J., Barone, A., Tassone, P., Tagliaferri, P., Del Vecchio, M.T., Pirtoli, L. and Correale, P., 2016. Tumor infiltrating T lymphocytes expressing FoxP3, CCR7 or PD-1 predict the outcome of prostate cancer patients

subjected to salvage radiotherapy after biochemical relapse. *Cancer Biology & Therapy,* 17 (11), 1213-1220.

Nelson, B.H., 2004. IL-2, regulatory T cells, and tolerance. *Journal of Immunology (Baltimore, Md.: 1950),* 172 (7), 3983-3988.

Nelson, W.G., De Marzo, A.M. and Isaacs, W.B., 2003. Prostate cancer. *The New England Journal of Medicine,* 349 (4), 366-381.

Ness, N., Andersen, S., Valkov, A., Nordby, Y., Donnem, T., Al-Saad, S., Busund, L.T., Bremnes, R.M. and Richardsen, E., 2014. Infiltration of CD8+ lymphocytes is an independent prognostic factor of biochemical failure-free survival in prostate cancer. *The Prostate,* 74 (14), 1452-1461.

Nizard, M., Roussel, H., Diniz, M.O., Karaki, S., Tran, T., Voron, T., Dransart, E., Sandoval, F., Riquet, M., Rance, B., Marcheteau, E., Fabre, E., Mandavit, M., Terme, M., Blanc, C., Escudie, J.B., Gibault, L., Barthes, F.L.P., Granier, C., Ferreira, L.C.S., Badoual, C., Johannes, L. and Tartour, E., 2017. Induction of resident memory T cells enhances the efficacy of cancer vaccine. *Nature Communications,* 8, 15221.

Nouri-Shirazi, M., Banchereau, J., Bell, D., Burkeholder, S., Kraus, E.T., Davoust, J. and Palucka, K.A., 2000. Dendritic cells capture killed tumor cells and present their antigens to elicit tumor-specific immune responses. *Journal of Immunology (Baltimore, Md.: 1950),* 165 (7), 3797-3803.

Nurieva, R., Wang, J. and Sahoo, A., 2013. T-cell tolerance in cancer. *Immunotherapy,* 5 (5), 513-531.

Oizumi, S., Deyev, V., Yamazaki, K., Schreiber, T., Strbo, N., Rosenblatt, J. and Podack, E.R., 2008. Surmounting tumor-induced immune suppression by frequent vaccination or immunization in the absence of B cells. *Journal of Immunotherapy (Hagerstown, Md.: 1997),* 31 (4), 394-401.

Olson, B.M., Frye, T.P., Johnson, L.E., Fong, L., Knutson, K.L., Disis, M.L. and McNeel, D.G., 2010. HLA-A2-restricted T-cell epitopes specific for prostatic acid phosphatase. *Cancer Immunology, Immunotherapy: CII,* 59 (6), 943-953.

Olson, B.M., Jankowska-Gan, E., Becker, J.T., Vignali, D.A., Burlingham, W.J. and McNeel, D.G., 2012. Human prostate tumor antigen-specific CD8+ regulatory T cells are inhibited by CTLA-4 or IL-35 blockade. *Journal of Immunology (Baltimore, Md.: 1950),* 189 (12), 5590-5601.

Omilusik, K.D., and Goldrath, A.W., 2017. The origins of memory T cells. *Nature,* 552 (7685), 337-339.

Ossendorp, F., Mengede, E., Camps, M., Filius, R. and Melief, C.J., 1998. Specific T helper cell requirement for optimal induction of cytotoxic T lymphocytes against major histocompatibility complex class II negative tumors. *The Journal of Experimental Medicine,* 187 (5), 693-702.

Ostroumov, D., Fekete-Drimusz, N., Saborowski, M., Kuhnel, F. and Woller, N., 2018. CD4 and CD8 T lymphocyte interplay in controlling tumor growth. *Cellular and Molecular Life Sciences: CMLS,* 75 (4), 689-713.

Parker, C., Nilsson, S., Heinrich, D., Helle, S.I., O'Sullivan, J.M., Fossa, S.D., Chodacki, A., Wiechno, P., Logue, J., Seke, M., Widmark, A., Johannessen, D.C., Hoskin, P., Bottomley, D., James, N.D., Solberg, A., Syndikus, I., Kliment, J., Wedel, S., Boehmer, S., Dall'Oglio, M., Franzen, L., Coleman, R., Vogelzang, N.J., O'Bryan-Tear, C.G., Staudacher, K., Garcia-Vargas, J., Shan, M., Bruland, O.S., Sartor,

O. and ALSYMPCA Investigators, 2013. Alpha emitter radium-223 and survival in metastatic prostate cancer. *The New England Journal of Medicine,* 369 (3), 213-223.

Parkin, J., and Cohen, B., 2001. An overview of the immune system. *Lancet (London, England),* 357 (9270), 1777-1789.

Pascolo, S., Bervas, N., Ure, J.M., Smith, A.G., Lemonnier, F.A. and Perarnau, B., 1997. HLA-A2.1-restricted education and cytolytic activity of CD8 (+) T lymphocytes from beta2 microglobulin (beta2m) HLA-A2.1 monochain transgenic H-2Db beta2m double knockout mice. *The Journal of Experimental Medicine,* 185 (12), 2043-2051.

Pasero, C., Gravis, G., Guerin, M., Granjeaud, S., Thomassin-Piana, J., Rocchi, P., Paciencia-Gros, M., Poizat, F., Bentobji, M., Azario-Cheillan, F., Walz, J., Salem, N., Brunelle, S., Moretta, A. and Olive, D., 2016. Inherent and Tumor-Driven Immune Tolerance in the Prostate Microenvironment Impairs Natural Killer Cell Antitumor Activity. *Cancer Research,* 76 (8), 2153-2165.

Patel, P.M., Ottensmeier, C.H., Mulatero, C., Lorigan, P., Plummer, R., Pandha, H., Elsheikh, S., Hadjimichael, E., Villasanti, N., Adams, S.E., Cunnell, M., Metheringham, R.L., Brentville, V.A., Machado, L., Daniels, I., Gijon, M., Hannaman, D. and Durrant, L.G., 2018. Targeting gp100 and TRP-2 with a DNA vaccine: Incorporating T cell epitopes with a human IgG1 antibody induces potent T cell responses that are associated with favourable clinical outcome in a phase I/II trial. *Oncoimmunology,* 7 (6), e1433516.

Pedersen, G.K., Andersen, P. and Christensen, D., 2018. Immunocorrelates of CAF family adjuvants. *Seminars in Immunology,* 39, 4-13.

Pernar, C.H., Ebot, E.M., Wilson, K.M. and Mucci, L.A., 2018. The Epidemiology of Prostate Cancer. *Cold Spring Harbor Perspectives in Medicine,* 8 (12), 10.1101/cshperspect.a030361.

Peshwa, M.V., Shi, J.D., Ruegg, C., Laus, R. and van Schooten, W.C., 1998. Induction of prostate tumor-specific CD8+ cytotoxic T-lymphocytes in vitro using antigen-presenting cells pulsed with prostatic acid phosphatase peptide. *The Prostate,* 36 (2), 129-138.

Petrylak, D.P., Tangen, C.M., Hussain, M.H., Lara, P.N.,Jr, Jones, J.A., Taplin, M.E., Burch, P.A., Berry, D., Moinpour, C., Kohli, M., Benson, M.C., Small, E.J., Raghavan, D. and Crawford, E.D., 2004. Docetaxel and estramustine compared with mitoxantrone and prednisone for advanced refractory prostate cancer. *The New England Journal of Medicine,* 351 (15), 1513-1520.

Petrylak, D.P., Vogelzang, N.J., Chatta, G.S., Fleming, M.T., Smith, D.C., Appleman, L.J., Hussain, A., Modiano, M., Singh, P., Tagawa, S.T., Gore, I., McClay, E.F., Mega, A.E., Sartor, A.O., Somer, B.G., Wadlow, R.C., Shore, N.D., Stambler, N., DiPippo, V.A. and Israel, R.J., 2015. A phase 2 study of prostate specific membrane antigen antibody drug conjugate (PSMA ADC) in patients (pts) with progressive metastatic castration-resistant prostate cancer (mCRPC) following abiraterone and/or enzalutamide (abi/enz). *Jco,* 33 (7), 144-144.

Pipkin, M.E., Sacks, J.A., Cruz-Guilloty, F., Lichtenheld, M.G., Bevan, M.J. and Rao, A., 2010. Interleukin-2 and inflammation induce distinct transcriptional programs that promote the differentiation of effector cytolytic T cells. *Immunity,* 32 (1), 79-90.

Podrazil, M., Horvath, R., Becht, E., Rozkova, D., Bilkova, P., Sochorova, K., Hromadkova, H., Kayserova, J., Vavrova, K., Lastovicka, J., Vrabcova, P., Kubackova, K., Gasova, Z., Jarolim, L., Babjuk, M., Spisek, R., Bartunkova, J. and Fucikova, J., 2015. Phase I/II clinical trial of dendritic-cell based immunotherapy (DCVAC/PCa) combined with chemotherapy in patients with metastatic, castration-resistant prostate cancer. *Oncotarget,* 6 (20), 18192-18205.

Potosky, A.L., Davis, W.W., Hoffman, R.M., Stanford, J.L., Stephenson, R.A., Penson, D.F. and Harlan, L.C., 2004. Five-year outcomes after prostatectomy or radiotherapy for prostate cancer: the prostate cancer outcomes study. *Journal of the National Cancer Institute,* 96 (18), 1358-1367.

Pritchard, C.C., Morrissey, C., Kumar, A., Zhang, X., Smith, C., Coleman, I., Salipante, S.J., Milbank, J., Yu, M., Grady, W.M., Tait, J.F., Corey, E., Vessella, R.L., Walsh, T., Shendure, J. and Nelson, P.S., 2014. Complex MSH2 and MSH6 mutations in hypermutated microsatellite unstable advanced prostate cancer. *Nature Communications,* 5, 4988.

Pudney, V.A., Metheringham, R.L., Gunn, B., Spendlove, I., Ramage, J.M. and Durrant, L.G., 2010. DNA vaccination with T-cell epitopes encoded within Ab molecules induces high-avidity anti-tumor CD8+ T cells. *European Journal of Immunology,* 40 (3), 899-910.

Qazilbash, M.H., Wieder, E., Thall, P.F., Wang, X., Rios, R., Lu, S., Kanodia, S., Ruisaard, K.E., Giralt, S.A., Estey, E.H., Cortes, J., Komanduri, K.V., Clise-Dwyer, K., Alatrash, G., Ma, Q., Champlin, R.E. and Molldrem, J.J., 2017. PR1 peptide vaccine induces specific immunity with clinical responses in myeloid malignancies. *Leukemia,* 31 (3), 697-704.

Quezada, S.A., Simpson, T.R., Peggs, K.S., Merghoub, T., Vider, J., Fan, X., Blasberg, R., Yagita, H., Muranski, P., Antony, P.A., Restifo, N.P. and Allison, J.P., 2010. Tumor-reactive CD4 (+) T cells develop cytotoxic activity and eradicate large established melanoma after transfer into lymphopenic hosts. *The Journal of Experimental Medicine,* 207 (3), 637-650.

Quinn, D.I., Petrylak, D.P., Pieczonka, C.M., Sandler, A., DeVries, T., Sheikh, N.A. and Drake, C.G., 2014. A randomized phase II, open-label study of sipuleucel-T with concurrent or sequential enzalutamide in metastatic castration-resistant prostate cancer (mCRPC). *Jco,* 32 (15), e16071-e16071.

Quinn, M., and Babb, P., 2002. Patterns and trends in prostate cancer incidence, survival, prevalence and mortality. Part I: international comparisons. *BJU International,* 90 (2), 162-173.

Quintero, I.B., Araujo, C.L., Pulkka, A.E., Wirkkala, R.S., Herrala, A.M., Eskelinen, E.L., Jokitalo, E., Hellstrom, P.A., Tuominen, H.J., Hirvikoski, P.P. and Vihko, P.T., 2007. Prostatic acid phosphatase is not a prostate specific target. *Cancer Research,* 67 (14), 6549-6554.

Rammensee, H.G., Falk, K. and Rotzschke, O., 1993. Peptides naturally presented by MHC class I molecules. *Annual Review of Immunology,* 11, 213-244.

Reading, J.L., Galvez-Cancino, F., Swanton, C., Lladser, A., Peggs, K.S. and Quezada, S.A., 2018. The function and dysfunction of memory CD8 (+) T cells in tumor immunity. *Immunological Reviews,* 283 (1), 194-212.

Reis, S.T., Pontes-Junior, J., Antunes, A.A., Sousa-Canavez, J.M., Abe, D.K., Cruz, J.A., Dall'oglio, M.F., Crippa, A., Passerotti, C.C., Ribeiro-Filho, L.A., Viana, N.I., Srougi, M. and Leite, K.R., 2011. Tgf-beta1 expression as a biomarker of poor prognosis in prostate cancer. *Clinics (Sao Paulo, Brazil),* 66 (7), 1143-1147.

Rekoske, B.T., Smith, H.A., Olson, B.M., Maricque, B.B. and McNeel, D.G., 2015. PD-1 or PD-L1 Blockade Restores Antitumor Efficacy Following SSX2 Epitope-Modified DNA Vaccine Immunization. *Cancer Immunology Research,* 3 (8), 946-955.

Richards, J., Lim, A.C., Hay, C.W., Taylor, A.E., Wingate, A., Nowakowska, K., Pezaro, C., Carreira, S., Goodall, J., Arlt, W., McEwan, I.J., de Bono, J.S. and Attard, G., 2012. Interactions of abiraterone,

eplerenone, and prednisolone with wild-type and mutant androgen receptor: a rationale for increasing abiraterone exposure or combining with MDV3100. *Cancer Research,* 72 (9), 2176-2182.

Riches, J.C., Davies, J.K., McClanahan, F., Fatah, R., Iqbal, S., Agrawal, S., Ramsay, A.G. and Gribben, J.G., 2013. T cells from CLL patients exhibit features of T-cell exhaustion but retain capacity for cytokine production. *Blood,* 121 (9), 1612-1621.

Ricupito, A., Grioni, M., Calcinotto, A., Hess Michelini, R., Longhi, R., Mondino, A. and Bellone, M., 2013. Booster vaccinations against cancer are critical in prophylactic but detrimental in therapeutic settings. *Cancer Research,* 73 (12), 3545-3554.

Roberts, A.D., Ely, K.H. and Woodland, D.L., 2005. Differential contributions of central and effector memory T cells to recall responses. *The Journal of Experimental Medicine,* 202 (1), 123-133.

Roden, A.C., Moser, M.T., Tri, S.D., Mercader, M., Kuntz, S.M., Dong, H., Hurwitz, A.A., McKean, D.J., Celis, E., Leibovich, B.C., Allison, J.P. and Kwon, E.D., 2004. Augmentation of T cell levels and responses induced by androgen deprivation. *Journal of Immunology (Baltimore, Md.: 1950),* 173 (10), 6098-6108.

Rojas-Martinez, A., Manzanera, A.G., Sukin, S.W., Esteban-Maria, J., Gonzalez-Guerrero, J.F., Gomez-Guerra, L., Garza-Guajardo, R., Flores-Gutierrez, J.P., Elizondo Riojas, G., Delgado-Enciso, I., Ortiz-Lopez, R., Aguilar, L.K., Butler, E.B., Barrera-Saldana, H.A. and Aguilar-Cordova, E., 2013. Intraprostatic distribution and long-term follow-up after AdV-tk immunotherapy as neoadjuvant to surgery in patients with prostate cancer. *Cancer Gene Therapy,* 20 (11), 642-649.

Rollings, C.M., Sinclair, L.V., Brady, H.J.M., Cantrell, D.A. and Ross, S.H., 2018. Interleukin-2 shapes the cytotoxic T cell proteome and immune environment-sensing programs. *Science Signaling,* 11 (526), 10.1126/scisignal.aap8112.

Romee, R., Rosario, M., Berrien-Elliott, M.M., Wagner, J.A., Jewell, B.A., Schappe, T., Leong, J.W., Abdel-Latif, S., Schneider, S.E., Willey, S., Neal, C.C., Yu, L., Oh, S.T., Lee, Y.S., Mulder, A., Claas, F., Cooper, M.A. and Fehniger, T.A., 2016. Cytokine-induced memory-like natural killer cells exhibit enhanced responses against myeloid leukemia. *Science Translational Medicine,* 8 (357), 357ra123.

Rosenberg, S.A., 2014. IL-2: the first effective immunotherapy for human cancer. *Journal of Immunology (Baltimore, Md.: 1950),* 192 (12), 5451-5458.

Ross, S.H., and Cantrell, D.A., 2018. Signaling and Function of Interleukin-2 in T Lymphocytes. *Annual Review of Immunology,* 36, 411-433.

Ross, S.H., Rollings, C., Anderson, K.E., Hawkins, P.T., Stephens, L.R. and Cantrell, D.A., 2016. Phosphoproteomic Analyses of Interleukin 2 Signaling Reveal Integrated JAK Kinase-Dependent and -Independent Networks in CD8 (+) T Cells. *Immunity,* 45 (3), 685-700.

Routy B, Le Chatelier E, Derosa L, Duong CPM, Alou MT, Daillere R, Zitvogel L. Gut microbiome influences efficacy of PD-1-based immunotherapy against epithelial tumors. Science. 2018;359(6371):91–7.

Russell, J.H., and Ley, T.J., 2002. Lymphocyte-mediated cytotoxicity. *Annual Review of Immunology,* 20, 323-370.

Saad, F., 2013. Evidence for the efficacy of enzalutamide in postchemotherapy metastatic castrate-resistant prostate cancer. *Therapeutic Advances in Urology,* 5 (4), 201-210.

Saif, J.M., Vadakekolathu, J., Rane, S.S., McDonald, D., Ahmad, M., Mathieu, M., Pockley, A.G., Durrant, L., Metheringham, R., Rees, R.C. and McArdle, S.E., 2014. Novel prostate acid phosphatase-based peptide vaccination strategy induces antigen-specific T-cell responses and limits tumour growth in mice. *European Journal of Immunology,* 44 (4), 994-1004.

Sakaguchi, S., Yamaguchi, T., Nomura, T. and Ono, M., 2008. Regulatory T cells and immune tolerance. *Cell,* 133 (5), 775-787.

Sakhdari, A., Mujib, S., Vali, B., Yue, F.Y., MacParland, S., Clayton, K., Jones, R.B., Liu, J., Lee, E.Y., Benko, E., Kovacs, C., Gommerman, J., Kaul, R. and Ostrowski, M.A., 2012. Tim-3 negatively regulates cytotoxicity in exhausted CD8+ T cells in HIV infection. *PloS One,* 7 (7), e40146.

Salinas, C.A., Tsodikov, A., Ishak-Howard, M. and Cooney, K.A., 2014. Prostate cancer in young men: an important clinical entity. *Nature Reviews.Urology,* 11 (6), 317-323.

Sallusto, F., Lenig, D., Forster, R., Lipp, M. and Lanzavecchia, A., 1999. Two subsets of memory T lymphocytes with distinct homing potentials and effector functions. *Nature,* 401 (6754), 708-712.

Santegoets, S.J., Stam, A.G., Lougheed, S.M., Gall, H., Jooss, K., Sacks, N., Hege, K., Lowy, I., Scheper, R.J., Gerritsen, W.R., van den Eertwegh, A.J. and de Gruijl, T.D., 2014. Myeloid derived suppressor and dendritic cell subsets are related to clinical outcome in prostate cancer patients treated with prostate GVAX and ipilimumab. *Journal for Immunotherapy of Cancer,* 2, 31-014-0031-3. eCollection 2014.

Santegoets, S.J., Stam, A.G., Lougheed, S.M., Gall, H., Scholten, P.E., Reijm, M., Jooss, K., Sacks, N., Hege, K., Lowy, I., Cuillerot, J.M., von Blomberg, B.M., Scheper, R.J., van den Eertwegh, A.J., Gerritsen, W.R. and de Gruijl, T.D., 2013. T cell profiling reveals high CD4+CTLA-4 + T cell frequency as dominant predictor for survival after prostate GVAX/ipilimumab treatment. *Cancer Immunology, Immunotherapy: CII,* 62 (2), 245-256.

Scheiermann, J., and Klinman, D.M., 2014. Clinical evaluation of CpG oligonucleotides as adjuvants for vaccines targeting infectious diseases and cancer. *Vaccine,* 32 (48), 6377-6389.

Schellhammer, P.F., Chodak, G., Whitmore, J.B., Sims, R., Frohlich, M.W. and Kantoff, P.W., 2013. Lower baseline prostate-specific antigen is associated with a greater overall survival benefit from sipuleucel-T in the Immunotherapy for Prostate Adenocarcinoma Treatment (IMPACT) trial. *Urology,* 81 (6), 1297-1302.

Schenkel, J.M., Fraser, K.A., Beura, L.K., Pauken, K.E., Vezys, V. and Masopust, D., 2014. T cell memory. Resident memory CD8 T cells trigger protective innate and adaptive immune responses. *Science (New York, N.Y.),* 346 (6205), 98-101.

Scher, H.I., Fizazi, K., Saad, F., Taplin, M.E., Sternberg, C.N., Miller, K., de Wit, R., Mulders, P., Chi, K.N., Shore, N.D., Armstrong, A.J., Flaig, T.W., Flechon, A., Mainwaring, P., Fleming, M., Hainsworth, J.D., Hirmand, M., Selby, B., Seely, L., de Bono, J.S. and AFFIRM Investigators, 2012. Increased survival with enzalutamide in prostate cancer after chemotherapy. *The New England Journal of Medicine,* 367 (13), 1187-1197.

Scholz, M., Yep, S., Chancey, M., Kelly, C., Chau, K., Turner, J., Lam, R. and Drake, C.G., 2017. Phase I clinical trial of sipuleucel-T combined with escalating doses of ipilimumab in progressive metastatic castrate-resistant prostate cancer. *ImmunoTargets and Therapy,* 6, 11-16.

Schreiber, T.H., Deyev, V.V., Rosenblatt, J.D. and Podack, E.R., 2009. Tumor-induced suppression of CTL expansion and subjugation by gp96-Ig vaccination. *Cancer Research,* 69 (5), 2026-2033.

Schweizer, M.T., Cheng, H.H., Tretiakova, M.S., Vakar-Lopez, F., Klemfuss, N., Konnick, E.Q., Mostaghel, E.A., Nelson, P.S., Yu, E.Y., Montgomery, B., True, L.D. and Pritchard, C.C., 2016. Mismatch repair deficiency may be common in ductal adenocarcinoma of the prostate. *Oncotarget,* 7 (50), 82504-82510.

Schymura, M.J., Kahn, A.R., German, R.R., Hsieh, M.C., Cress, R.D., Finch, J.L., Fulton, J.P., Shen, T. and Stuckart, E., 2010. Factors associated with initial treatment and survival for clinically localized prostate cancer: results from the CDC-NPCR Patterns of Care Study (PoC1). *BMC Cancer,* 10, 152-2407-10-152.

Sckisel, G.D., Mirsoian, A., Minnar, C.M., Crittenden, M., Curti, B., Chen, J.Q., Blazar, B.R., Borowsky, A.D., Monjazeb, A.M. and Murphy, W.J., 2017. Differential phenotypes of memory CD4 and CD8 T cells in the spleen and peripheral tissues following immunostimulatory therapy. *Journal for Immunotherapy of Cancer,* 5, 33-017-0235-4. eCollection 2017.

Seaman, M.S., Peyerl, F.W., Jackson, S.S., Lifton, M.A., Gorgone, D.A., Schmitz, J.E. and Letvin, N.L., 2004. Subsets of memory cytotoxic T lymphocytes elicited by vaccination influence the efficiency of secondary expansion *in vivo*. *Journal of Virology,* 78 (1), 206-215.

Sette, A., Vitiello, A., Reherman, B., Fowler, P., Nayersina, R., Kast, W.M., Melief, C.J., Oseroff, C., Yuan, L., Ruppert, J., Sidney, J., del Guercio, M.F., Southwood, S., Kubo, R.T., Chesnut, R.W., Grey, H.M. and Chisari, F.V., 1994. The relationship between class I binding affinity and immunogenicity of potential cytotoxic T cell epitopes. *Journal of Immunology (Baltimore, Md.: 1950),* 153 (12), 5586-5592.

Sfanos, K.S., Bruno, T.C., Maris, C.H., Xu, L., Thoburn, C.J., DeMarzo, A.M., Meeker, A.K., Isaacs, W.B. and Drake, C.G., 2008. Phenotypic analysis of prostate-infiltrating lymphocytes reveals TH17 and Treg skewing. *Clinical Cancer Research: An Official Journal of the American Association for Cancer Research,* 14 (11), 3254-3261.

Sfanos, K.S., Bruno, T.C., Meeker, A.K., De Marzo, A.M., Isaacs, W.B. and Drake, C.G., 2009. Human prostate-infiltrating CD8+ T lymphocytes are oligoclonal and PD-1+. *The Prostate,* 69 (15), 1694-1703.

Sfanos, K.S., and De Marzo, A.M., 2012. Prostate cancer and inflammation: the evidence. *Histopathology,* 60 (1), 199-215.

Sharma, R., and Das, A., 2018. IL-2 mediates NK cell proliferation but not hyperactivity. *Immunologic Research,* 66 (1), 151-157.

Sharpe, A.H., Wherry, E.J., Ahmed, R. and Freeman, G.J., 2007. The function of programmed cell death 1 and its ligands in regulating autoimmunity and infection. *Nature Immunology,* 8 (3), 239-245.

Shaulov, A., and Murali-Krishna, K., 2008. CD8 T cell expansion and memory differentiation are facilitated by simultaneous and sustained exposure to antigenic and inflammatory milieu. *Journal of Immunology (Baltimore, Md.: 1950),* 180 (2), 1131-1138.

Sheikh, N.A., Petrylak, D., Kantoff, P.W., Dela Rosa, C., Stewart, F.P., Kuan, L.Y., Whitmore, J.B., Trager, J.B., Poehlein, C.H., Frohlich, M.W. and Urdal, D.L., 2013. Sipuleucel-T immune parameters correlate with survival: an analysis of the randomized phase 3 clinical trials in men with castration-resistant prostate cancer. *Cancer Immunology, Immunotherapy: CII,* 62 (1), 137-147.

Shimura, S., Yang, G., Ebara, S., Wheeler, T.M., Frolov, A. and Thompson, T.C., 2000. Reduced infiltration of tumor-associated macrophages in human prostate cancer: association with cancer progression. *Cancer Research,* 60 (20), 5857-5861.

Shin, M.S., Kim, H.S., Lee, S.H., Park, W.S., Kim, S.Y., Park, J.Y., Lee, J.H., Lee, S.K., Lee, S.N., Jung, S.S., Han, J.Y., Kim, H., Lee, J.Y. and Yoo, N.J., 2001. Mutations of tumor necrosis factor-related apoptosis-inducing ligand receptor 1 (TRAIL-R1) and receptor 2 (TRAIL-R2) genes in metastatic breast cancers. *Cancer Research,* 61 (13), 4942-4946.

Shroder, F.H., Damhuis, R.A., Kirkels, W.J., De Koning, H.J., Kranse, R., Nus, H.G. and Blijenberg, B.G., 1996. European randomized study of screening for prostate cancer--the Rotterdam pilot studies. *International Journal of Cancer,* 65 (2), 145-151.

Shui, I.M., Lindstrom, S., Kibel, A.S., Berndt, S.I., Campa, D., Gerke, T., Penney, K.L., Albanes, D., Berg, C., Bueno-de-Mesquita, H.B., Chanock, S., Crawford, E.D., Diver, W.R., Gapstur, S.M., Gaziano, J.M., Giles, G.G., Henderson, B., Hoover, R., Johansson, M., Le Marchand, L., Ma, J., Navarro, C., Overvad, K., Schumacher, F.R., Severi, G., Siddiq, A., Stampfer, M., Stevens, V.L., Travis, R.C., Trichopoulos, D., Vineis, P., Mucci, L.A., Yeager, M., Giovannucci, E. and Kraft, P., 2014. Prostate cancer (PCa) risk variants and risk of fatal PCa in the National Cancer Institute Breast and Prostate Cancer Cohort Consortium. *European Urology,* 65 (6), 1069-1075.

Silva, A., Mount, A., Krstevska, K., Pejoski, D., Hardy, M.P., Owczarek, C., Scotney, P., Maraskovsky, E. and Baz Morelli, A., 2015. The combination of ISCOMATRIX adjuvant and TLR agonists induces regression of established solid tumors *in vivo*. *Journal of Immunology (Baltimore, Md.: 1950),* 194 (5), 2199-2207.

Simon, S., and Labarriere, N., 2017. PD-1 expression on tumor-specific T cells: Friend or foe for immunotherapy? *Oncoimmunology,* 7 (1), e1364828.

Simon, S., Vignard, V., Florenceau, L., Dreno, B., Khammari, A., Lang, F. and Labarriere, N., 2015. PD-1 expression conditions T cell avidity within an antigen-specific repertoire. *Oncoimmunology,* 5 (1), e1104448.

Simons, J.W., and Sacks, N., *Granulocyte-macrophage colony-stimulating factor-transduced allogeneic cancer cellular immunotherapy: the GVAX vaccine for prostate cancer.* 2006

Slovin, S.F., Wang, X., Hullings, M., Arauz, G., Bartido, S., Lewis, J.S., Schöder, H., Zanzonico, P., Scher, H.I., Sadelain, M. and Riviere, I., 2013. Chimeric antigen receptor (CAR+) modified T cells targeting prostate-specific membrane antigen (PSMA) in patients (pts) with castrate metastatic prostate cancer (CMPC). *Jco,* 31 (6), 72-72.

Small, E.J., Lance, R.S., Gardner, T.A., Karsh, L.I., Fong, L., McCoy, C., DeVries, T., Sheikh, N.A., GuhaThakurta, D., Chang, N., Redfern, C.H. and Shore, N.D., 2015. A Randomized Phase II Trial of Sipuleucel-T with Concurrent versus Sequential Abiraterone Acetate plus Prednisone in Metastatic Castration-Resistant Prostate Cancer. *Clinical Cancer Research: An Official Journal of the American Association for Cancer Research,* 21 (17), 3862-3869.

Smith, D.S., and Catalona, W.J., 1995. Interexaminer variability of digital rectal examination in detecting prostate cancer. *Urology,* 45 (1), 70-74.

Smyth, M.J., Hayakawa, Y., Takeda, K. and Yagita, H., 2002. New aspects of natural-killer-cell surveillance and therapy of cancer. *Nature Reviews.Cancer,* 2 (11), 850-861.

Soares, A., Govender, L., Hughes, J., Mavakla, W., de Kock, M., Barnard, C., Pienaar, B., Janse van Rensburg, E., Jacobs, G., Khomba, G., Stone, L., Abel, B., Scriba, T.J. and Hanekom, W.A., 2010. Novel application of Ki67 to quantify antigen-specific in vitro lymphoproliferation. *Journal of Immunological Methods,* 362 (1-2), 43-50.

Sonpavde, G., Slawin, K.M., Spencer, D.M. and Levitt, J.M., 2010. Emerging vaccine therapy approaches for prostate cancer. *Reviews in Urology,* 12 (1), 25-34.

Spary, L.K., Salimu, J., Webber, J.P., Clayton, A., Mason, M.D. and Tabi, Z., 2014. Tumor stroma-derived factors skew monocyte to dendritic cell differentiation toward a suppressive CD14 (+) PD-L1 (+) phenotype in prostate cancer. *Oncoimmunology,* 3 (9), e955331.

Spies, E., Reichardt, W., Alvarez, G., Groettrup, M. and Ohlschlager, P., 2012. An artificial PAP gene breaks self-tolerance and promotes tumor regression in the TRAMP model for prostate carcinoma. *Molecular Therapy: The Journal of the American Society of Gene Therapy,* 20 (3), 555-564.

Sprent, J., Zhang, X., Sun, S. and Tough, D., 2000. T-cell proliferation *in vivo* and the role of cytokines. *Philosophical Transactions of the Royal Society of London.Series B, Biological Sciences,* 355 (1395), 317-322.

Steimle, V., C. A. Siegrist, A. Mottet, B. Lisowska-Grospierre, B. Mach. 1994. Regulation of MHC class II expression by interferon-γ mediated by the transactivator gene CIITA. *Science* 265:106.

Steinbrink, K., Graulich, E., Kubsch, S., Knop, J. and Enk, A.H., 2002. CD4 (+) and CD8 (+) anergic T cells induced by interleukin-10-treated human dendritic cells display antigen-specific suppressor activity. *Blood,* 99 (7), 2468-2476.

Steinman, R.M., 1991. The dendritic cell system and its role in immunogenicity. *Annual Review of Immunology,* 9, 271-296.

Stone, J.D., Chervin, A.S. and Kranz, D.M., 2009. T-cell receptor binding affinities and kinetics: impact on T-cell activity and specificity. *Immunology,* 126 (2), 165-176.

Street, S.E., Cretney, E. and Smyth, M.J., 2001. Perforin and interferon-gamma activities independently control tumor initiation, growth, and metastasis. *Blood,* 97 (1), 192-197.

Stutman O. Tumor development after 3-methylcholanthrene in immunologically deficient athymic-nude mice. Science. 1974;183:534–536.

Sutherland, J.S., Goldberg, G.L., Hammett, M.V., Uldrich, A.P., Berzins, S.P., Heng, T.S., Blazar, B.R., Millar, J.L., Malin, M.A., Chidgey, A.P. and Boyd, R.L., 2005. Activation of thymic regeneration in mice and humans following androgen blockade. *Journal of Immunology (Baltimore, Md.: 1950),* 175 (4), 2741-2753.

Tagawa, S.T., Milowsky, M.I., Morris, M., Vallabhajosula, S., Christos, P., Akhtar, N.H., Osborne, J., Goldsmith, S.J., Larson, S., Taskar, N.P., Scher, H.I., Bander, N.H. and Nanus, D.M., 2013. Phase II study of Lutetium-177-labeled anti-prostate-specific membrane antigen monoclonal antibody J591 for metastatic castration-resistant prostate cancer. *Clinical Cancer Research: An Official Journal of the American Association for Cancer Research,* 19 (18), 5182-5191.

Taitt, H.E., 2018. Global Trends and Prostate Cancer: A Review of Incidence, Detection, and Mortality as Influenced by Race, Ethnicity, and Geographic Location. *American Journal of Men's Health,* 12 (6), 1807-1823.

Takahashi, H., Feuerhake, F., Kutok, J.L., Monti, S., Dal Cin, P., Neuberg, D., Aster, J.C. and Shipp, M.A., 2006. FAS death domain deletions and cellular FADD-like interleukin 1beta converting enzyme inhibitory protein (long) overexpression: alternative mechanisms for deregulating the extrinsic apoptotic pathway in diffuse large B-cell lymphoma subtypes. *Clinical Cancer Research: An Official Journal of the American Association for Cancer Research,* 12 (11 Pt 1), 3265-3271.

Takase, H., Yu, C.R., Mahdi, R.M., Douek, D.C., Dirusso, G.B., Midgley, F.M., Dogra, R., Allende, G., Rosenkranz, E., Pugliese, A., Egwuagu, C.E. and Gery, I., 2005. Thymic expression of peripheral tissue antigens in humans: a remarkable variability among individuals. *International Immunology,* 17 (8), 1131-1140.

Tanaka K, Kasahara M (1998) The MHC class I ligand-generating system: roles of immunoproteasomes and the interferon-4gMY-inducible proteasome activator PA28. Immunological Reviews 163: 161–176.

Tario, J.D.,Jr, Chen, G.L., Hahn, T.E., Pan, D., Furlage, R.L., Zhang, Y., Brix, L., Halgreen, C., Jacobsen, K., McCarthy, P.L. and Wallace, P.K., 2015. Dextramer reagents are effective tools for quantifying CMV antigen-specific T cells from peripheral blood samples. *Cytometry.Part B, Clinical Cytometry,* 88 (1), 6-20.

Telesca, D., Etzioni, R. and Gulati, R., 2008. Estimating lead time and overdiagnosis associated with PSA screening from prostate cancer incidence trends. *Biometrics,* 64 (1), 10-19.

Teply, B.A., Luber, B., Denmeade, S.R. and Antonarakis, E.S., 2016. The influence of prednisone on the efficacy of docetaxel in men with metastatic castration-resistant prostate cancer. *Prostate Cancer and Prostatic Diseases,* 19 (1), 72-78.

Thomas, D.A., and Massague, J., 2005. TGF-beta directly targets cytotoxic T cell functions during tumor evasion of immune surveillance. *Cancer Cell,* 8 (5), 369-380.

Thompson, I.M., Pauler, D.K., Goodman, P.J., Tangen, C.M., Lucia, M.S., Parnes, H.L., Minasian, L.M., Ford, L.G., Lippman, S.M., Crawford, E.D., Crowley, J.J. and Coltman, C.A.,Jr, 2004. Prevalence of prostate cancer among men with a prostate-specific antigen level < or =4.0 ng per milliliter. *The New England Journal of Medicine,* 350 (22), 2239-2246.

Tian, S., Maile, R., Collins, E.J. and Frelinger, J.A., 2007. CD8+ T cell activation is governed by TCR-peptide/MHC affinity, not dissociation rate. *Journal of Immunology (Baltimore, Md.: 1950),* 179 (5), 2952-2960.

Tietze, J.K., Wilkins, D.E., Sckisel, G.D., Bouchlaka, M.N., Alderson, K.L., Weiss, J.M., Ames, E., Bruhn, K.W., Craft, N., Wiltrout, R.H., Longo, D.L., Lanier, L.L., Blazar, B.R., Redelman, D. and Murphy, W.J., 2012. Delineation of antigen-specific and antigen-nonspecific CD8 (+) memory T-cell responses after cytokine-based cancer immunotherapy. *Blood,* 119 (13), 3073-3083.

Topalian, S.L., Hodi, F.S., Brahmer, J.R., Gettinger, S.N., Smith, D.C., McDermott, D.F., Powderly, J.D., Carvajal, R.D., Sosman, J.A., Atkins, M.B., Leming, P.D., Spigel, D.R., Antonia, S.J., Horn, L., Drake, C.G., Pardoll, D.M., Chen, L., Sharfman, W.H., Anders, R.A., Taube, J.M., McMiller, T.L., Xu, H., Korman, A.J., Jure-Kunkel, M., Agrawal, S., McDonald, D., Kollia, G.D., Gupta, A., Wigginton, J.M. and Sznol, M., 2012. Safety, activity, and immune correlates of anti-PD-1 antibody in cancer. *The New England Journal of Medicine,* 366 (26), 2443-2454.

Topham, N.J., and Hewitt, E.W., 2009. Natural killer cell cytotoxicity: how do they pull the trigger? *Immunology,* 128 (1), 7-15.

Tough, D.F., and Sprent, J., 1998. Bystander stimulation of T cells *in vivo* by cytokines. *Veterinary Immunology and Immunopathology,* 63 (1-2), 123-129.

Tumeh, P.C., Harview, C.L., Yearley, J.H., Shintaku, I.P., Taylor, E.J., Robert, L., Chmielowski, B., Spasic, M., Henry, G., Ciobanu, V., West, A.N., Carmona, M., Kivork, C., Seja, E., Cherry, G., Gutierrez, A.J., Grogan, T.R., Mateus, C., Tomasic, G., Glaspy, J.A., Emerson, R.O., Robins, H., Pierce, R.H., Elashoff, D.A., Robert, C. and Ribas, A., 2014. PD-1 blockade induces responses by inhibiting adaptive immune resistance. *Nature,* 515 (7528), 568-571.

Ugel, S., De Sanctis, F., Mandruzzato, S. and Bronte, V., 2015. Tumor-induced myeloid deviation: when myeloid-derived suppressor cells meet tumor-associated macrophages. *The Journal of Clinical Investigation,* 125 (9), 3365-3376.

Van Rompay, M.I., Solomon, K.R., Nickel, J.C., Ranganathan, G., Kantoff, P.W. and McKinlay, J.B., 2019. Prostate cancer incidence and mortality among men using statins and non-statin lipid-lowering medications. *European Journal of Cancer (Oxford, England: 1990),* 112, 118-126.

Velcheti, V., Karnik, S., Bardot, S.F. and Prakash, O., 2008. Pathogenesis of prostate cancer: lessons from basic research. *The Ochsner Journal,* 8 (4), 213-218.

Viaud S, Saccheri F, Mignot G, Yamazaki T, Daillère R, Hannani D, Enot DP, Pfirschke C, Engblom C, Pittet MJ, Schlitzer A, Ginhoux F, Apetoh L, Chachaty E, Woerther PL, Eberl G, Bérard M, Ecobichon C, Clermont D, Bizet C, Gaboriau-Routhiau V, Cerf-Bensussan N, Opolon P, Yessaad N, Vivier E, Ryffel B, Elson CO, Doré J, Kroemer G, Lepage P, Boneca IG, Ghiringhelli F, Zitvogel L. The intestinal microbiota modulates the anti-cancer immune effects of cyclophosphamide. Science. 2013;342:971–976.

Vigano, S., Utzschneider, D.T., Perreau, M., Pantaleo, G., Zehn, D. and Harari, A., 2012. Functional avidity: a measure to predict the efficacy of effector T cells? *Clinical & Developmental Immunology,* 2012, 153863.

Vitkin, N., Nersesian, S., Siemens, D.R. and Koti, M., 2019. The Tumor Immune Contexture of Prostate Cancer. *Frontiers in Immunology,* 10, 603.

Vonderheide, R.H., and Glennie, M.J., 2013. Agonistic CD40 antibodies and cancer therapy. *Clinical Cancer Research: An Official Journal of the American Association for Cancer Research,* 19 (5), 1035-1043.

Voutsas, I.F., Anastasopoulou, E.A., Tzonis, P., Papamichail, M., Perez, S.A. and Baxevanis, C.N., 2016. Unraveling the role of preexisting immunity in prostate cancer patients vaccinated with a HER-2/neu hybrid peptide. *Journal for Immunotherapy of Cancer,* 4, 75-016-0183-4. eCollection 2016.

Wagstaffe, H.R., Mooney, J.P., Riley, E.M. and Goodier, M.R., 2018. Vaccinating for natural killer cell effector functions. *Clinical & Translational Immunology,* 7 (1), e1010.

Wang, M.C., Valenzuela, L.A., Murphy, G.P. and Chu, T.M., 1979. Purification of a human prostate specific antigen. *Investigative Urology,* 17 (2), 159-163.

Wang, W., Erbe, A.K., Hank, J.A., Morris, Z.S. and Sondel, P.M., 2015. NK Cell-Mediated Antibody-Dependent Cellular Cytotoxicity in Cancer Immunotherapy. *Frontiers in Immunology,* 6, 368.

Wang, X., He, Q., Shen, H., Lu, X.J. and Sun, B., 2019. Genetic and phenotypic difference in CD8 (+) T cell exhaustion between chronic hepatitis B infection and hepatocellular carcinoma. *Journal of Medical Genetics,* 56 (1), 18-21.

Wang, X., and Lin, Y., 2008. Tumor necrosis factor and cancer, buddies or foes? *Acta Pharmacologica Sinica,* 29 (11), 1275-1288.

Wang, Y.J., Fletcher, R., Yu, J. and Zhang, L., 2018. Immunogenic effects of chemotherapy-induced tumor cell death. *Genes & Diseases,* 5 (3), 194-203.

Wargowski, E., Johnson, L.E., Eickhoff, J.C., Delmastro, L., Staab, M.J., Liu, G. and McNeel, D.G., 2018. Prime-boost vaccination targeting prostatic acid phosphatase (PAP) in patients with metastatic castration-resistant prostate cancer (mCRPC) using Sipuleucel-T and a DNA vaccine. *Journal for Immunotherapy of Cancer,* 6 (1), 21-018-0333-y.

Wherry, E.J., and Kurachi, M., 2015. Molecular and cellular insights into T cell exhaustion. *Nature Reviews.Immunology,* 15 (8), 486-499.

Wherry, E.J., Teichgraber, V., Becker, T.C., Masopust, D., Kaech, S.M., Antia, R., von Andrian, U.H. and Ahmed, R., 2003. Lineage relationship and protective immunity of memory CD8 T cell subsets. *Nature Immunology,* 4 (3), 225-234.

Williams, J.B., Horton, B.L., Zheng, Y., Duan, Y., Powell, J.D. and Gajewski, T.F., 2017. The EGR2 targets LAG-3 and 4-1BB describe and regulate dysfunctional antigen-specific CD8+ T cells in the tumor microenvironment. *The Journal of Experimental Medicine,* 214 (2), 381-400.

Witherspoon, L., Breau, R.H. and Lavallee, L.T., 2019. Evidence-based approach to active surveillance of prostate cancer. *World Journal of Urology,* .

Wolchok, J.D., Yuan, J., Houghton, A.N., Gallardo, H.F., Rasalan, T.S., Wang, J., Zhang, Y., Ranganathan, R., Chapman, P.B., Krown, S.E., Livingston, P.O., Heywood, M., Riviere, I., Panageas, K.S., Terzulli, S.L. and Perales, M.A., 2007. Safety and immunogenicity of tyrosinase DNA vaccines in patients with melanoma. *Molecular Therapy: The Journal of the American Society of Gene Therapy,* 15 (11), 2044-2050.

Wong, P., and Pamer, E.G., 2004. Disparate in vitro and *in vivo* requirements for IL-2 during antigen-independent CD8 T cell expansion. *Journal of Immunology (Baltimore, Md.: 1950),* 172 (4), 2171-2176.

Wong, P., and Pamer, E.G., 2001. Cutting edge: antigen-independent CD8 T cell proliferation. *Journal of Immunology (Baltimore, Md.: 1950),* 166 (10), 5864-5868.

Xiang, W., Shi, R., Kang, X., Zhang, X., Chen, P., Zhang, L., Hou, A., Wang, R., Zhao, Y., Zhao, K., Liu, Y., Ma, Y., Luo, H., Shang, S., Zhang, J., He, F., Yu, S., Gan, L., Shi, C., Li, Y., Yang, W., Liang, H. and Miao, H., 2018. Monoacylglycerol lipase regulates cannabinoid receptor 2-dependent macrophage activation and cancer progression. *Nature Communications,* 9 (1), 2574-018-04999-8.

Xie Y, Akpinarli A, Maris C, Hipkiss EL, Lane M, Kwon EK, et al. Naive tumor-specific CD4(+) T cells differentiated in vivo eradicate established melanoma. The Journal of experimental medicine. 2010;207(3):651–67. Epub 2010/02/17. pmid:20156973; PubMed Central PMCID: PMCPmc2839147.

Yamamoto, R., Nishikori, M., Kitawaki, T., Sakai, T., Hishizawa, M., Tashima, M., Kondo, T., Ohmori, K., Kurata, M., Hayashi, T. and Uchiyama, T., 2008. PD-1-PD-1 ligand interaction contributes to immunosuppressive microenvironment of Hodgkin lymphoma. *Blood,* 111 (6), 3220-3224.

Yoshimoto S, Loo TM, Atarashi K, Kanda H, Sato S, Oyadomari S, Iwakura Y, Oshima K, Morita H, Hattori M, Honda K, Ishikawa Y, Hara E, Ohtani N. Obesity-induced gut microbial metabolite promotes liver cancer through senescence secretome. Nature. 2013;499:97–101.

Yuan, J., Ku, G.Y., Gallardo, H.F., Orlandi, F., Manukian, G., Rasalan, T.S., Xu, Y., Li, H., Vyas, S., Mu, Z., Chapman, P.B., Krown, S.E., Panageas, K., Terzulli, S.L., Old, L.J., Houghton, A.N. and Wolchok, J.D., 2009. Safety and immunogenicity of a human and mouse gp100 DNA vaccine in a phase I trial of patients with melanoma. *Cancer Immunity,* 9, 5.

Zitvogel L, et al. Cancer and the gut microbiota: an unexpected link. Sci Transl Med. 2015;7(271):271ps271.

Zhang, N., and Bevan, M.J., 2011. CD8 (+) T cells: foot soldiers of the immune system. *Immunity,* 35 (2), 161-168.

Zhao, S.G., Lehrer, J., Chang, S.L., Das, R., Erho, N., Liu, Y., Sjostrom, M., Den, R.B., Freedland, S.J., Klein, E.A., Karnes, R.J., Schaeffer, E.M., Xu, M., Speers, C., Nguyen, P.L., Ross, A.E., Chan, J.M., Cooperberg, M.R., Carroll, P.R., Davicioni, E., Fong, L., Spratt, D.E. and Feng, F.Y., 2019. The Immune Landscape of Prostate Cancer and Nomination of PD-L2 as a Potential Therapeutic Target. *Journal of the National Cancer Institute,* 111 (3), 301-310.

Zhou, F., 2009. Molecular mechanisms of IFN-gamma to up-regulate MHC class I antigen processing and presentation. *International Reviews of Immunology,* 28 (3-4), 239-260.

Zhou, X., Sun, L., Jing, D., Xu, G., Zhang, J., Lin, L., Zhao, J., Yao, Z. and Lin, H., 2018. Galectin-9 Expression Predicts Favorable Clinical Outcome in Solid Tumors: A Systematic Review and Meta-Analysis. *Frontiers in Physiology,* 9, 452.

Zhu, Z., Cuss, S.M., Singh, V., Gurusamy, D., Shoe, J.L., Leighty, R., Bronte, V. and Hurwitz, A.A., 2015. CD4+ T Cell Help Selectively Enhances High-Avidity Tumor Antigen-Specific CD8+ T Cells. *Journal of Immunology (Baltimore, Md.: 1950),* 195 (7), 3482-3489.